

Universität
Rostock



Traditio et Innovatio

Scenario-based Optimization of Merchant Vessels

Dissertation

to obtain the academic degree of

Doktor-Ingenieur (Dr.-Ing.)

of the Faculty of Mechanical Engineering and Marine Technology
of the University of Rostock

submitted by

Dipl.-Ing. Jonas Conradin Wagner

born on 28.04.1982 in Stuttgart, Germany

Rostock, September 25, 2018



Dieses Werk ist lizenziert unter einer
Creative Commons Namensnennung - Weitergabe unter gleichen Bedingungen 4.0
International Lizenz.

Reviewer:

1st reviewer: Prof. Dr.-Ing. Robert Bronsart
Fakultät für Maschinenbau und Schiffstechnik, Universität Rostock
2nd reviewer: Prof. Dr.Eng./Hiroshima Univ. Patrick Kaeding
Fakultät für Maschinenbau und Schiffstechnik, Universität Rostock

Date of submission: 13. July 2017
Date of defence: 25. June 2018

“Nukular... das Wort heißt Nukular!”

Homer S.

Abstract

Due to the world economic crisis and its implications as well as other economic effects, the way of designing ships has been exposed to substantial changes. In search of vessels that offer an increased life-time performance, the designers' attention has more and more been shifting towards holistic ship design strategies. Regarding the ship hull form, this raises the need to optimize hull forms with respect to their overall service time performance instead of focusing on an unrealistic single design condition.

In order to contribute to this objective, this thesis aims at the development, implementation and exemplary application of a scenario-based design methodology that enables to predict a vessel's future operational profile and to consider its corresponding operating conditions in the design process. Thereby, the respective operating conditions - consisting of speed, draught and sea state information - are derived from a simulation of the vessel's full service time, which is mainly driven by the specification of the vessel's trade (transport task and route) and a set of variable economic and ecological surrounding conditions. These conditions include mathematical descriptions of the expected development of the world's transport demand and fuel oil prices as well as a statistical model of the weather conditions along the vessel's route. The simulation is capable of calculating the vessel's reaction to the varying surrounding conditions by considering details such as a fuel cost-driven owner's decision for slow steaming, weather-caused delays and schedule-keeping, maintenance periods, local speed and draught limitations and the need to switch to alternative fuels in environmentally sensitive areas.

In order to account for unforeseen developments and the generally lacking knowledge about the future, the development of the economic surrounding conditions is subjected to stochastic fluctuations. For the purpose of depicting all possibly upcoming operating conditions, a Monte-Carlo approach is applied, meaning that the simulation is repeated under constantly varying surrounding conditions and by collecting all resulting operating conditions until the aggregated distribution of these conditions reaches convergence. The convergence determination is thereby done using a *Hellinger distance*-based abort criterion.

The most relevant of all detected operating conditions are chosen on the basis of the time spent and the net present value of the fuel costs to be paid at that condition. These selected conditions can then be transferred into the objective function of a subsequent hull form optimization of a parametrically modeled vessel and provide a solid basis for a robust and holistic ship design.

Contents

1. Introduction and Motivation	1
1.1. Research Objectives	4
1.2. Outline	5
2. Fundamentals of Scenario-based Ship Design	6
2.1. History of Scenario Methods	6
2.2. Working Principle	9
2.2.1. Scenario Types	10
2.2.2. Structure and Terminology	11
2.2.3. Scenario Setup	12
2.3. Scenario Methods in Shipbuilding	14
2.4. Assessment of Ship Designs	20
2.4.1. Life Cycle Assessment	20
2.4.2. Economic Key Performance Indicators	21
2.4.3. Social and Environmental Performance Indicators	22
3. Scenario Development	25
3.1. Basic Considerations	25
3.1.1. Input	25
3.1.2. Scenario Descriptors	26
3.1.3. Utilization of Data	30
3.2. Scenario Development Methodology	30
3.3. Modeling of Scenario Environment	34
3.3.1. Trade	34
3.3.2. Fuel Oil Prices	37
3.3.3. Transport Demand	44
3.3.4. Weather	45
3.4. Calculation of Scenario Descriptors	47
3.4.1. Dry Dock	47
3.4.2. Sea State	48
3.4.3. Speed	50
3.4.4. Time	53
3.4.5. Fuel Oil Price	53
3.4.6. Transport Demand	55
3.4.7. Slow Steaming	55
3.4.8. Draught	56
3.5. Uncertainty Handling	58
3.6. Development of Objective Operating Conditions	62

4. Proof of Concept	66
4.1. Trade	66
4.2. Fuel Oil Prices	68
4.3. Weather	72
4.4. Vessel Response	72
5. Implementation	77
5.1. Scenario In- and Output	77
5.2. Ship Model	78
5.3. Resistance Calculation	78
6. Optimization Examples	80
6.1. Case One: Duisburg Test Case	80
6.1.1. Ship Model	80
6.1.2. Trade Description	83
6.1.3. Scenario Setup	84
6.1.4. Objective Function and Optimization Setup	86
6.1.5. Results	87
6.1.6. Sensitivity Analysis	89
6.2. Case Two: 3500 TEU Container Vessel	91
6.2.1. Ship Model	91
6.2.2. Trade Description	93
6.2.3. Scenario Setup	95
6.2.4. Objective Function and Optimization Setup	97
6.2.5. Results	100
6.2.6. Sensitivity Analysis	107
6.3. Case Three: Passenger Vessel	107
6.3.1. Ship Model	109
6.3.2. Trade Description	109
6.3.3. Scenario Setup	110
6.3.4. Objective Function and Optimization Setup	111
6.3.5. Results	112
7. Conclusion	114
7.1. Summary	114
7.2. Limitations and Discussion	115
7.3. Outlook and further Work	117
A. Appendix	119
A.1. Introduction	119
A.2. Proof of Concept	120
A.3. Optimization of Duisburg Test Case	121
A.3.1. Ship Model	121
A.3.2. Trade Description	122
A.3.3. Scenario Setup	124
A.3.4. Objective Function	125

Contents

A.4. Optimization of 3500 TEU Container Vessel	127
A.4.1. Ship Model	127
A.4.2. Trade Description	128
A.4.3. Scenario Setup	131
A.4.4. Objective Function	132
A.4.5. Results	134
A.5. Optimization of Passenger Vessel	136
A.5.1. Trade Description	136
A.5.2. Scenario Setup	142
Bibliography	144

List of Figures

1.1.	Development of Baltic Exchange Dry Index (2007 to 2013)	2
1.2.	Operating conditions of a 3750 <i>TEU</i> container vessel	3
2.1.	Feedback loop of population, capital, agriculture and pollution	8
2.2.	Prognosis vs. scenario approach	10
2.3.	Hierarchical structure of scenario components	12
2.4.	<i>Quantum</i> container ship concept	15
3.1.	Transport demand, OECD Industrial Production Index and gross domestic product	28
3.2.	General schema of the scenario-based optimization approach	31
3.3.	Scenario development process	32
3.4.	Scenario development within each Monte-Carlo cycle	33
3.5.	Schematic trade description Rotterdam - New York	37
3.6.	Development of fuel oil prices from 1987 to 2014	38
3.7.	Exemplary simple symmetric random walk on integer number line	39
3.8.	Random walks of length 100	40
3.9.	Flow chart of fuel oil price simulation	42
3.10.	Flow chart of fuel oil price crisis simulation	42
3.11.	Flow chart of transport demand simulation	45
3.12.	Position of seaway points	46
3.13.	Schema of manifestation calculation within each route segment	48
3.14.	Sampling from a discrete cumulative distribution function	49
3.15.	Flow chart of speed calculation	51
3.16.	Comparison of reactions to speed changes	52
3.17.	Flow chart of time calculation	54
3.18.	Flow chart of fuel oil price calculation	55
3.19.	Flow chart of transport demand calculation	56
3.20.	Reaction to an exemplary slow steaming decision	57
3.21.	Flow chart of draught calculation	58
3.22.	Comparison of three histograms using <i>Hellinger distance</i>	61
3.23.	Exemplary <i>Hellinger distance</i> development	62
3.24.	Joint vs. marginal frequencies	64
4.1.	Exemplary fuel oil price development after 1000 Monte-Carlo cycles	69
4.2.	Selected single fuel oil price developments	69
4.3.	Distribution of fuel oil prices after 1000 Monte-Carlo cycles	70
4.4.	Exemplary FOP development including crises after 1000 Monte-Carlo cycles . .	71
4.5.	Selected single fuel oil price developments including crises	71
4.6.	Comparison between original and simulated sea state distribution	72
4.7.	Exemplary distribution of speed and wave heights	75

List of Figures

6.1. Bulbous bow parameters	81
6.2. Principle of bulbous bow breadth variation	82
6.3. Global container trade	85
6.4. Development of fuel oil prices of all 25 000 Monte-Carlo cycles	88
6.5. Body plan of 3500 <i>TEU</i> container vessel	92
6.6. Speed-resistance-curves of original hull form	93
6.7. Total wave height and period distribution of the 3500 <i>TEU</i> container vessel	99
6.8. Results of Ensemble Investigation	101
6.9. Body plan of optimized hull form	102
6.10. Comparison of speed-resistance-curves	103
6.11. Comparison of wave elevation and pressure distribution at OC ₃	105
6.12. Comparison of wave elevation and pressure distribution at OC ₅	105
6.13. Comparison of speed-resistance-curves	108
6.14. Total wave height and period distribution of passenger vessel	112
A.1. Development of HARPEX Index since 2006	119
A.2. Distribution of FOP development including crises after 1000 Monte-Carlo cycles	120
A.3. Principle of bulbous bow length variation	121
A.4. Principle of bulbous bow height variation	121
A.5. Transport task of Duisburg Test Case	122
A.6. Allocation of transport task onto seaway points	122
A.7. Distribution of fuel oil price values after ten years	125
A.8. Distribution of transport demand values after ten years	126
A.9. Wave resistance-curves of original hull form	127
A.10. Frictional resistance-curves of original hull form	128
A.11. <i>Hellinger</i> criterion development of last 10 000 Monte-Carlo cycles	132
A.12. Total speed and draught distribution of 3500 <i>TEU</i> container vessel	133
A.13. Wave resistance-curves of optimized hull form	134
A.14. Frictional resistance-curves of optimized hull form	135
A.15. Total resistance-curves of optimized hull form	136

List of Tables

2.1. Comparison of design approaches	19
3.1. Exemplary slow steaming decision table	29
3.2. Traditional route description Rotterdam - New York	34
3.3. Route description Rotterdam - New York	34
3.4. Exemplary extract of a seaway scatter table entry	46
3.5. Decision table for speed reductions due to wave height	52
3.6. Exemplary objective operating conditions	65
3.7. Exemplary objective operating conditions including merged $H_{1/3}$ bins	65
4.1. Example trade characteristics	66
4.2. Exemplary objective operating conditions (initial case)	67
4.3. Exemplary objective operating conditions (with local speed restriction)	67
4.4. Exemplary objective operating conditions (with speed and draught restrictions)	68
4.5. Exemplary economic scenario development parameters	73
4.6. Exemplary objective operating conditions (with and without considering FOPs)	73
4.7. Exemplary objective operating conditions (considering slow steaming)	74
4.8. Exemplary objective operating conditions (considering slow steaming and weather)	74
4.9. Theoretical objective operating conditions (without fuel oil prices)	76
6.1. Main dimensions of Duisburg Test Case	81
6.2. Boundaries of bulbous bow variation	82
6.3. Speed reduction due to wave height	84
6.4. Economic scenario development descriptors	86
6.5. Objective operating conditions (including fuel oil prices)	87
6.6. Objective operating conditions (excluding fuel oil prices)	89
6.7. Best performing variants vs. number of objective operating conditions	90
6.8. Best performing variants vs. number of objective operating conditions	90
6.9. Main dimensions of 3500 <i>TEU</i> container vessel	91
6.10. Boundaries of bulbous bow variation	92
6.11. Speed reduction due to wave height	96
6.12. Economic scenario development descriptors	96
6.13. List of top 50 operating conditions	98
6.14. Objective operating conditions (including fuel oil prices)	99
6.15. Resistance values of initial variant	100
6.16. Starting variants for Tangent Search optimization	102
6.17. Optimized vessel performance per objective operating condition	104
6.18. Main dimensions of passenger vessel	108
6.19. Economic scenario development descriptors	111
6.20. Objective operating conditions	113

List of Symbols

A.1. Calculation of route segment characteristics	120
A.2. Objective operating conditions (without fuel oil prices)	133

List of Symbols

B_{wl}	Breadth at water line
c_B	Block coefficient
$C_{f,j}$	CO ₂ emission rate of fuel type j
CF_t	Cash flow at time t
$C_{o,t}$	Cash outflow at time t
D	Travel distance
$\Delta FOP(t_j)$	Development of $FOP(t)$ at time step t_j since t_{j-1}
ΔFOP_{ECA}	Fuel cost difference at emission control areas
D_m	m^{th} descriptor
η_D	Propulsion efficiency
η_H	Hull efficiency
η_O	Propeller efficiency
η_R	Rotative efficiency
FC_j	Mass of consumed fuel of type j
$fluc_{FOP}$	Fluctuation of fuel oil price
$fluc_{TD}$	Fluctuation of transport demand
\overline{FOP}	Time-averaged fuel oil price
$FOP_{ECA,i}$	ECA-adjusted fuel oil price at route segment i
FOP_i	Fuel oil price at route segment i
FOP_{t_j}	Fuel oil price at time step t_j
$F_X(x)$	Discrete cumulative distribution function
$f_X(x)$	Discrete probability mass function
$F_X^{-1}(x)$	Inverse discrete cumulative distribution function
gt	Gross tonne

List of Symbols

$H_{1/3}$	Significant wave height
$H(P, Q)$	<i>Hellinger distance</i> of discrete probability distributions P and Q
i	Route segment indicator
i_r	Interest rate
k	Form factor
kn	Knots
L_B	Longitudinal position of bulbous bow tip
L_{pp}	Length between perpendiculars
$M_{i,p}$	p^{th} manifestation of descriptor i
m_{cargo}	Carried cargo
mt	Metric tonne
μ	Expected value
$\mu_{FOPCrisisDur}$	Expected value of fuel oil price crisis duration
μ_{RW}	Expected value of a random walk-based distribution
$\mu_{TDCrisisDur}$	Expected value of transport demand crisis duration
∇	Displacement
NCF_t	Net cash flow at time t
$\mathcal{N}(\mu, \sigma)$	Normal distribution with expected value μ and standard deviation σ
n_{MC}	Number of Monte-Carlo cycles
$n_{MC,min}$	Minimum number of needed Monte-Carlo cycles
n_{empty}	Number of transported TEUs (empty)
n_{full}	Number of transported TEUs (full)
n_{total}	Total number of possible descriptor manifestations
n_x	Number of possible manifestations of descriptor x
OC_i	Operating condition(s) at route segment i
OC_{MC}	Aggregated operating condition(s) of one Monte-Carlo cycle
OC_{Total}	Aggregated operating condition(s) of all Monte-Carlo cycles
P	75 % of installed shaft power
p	Success probability

List of Symbols

P_B	Break power
P_D	Delivered power
P_E	Effective power
$P_{E,total}$	Weighted effective power
$P_{FOPCrisis}$	Occurrence probability of fuel oil price crises
p_k	k^{th} value of discrete probability distribution P
q_k	k^{th} value of discrete probability distribution Q
$P_{RiseFOP}$	Probability of rising fuel oil prices
P_{RiseTD}	Probability of rising transport demand
$P_{TDcrisis}$	Occurrence probability of transport demand crises
P_x	Breadth shift of bulbous bow in longitudinal direction
P_y	Breadth shift of bulbous bow in transverse direction
P_z	Breadth shift of bulbous bow in vertical direction
R_{AW}	Added resistance in seaways
$R_{AW,total}$	Weighted added resistance in seaways
R_{Drift}	Resistance due to drift forces
R_F	Frictional resistance
R_T	Total resistance
R_{T,OC_i}	Total resistance at operating condition i
$R_{T,total}$	Weighted total resistance
R_W	Wave resistance
R_{Wind}	Wind resistance
S	Wetted surface
SFC	Specific fuel consumption
s_i	Length of route segment i
σ	Standard deviation
$\sigma_{FOPCrisisDur}$	Standard deviation of fuel oil price crisis duration
$\sigma_{\mathcal{N}}$	Standard deviation of normal distribution
σ_{RW}	Standard deviation of a random walk-based distribution

List of Symbols

$\sigma_{Rademacher}$	Standard deviation of <i>Rademacher distribution</i>
σ_{Steps}	Standard deviation of step distribution
$\sigma_{TDCrisisDur}$	Standard deviation of transport demand crisis duration
T	Draught
T_1	Center of gravity period
T_D	Design draught
$t_{delay,i}$	Delay at route segment i
TD_i	Transport demand at route segment i
t_{dock}	Dry-docking time
T_i	Draught at route segment i
t_i	time spent at route segment i
$t_{intended,i}$	Intended passing time of route segment i
T_{LSW}	Light draught
T_{max}	Global draught restriction (maximum)
t_{max}	Service time horizon
$T_{max,local,i}$	Local draught restriction (maximum) at route segment i
T_{min}	Global draught restriction (minimum)
$T_{min,local,i}$	Local draught restriction (minimum) at route segment i
T_p	Peak period
TP	Transport performance
$t_{total,i}$	Total operating time at route segment i
T_z	Zero upcrossing period
U	Sampled probability value
v	Speed
v_D	Design speed
v_i	Speed at route segment i
$v_{initial,i}$	Initial speed value at route segment i
$v_{intended,i}$	Intended speed at route segment i
v_{max}	Global speed restriction (maximum)

List of Symbols

$v_{max,local,i}$	Local speed restriction (maximum) at route segment i
v_{min}	Global speed restriction (minimum)
$v_{min,local,i}$	Local speed restriction (minimum) at route segment i
v_{OC_i}	Speed of operating condition i
V_{ref}	Reference speed
$v_{ssc,i}$	Slow steaming-corrected speed at route segment i
$v_{wc,i}$	Weather-corrected speed at route segment i
w_{cum}	Cumulative weighting of operating condition(s)
w_{OC_i}	Weighting of operating condition i
W_P	Payload
w_{Total,OC_i}	Weighting of operating condition i with respect to total service time
Z_B	Vertical position of bulbous bow tip

List of Abbreviations

ASCII	American Standard Code for Information Interchange
BIP	Binary Integer Programming
CDF	cumulative distribution function
CRF	capital recovery factor
DNV	Det Norske Veritas
DoE	Design of Experiment
DTC	Duisburg Test Case
DWT	deadweight tonnage
ECA	emission control area
ECPTS	European Conference on Production Technologies in Shipbuilding
EEDI	Energy Efficiency Design Index
EEOI	Energy Efficiency Operational Indicator
EIA	United States Energy Information Administration
FEU	forty foot equivalent unit
FOP	fuel oil price
GDP	gross domestic product
GBN	Global Business Network
HARPEX	Harper Petersen Charter Rate Index
HFO	heavy fuel oil
HSVA	Hamburgische Schiffbau-Versuchsanstalt
IGES	Initial Graphics Exchange Specification
IMO	International Maritime Organization
IPCC	Intergovernmental Panel on Climate Change
ISSC	International Ship and Offshore Structures Congress
ITTC	International Towing Tank Conference
KCS	KRISO Container Ship
KPI	key performance indicator
LCA	life cycle assessment
LCC	life cycle costing
LNG	liquefied natural gas

List of Abbreviations

LR	Lloyds Register
MARPOL	International Convention for the Prevention of Pollution from Ships
MBI	market-based instrument
MEPC	Marine Environment Protection Committee
MOGA	multi-objective genetic algorithm
MC	Monte-Carlo
MCM	Monte-Carlo method
MDO	marine diesel oil
MGO	marine gas oil
MIC-MAC	Matrice d'Impacts Croisés - Multiplication Appliquée à un Classement
MIT	Massachusetts Institute of Technology
NGO	non-governmental organization
NMS	Nelder Mead Simplex
NPV	net present value
NPVI	net present value index
NMVOC	non methane volatile organic compounds
OC	operating condition
OOC	objective operating condition
PDF	probability density function
PMF	probability mass function
PMM	planar motion mechanism
PSO	particle swarm optimization
PV	present value
RANSE	Reynolds-Averaged Navier-Stokes Equation
RDO	robust design optimization
RFR	required freight rate
ROI	return of investment
SECA	sulphur emission control area
SEEMP	Ship Energy Efficiency Management Plan
SMF	ship merit factor
STL	Stereolithography
TBT	Tributyltin
TD	transport demand
TEU	twenty foot equivalent unit
TS	Tangent Search

List of Abbreviations

UNCTAD	United Nations Conference On Trade And Development
VDMA	Verband Deutscher Maschinen- und Anlagenbau
XML	Extensible Markup Language

1. Introduction and Motivation

In recent years, the shipping industry has experienced drastic changes. At first, the world economic crisis starting in 2008 should be mentioned. In the course of this crisis, shippers have been facing two problems: a decelerating transport demand due to the - regarding Europe at best - stagnating global economy and collapsing freight rates caused by overcapacities and the introduction of constantly growing vessels. As an illustration, the development of the *Baltic Exchange Dry Index* from 2007 to 2013 is given in Figure 1.1. Focusing onto the containerized trading, the market situation shows almost the same behavior, which can be seen in the development of the corresponding *Harper Petersen Charter Rate Index (HARPEX)* for containerized goods given in Figure A.1 in the Appendix. It appears that even though the shipping demand slowly recovers, the freight rates stay at a low level with a tendency to decrease even further (Jah and Christie, 2015). Resulting from the constantly falling daily earnings, there is a severe financial pressure on ship owners, forcing them to improve their vessel's efficiency or to file for bankruptcy (UNCTAD Secretariat, 2015).

In order to cope with these challenges, slow steaming has become a popular instrument for reducing the operational costs while at the same time solving the problem of decreased transport demand. According to Bergh (2010), approximately 80 % of all vessels serving on Asia-Europe loops have switched to slow steaming operation indicated by a speed drop from 24 to 25 *kn* to 17 to 18 *kn* or even less. While not being applied to that extent at all other trades, there seems to be a general trend for retaining the slow steaming even in case the market situation recovers (UNCTAD Secretariat, 2015).

Despite the crisis and its consequences, there are other issues affecting the operation of merchant vessels. One of these issues can be identified in the so-called cascading effect. Driven by both, the economic pressure as well as the expansion of the Panama Canal, an increasing number of steadily growing large container vessels ($> 16\,000\ TEU$) has entered the market. While being able to transport more goods at a lower cost level, these vessels force operators to cascade their vessels to secondary and regional routes (UNCTAD Secretariat, 2013). At these trades the vessels often have to operate under conditions they have not initially been designed for.

It becomes apparent that both - the slow steaming as well as the cascading effect - have a significant impact on the way that ships are operated, which force vessels to adapt to changing operating conditions. In this context, changing operating conditions are understood as modifications to a vessel's speed, its draught and trim as well as its environmental conditions like sea states, wind and currents. While not being considered within the vessel's initial design, they are often being referred to as off-design conditions. These conditions affect a lot of efficiency-related matters, for example powering, propulsion, resistance and seakeeping. From all of these impacts, the effect of draught, trim and speed on the vessel's propulsion and resistance characteristics can be considered to be the most influential. Especially the extreme bulbous bow forms resulting from hull form optimizations onto high speeds and draughts as done prior to the economic crisis have shown to be highly prone to speed and draught variations. Experiments at the Hamburgische Schiffbau-Versuchsanstalt (HSVA) indicated an increase in required power

1. Introduction and Motivation

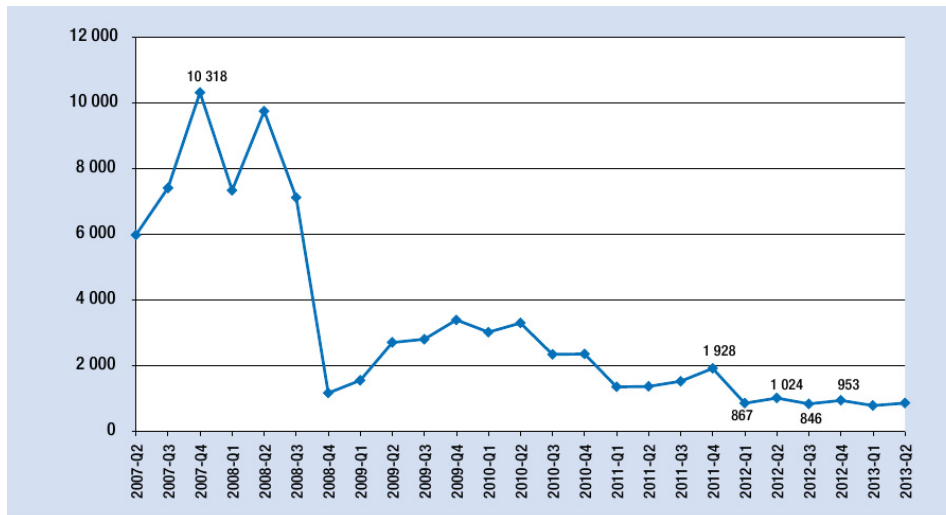


Figure 1.1.: Development of Baltic Exchange Dry Index (2007 to 2013) (UNCTAD Secretariat, 2013)

of about 15% in case a bulbous bow-equipped vessel operates at 80% speed and 70% draught (Hollenbach and Reinholz, 2011). In addition to that, the application of bulbous bows can be questioned with respect to their performance in waves (Chuang and Steen, 2012). Regarding propulsion, a decreasing draught becomes at least problematic in case the propeller pierces the surface (Holtrop, 1984; Minsaas et al., 1986). Furthermore, the propulsion efficiency is sensitive to rough waters as well as speed changes, too (Carlton, 2012). All of these effects lead to the problem of ships being - to a varying extent - less effective when operating at off-design conditions.

In order to illustrate the magnitude of this problem, an analysis of the noon-to-noon reports of a medium sized panamax container vessel (3750 TEU) of a German shipping company has been carried out. The data covered a period from 2007 to 2012 and did not consider any pilotage segments. As it can be seen in Figure 1.2, the vessel encounters moderate slow steaming and spends most of its time at conditions that differ from its designated design condition of $v = 21.5 \text{ kn}$ and $T = 12.0 \text{ m}$. In particular, the speed reduction to 17 to 19 kn is visible. The draughts also show a high variation, ranging from 7.5 m to the scantling draught, presumably due to the decelerated transport demand. Concluding this example, the vessel's design conditions add up to less than 1% of its total operating time.

As the indicated operation under non-efficient conditions means a waste of resources and resulting a loss of profit, it appears to be a strong motivation for rethinking the traditional way of designing vessels. Additionally, great efforts have been made in order to reduce the environmental footprint of the world's merchant fleet. These efforts resulted in a number of statutory provisions that force ships to operate in a more energy efficient way and further urge ship designers and operators to head for innovative solutions.

According to Gershanik (2011) the main factors for reducing both, the costs and the environmental footprint, are

- an increase of machinery efficiency,
- maintaining the vessel's technical condition,

1. Introduction and Motivation

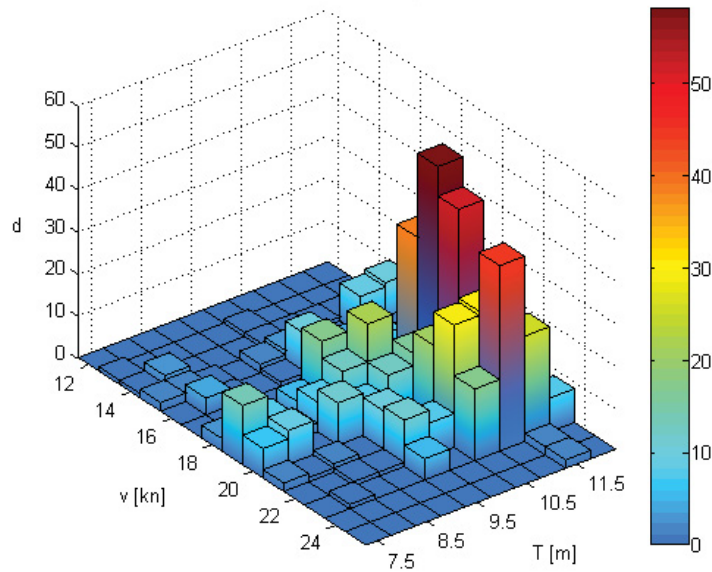


Figure 1.2.: Operating conditions of a 3750 TEU container vessel

- an optimized routing,
- the evaluation of optimal operational engine modes and
- an improvement of the vessel's hull form and propeller.

As also stated there, the possibilities of increasing the machinery efficiency are tending to zero within the near future. While the following three points address ship operators, from the designer's point of view the hydrodynamic factors gain in importance. Accordingly, a new way of designing ship hull forms and propulsion units has been established. These new design methodologies target a rather holistic approach by trying to consider more than one operating condition within the design objectives. While "more than one" currently in most cases means a number between two and four, the focus on a vessel's life-time performance and resulting the consideration of complete operational profiles is supposed to become a standard approach in the future (Hochkirch and Bertram, 2012).

This approach of designing ships with respect to operational profiles raises the question on how to determine these profiles. In practice, it has become common to rely on data collected in the past, for example noon-to-noon reports of existing vessels. This approach works as intended as long as the new vessel is supposed to operate on the same trade and has comparable main dimensions. Unfortunately, this is rather an exceptional than the normal case. In most cases, the newly developed vessel will feature larger dimensions if at all serving the same route. Also when thinking of retrofitting purposes (for example resulting from the cascading effect), data from the past only work, if a comparable vessel has already been operating on the new route for an adequate period of time.

Another disadvantage of data from the past exists in their reliability. The collection of ship operational data is exposed to a long list of potential disruptive factors. While the ship's speed through water as well as over ground can be determined comparatively accurate, a precise

draught monitoring is a complex task. Even though the draught can be determined in port, this data does not hold for the transit, due to dynamic trim and sinkage effects. While in transit, the draught measuring is usually hampered by the current sea state and the resulting ship motions. The sea states itself are often estimated instead of measured, due to lacking equipment. Additionally and concerning all on-board measurements, only a small (yet rising) number of vessels has been equipped with tools for fully automated data collection. As the collection of operational data is often not of the crew's primary interest, many manually generated noon-to-noon reports offer gaps or inconsistencies. Despite this issue, another fundamental disadvantage of the usage of past data consists in the lacking possibility to illustrate future developments that might affect the operation of a designated vessel. Examples for these influences could be rules and regulations, fuel oil prices, the development of global and local economies as well as environmental or social incidents.

The contrary approach of using forecasted operational profiles is comparatively new to the shipping industry and tries to address the previously mentioned problems. As it will be shown in Chapter 2, there exists a set of tools for revealing potential future developments, with some of them already being implemented within the maritime context. Nevertheless, most of these methods are still based on ideal, inflexible assumptions and suffer from the lack of possibilities for modeling external influences and their respective impact on the structure of the operational profile.

Resulting from these circumstances, the research objectives as given in the following section arise.

1.1. Research Objectives

This thesis aims at the development and implementation of a scenario-based design methodology that enables to predict a vessel's future operational profile and to consider its corresponding operating conditions in the design process. This should allow to optimize a hull form with respect to its life-time performance instead of focusing on an unrealistic single design condition. It should be noted that in this context the life-time performance has to be considered as a function of the chosen business model and therefore does not necessarily refer to the total life span of a vessel (especially during crises, business models focus on time spans much less than 25 years). The intended approach shall make use of scenario methods in order to satisfy the following requirements:

- Enable a system that allows the simulation of a vessel's full service time in order to derive its most probable operating conditions. These operating conditions should contain speed, draught and sea state information.
- The simulation shall be based on the definition of a specific trade (transportation task and route to serve on) and a set of external parameters that affect the vessel's operation. The dependencies and interrelations of all of these parameters shall be modeled mathematically. The whole system has to be fully customizable, which includes the modeling and the impact of the external parameters as well as the corresponding vessel's reaction.
- The system shall be able to consider deviations to the above mentioned specifications in order to reveal unexpected developments, such as the strong increase of fuel oil prices until mid 2014 and its subsequent collapse. Therefore, stochastic fluctuations and the possibility of shocks or crisis have to be taken into account. A method has to be provided

1. Introduction and Motivation

that allows to handle these uncertainties and to include their consequences within the operational profile.

- The selection of the most promising operating conditions to optimize onto should be done with respect to economic aspects. Therefore, despite their probability of occurrence, additional economic factors shall be taken into account when determining the optimization's objective operating conditions.

The methodology mainly addresses container vessels, but should also be usable for other merchant vessels as well. It shall additionally be applicable to new buildings as well as retrofitting projects. When successful, the intended approach should mark a small step towards the goal of robust, holistic ship design.

1.2. Outline

This thesis structures as follows: Within Chapter 2, an introduction to scenario methods, their basic functionality and terminology as well as examples of their implementation within the maritime environment are given. Additionally, a short overview on the different assessment methods for ship designs is provided. Chapter 3 contains a detailed description of the targeted scenario-based optimization approach and introduces the basic working principle, the modeling and the calculation of the respective scenarios. The chapter closes with information on the uncertainty handling and the identification of the objective operating conditions. The proof of concept regarding the scenario development's functionality is done in Chapter 4. After a short description of the implementation of the scenario development tool and the optimization environment in Chapter 5, the scenario-based optimization approach is applied to three exemplary use cases, which are presented in Chapter 6. Finally, Chapter 7 contains the discussion on the achieved results and an outlook to possible future work.

2. Fundamentals of Scenario-based Ship Design

Within this chapter, a basic introduction on the methods being applied within the targeted approach are presented. As the working principle of ship hull form optimizations are assumed to be well known, this chapter concentrates on the other parts of the scenario based optimization approach. Therefore, various aspects of scenario methods are exposed, including a short overview concerning the various assessment possibilities for ship designs. Finally, a literature review on application examples of scenario-related design and optimization approaches within the maritime transport industry is presented.

According to Shoemaker (1993), scenario methods are a powerful tool for triggering new developments due to their ability of stretching peoples' thinking, which is achieved by bringing up futures not yet considered. In general, the evaluation of specific problems regarding future developments is done by modeling a corresponding system of the problem's dependencies and interdependencies, followed by running this model under varying preconditions. This approach does not result in one specific prediction, but a certain number of possible future contingencies, often bringing up unconventional paths and allowing to deduce strategies that in many cases differ from the standard "business as usual" procedures. This ability has made scenario methods being successfully used within different fields of strategic business, social and political planning.

While being widely used it has to be noted that there neither exists a consistent definition of scenario methods nor a distinctive theoretical or methodological procedure of application (Kossow and Gaßner, 2007). As also the terminology is not consistent but varying between different sources, it has been decided to make use of the terms and conventions defined by Mißler-Behr (1993) within this thesis.

2.1. History of Scenario Methods

Originating from the military intelligence, the predecessor of scenario methods - the so-called *war games* - have been set up in order to allow policy makers to simulate possible effects and consequences of potential decisions to be made in the upcoming future and to reduce the risk of making bad decisions in real life. Based on this, the idea of simulating future developments under consideration of fluctuating surrounding conditions in order to draw conclusions and make decisions has been transferred into the civil fields of social science and business management.

One of the first companies applying scenario methods has been Shell, helping them to survive the oil price crisis in the 1973s and to foresee the fall of communism in Russia as well as its impact on global gas prices in 1983 (Ringland, 1998). The company is still active in the field of creating and analyzing scenarios, which is reflected in their *Global Scenarios* series, wherein constantly updated future visions are presented. The latest issue has been published in 2011 and addresses the global energy development up to the year 2050 (Shell International BV, 2011). In Shell International BV (2008) there even exists a guide on how to set up and make use of scenarios.

2. Fundamentals of Scenario-based Ship Design

With Shell certainly being the most prominent example for the successful implementation of scenario methods, there are many other companies that achieved comprehensive results. Exemplarily, Ringland (1998) lists

- Electrolux, changing the strategic agenda of their commercial cleaning business from exclusively acting as a supplier to selling services instead of products,
- Erste Allgemeine Versicherung (an Austrian insurance company), being one of the first companies to enter the central European markets by foreseeing the fall of the Berlin Wall,
- European Computer-Industry Research Center (ECRC), trying to uncover future developments of the European IT industry in 1993 in order to focus their research programs,
- British Airways, at this time being the world's largest international passenger carrier, developing new strategies and a long-term business plan in 1994.

As the modeling as well as the correct interpretation of scenarios is a complex and time consuming task not many companies are willing to take, there are consulting companies specializing onto scenario based business advisory. One example for this is the Global Business Network (GBN), founded in 1987 amongst others by Peter Schwartz, who has previously been responsible for the strategic scenario planning at Shell (Ringland, 1998). This consultant company consisted of a large group of experts from different fields, not only including mathematics, IT experts and economists but also political scientists, environmentalists and even science fiction writers and musicians (Lohr, 1998). This broad mixture of expertise allowed the company to offer scenario analysis for all kind of companies, to hold scenario planning workshops and to publish an extensive guide for using scenario methods within non-profit organizations (Scearce and Fulton, 2004).

As well as for business matters, examples for the application of scenario methods within non-profit and non-governmental organizations (NGOs) can be found. The first time that scenarios created by a NGO received a recognizable public perception happened after the publication of the first *The Limits to Growth* report by the Club of Rome with support of the Massachusetts Institute of Technology (MIT) in 1972. Within this study, the global implications of human action with respect to environmental and social issues has been simulated by using scenario methods. As described in Meadows (1973), the utilized simulation model named *World3* took care about the five main variables

- world population,
- industrialization,
- food production,
- non-renewable resource depletion and
- pollution.

Each of these variables is driven by a number of sub-variables, forming so-called *feedback loops* of casual relationships. As an example, the feedback loop of the variables population, capital, agriculture and pollution is given in Figure 2.1. The development of all contained variables has been based on different prognosis by the authors and led in most cases to the result, that by

2. Fundamentals of Scenario-based Ship Design

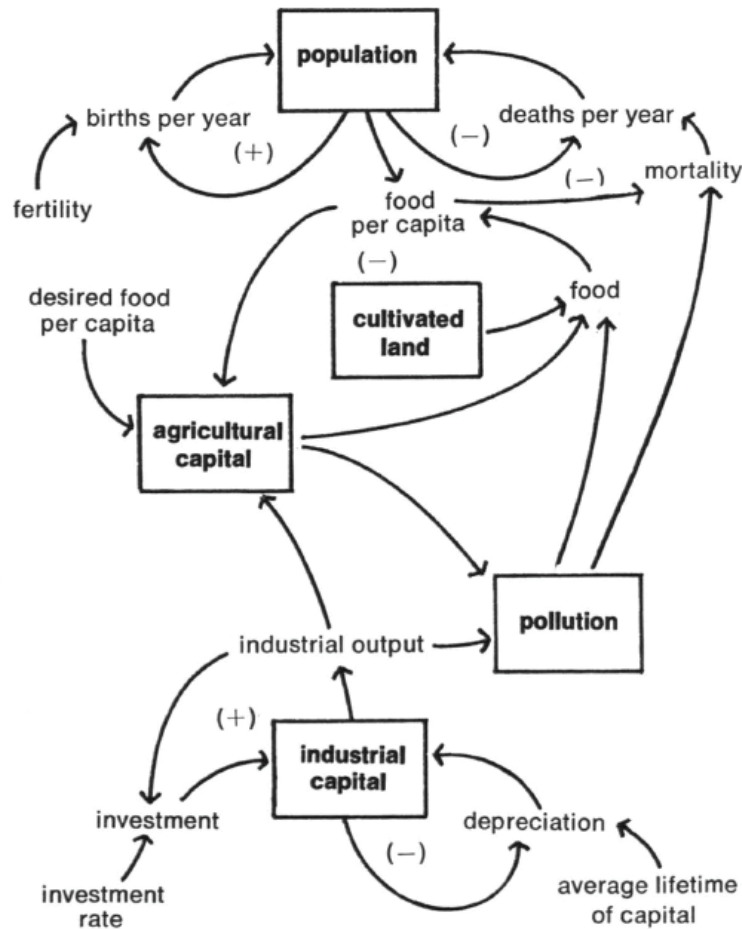


Figure 2.1.: Original feedback loop of population, capital, agriculture and pollution as given in Meadows et al. (1972)

continuing exponential growth of all five variables (the *business-as-usual scenario*) the natural resources of the earth will be expired within the next hundred years (Meadows et al., 1972). Within the updated version of 2004, this collapse is predicted for the year 2030 (Meadows et al., 2004). Although many economists - for example Cole (1973) - and even the authors itself (Meadows, 1982) criticized their model or the prognosis used therein, this constantly updated study has been sold approximately 30 000 000 times according to Simmons (2000), received huge attention especially within NGOs and can be considered to have a strong influence on the public discourse (Bardi, 2011).

Another early example of a study based on even more advanced scenario methods can be found in the *Global 2000* report, commissioned by US President Jimmy Carter in 1977 and published in 1980 (Barney, 1980). Using a comparable approach as the *Limits to Growth* study but involving the input of 14 US government agencies, this report targeted the development of mankind and its environment up to the year 2000. As well as its preceding study by the Club of Rome, the *Global 2000* report concluded “global problems of alarming proportions by the year 2000” and gained huge attention especially by environmental NGOs.

A problem both studies face, consists in their lack of acceptance outside of NGOs. This lack

is based on the impression that not all developed scenarios - for example the *run-out of natural resources in the year 2000* scenario - have come true and therefore the method itself can not be considered to be reliable, which is a basic mistake that is often made when discussing the results of scenario methods.

A - regarding the public acceptance - more succesful and regularly updated series of reports basing on scenario methods are the *IPCC Assessment Reports* (IPCC, 2015) of the Intergovernmental Panel on Climate Change (IPCC), which has been awarded the 2007 Nobel Peace Price (sharing with Al Gore). These reports address the scientific and technical assessment of climate change and are updated every five to seven years, starting with the first issue in the year 1988. Within the reports, a comprehensive world model has been set up, which is used to generate a small number of scenarios in order to initiate necessary discussions and to cope with the climate change impacts. In addition to the description of the model itself, the dependencies, impacts and interactions modeled therein and the outlines of the different work groups contributing to the report, so-called *Pathways for adaption, mitigation and sustainable development*, are offered within a special summary for policy-makers (IPCC, 2014).

Further examples of sceanrio usage within the public and corporate field can be found in Greeuw et al. (2000), Ringland (1998) and van Notten et al. (2003).

2.2. Working Principle

In order to describe the basic working principle of scenarios methods, it is useful to primarily make a distinction between scenario methods and prognosis. In general, scenario methods focus on possible developments within a larger time span of up to 20 years or more, while prognosis are usually used to forecast more contemporary developments of a few years. Furthermore, the outcome of a prognosis normally consists of a single concrete value, development or statement, while scenario methods provide more than just one answer by raising a cone of possible developments, which is based on the fact that far future developments are usually subjected to larger uncertainties than short-range forecasts. Simplified, scenario methods could be illustrated as an accumulation of multiple long-term prognosis done under consideration of varying boundary conditions.

Another difference exists in the fact that scenario methods can not only be used when it comes to mathematically based developments (such as economic forecasts), but within the fields of political or social matters, where so-called *soft factors*, like human behaviors that are difficult to model by mathematics, are important. Therefore, scenario methods more than prognosis usually account for the path of a certain development. In fact, in some cases the *how* of a specific development can be more important than the final result itself, mostly applying for the usage within the above mentioned political or social environment.

These differences are reflected within Figure 2.2, where the typical scheme of a traditional prognosis and a scenario approach are given. Thereby, the gray line indicates observations of an unspecified parameter from the past until the present day. The red line represents a traditional prognosis made on the basis of the averaged growth of the past (marked by the dashed red line) and results in a single situation at the end of the forecast horizon. In contrast to this, the dashed blue line and the resulting situation at the forecast horizon represents just one of many possible parameter developments. It can furthermore be seen that the path of the scenario development can be retraced at any point along the time line, allowing it to analyze the development process and to identify disrupting events, critical influences or key driving

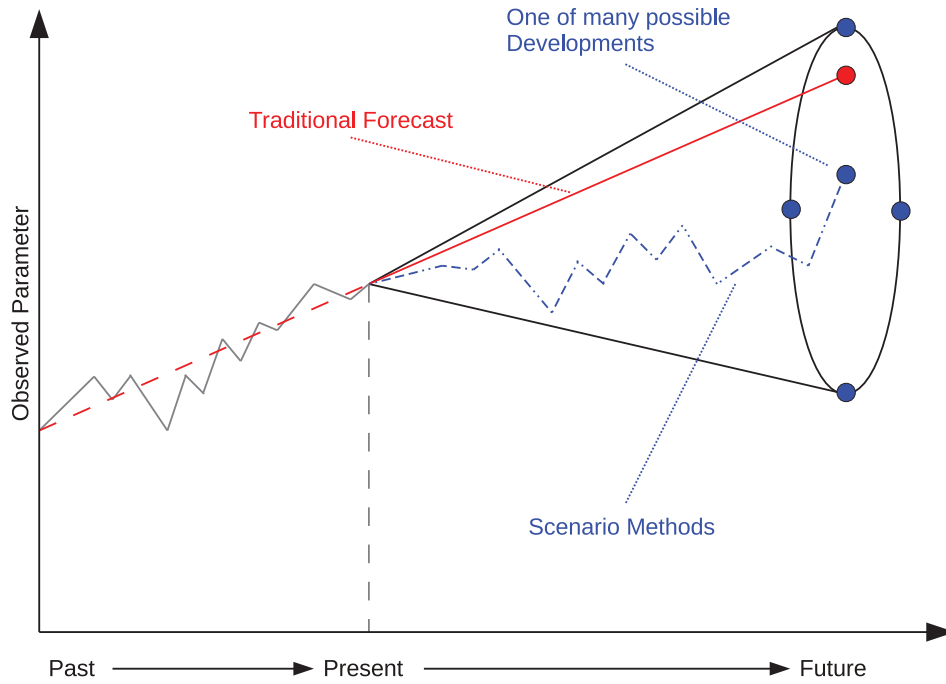


Figure 2.2.: Prognosis vs. scenario approach (Shoemaker, 1993)

factors.

The total of all possible developments would sum up to the depicted scenario cone, usually opening up with increasing time due to the growing uncertainty level of knowledge about the future (although there might be setups leading to constant or even narrowing borders). The blue dots at the borders of the forecast horizon mark so-called *extreme scenarios*, usually being referred to as *best case* or *worst case* of a specific development possibility. It should be noted that the borders of a scenario cone necessarily neither need to be linear or defined by a however looking mathematical function nor represent the most unlikely developments, as both is dependent on the setup and the type of the respective scenario.

2.2.1. Scenario Types

Before going into the details on how to model scenarios, a distinction of the different scenario types has to be done. Following the explanations of Kossow and Gaßner (2008), scenarios can either be one of the following types:

- explorative or normative,
- quantitative or qualitative.

Explorative (also called descriptive) methods lead to a set of possible future events aiming to answer the question “What if?”. Based on the present, this is done by identifying key driving factors and their respective consequences and developing them into the future. Within explorative scenarios, occurrence probabilities are usually of great importance. In contrast to this, normative scenarios try to answer the questions “How should the future look like?” or “How does one come to a specific future?”. Therefore, the perspective of the normative

approach heads from the future to the present. Occurrence probabilities are used only in exceptional circumstances, which is based on the assumption that the occurrence probability of a specific event is influenced by the decisions to be done in order to reach it.

The second distinguishing feature relates to the type of information to be included within the scenario. When utilizing a quantitative scenario model, the model as well as its corresponding interrelations can be set up mathematically, while the results can be analyzed in the same way. Scenarios of this kind are usually applied within mathematically easy describable contexts, for example for demographic studies or in the area of business sciences. Qualitative scenarios are used, if there is no sense in describing a problem using a quantitative approach. Examples for this are politics, social science or cultural problems. As the degree of formalizations of these scenarios is much lower than the one of the quantitative methods, their modeling usually has a more narrative character. Although this might in some cases not seem to be an approach that meets scientific requirements, qualitative, narrative scenarios have the advantage of being able to address larger time horizons. This is due to the fact that quantitative descriptions or information lose their plausibility when it comes to longer development perspectives of 10 to 25 years or more. According to van Notten et al. (2003), they are furthermore used in case of complex situations with high levels of uncertainty. As stated there, also mixed approaches exist, which are usually characterized by a complex modeling methodology, but on the other hand offer a higher consistency and robustness than its individual constituent parts.

Another distinction given in Kossow and Gaßner (2008) can be made on the basis of the time horizon. It is distinguished between short-term, mid-term and long-term scenarios, running from up to 10 over up to 25 to more than 25 years. van Notten et al. (2003) furthermore mention a distinction addressing the temporal nature of the scenario. As stated there, scenario methods can be divided into approaches producing chain scenarios or end-state (also: snapshot) scenarios. The former ones can be understood as films, describing the complete path of a certain development up to its end-state. Contrarily, snapshot scenarios are like a photograph, only describing the end-state of a development by only implicitly considering the path that led to this result.

2.2.2. Structure and Terminology

According to Mißler-Behr (1993), scenarios can be subdivided into specific fields of interest in order to delimit the different influence factors and therefore to structure the scenario development process. The composition of these so-called *environments* is given in Figure 2.3. Each environment consists of a number of influence factors, the so-called *descriptors*. Examples for these could be found in the descriptors *growth of gross domestic product (GDP)* and *interest rate* grouped within the environment *economic situation*. In general, descriptors can be split into critical and non-critical ones, differing in the ability to have changing manifestations. Critical descriptors form the basis of any scenario development process and can take any value within specified borders, which allows interpreting them as variables with the manifestations being their variable values. Non-critical descriptors are usually used in order to depict complete scenarios also including static but relevant information, for example descriptors that are not supposed to change during the scenario development process. Regarding the two exemplary descriptors mentioned above, the growth of the GDP can be considered to represent a critical and the interest rate (often set as a constant value within profitability calculations) a non-critical descriptor.

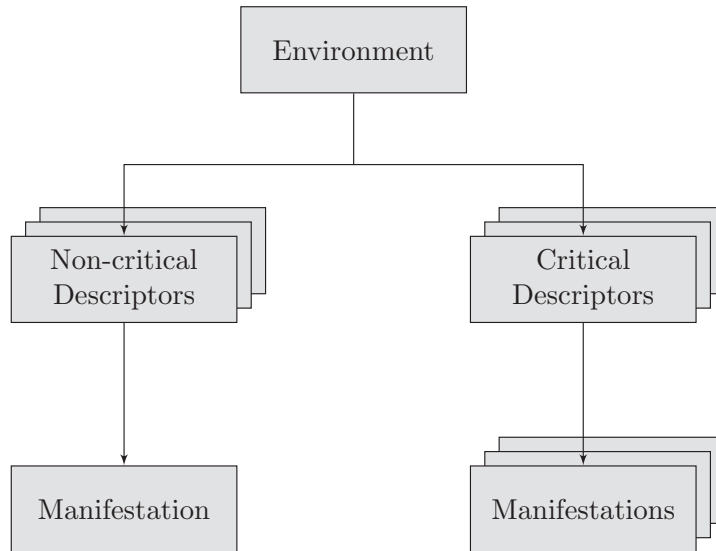


Figure 2.3.: Hierarchical structure of scenario components (Mißler-Behr, 1993)

The total number of possible manifestations can be determined through

$$n_{total} = \sum_{i=1}^m \sum_{j=1}^p M_{i,j}, \quad (2.1)$$

with m being the number of descriptors (D_1, \dots, D_m), each having p possible manifestations ($M_{i,1}, \dots, M_{i,p}$). In general, n_{total} takes comparatively small values in case of narrative scenarios, as those are focusing on qualitative instead of quantitative descriptor manifestations. When developing mathematically based scenarios, the number of manifestations is usually higher. In case of mathematically developed scenarios with non-discrete manifestations, n_{total} can not be determined prior to the full scenario development, as in those cases n_{total} is dependent on the binning of the resulting manifestations.

It should be noted that not all theoretically possible manifestations need to come up during the scenario development.

2.2.3. Scenario Setup

The general setup of the scenario modeling as it will be used within this thesis has been described in Wagner and Bronsart (2012) and can be divided into the following four major steps:

1. problem definition and specification of boundaries,
2. system build-up,
3. scenario creation,
4. scenario analysis / drawing of conclusions.

Within the first step, the problem to be examined is defined, which includes the formulation of a targeted question as well as a delimitation of areas not to be included. In case of a normative approach, the objective to be reached would be framed within this step.

2. Fundamentals of Scenario-based Ship Design

Step two - the system build-up - can be considered to be the most complex and time consuming task within the scenario setup. Within this step the questions

- Which descriptors shall be used to describe the system?
- How do they describe it / what is their precise influence?
- Are there any interconnections between them?

are addressed. The answer to the first question can be given comparatively easy, as it usually evolves from the initial problem definition and can freely be chosen by the user. In contrast, the second and third question can cause extensive and time consuming analyses, as their answers are of great importance regarding the plausibility and reliability of the scenarios to be created. Especially in case of complex scenario models with a high number of descriptors, the number of relationships and interrelationships to be investigated and resulting the effort to be put into these investigations can become the largest part (regarding the temporal effort) of the whole scenario development process. The main task is to determine cause and effect chains of each descriptor that should be included within the scenario model. These chains have to be expressed in narrative or mathematical form (depending on the scenario's characteristics), for which a detailed survey of causes and impacts is needed. Thereby, one of the main challenges exists in the need to examine each descriptor separately in order to only consider direct instead of indirect influences from one descriptor onto another. Furthermore, it has to be taken care of causal loops, either direct or indirect. These loops - for example a direct loop of the gross domestic product influencing the fuel oil prices again influencing the gross domestic product - can lead to an unwanted overvaluation of the respective descriptors, causing inconsistent and unreasonable scenarios. Especially indirect loops being "hidden" within chains with more than two links can be challenging to detect. As potential problems due to these causal loops also increase with a growing number of scenario descriptors, their number should be kept at a manageable amount. As an example, Kossow and Gaßner (2008) recommend to focus on a number of 10 to at the maximum 20 descriptors. In order to find the most important (meaning the most influential) descriptors and to reduce their number, different approaches for analyzing the descriptors' influence on the system and for uncovering causal loops exist:

- Influence Matrix and System Grid,
- Triangulation Method,
- Matrice d'Impacts Croisés - Multiplication Appliquée à un Classement (MIC-MAC) Analysis.

All three methods create a ranking order of all descriptors included within a scenario model by splitting them into rather active or passive ones. While the first two approaches are only capable of considering direct dependencies, the MIC-MAC Analysis are a powerful tool for detecting causal loops due to indirect dependencies. Based on this ability, the MIC-MAC Analysis has become a widely used tool, for example within the previously mentioned study of the ECRC (Ringland, 1998). Further explanations on the working principle and the advantages and disadvantages of these methods as well as examples of usage and a comparison of the results can be found in Wagner and Bronsart (2012). As also stated there, it should be noted that these methods should only be used in order to detect the most relevant descriptors. They do not enable the user to make statements about how descriptors are related to each other. Further

literature concerning this part of the scenario setup and the selection of relevant descriptors can be found in Reibnitz (1991), Wessels (1981), Hauke (1992), Godet (1987) and Mißler-Behr (1993).

Step three of the scenario setup consists in the actual development of the scenarios, which is done by running the previously set up model. In case of a mathematically formulated scenario model, there usually exist corresponding computational algorithms (if not, they can be developed), which in the following can easily be computed. In case of narrative scenario models, the final scenarios need to be “told”. This can be done on the one hand by actually verbally developing different “stories” based on the scenario model or on the other hand by using structured approaches or computational algorithms. In case of discrete descriptors (for example the descriptor *tightening of environmental policies* becoming either high, medium or low), this storytelling could be done via matrices or decision trees. In that case - and after the development of all possible scenarios - a small number of them will be picked in order to be analyzed. Another approach exists in merging related scenarios into a few representative reference scenarios. In most cases, this procedure of choosing only a few out of the whole of the developed scenarios is useful, because of the strategic nature of the problems to be solved. This implies that not every single deviation from an identified major development needs to be considered. Relating to Figure 2.2 on page 10, it could be sufficient to only discuss the four extreme and one additional medium scenario.

Finally within step four, the evaluation of the chosen scenarios - or in case of a normative approach the chosen paths - is done. The type of evaluation depends on the initial problem to be solved as well as on the chosen scenario type and can range from purely statistical analysis to strategic debating.

As within this thesis only a short introduction on scenario methods can be given, further literature on the topic can be found for example in Mietzner and Reger (2004), Mietzner (2009), Kossow and Gaßner (2008) and Greeuw et al. (2000).

2.3. Scenario Methods in Shipbuilding

In contrast to other industries, the application of scenario methods is a comparatively young field within the maritime industry. Only since approximately 2008 and the beginning of the world economic crisis and the associated incipient rethinking of operating and designing ships, these methods received common attention. Since then, scenario methods can in most cases be found in the field of strategic planning and general market development, while their usage for the actual design or re-design of ships - as it is intended to strive for within this thesis - rarely comes to public. The main reason for this could be the fact that shipyards as well as component suppliers or design offices normally aren't interested in publishing their design methodologies, as their business success depends on keeping them secret.

One example on how the design of a vessel with respect to results gained from scenario methods could look like has been published by DNV (2010). The concept of a 6210 *TEU* container vessel as presented there has, amongst others, been developed on the basis of different transport and market scenarios. Resulting, the vessel has been given a slender hull form ($c_B = 0.57$) with a wide double side deck for increased container storage and a dual fuel marine diesel oil (MDO) / liquefied natural gas (LNG) drive concept with two Azipod propulsors. Thereby, the final hull design has been the result of an optimization with a parametrically modeled hull form under consideration of calm water resistance and added resistance in seaways.



Figure 2.4.: *Quantum* container ship concept, (DNV, 2010)

As the main goal of this design study has been to open a window to possible future ship designs and to inspire the maritime industry, the *Quantum* concept neither reflects an - according to the regulations - valid ship design nor claims to exist in full in the future. Considering this, an impression of this vessel is given in Figure 2.4.

While only being a small part within the *Quantum* study, scenario methods have been the main topic within the comprehensive *Shipping 2020* report, which has been presented in DNV (2012) and targets on giving an outlook onto likely outcomes of technology uptake in the maritime industry. The scenarios developed within this study considered the descriptors economic growth (in the western world as well as in China and India), the status of ballast water, sulphur and carbon regulation, heavy fuel oil (HFO), marine gas oil (MGO) and LNG prices, the size of the world merchandise fleet, its design and the accessibility to capital. Some of these descriptors have been given a qualitative (e.g. fuel oil prices and economic growth) and some a narrative character (e.g. regulations, design). It has to be noted that - in a first step - most of the included descriptors have not been allowed to develop completely freely (by means of random-based or stochastic algorithms) but were given a few predefined trend alternatives. By combining these alternatives, four basic scenarios forming a rough development setting have been built, which in the following served as the starting point for the creation of a high number of simulation runs that might be considered as sub-scenarios. Within these sub-scenarios, the actual manifestations of fuel oil prices and technology costs and resulting from that the fleet development as well as the corresponding technology investment decisions have been simulated on the basis of stochastically modeled processes. These simulations furthermore included different ship owner characteristics and technology investment cost adjustments on the basis of learning effects. As well as for the scenario approach introduced within this thesis, the *Shipping 2020* study made use of discrete event and Monte-Carlo (MC) sampling. In the end, the data gained from these simulations have been analyzed in order to figure out, which technologies at what costs are most likely to be adopted within the future.

Even though this study is based on a comprehensive simulation model fed by a huge database (sources have, amongst others, been International Maritime Organization (IMO), Det Norske Veritas (DNV) and United States Energy Information Administration (EIA) researches, studies and databases) and features a common and widely used procedure for creating scenarios, there

2. Fundamentals of Scenario-based Ship Design

are some drawbacks. As an example for these, the fuel oil price development can be quoted, which has been given three basic alternative development possibilities, namely a worst case, a best case and a reference scenario. Regarding the end of the year 2015, the worst case scenario predicts a fuel oil price of roughly 1100 \$/mt, the reference scenario 750 \$/mt and the best case scenario 300 \$/mt. Although the best case scenario comes at least close to the current fuel oil prices, this development has not been included within the four finally chosen scenarios, while even the 750 \$/mt reference scenario is part of only one of them. Despite this problem, the scenario model itself as well as its results have been constantly updated and used to develop further concept vessels like the LNG driven *Quantum 9000* container vessel presented in DNV and MAN Diesel & Turbo (2011) in order to support the goal of taking a glance at possible future vessel designs.

Another example of scenario methods applied by a classification society (in this case Lloyds Register (LR)) in order to depict possible future market developments can be found in Fang et al. (2013) and Argyros et al. (2014), with the first one rather focusing onto general maritime industry trends and the latter concentrating on fuel oil prices. The *Global Marine Trends 2030* study (Fang et al., 2013) has been conducted in order to identify upcoming challenges to the maritime industry as well as to start a debate about its future shape. Therefore, mainly qualitative scenario methods have been utilized, resulting in three scenarios (*Global Commons*, *Status Quo* and *Competing Nations*) that cover, amongst others, demographics, economy, natural resources and environmental issues. In accordance with the narrative character of the overall method, these scenarios and their paths have been called *scenario stories* throughout the publication. The impact of the three scenarios have then been simulated with respect to various aspects of the commercial, naval and offshore energy sector. Furthermore, six additional disruptive events have been defined, which are not included within the chosen scenarios but especially mentioned in order to raise their awareness due to their supposed strong impact onto the maritime industry.

Referring to and based on the above study, the *Global Marine Fuel Trends 2030* report has been published in Argyros et al. (2014). It presents a more detailed view onto the specifics of different fuel markets and the resulting progression of the global fleet of container ships, bulk and general cargo carriers and tankers. By utilizing a comparable approach with the same basic assumptions as done within its predecessor, three basic fuel scenarios have been set up and in the following been run through and analyzed by the help of a global transport model, simulating the world fleet development due to industry stakeholders' and ship operators' behavior, technological developments and regulations. Resulting, the impact of each scenario with respect to fuel demand and the corresponding prices, technology costs, emissions and even ship operations has been presented.

A similar approach has been utilized by Wärtsilä within their *Shipping Scenarios 2030*, which has been published in 2010 (Wärtsilä, 2010b). Therein, five descriptors have been defined, namely trade and economic growth, response to climate change and sustainability issues, geopolitical issues and global leadership, solutions to deal with scarcity issues and control of power. The respective manifestation combinations have been summed up in three narrative scenarios (*Rough Seas*, *Open Oceans* and *Yellow River*), each leading to distinct cause-and-effect chains and event timelines. Additionally to the study, an interactive website has been set up, introducing additional information as well as some basic ship concepts matching the respective scenarios (Wärtsilä, 2010a).

Although the above examples might give the opposite impression, scenario methods within the maritime industry must not inevitably be utilized by certain companies and afterwards be

2. Fundamentals of Scenario-based Ship Design

published in form of brochures or technical reports. In 2010 and 2013, the German industry association Verband Deutscher Maschinen- und Anlagenbau (VDMA) held two conferences on scenarios that targeted the future development of the marine equipment industry (Schlegel, 2011; Mutschler, 2013). Being open to attend for members of the VDMA only, the questions to be targeted and the therefore needed scenario input have been defined in a first meeting, while in a second meeting the resulting findings have been presented and discussed. As these conferences were aiming at general strategic developments of a whole business field, a narrative scenario modeling approach has been used.

Due to the fact that the setup, execution and analysis of scenario methods implies a huge effort (especially when it comes to comprehensive models) and furthermore requires contributions from many adjacent disciplines, their application within the academic field can be considered to be rare. Regarding the actual ship design and neglecting the risk-based design methodology often mixed up therewith, there are only a few approaches loosely related to scenario methods. Most of them deal with the design of ships under uncertainties and classify into the closely related category of “classic” robust design optimization (RDO).

An introduction to these classic RDO problems and how to deal with them can be found in Diez and Peri (2009). Therein, the general concept of formulating and solving RDO problems by the help of particle swarm algorithms is described. Furthermore, exemplary particle swarm optimizations (PSOs) of the main dimensions of a bulk carrier with respect to uncertain speed, round trip distance and port handling rate distributions are presented and compared to standard deterministic approaches. The same optimization example has been used in Diez and Peri (2010) for the introduction of another way of solving RDO problems, namely a two-stage stochastic programming formulation, which can be understood as a nested minimization approach. The particle swarm optimization concept has also been adopted in Diez et al. (2013) for a multi-objective optimization regarding the resistance reduction and operability increase of a catamaran under a wide range of Froude numbers (from 0.115 to 0.575) and variable sea states. Comprehensive literature re- and overviewing robust optimization methods can be found in Beyer and Sendhoff (2007) and Park et al. (2006).

An approach targeting at actually modeling future deployments has been presented in Erikstad et al. (2011). Focusing on non-cargo ships, the basic idea of this scenario based model consists in setting up possible future contract or market scenarios and evaluating a fixed number of possible design solutions with respect to their respective revenue. Thereby, the contract scenarios feature different requirements, durations, starting times and revenues in form of daily rates. The different vessel design alternatives - which in this context need to be understood as a simple cumulation of feasible design properties combinations - are indicated by their acquiring costs and their capability of matching the previously modeled contract scenarios. As these contracts and design alternatives are forming a network, the task of finding the design variant with the highest income can be done using a Binary Integer Programming (BIP) model. It has to be noted that this approach goes a bit further than standard design approaches, as the result does not only include a design proposal, but additionally a list of contracts to be concluded. This approach is even more interesting, as the contract scenarios do not need to reflect the current situation, but can be randomly generated from a specific distribution of contract properties, which allows the consideration of uncertainties. Furthermore, the model can be expanded to be used with fleets instead of single vessels.

It has to be noted that - stepping away from design issues of single ships - fleet management in general is a field, where scenario methods can effectively be applied in order to support decision making of any kind. An example for this can be found in Meng and Wang (2011),

2. Fundamentals of Scenario-based Ship Design

where the respective advantages of buying or chartering ships when facing an uncertain future have been investigated.

The usage of probability density functions (PDFs) of speed and / or draught values as the basis for ship hull form optimizations has been applied by Temple and Collette (2012). Within their study, two vessels (the DTMB-5145 naval combatant vessel and the KRISO Container Ship (KCS)) have been optimized with respect to their lifetime resistance as well as their initial building costs, with the latter being derived from the vessel's build complexity, namely the backset and curvature of the hull plating. The lifetime resistance results from the integral over the speed dependent total resistance (which has been estimated by the help of the thin ship theory) multiplied by the PDF of the respective vessel's speeds. The speed values included within these PDFs have been deduced from the KCS' design speed (in form of a unimodal distribution) and the endurance and mission speed (in form of a bimodal distribution) of the DTMB-5145, respectively. Due to the fact that reducing the building costs and the lifetime resistance often are opposing tasks, a multi-objective genetic algorithm (MOGA) has been applied in order to solve the problem. Resulting, a Pareto front of suitable design variants could be developed.

Joint probability density functions have been used in Kramer et al. (2010) in order to optimize a waterjet propulsor for a surface effect ship. Even though this might not be a typical basic design task, the approach presented there is of interest, because it introduces the combination of the vessel's lifetime speed distribution with a distribution of its resistance variation associated with different operating conditions. In particular, model test-based speed-resistance-functions have been supplied for operation in different water depths and sea states. The resulting PDF has been combined with the speed distribution, forming a probabilistic design space, which as a whole serves as the basis for the overall efficiency evaluation of the waterjet variants.

Another approach considering PDFs of operating conditions can be found in Eljardt (2010). Even though this dissertation likewise rather focuses on the vessel's propulsion than its hull form, it evolves the concept of applying statistical distributions in order to serve as input for any sort of optimization. Additional to the distribution of the ship's speed, its trim distribution as well as environmental data such as sea state and wind conditions have been considered. All of these data have been determined on the basis of statistical analyses or prognoses. Following, a Monte-Carlo sampling algorithm has been set up on the basis of these distributions in order to create a set of operating conditions, each of them consisting of a combination of particular parameter values. These operating conditions have in the following been used as part of the objective function in order to minimize the vessel's overall required power. With the idea of coupling stochastic simulation procedures with an optimization onto more than one operating condition, this approach comes comparably close to the one presented in this thesis, even though it does not include the actual scenario development and lacks the consideration of joint distributions (whose importance will be explained in Section 3.6). In Table 2.1 a comparison of those approaches that actually lead to a specific (ship) design and the targeted scenario-based design approach is given.

There are further publications claiming to optimize ship hull forms on the basis of scenario methods (for example Ayob et al. (2011)), but in most cases this merely covers the inclusion of more than one operating condition (with these conditions often being reduced to a single speed value only) within the objective function. In other cases, the term scenario is used to indicate a specific phase within a vessel's life cycle, for example in Fischer et al. (2012). In Koutroukis et al. (2013), the scenario term is used for a set of assessment procedures that reflect varying requirements preferences. Usually, all of these publications have in common that there neither

Reference	Considered Parameters	Scenario Approach	Data Source	Development Uncertainties	Cost Model	Joint / Single Probabilities
DNV (2010)	Speed Draught Sea State	explorative qualitative quantitative short term snapshot	Forecast	no	no	unknown
Erikstad et al. (2011)	Contracts	explorative quantitative short term chain	Forecast	yes	yes	n.a.
Temple and Collette (2012)	Speed Draught	none	Past	no	yes	Single
Kramer et al. (2010)	Speed Resistance	none	Past	no	no	Joint
Eljardt (2010)	Speed Trim Sea State Wind	none	Past & Forecast	no	no	Single
Intended Approach	Speed Draught Sea State (expandable)	explorative quantitative short term chain	Past & Forecast	yes	yes	Joint

Table 2.1.: Comparison of design approaches. *Considered Parameters* refers to the parameters included within the device's objective function, while *Scenario Approach* indicates, whether - and if yes which - type of scenario-based approach for detecting these parameters has been used. *Data Source* points out, whether the needed input is based on past or forecasted data. *Development Uncertainties* and *Cost Model* indicate the consideration of uncertainties and the usage of any sort of cost model when evaluating a design. Finally, *Joint / Single Probabilities* refers to an approaches ability to deal with joint probabilities in case it features more than one parameter within its objective function.

exists an actual development of scenarios nor a consideration of any kind of uncertainties. As far as the author is aware of, the intended design approach of telling the vessel's lifetime story in advance in order to afterwards draw conclusions with respect to its properties has not been realized within the maritime business up to the present day.

2.4. Assessment of Ship Designs

As presented in the previous section, there exists a wide range of scenario-related approaches for finding an optimum design solution. Sharing the basic principle of determining the optimization's environment conditions by means of however implemented future modeling tools, all of them differ in the formulation of their optimization's objective function. Regarding the optimization of ship hull forms, this objective function and the question, how and on what basis to assess the different design alternatives is of great importance. Focusing on classic design approaches, the most common objectives (providing that specific basic requirements like payload or design speed are met) are on the one hand the reduction of such characteristic values like the vessel's wave, frictional or total resistance or its propulsion power or - on the other hand - the improvement of properties being harder to determine like maneuverability or sea-keeping characteristics. As well as for the design methodology itself, the world economic crisis had a remarkable impact on the assessment of ship designs, shifting the focus from the above mentioned classic targets to a more all-embracing, cost-based view. This is reflected by the introduction of life cycle assessment (LCA) or life cycle costing (LCC) methods in conjunction with economic key performance indicators (KPIs) in order to measure the benefit of a certain ship design. Additionally, external environmental issues are becoming increasingly important, even though this might - aside from its consideration due to legislation - not be reflected within ship hull form optimization targets, yet.

2.4.1. Life Cycle Assessment

The consideration of life cycle methods has made its way into many areas of the ship design process, such as risk based design or risk management (Vassallos, 2012), holistic design (Papanikolaou, 2010) and hull design. As the latter two are in the main scope of this thesis, a few literature examples will be given in the following.

An overview on the current status of life cycle assessments within the ship design context has been done in Aspen et al. (2012). This publication monitors existing software implementations and furthermore explores the possibilities of the LCA approach for decision-making within the design process and identifies still existing challenges. The authors conclude that - even though the life cycle assessment is an already widely used tool within other industries - the maritime industry faces methodological difficulties, mainly regarding the definition of the functional unit and the system boundaries as well as the collection of data. Another overview rather focusing onto the methodology of life cycle assessments and its application within the maritime business can be found in GAUSS (2011). Therein, a detailed distinction between the different types of LCAs accompanied by many application examples as well as proposals for future usage is given.

Within Fischer et al. (2012), a life cycle performance assessment approach has been presented that tries to cope with these difficulties and targets the assessment of any kind of technical solution on the basis of a wide range of economic, social and safety KPIs. Therefore, a data model has been set up, which allows the user to implement the technical component to be observed including its attributes regarding performance, cost, revenue and safety issues. Additionally,

scenarios come into usage, but - as already mentioned earlier - only in terms of specific life cycle phases the vessel runs through, such as construction, operation, maintenance and dismantling. These scenarios are accompanied by a set of global values, describing fuel oil price development, discount and currency exchange rates alongside with technical and other variables. Based on this input, the tool calculates the life cycle KPIs

- net present value (NPV) and risk-adjusted NPV,
- global warming, acidification and eutrophication potential,
- airborne and underwater noise and
- social welfare index.

It has to be noted that according to the authors there is no possibility of including development uncertainties. In case robust assessments need to be done, the program has to be run through many times by constantly varying the included variables and functions.

When using life cycle methods, the evaluation of the specific design variants is an important aspect. Usually, a set of performance indicators is defined in order to perform the assessment. As a few of them have already been mentioned in the above examples, the most common KPIs will be introduced within the next subsections.

2.4.2. Economic Key Performance Indicators

Despite technical performance characteristics, economic KPIs are still the most important ones when it comes to the interests of shipping companies and funding or investment banks. The most common KPI in this context is the NPV. The net present value represents the current value of all costs and benefits (equaling all cash flows) within a designated period of time (regarding maritime transport in most cases the service or chartering time of a vessel). It is therefore widely used for comparing possible profits resulting from different investment alternatives or as a tool for supporting investment decision making. The present value of any cash flow can be discounted to the present day via

$$PV = \frac{CF_t}{(1 + i_r)^t}, \quad (2.2)$$

with CF_t being the particular cash flow at a future time t (in hours, years or in general any period) and i_r representing the interest rate, which needs to be adapted accordingly. Considering a period of time with a set of various costs and benefits, the NPV sums up to

$$NPV = \sum_{t=0}^{t_{end}} \frac{NCF_t}{(1 + i_r)^t}, \quad (2.3)$$

with NCF_t being the net cash flow, consisting of the difference of cash inflow and cash outflow at each point in time t . A higher NPV therefore indicates a better investment than a lower one. As the NPV does not consider limited investment resources, Benford (1980) proposes derivatives, such as a net present value index (NPVI), which indicates the NPV in relation to needed investments of any kind (capital, man-hours, et cetera).

Within the maritime transport business, the required freight rate (RFR) is of special relevance. In general, it indicates the minimum benefits per unit load (mostly TEUs) that need

2. Fundamentals of Scenario-based Ship Design

to be generated in order to cover a vessel's expenses, meaning that the overall NPV becomes zero. As done above, all expenses have to be interest adjusted. Therefore, the required freight rate for regaining a certain investment can be calculated via

$$RFR = \frac{C_o \cdot CRF}{TP}, \quad (2.4)$$

with C_o being a cash outflow (investment), while CRF represents the capital recovery factor. TP indicates the total transport performance of a certain period in $TEU \cdot nm$ in case of a container vessel. The capital recovery factor calculates as

$$CRF = \frac{i_r \cdot (1 + i_r)^t}{(1 + i_r)^t - 1}. \quad (2.5)$$

In compliance with Equation 2.3, the RFR covering all present and future investments yields to

$$RFR = \frac{\sum_{t=0}^{t_{end}} C_{o,t} \cdot CRF_t}{TP}. \quad (2.6)$$

In most maritime business cases, the RFR is the performance indicator finally to be minimized. One reason for this can be found in the fact that this KPI, in contrast to the NPV and the NPVI, does not depend on often hardly predictable future incomes.

An alternative performance indicator especially used when targeting onto a vessel's resistance or powering minimization exists in the ship merit factor (SMF). This measurement is especially useful as it specifically focuses on the transport costs related to one unit of - however defined - cargo, instead of keeping track of future and therefore uncertain revenues. In its basic form, the ship merit factor has been introduced by Cheng (1968) as

$$SMF = k \cdot \frac{P_B}{C_o} \cdot \frac{W_P}{v_D}, \quad (2.7)$$

with P_B being the main engine's delivered power and C_o the cash outflow of one year (including capital costs), W_P representing the designed payload in tons and v_D the design speed in knots. k represents a service constant, consisting of a range of factors considering the loading capacity utilization, an averaged operating speed, the vessel utilization in terms of service hours and a port time / sea time ratio.

2.4.3. Social and Environmental Performance Indicators

In addition to the traditional, mainly economic performance indicators, other possibilities of evaluating a ship design exist and will briefly be presented in the following. In some of the previously introduced approaches, e.g. Fischer et al. (2012), the environmental impact of design solutions has been included into the assessment procedure, which has become more and more popular within recent years, mostly due to a rising awareness of the induced costs, not only for ship operators due to environmental taxes or disposal costs but also for the public. Even though a precise determination of these costs is still a challenging task, there do exist studies and regulations targeting this challenge or at least providing tools for reducing the environmental footprint. Some of these attempts will briefly be presented in the following.

The best known environmental performance indicator within the maritime industry exists in the Energy Efficiency Design Index (EEDI), which has been developed by the IMO as

2. Fundamentals of Scenario-based Ship Design

an amendment to the International Convention for the Prevention of Pollution from Ships (MARPOL) Annex VI regulations in order to increase the energy efficiency of vessels and to reduce their overall emissions of greenhouse gases (IMO, 2012a,b). Adopted in 2012, the EEDI is required to be determined for every cargo vessel greater than 400 *gt* and being built as of January 2013. Its basic principle is to correlate a vessel's CO₂ emissions with its transport work measured in ton-miles. While the original formula for the calculation of the EEDI is of a higher complexity and consists of various terms and factors, a simplified formula that sufficiently illustrates the working principle is given in ICCT (2011) as

$$EEDI = \frac{P \cdot SFC \cdot C_{f,j}}{DWT \cdot v_{ref}}, \quad (2.8)$$

where P indicates 75% of the installed shaft power, SFC the engine's specific fuel consumption and $C_{f,j}$ the fuel type-specific CO₂ emission rate. The transport work is defined by the product of the vessel's deadweight tonnage DWT (for container ships only 75% DWT) and a reference speed v_{ref} , which equals the design speed at maximum design load condition and P . Calculated that way, the so-called *Attained EEDI* will be checked against a reference line (called *Required EEDI*), which is based on a regression of already existing vessels being built between 1999 and 2009. As this reference line will be lowered within fixed periods, each ship operator is urged to prepare a Ship Energy Efficiency Management Plan (SEEMP) for all of his vessels that provides technologies for efficiency performance monitoring and supports the implementation of new performance optimizing technologies. Supporting, the IMO developed guidelines for the voluntary use of the Energy Efficiency Operational Indicator (EEOI), which can be thought of as closely related to the EEDI, but focusing on environmental friendly operation of ships and fleets. As the EEOI serves the goal of monitoring and controlling a vessel's greenhouse gas emissions during operation, its basic structure equals the EEDI with the difference of using specific voyage data instead of design parameters and correction factors. Its value can be determined for any voyage, trade or time period via

$$EEOI = \frac{\sum_j FC_j \cdot C_{f,j}}{m_{cargo} \cdot D}, \quad (2.9)$$

where j indicates the fuel type, FC_j the mass of the consumed fuel j , $C_{f,j}$ a fuel mass to CO₂ conversion factor for fuel j , m_{cargo} the cargo carried (usually in tons, *TEU* or number of passengers in case of passenger vessels) and D the traveled distance in *nm* (IMO, 2009). Using the EEOI in conjunction with the SEEMP, ship operators shall be able to keep track of the gainings of each newly installed performance optimizing device or any change in operation in order to eventually reduce the environmental footprints of their fleets. Even though there exists a strong debate on the general structure, the implementation and the actual effect of the EEDI and its accompanying guidelines, it has become the only non-economic KPI regularly being considered within the design or re-design of cargo vessels.

While this index only focuses on the operational phase and especially on CO₂ (by ignoring further harmful emissions), other approaches targeting the evaluation of social and / or environmental footprints have been developed, even though none of them can be considered to have a comparable impact onto the maritime industry as the EEDI.

In Singh et al. (2009), a comprehensive overview on general sustainability assessment methods is given. This overview does, amongst others, not only cover innovation and technology,

2. Fundamentals of Scenario-based Ship Design

development and economy-based indices but also sustainability indices for assessing cities, policies and industries. The - regarding the design of ships - most interesting category of product based sustainability indices only contains two entries, the first one being a life cycle index comprising of (not further specified) environmental, cost, technology and socio-political factors. The second one refers to the automotive industry, namely the *Ford of Europe's Product Sustainability Index*. This index is focusing on eight environmental, social and economic categories like global warming potential, safety and life cycle cost of ownership in order to assess any vehicle's attributes.

Especially focusing on shipping transport, in Fet and Sjørgård (1999) a state of the art report in conjunction with a workshop on the needs and requirements for developing a standard life cycle assessment tool has been published. Therein, the authors urge the inclusion of all stages of a vessel's life, the consideration of additional toxic substances as well as the development of alternative impact categories in order to widen the environmental performance monitoring to a truly holistic life cycle assessment. Supporting this goal, a list of tasks targeting a code of practice for life cycle evaluations of transport modes is provided.

A general comparison of all transport modes on the basis of their respective environmental performance has been presented in Fet et al. (2001). This study is specifically interesting due to the fact that the authors suggest actual environmental performance indicators. Accordingly, the categories

- climate change (CO₂, N₂O and CH₄),
- acidification (SO₂, NO_x and NH₃),
- toxic contamination (Pb and Tributyltin (TBT)),
- local air pollution (dust),
- photo oxidant formation (non methane volatile organic compounds (NMVOC)),
- noise (measuring the area having a noise exposure ≥ 55 dBA),
- eutrophication (NH₃ and NO_x),
- total energy consumption and
- land use in m^2

have been defined. Following, the corresponding values of each transport mode have been scaled in relation to the transport capacity for the purpose of comparison. Even though an additional characterization factor for each of the impact categories has been provided in order to allow a grading of the respective compounds, a conversion of the resulting overall environmental performance into monetary values in terms of operator or public costs could not be found. The same applies to the sustainable development index presented in Krajnc and Glavič (2005), where also environmental, economic and social indicators (of companies) have been associated into an overall performance indicator.

Despite the already implemented EEDI, most of these approaches (except for the last two) suffer from the problem of being rather unspecific in its definition and / or providing non-absolute values. In case enough data is available (or can be deduced from other vessel characteristics), at least the environmental performance as presented in Fet et al. (2001) and Fischer et al. (2012) could be evaluated within a hull form optimization process.

3. Scenario Development

The overall goal of the scenario methods presented in this thesis is to develop a distribution of the most probably upcoming operation conditions, a to-be-designed vessel could stay in during its scheduled operating time. This data - or parts of it - should in the following be used in order to set up a basis for the optimization of a parametrically modeled ship hull form in order to find the most efficient variant regarding the vessel's lifetime energy consumption or fuel costs.

3.1. Basic Considerations

Considering the initial idea of catching a glimpse onto possible future developments and following the explanations given in Section 2.2.1, the chosen scenario method should have an explorative character. Regarding the type of information used therein, a quantitative approach has been chosen. This decision results from the type of included descriptors, as all of them need to take specific values, while their development and interrelations should be displayed using mathematical functions. The only argument against the quantitative approach exists in its lacking ability for addressing large time horizons. But in fact, although ships usually operate for up to 25 years or even longer, most shipping companies do not target time horizons of more than three years, especially in times of a crisis. As it has furthermore been mentioned, not only the final end state but the complete path of the scenario development should be used in order to determine the most probable operating conditions of the vessel. Resulting, the explorative, quantitative and - following the distinctions of Kossow and Gaßner (2008) and van Notten et al. (2003) - short-term, chain scenario approach has been considered suiting the needs.

The chosen scenario approach differs from any of the methods presented in Section 2.3 as it completely bases on mathematically formulated algorithms. No narrative elements will be included, as for example done in DNV (2010). The fundamental idea for this decision is, that omitting a few or even a single possible scenario development by preselecting specific development paths as done within the *Quantum* project should be avoided, even though the modeling as well as the simulation effort might consequently increase. In the attempt of trying to not exclusively focus on individual extreme or other selectively chosen but all possible scenarios, the attempted approach tries to break new grounds.

Furthermore, it classifies between the classic design and the holistic approach as presented in Papanikolaou (2010) by focusing on the expenditure side only and by not considering all phases of a complete life cycle (concept and detailed design, construction, operation, scrapping) but at least the one being most important with respect to operating costs.

3.1.1. Input

In order to meet the requirements discussed in Section 1.1, a transportation task consisting of a description of the trade and the amount of goods to be transported accompanied by some basic constraints and decisions, which will be described in more detail in Section 3.2, have to be

3. Scenario Development

defined and used as input to the scenario development. Furthermore, input regarding possible future developments affecting the operating conditions of the vessel has to be given.

3.1.2. Scenario Descriptors

The decision on which descriptors to be included within the scenario development has been made due to the following considerations:

In a first step, the descriptors to be monitored and to actually form the operating conditions onto which the hull form will later be optimized onto have been chosen. Essential for a contemporary optimization is the consideration of the parameters speed and draught, which therefore have to be included as descriptors. Furthermore, two descriptors displaying sea state conditions, namely the significant wave height and the wave period will be included. The decision towards these two parameters instead of for example complete wave spectra has been made due to the fact that on the one hand enough data (respectively scatter tables) are available and these data on the other hand can easily be fed to the later used resistance calculation tools as recognized input. The decision on how to specifically apply these data to the methods used within the optimization of the vessel's hull form has been left to the user.

In a second step, it has been decided that the descriptors draught and speed should mainly be modified due to the manifestations of the descriptors transport demand (TD) and fuel oil price (FOP). This decision is based on the outcome of a survey being done amongst the participants of the fifth European Conference on Production Technologies in Shipbuilding (ECPTS) in 2012. Within this survey, amongst others, the question for the most important driving factors for the operation of cargo vessels in relation to their speed and loading conditions has been asked. Despite the more social or political and also harder representable factors like financing issues, port infrastructure, environmental policy development, piracy and local conflicts, in almost every list the factors fuel oil price and / or worldwide or local transport demand ranked among the top five. Another high-rated factor existed in the (required) freight rates, but as those are directly related to both, the fuel oil price and the transport demand on the expenditure side, while the revenue side has been agreed to not be considered within the scenario approach, the freight rate has been decided to be representable by the two mentioned descriptors and therefore to be negligible. Resulting, the two most important questions to be answered regarding the vessel's speed and draught manifestations are on the one hand how many goods have to be transported and on the other hand which price needs to be paid to do so.

Regarding the second question, the total costs - or in this case, where the overall goal is assumed to exist in optimizing the expenditures, the variable costs - can easily be broken down onto the bunker costs, as those are the only ones being both variable and by means of percentage big enough to have a recognizable impact. This has for example been shown in World Shipping Council (2008) as well as within work package 1.3 of the related research project *PerSee* (Bronsart et al., 2016), which means that the modeling of the fuel oil prices becomes important.

In literature, many different influence factors onto the development of fuel oil prices can be found, although in most cases their actual impact can not sufficiently be determined. As an example, in Kilian (2014) a comprehensive survey of causes and consequences of oil price shocks has been published. The influencing factors - regardless the strength and effective direction of their actual impact - listed therein are the flow supply, correspondingly the flow demand, expectations of future oil shortfalls and financial speculation. Furthermore, the role of the OPEC is mentioned there, even though their significance to the oil price development is

3. Scenario Development

doubted. The *Leibniz Institute for Economic Research* identified the expanding global economy, political instabilities within relevant oil-producing areas and natural disasters as the main reasons for rising oil prices (Schirwitz and Vogt, 2005). When focusing on local instead of global price developments, additionally the currency and the inflation rate needs to be taken into consideration.

Due to the fact that many of these influencing factors can be transformed or broken down into each other and by neglecting political and social developments as well as environmental issues, which shall not directly be modeled within the attempted explorative quantitative scenario approach, the most common influences regarding the fuel oil price development can be determined as

- gross domestic product or the correlating oil demand,
- Euro / Dollar currency rate,
- oil delivery rate,
- oil reserves and
- degree of extraction technology.

In Wagner and Bronsart (2012), various methods have been used in order to sort these influence factors according to their respective impact, to analyze their interdependencies and to filter the most relevant ones with respect to their importance regarding the oil price modeling. When analyzing those factors by using the influence matrix in conjunction with a system grid as described in Mißler-Behr (1993) and Reibnitz (1991), the triangulation method developed by Wessels (1981) and Hauke (1992) and MIC-MAC analysis presented for example in Arcade (1999) and Godet (1987), a complex mesh of dependencies and interdependencies arises, which points to a high modeling and especially analyzing effort. As it should not be focused on the modeling of economic relations but on the impact of single economic factors (in this case the fuel oil price) within this thesis, this complex modeling of many interrelated descriptor development functions has been skipped on behalf of supplying an easy method, which is able to understand and make use of any single development function onto which a users' knowledge can easily be applied.

Besides the question of how to model fuel oil prices in general, the question of which specific prices to be modeled needs to be answered. It has been decided that two different fuel oil types should be considered within the scenario development: a standard type accompanied by a second fuel type for special purposes. Therefore, the basic assumption of the vessel usually burning HFO has been made. Only in case it operates in special emission control areas or other areas of strict environmental regulations like inland waterways or ports, an alternative fuel will be used. As this alternative fuel - regardless of being MGO, LNG or any other - will be spent at different, presumably higher costs, a price difference between the alternative fuel and the standard HFO needs to be defined. When comparing the development of different bunker prices, it can be seen that they run almost parallel with only slight deviations. As for example the MGO price is unlikely to increase while the price for HFO is decreasing, an approach of specifying a possibly time-dependent price difference instead of an independent development function for alternative fuels has been favored. This reflects a modeling approach which has also been used for simulating the MGO and LNG price development within the previously mentioned *Shipping 2020* study done in DNV (2012). Thereby, the focus on only two different

3. Scenario Development

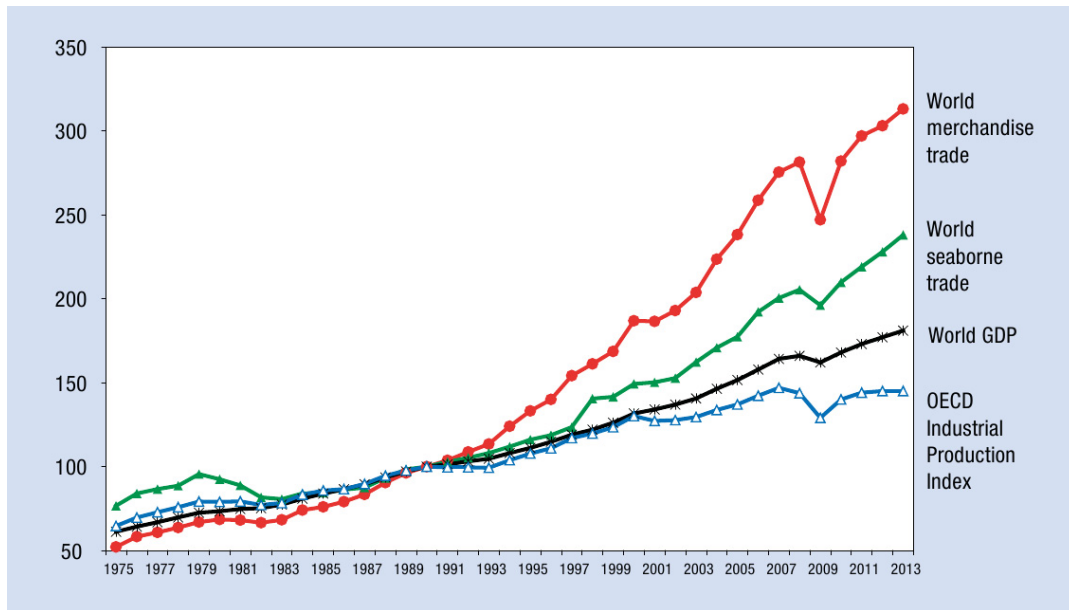


Figure 3.1.: Transport demand, OECD Industrial Production Index and gross domestic product (1973 to 2013, 1990 = 100), (UNCTAD Secretariat, 2013)

fuel types is considered to be sufficient, resulting from the fact that in most cases vessels are equipped with only one emission reducing technology at once. In case of a scheduled system change - for example from HFO / MGO to HFO / LNG dual fuel usage - the correspondingly changing costs can easily be represented by specifying a jump within the development of the price difference.

Regarding the question about the transport demand and looking at the data of global seaborne trade for example given in UNCTAD Secretariat (2013) and presented in Figure 3.1, a high correlation to the development of the gross domestic product can be identified. This appears to be legit, as approximately 95% of the world trade is being covered using ships, wherefore changes in the GDP directly and with similar impact affect the transport demand. When only focusing onto containerized trade, the United Nations Conference On Trade And Development (UNCTAD) states in its 2013 *Review of Maritime Transport* that the transport demand development has been following the performance of the GDP with a multiplier effect usually ranging between three and four, (UNCTAD Secretariat, 2013). Due to the fact that changes in the GDP apply to the transport demand at it's face value and it additionally and in analogy to the fuel oil prices appears to be complicated and also out of scope to identify the parameters influencing the GDP, it has been decided to directly model the transport demand via a respective development function.

For this reason it has also been decided to model the transport demand and the fuel oil prices independently from each other. This is based on the assumption that if the user would identify a relationship between these two descriptors, this could directly be displayed within the respective development functions, e.g. by giving them the same average increase or a larger jump at the the same point in time. This would in combination with the Monte-Carlo approach introduced in Section 3.5 in most cases (but depending on the likeliness of possibly occurring fuel oil price and transport demand crisis, see Sections 3.3.2 and 3.3.3) lead to the intended dependent development.

3. Scenario Development

Transport Demand [%]	Fuel Oil Price [\$/t]	$v_{SlowSteaming}$ [kn]
≤ -2.0	≥ 450.0	14.0
	≥ 500.0	12.0
	≥ 550.0	10.0
≤ 0.0	≥ 450.0	15.0
	≥ 500.0	13.0
	≥ 550.0	11.0
≤ 2.0	≥ 450.0	17.0
	≥ 500.0	16.0
	≥ 550.0	15.0

Table 3.1.: Exemplary slow steaming decision table

It has to be noted that in order to simulate the respective manifestations of these two descriptors, further descriptors are needed that will be introduced in Section 3.3.

Additionally to the reaction of the draught and speed manifestations to changes in the fuel oil price and the transport demand, further descriptors influencing these two will be considered within the scenario development, most of them due to discussions with shipping companies. Regarding descriptors influencing the vessel's draught, only local draught restrictions as they can for example be found in ports or pilotage areas are taken into consideration. As despite loading and local restrictions no other draught changes will be considered, this is especially important as a draught restriction in a forthcoming route segment also limits the maximum draught along the complete route to this specific segment. The possibility of loading and dumping of ballast water during open sea passages has been left out, as ballasting - according to a ship owner's statement - does not follow a specific schedule and its results are not predictable. The lack of this possibility can be counteracted by specifying an overall minimum draught within the scenario development the vessel can not fall below in any case. Doing this, the appearance of too low draughts can be bypassed while simulating a sort of ballasting to be done in ports.

Regarding descriptors with an impact on the vessel's speed, more parameters are to be considered. At first, there are the same local restrictions to be taken into consideration as for the draught. With respect to their specific impact, there only exists one single difference as the local speed restrictions do not influence the speed of previous route segments.

One major function to be included is the possibility to operate the vessel in slow steaming mode. As slow steaming should only be applied in case of a crisis, it can not be modeled statically like it is for example possible for the trade. It should rather be a decision being dependent on one or more descriptors within the scenario model, with the transport demand on the one and the fuel oil price on the other hand being the most obvious ones. It has furthermore being pointed out by the shipping company that there neither exists *the* decision for slow steaming nor a specific slow steaming speed that should be applied to a vessel. Instead, the decision for operating with reduced speed can change between different trades while the speeds traveled with are allowed to vary within specific boundaries. Therefore, the decision which speed to apply should in the best case be made on the basis of a matrice like the one exemplary presented in Table 3.1. But as it turned out that most ship owners and operators are not able to specify a table with this degree of accuracy, it has been decided to only use a fuel oil price-based slow steaming decision within the scenario approach of this thesis.

3. Scenario Development

Another descriptor mentioned by the ship owner being of high importance exists in the weather conditions the vessel operates in. The scenario development should offer the possibility to reduce the vessel's speed in case it meets rough weather conditions. The main parameter to be observed should thereby be the wave height, which is easier and more accurately to observe than wave periods or other related criteria. As it has already been mentioned that weather conditions will be included anyway, the decision to reduce the ship's speed can be made on the basis of those calculations by using a matrix equivalent to the one utilized for the slow steaming decision.

An important boundary condition to be considered exists in the need to meet the scheduled time slots in ports. Especially in times of a prospering world trade and therefore high port utilization quotas, missing one's time slot can lead to waiting times ranging from a few hours to even days. Within this time, the vessel remains purposeless in a state of only creating costs while not generating any income, which is a state a ship owner usually tries to avoid under all circumstances. This results in the need to include descriptors taking care of the time to make up in order to reach the next destination in time.

The last descriptors to be included within the scenario development exist in the need for maintenance. It should be possible to specify a certain maintenance period after which the vessels has go into dry dock for a specific period of time. Those descriptors do neither influence the vessel's speed nor its draught, but they are of importance as it comes to bunker costs and are furthermore essential when aiming at modeling a realistic ship life.

3.1.3. Utilization of Data

The scenario method will use all given input to run through a specific number of life cycles creating randomly varying vessel "lifes", intendedly in the end covering all future developments of the specified descriptors and their respective possible combinations. All operating conditions appearing within these runs will be clustered according to user-given constraints and then summed up by using specific weightings. As the following hull form optimization shall be done with respect to the fuel oil costs, those weightings should not only be based on the "classic" parameter *time spend in a specific operating condition* but should also consider an economic KPI, namely the NPV of the costs to be spent at the specific operating condition.

Based on the resulting distribution of all of these operating conditions, the most relevant ones (those having the highest frequency of occurrence or NPV-adjusted weightings) will be selected in order to form the basis for the following optimization, which is intended to follow a standard hull form optimization schema.

The resulting general schema of the intended scenario approach has primarily been described in Wagner and Bronsart (2011) and is illustrated in Figure 3.2.

3.2. Scenario Development Methodology

The actual scenario development methodology will be introduced within this section in more detail by evolving the *Scenario Development*-blackbox of Figure 3.2 into more sophisticated process descriptions with constantly decreasing levels of abstraction.

The first abstraction decrease consists in specifying the in- and output of the scenario development. As already mentioned in the previous section, input regarding the scenario development specifications, trade description and weather conditions has to be handed over to the method. While the scenario development specifications consist of a simple list of distinct values and

3. Scenario Development

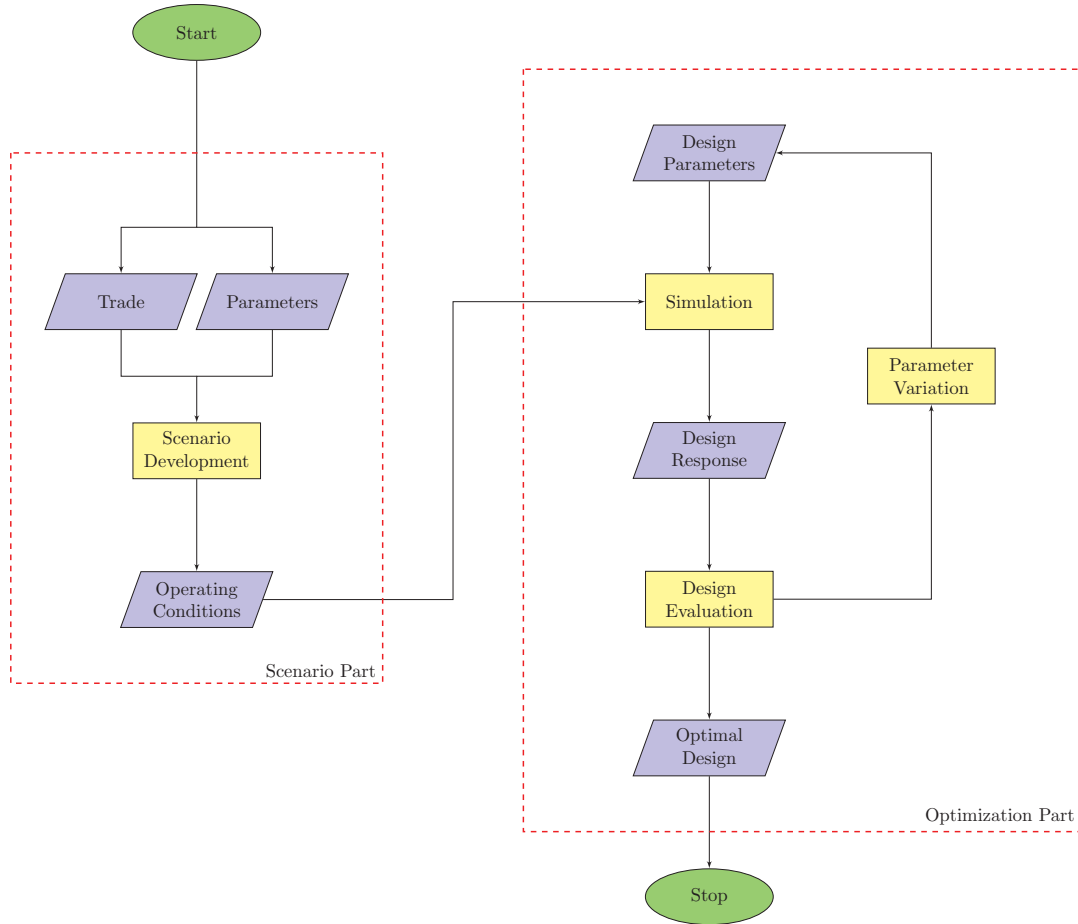


Figure 3.2.: General schema of the scenario-based optimization approach

functions being described in the following sections, the trade description and the weather conditions have to be given in form of arrays. A more detailed description of the latter two will be given in the sections 3.3.1 and 3.3.4. The output of the method will on the one hand be a five-dimensional array including all calculated operating conditions and on the other hand a list including a user-specified number of objective operating conditions (OOCs) to be used as the basis for the optimization process, both clustered according to predefined user specifications. Furthermore, a log file for monitoring and analyzing purposes will be generated.

Focusing on the scenario development process, it has to be noted that not only one but many different vessel lives will be simulated in order to cover as many future developments as possible. This is reflected in the MC segment of Figure 3.3. While the details on how this is handled are explained in Section 3.5, it should for now be sufficient to mention that the Monte-Carlo algorithm constantly repeats the scenario development process using randomly changing surrounding conditions until a certain abort criterion has been reached. When this is done, the objective operating conditions will be derived as presented in Section 3.6 from the aggregated data generated by all MC cycles.

The simulation of each single vessel life is done following the schema given in Figure 3.4. At the begin of each MC cycle, the development of the surrounding descriptors *fuel oil price* and *transport demand* is calculated. In contrast to the rest of the scenario development, this is

3. Scenario Development

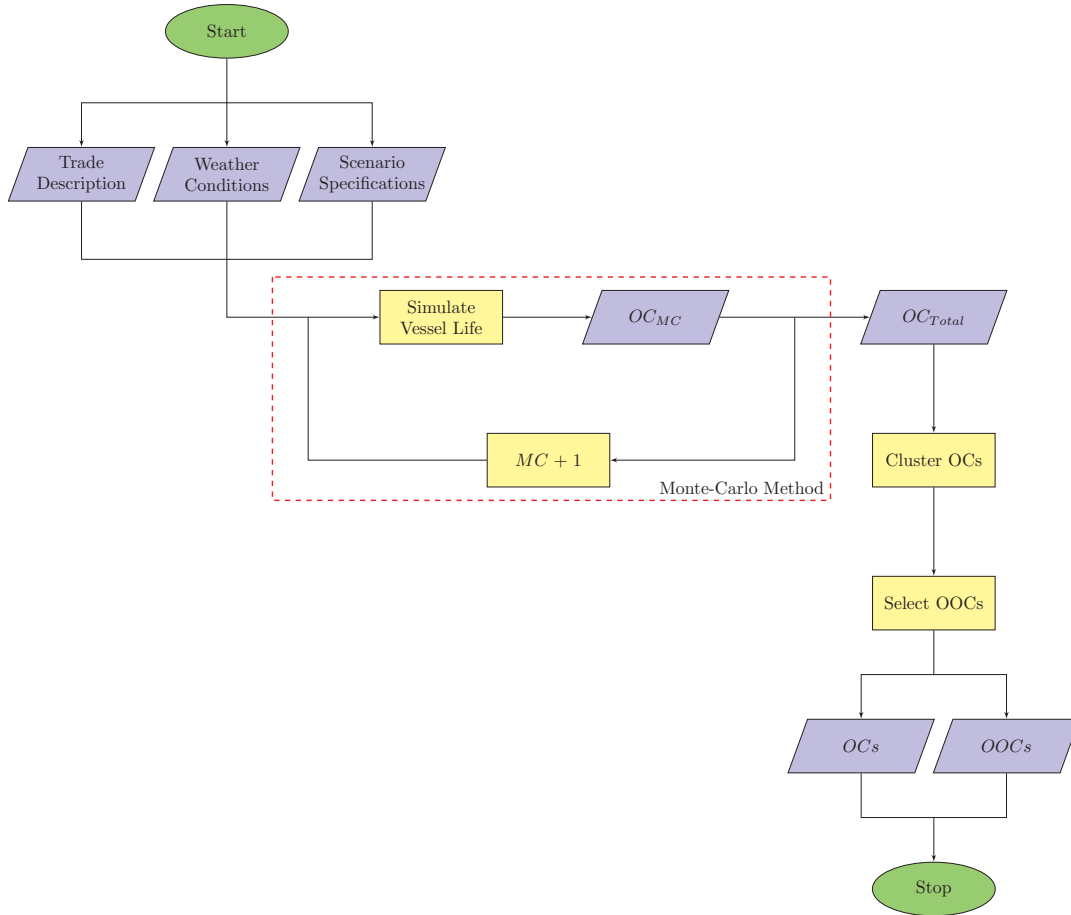


Figure 3.3.: Scenario development process

done for the complete operating time at once. Afterwards, the vessel starts operating onto its designated route until the specified time horizon t_{max} has been reached and the current route segment has completely been passed through¹. The vessel's specific operating and surrounding conditions at each route segment i are determined in form of the following calculations:

Sea State: simulates the properties of the current sea state (wave period T_1 and significant wave height $H_{1/3}$) of the respective route segment, see Section 3.4.2.

Speed: determines the vessel's speed by taking into consideration the initially intended service speed taken from the trade descriptions as well as possible speed reductions due to an owner's decision for slow steaming or challenging weather conditions and increasing speeds caused by the need to keep the schedule. Furthermore, local boundary conditions, such as minimum and maximum speeds for example in ports or pilotage passages are considered, see Section 3.4.3.

Draught: evaluates the vessel's draught on the basis of a specified initial draught or via the respective loading, see Section 3.4.8.

¹The definition of route segments will be given in Section 3.3.1.

3. Scenario Development

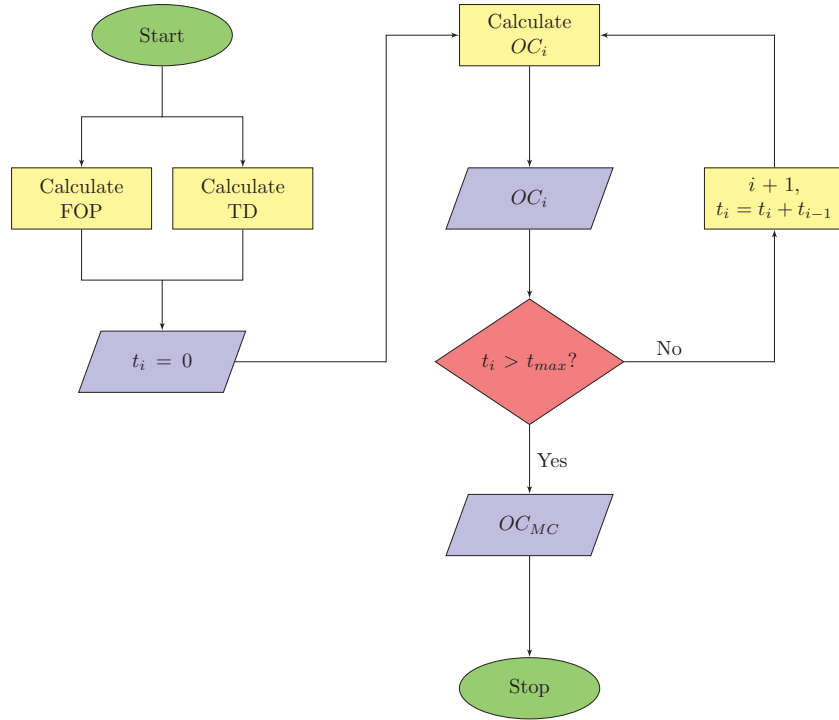


Figure 3.4.: Scenario development within each Monte-Carlo cycle

Time: calculates the time the vessel spends within a route segment while having constant operating conditions. Additionally, port lay times as well as times of dry-docking are considered, see Section 3.4.4.

Fuel Oil Price: determines the price, the ship owner has to pay for the fuel consumed by the vessel on the respective route segment, see Section 3.4.5.

Transport Demand: calculates the transport demand within each port, see Section 3.4.6.

Additionally to these descriptors that directly merge into the objective operating conditions, the following properties need to be checked within each route segment:

Dry Dock: the need for the vessel to go into dry dock for maintenance.

Speed Reduction: possible speed reductions due to harsh weather conditions.

Slow Steaming: the ship owner's decision for operating in slow steaming mode.

Within the following sections, the description of the trade, the modeling of the development functions for fuel oil prices and transport demand and the calculation of the vessel's specific conditions regarding speed, draught, time and sea state will be described in more detail. For convenience reasons this will be done without considering uncertainties, whose handling by the usage of Monte-Carlo methods will be illustrated in Section 3.5. The full particulars on how to develop the final objective operating conditions will eventually be presented in Section 3.6.

3. Scenario Development

Day	Type	Port
1	Port	Rotterdam, Netherlands
2 to 10	Transit	-
11	Port	New York, USA

Table 3.2.: Traditional route description Rotterdam - New York

Distance [nm]	Type	Port
0	Port	Rotterdam, Netherlands
5	Pilotage	-
3270	Transit	-
5	Pilotage	-
0	Port	New York, USA

Table 3.3.: Route description Rotterdam - New York as used within the scenario development

3.3. Modeling of Scenario Environment

3.3.1. Trade

The term *trade* marks the designated service operation of a certain vessel. In general linguistic usage, this includes the description which routes and ports the vessel operates on. Usually, a description of a trade consists of a list of ports accompanied by the respective time slots. In some cases the amount of goods to be transported can be included, too. Within the context of this work, the term *trade* covers not only a more detailed description of the vessel's ports of call but also information about the intended loading, timetable, sea areas and local boundary conditions.

While everything else within the scenario creation process is flexible and can change due to surrounding conditions (descriptors), the trade of the designated vessel is fixed as it serves as the backbone of the scenario development. During the scenario development process, the vessel will run through its specified trade until the designated time horizon has been reached, making it unnecessary to display the whole service period-covering movements of the vessel. In order to avoid gaps within a trade, it should be modeled as one to be repeated round-trip, with one port serving as starting and ending point.

In contrast to traditional trade descriptions, it has been decided to use a distance-based approach instead of a time-based one, meaning that different parts of a round-trip are indicated by nautical miles instead of days or hours. As an example, a transit from Rotterdam, Netherlands to New York, USA would be displayed in the traditional way as shown in Table 3.2. A description of the same transit using the schema of this work is given in Table 3.3. It has to be noted that both descriptions are only trimmed-down examples and can not be considered to be complete, they shall just indicate the different representation approaches.

Using the distance-based approach, a specific route has to be divided into route segments, each representing one part of the trade with constant characteristics. In the example given above, this would be the five segments *Port* (two times), *Pilotage* (two times) and *Transit*. As the assumption of constant characteristics over the whole distance of the respective segment may be correct for the port and the short pilotage segments, it should not apply to the comparatively

3. Scenario Development

long transit segment, where for example the weather conditions can not be considered to remain constant. Therefore, if one wants to include zones of different weather conditions on the route, he would have to subdivide the route segment into one or more sub-segments, each with constant weather conditions.

In comparison with a time-based schedule, the distance-based approach allows simulating time delays due to rough swell and a flexible speed management (both being explained in Sections 3.4.4 and 3.4.3) by the drawback of not being able to simulate a vessel bypassing zones with bad weather conditions or an unexpected change in the trade due to altered economic surrounding conditions. However, planned trade changes after for example three years can easily be modeled by calculating the time needed to operate on the initial trade, looping this trade within the trade description until three years have passed and finally adding and looping the second trade until the end of the intended service period has been reached. The only downside of this approach exists in the fact that - due to altering surrounding conditions - the operating time of a trade can change and therefore the point in time at which the trade changes may not be fixed.

As the trade description used within this work not only consists of the elements presented in the above example, a list of all information to be included is given in the following:

Distance: distance of the respective route segment (instantaneous, in contrast to traditional route descriptions, where mostly cumulative values for times and distances are given) in *nm*. Has to be zero in case of a port.

Sea Area ID: assignment ID for mapping the actual route segment to a specific sea state area. Has to be zero in ports.

Emission Control Area: indicates the share of emission control areas (ECAs) or other regions with special environmental laws applying.

Initial Speed: intended speed value of the vessel. Must not equal the resulting vessel speed at this segment as it can be modified during the scenario development process. Specification in *kn*.

Initial Draught: intended draught value of the vessel. Must not equal the resulting vessel draught at this segment as it can be modified during the scenario development process. Specification in *m*.

Lay Time: lay time spent for loading and unloading in ports. Only needed in route segments defined as ports and otherwise zero. Specification in *h*.

Port Type: specifies the type of a port. The following variants are possible:

- no port: inland waterways, pilotage area or open sea.
- main port, denoting one of the most important ports within the designated route, normally the start or end point of a trade. Only at ports of this type slow steaming decisions can be made.
- docking port, indicating that this is
 - the port with the closest distance to the preferred dockyard of the vessel or
 - one of many harbours, in who's near vicinity the vessel can be dry-docked.

3. Scenario Development

The specification of a docking port is important for simulating the vessel's operating time.

- refueling port, meaning that exclusively at these ports the ship will be refueled. This information has an influence on the economic evaluation of the generated operating conditions.
- both, main and docking port.
- both, main and refueling port.
- both, docking and refueling port.
- combination of all three, main, docking and refueling port.
- standard, neither main nor docking nor refueling port.

TEU (full): number of full TEUs the vessel will have loaded when leaving port.

TEU (empty): number of empty TEUs the vessel will have loaded when leaving port.

Minimum local Speed: position-dependent minimum speed in kn , for example due to canal passage restrictions. Has to be zero in case there is no restriction.

Maximum local Speed: position-dependent maximum speed in kn . Has to be zero in case there is no restriction.

Maximum local Draught: position-dependent maximum draught in m . This parameter can be set due to canal, river or harbour limitations. If specified as zero, there is no limitation.

It has to be noted that the necessity to specify values for the initial draught, TEU (full) and TEU (empty) depends on the decision, whether a loading-draught-function shall be used in order to calculate the vessel's draught (see Section 3.4.8 for details). However, as it is only possible to specify twenty foot equivalent units (TEUs), forty foot equivalent units (FEUs) have to be converted into TEUs. In case other loadings than standard TEUs need to be specified (for example when applying the scenario method onto a bulk carrier), this has to be done via the loading-draught-function being introduced in Section 3.4.8.

On the basis of these descriptions, the vessel's detailed "life", meaning the succession of its actual operating conditions along the trade segments, is simulated. In order to clarify this approach, a graphical schematic description of the previously mentioned example trade covering the descriptors speed, time and sea area (reflecting the corresponding weather conditions and for convenience reasons indicated by numbers, see Section 3.4.2) over the constantly increasing travel distance can be found in Figure 3.5. This schematic figure will be used to explain, how the scenario development works, and will therefore constantly be updated and amended throughout this chapter.

On the bottom of the picture the travel distance is given along the horizontal axis, indicating the total 3280 nm of the trade. The dashed vertical lines distinguish between different route segments with a distance > 0 , for example between the pilotage and the transit segment or between two transit segments heading through different sea areas. As a vessel is considered to not move within a port (possible movements due to in-port maneuvering or berth shifting can be reflected by including them within the pilotage segment), ports do not appear in this view but as a dashed line, usually between two pilotage segments. In Figure 3.5, the two outer lines represent the ports of Rotterdam and New York. Above the distance axis, the sea areas of the

3. Scenario Development

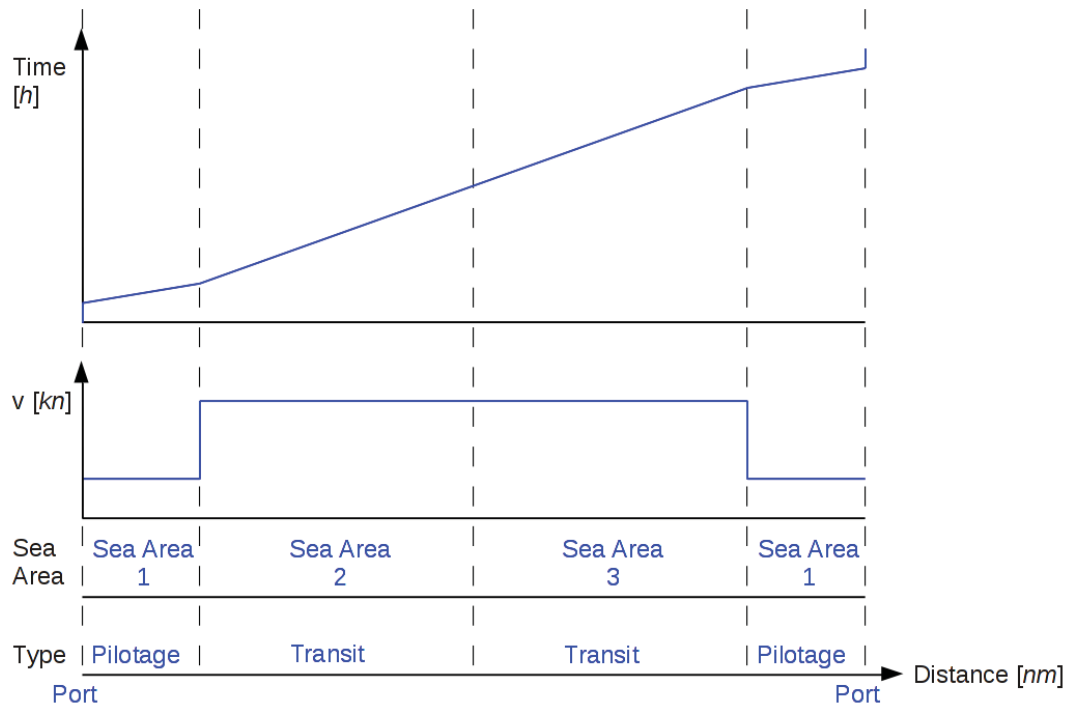


Figure 3.5.: Schematic trade description Rotterdam - New York

respective route segments can be found. Thereby, sea area 1 could indicate a typical pilotage area with usually calm sea states, while areas 2 and 3 may represent zones of rougher weather. However at this point, the sea areas are of interest only in terms of splitting the transit segment into two parts. The third part of the diagram contains the speed process, followed by the course of time. As the speed values always have to remain constant over a route segment and the time needed to adjust a new speed level has been decided to be negligible, the speed development has the form of a step function. Based on this, the traveling time can be differentiated, resulting in a constantly increasing linear function. In case of a port, this function shows discontinuities due to the fact, that time is spent without moving the vessel.

3.3.2. Fuel Oil Prices

Despite the trade description, one of the key driving factors of the scenario development is the descriptor *fuel oil price (FOP)*. As already mentioned in Chapter 1, increasing fuel oil prices in conjunction with a low transport demand can lead to the ship operator's decision to run his vessels in slow steaming mode. While the actual effect of a high fuel oil price onto the vessel's speed will be described in Section 3.4.3, the calculation methodology, adjustment options and utilization of the fuel oil price simulation will be presented in the following.

In literature, many attempts to the accurate forecasting of FOPs can be found. Both universities and private companies as well as public institutions have been trying to find different solutions for this complex problem. The main problem when dealing with FOP prognosis exists in the complexity and the mutual influences of the many driving factors, which can not easily be unraveled. Therefore, based on the perspective onto the problem, different types of solving the issue have been developed. One approach exists in the application of stochastic models

3. Scenario Development

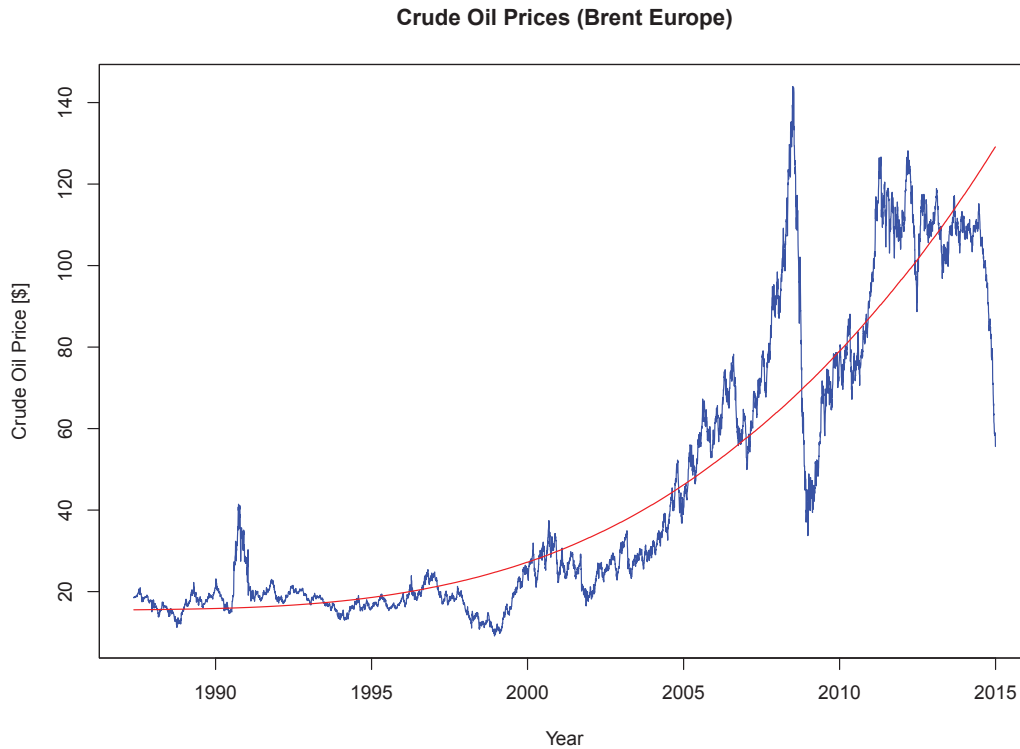


Figure 3.6.: Development of fuel oil prices from 1987 to 2014 (source: Federal Reserve Bank of St. Louis (2015)). Red: regression function.

while using data series from the past and trying to find specific patterns and characteristics (for example done in Zhang et al. (2008)) in order to afterwards apply those findings to forecasting algorithms (as for example done in Stefanakos and Schinas (2014)). Another variant of this approach can be found in the usage of artificial neural networks, which make use of machine learning strategies and which are commonly used for problems, where specific functions need to be deduced from a huge number of observations. Popular examples for this are voice recognition, machine vision and general data mining. One example for the application of these methods for FOP prognosis is given in Jammazi and Aloui (2012). In addition, there is the attempt of focusing on specific driving factors, e.g. the gross domestic product, stock market activities or the oil extraction rate. An example for the latter one can be found in Rehrl and Friedrich (2006).

Within this work it is not intended to compete with one of the above mentioned solutions but rather to provide a method that allows for an easy modeling of FOP development functions and that is able to reflect the knowledge gained from one of the presented approaches. Therefore, it has been chosen to model the FOP development on the basis of a basic development function, which is superimposed by various stochastic fluctuations. This approach is loosely based on the idea for example presented by Kaboudan (2001) and Jammazi and Aloui (2012) that oil prices follow cyclical patterns, which are “typically governed by non constant periodicity and variations within an escalating or a decreasing period”.

When looking at the FOP development of the last 27 years as given in Figure 3.6, a basic

3. Scenario Development

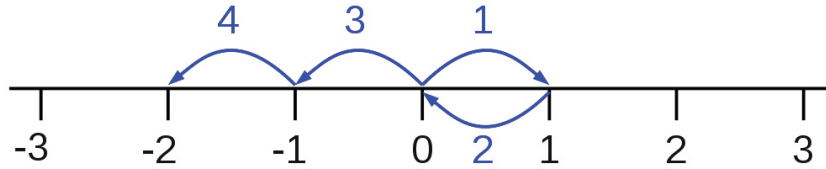


Figure 3.7.: Exemplary simple symmetric random walk on integer number line (based on Henze (2013))

trend function gained from a robust regression can be drawn. While for example in the years 1988 to 1997 the FOP development follows the trend function with only small deviations, there are a few distinct periods for example in 2008 and 2011, at which the oil price shows an extreme behaviour, which are usually referred to as crises. It has to be noted that after those periods - following the statement of Jammazi and Aloui (2012) - the FOP development again follows the basic trend function, even though it might have shifted. It appears that the simulation approach should be able to cope with both the smaller and the more rarely occurring but larger deviations.

One suitable approach for achieving this aim exists in the usage of a modified random walk algorithm. Random walk algorithms are a common stochastic instrument within the field of modeling (not only) economic processes and have been described for the first time in 1905 by the English mathematician Karl Pearson. As the mathematical basics quickly become quite complex, the focus within this thesis will be set on the working principle and some basic properties. For further lecture, the fundamental works of Spitzer (2001) and Lawler and Limic (2010) are recommended.

The basic principles of a random walk simulation can be explained best by the example of a simple symmetric random walk on an one-dimensional integer number line starting at 0 and moving with an equal probability $+1$ or -1 with every step. An example of such a walk with four steps can be seen in Figure 3.7. It appears that for example a particle within each of the four steps randomly jumps to one of its neighboring integers. As the probability for moving forwards or backwards equals 50 %, the particle won't move into one preferred direction, which is why this walk is called a *symmetric walk*.

Even though the random walk is symmetric, it can be seen that if one would repeat a random walk with a larger number of steps (for example $n = 100$) i times, the individual paths of the particles would not constantly alter around zero but develop a flat progression above or below zero, which is shown in Figure 3.8 for an exemplary number of 10 walks.

Using the central limit theorem, it can be proven that when repeating the random walk i times, the probabilities of a particle ending up at a specific place (integer) $x_{i,n}$ after n steps approach a normal distribution with an expected value of $\mu_{RW} = 0$ and a standard deviation of

$$\sigma_{RW} = \sqrt{n} \cdot \sigma_{Steps}, \quad (3.1)$$

with σ_{Steps} being the standard deviation of the step distribution, which consists of the standard deviation of the distribution itself times the actual step size (Henze, 2013). In the above given example, the random walk can be considered as a series of *Rademacher* distributed steps, which leads to

$$\sigma_{Steps} = \sigma_{Rademacher} = 1 \quad (3.2)$$

3. Scenario Development

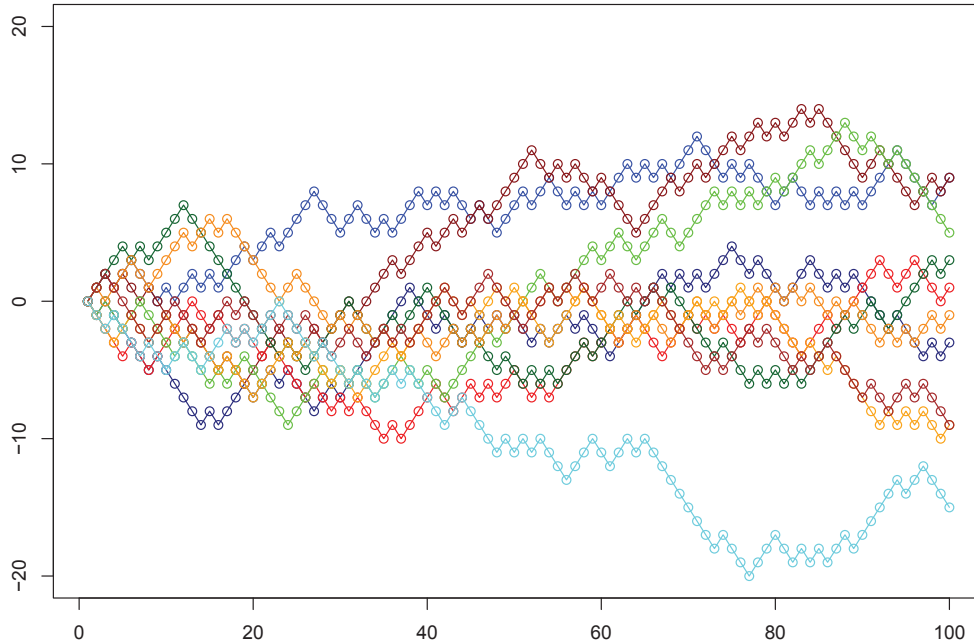


Figure 3.8.: Random walks of length 100

and therefore

$$\sigma_{RW} = \sqrt{100} \cdot \sigma_{Steps} = 10. \quad (3.3)$$

This characteristic is approved by the behavior of the random walks presented in Figure 3.8.

As the above presented simple random walk will not meet the requirements for realistic fuel oil price simulations, a more advanced variant is needed. Therefore, the distribution of the steps need to be changed from a *Rademacher* to a normal distribution of non-discrete step sizes, allowing the random walk to take any value within a given range. Furthermore, a so-called *drift* needs to be added, which means that the mean step size differs from zero, giving the walk a specific direction. Random walk models of this type are sometimes being referred to as *Gaussian random walks* and are widely used for modeling economic processes. When specifying a correct basic development function for the drift and a corresponding fluctuation for the step size, FOP developments can be generated that accurately reproduce main parts of the FOP regression curve given in Figure 3.6.

Although this method allows to simulate FOP developments close to a predefined expectation, scenario methods should also be able to reveal unforeseen developments. Regarding fuel oil prices, these would be oil crises or other disruptive events causing periods of dramatically rising or decreasing prices. One way to include this functionality within the *Gaussian random walk* model exists in specifying large step sizes. But as this would not ensure constantly in- or decreasing prices but also lead to unrealistic jumps between the high and low end of the step scale and would furthermore blur the underlying development function, it has been decided to add disruptive events to the model instead.

3. Scenario Development

When looking at the FOP development in Figure 3.6, it can be seen that the unevenly arising crises differ in impact and duration. As it is not intended to model the causes but only the effects of these crises, a stochastic approach considering the observations of their behavior is sufficient². It has to be noted that in contrast to the real development but for reasons of simplicity a crisis in this context is understood as a period of constantly in- or decreasing fuel oil prices. Keeping that in mind, three main characteristics of oil price crises can be identified:

Occurrence Frequency: probability of how often a crisis will arise within a specific time frame.

Type: direction of the FOP development, either up- or downwards.

Duration: time of constantly in- or decreasing FOP development.

The first parameter applies to all crisis and can easily be implemented into the crisis simulation via random sampling whilst the two other parameters differ for each crisis and therefore need to be simulated using a stochastic approach. For the impact, a simple random selection algorithm can be used, which decides for in- or decreasing developments according to a given probability. The varying duration of a crisis is considered to be normally distributed, therefore it can be modeled on the basis of a specific expected value μ and a standard deviation σ .

Summing up, the above presented ideas lead to a simulation algorithm with one basic input function and five parameters, one for the stochastic fluctuation added to the basic function and four for controlling the occurrence of crises. By specifying the time-dependent function $FOP(t)$, the general development of the fuel oil prices is given, for example based on forecasts of a shipping company. The development's maximum allowed deviation can be specified in $\$/h$ by using the fluctuation parameter $fluc_{FOP}$. The parameters to determine crises are oriented towards the above mentioned crises characteristics: the occurrence probability $P_{FOPCrisis}$ has to be given in $\%/h$, the probability for rising prices in case of a crisis $P_{RiseFOP}$ in $\%$, respectively. Furthermore, the duration of upcoming crises can be controlled using a crisis standard duration $\mu_{FOPCrisisDur}$ and the duration's standard deviation $\sigma_{FOPCrisisDur}$, both to be specified in h .

The resulting simulation algorithm's flow chart for a single time step is presented in Figure 3.9. The basic idea is to simulate the FOP development (and accordingly the transport demand, see Section 3.3.3) over the complete operating time on a daily basis before starting the rest of the scenario simulation process. Thereby, the FOP simulation for all time steps follows the same patterns. At first it is determined, whether there is a crisis at the present time or not. It can be seen that in case there is no crisis, based on the specified occurrence probability it is evaluated, whether - and if yes with what characteristics - a new crisis will occur within the next time step. This process - presented here only in a simplified form - is shown in more detail in Figure 3.10. The specific crisis characteristics to be determined within this process are the crisis duration (calculated via the normal distribution $\mathcal{N}(\mu_{FOPCrisisDur}, \sigma_{FOPCrisisDur})$) and the crisis development type, meaning the decision for in- or decreasing fuel oil prices.

Subsequently, the FOP at the time t_j with j being the specific time step will be calculated via

$$FOP_{t_j} = \mathcal{N}(FOP_{t_{j-1}} + \Delta FOP(t_j), \frac{fluc_{FOP}}{3}). \quad (3.4)$$

Thereby, the expected value of the normal distribution corresponds to the expected development during the respective time step ($\Delta FOP(t_j)$) starting from the FOP value of the last step. The

²According to Narayan and Narayan (2007), oil price shocks have inconsistent, permanent and asymmetric effects on the subsequent price development. Nevertheless, it has been decided to neglect these implications within the FOP modeling due to reasons of simplicity.

3. Scenario Development

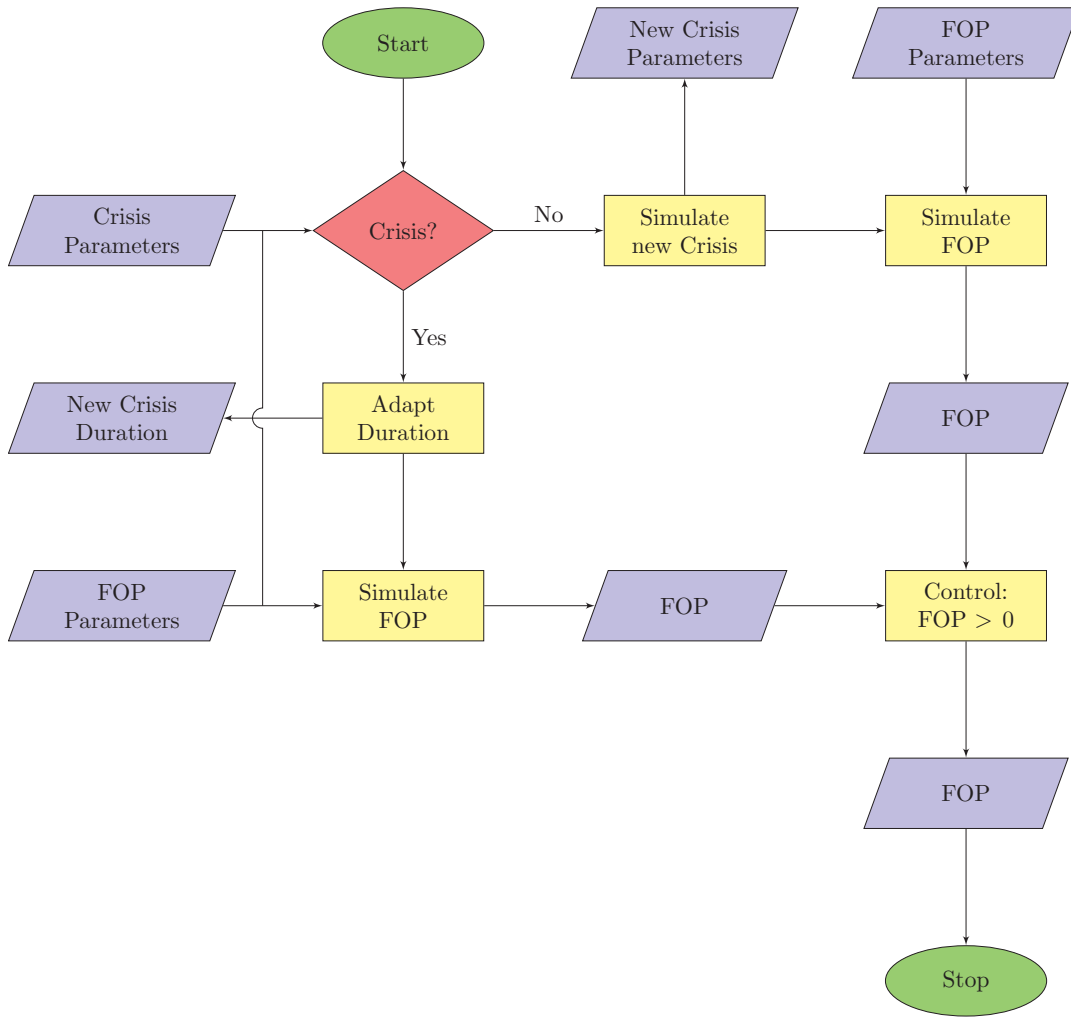


Figure 3.9.: Flow chart of fuel oil price simulation

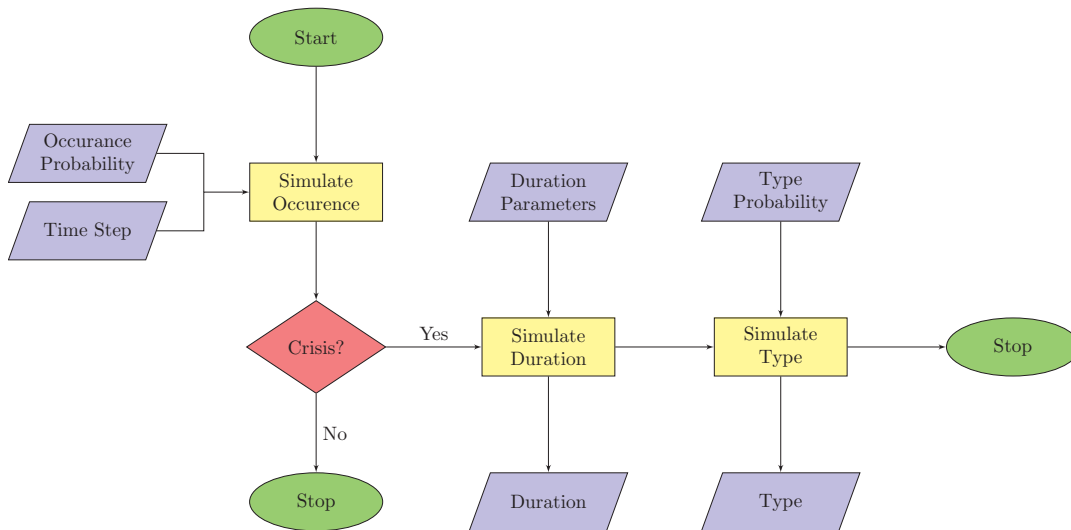


Figure 3.10.: Flow chart of fuel oil price crisis simulation

3. Scenario Development

calculation of $\Delta FOP(t_j)$ is needed due to the possibility of specifying not only linear but arbitrary developments, such as discontinuous functions. The corresponding standard deviation is approximated by dividing the specified maximum fluctuation by three. This simplification has the downside of allowing step sizes larger than the given maximum fluctuation value, but as those in most cases only slightly larger steps have a likeliness of approximately 0.27%, they have been considered to be negligible.

In case there already is a crisis apparent, only the length of the current time step is subtracted from the crisis duration, while the rest of the crisis parameters remain untouched. The FOP calculation itself follows the same patterns as above with the only difference of ensuring the newly simulated FOP being higher or - according to the crisis type - lower than the development function-adjusted value of the last time step. The adjustment includes that in case the increase of the basic development function during a specific time step is higher than the specified maximum fluctuation value, increasing FOP developments can come up, even if a crisis of the decreasing prices type is apparent.

The last step in both cases consists in preventing the FOP values to become smaller than zero. The final FOP value for the current time step is stored and the whole simulation process with updated parameters starts again until the end of the specified service horizon. Resulting, a list containing the fuel oil prices for each day of the vessel's specified operating time is passed to the remaining parts of the scenario creation.

The advantage of the presented approach is the ability to use any kind of function for describing the general FOP development, allowing for example to specify a fixed crisis at a certain point in time. Even discontinuities are allowed within the basic function, which might not be relevant for the oil prices itself but offers the possibility of mapping other costs onto the fuel oil price. An example for this might be found in environmental policies coming into effect in form of market-based instruments (MBIs). In combination with the development function of the price difference between standard and alternative fuel, which is also capable of handling discontinuities, a flexible system is offered that allows to represent all modifications affecting the vessel's main engine.

It should be noted that within the scenario development process only the global fuel oil price development can be displayed, local particularities will not be taken into consideration.

Regarding the usage of the FOP simulation within the scenario development process, it has furthermore to be noted that according to Equation 3.1 the distribution of the generated values is dependent on the number of steps: the more steps per period the smaller the standard deviation of the resulting values. Using the given formula, an example FOP simulation not considering any crises but with a time horizon of 2 hours, a basic development function constantly staying at $FOP(t) = 500 \$$ and a normally distributed fluctuation with a maximum step size of $1 \$/h$ leads to a distribution with

$$\sigma_{RW} = \sqrt{1} \cdot \sigma_{\mathcal{N}(0,1)} \cdot 2 = 2 \quad (3.5)$$

when using only one step. In case of two steps the distribution leads to

$$\sigma_{RW} = \sqrt{2} \cdot \sigma_{\mathcal{N}(0,1)} \cdot 1 = 1.41. \quad (3.6)$$

This means that any change in the number of steps or - referring to a constant time frame - the spacing between the steps consequently leads to changes in the properties of the resulting distribution. This behavior can be considered to be noncritical and easily manageable as long as the spacing of the steps remain constant over time. If - as it is the case here - the steps

3. Scenario Development

have varying spacings due to route segments with different lengths and speeds, the calculation of the resulting FOP distribution may be hampered but still possible. This is reflected by the fact that repeating the simulation under these conditions will most probably lead to the same results. But if in addition to this the calculated value at a specific point in time had an influence onto the following step size, the calculation of the resulting distribution's properties can not be done at reasonable expense. This case might occur if for example a high fuel oil price causes the ship operator to reduce the vessel's speed, which results in longer times spent within the following route segments. Due to this, the number of simulation steps would decrease while under consideration of Formula 3.1 the standard deviation of the resulting FOP distribution at the end of the simulation time would increase. Although this might not be a problem for the simulation algorithm itself, it becomes important when it comes to controlling the scenario development process by the user. In case one wants to achieve a specific standard deviation, this can only be done via adapting the FOP simulation step sizes, which requires the calculability of the resulting distribution of fuel oil prices.

As - resulting from these thoughts - within this approach constant time steps of 24 hours are used, the value for the stochastic fluctuation can be appropriately adapted, if a specific fluctuation range at the end of the designated time horizon needs to be achieved. The additional crises simulation is not considered within Equations 3.5 and 3.6, but it has the potential to blur the distribution due to the fact that although the appearance of crises is uniformly and their duration normally distributed, the respective crises impact follows a *Bernoulli distribution* with the success probability p specified through $P_{RiseFOP}$. Nevertheless, in practice this issue is not of major importance, as the likeliness of a crisis is usually low enough to not notably disturb the distribution.

Examples on the general usage and on how to adapt the fluctuation rate can be found in Section 4.2.

3.3.3. Transport Demand

Alongside the fuel oil price, the transport demand is the second key driving descriptor of the scenario development. While the former is mainly influencing the vessel's speed, changes to the transport demand are being reflected by the draught, which is explained in Section 3.4.8. The transport demand itself is not reflected by an absolute value but by its relative change in %, based on the initial value at the begin of the simulation. It has to be noted that - also in compliance with the fuel oil prices - only the global transport demand is modeled, while local particularities can not be considered.

For the prognosis of the transport demand, the same presumptions and preconditions as for the fuel oil prices apply. Therefore, its simulation follows the principles explained in the previous section, including the *Gaussian random walk* with drift and the additional crises simulation, which leads to the corresponding flow chart given in Figure 3.11. Transport demand crises arise equally but independent of those of the fuel oil price, as it has been discussed in Section 3.1. Resulting, the parameters to control the transport demand simulation are similarly named $TD(t)$, $fluct_{TD}$, $P_{TDCrisis}$, P_{RiseTD} , $\mu_{TDCrisisDur}$ and $\sigma_{TDCrisisDur}$. Apart from its possibility to take values smaller than zero, the only difference consists in the respective units, as both the basic transport demand development function as well as the fluctuation have to be specified in %/h.

3. Scenario Development

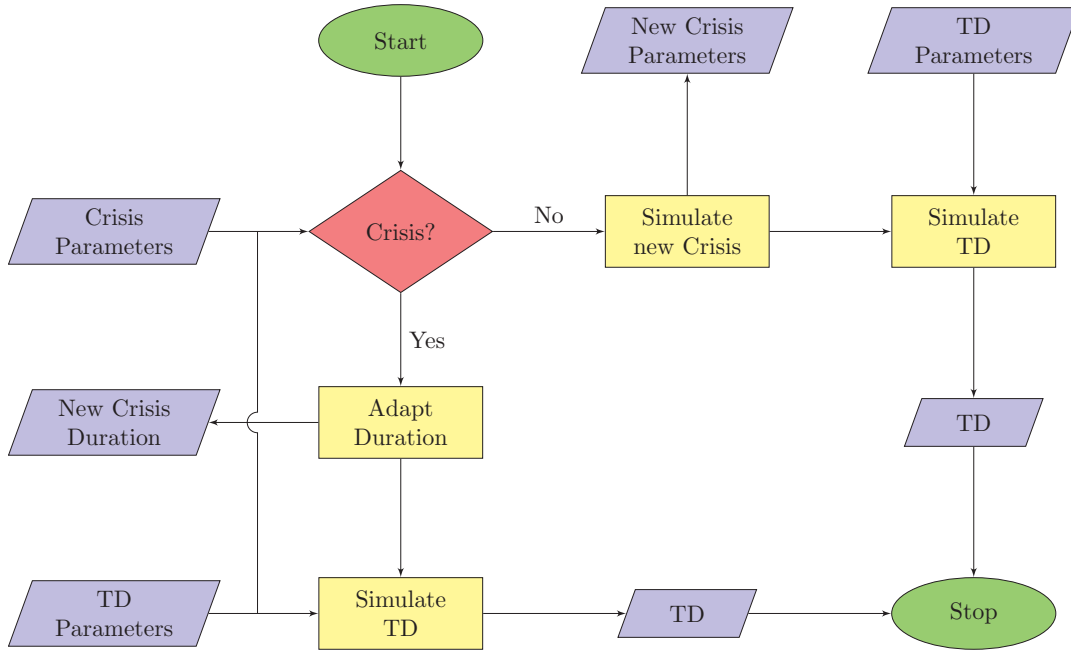


Figure 3.11.: Flow chart of transport demand simulation

3.3.4. Weather

As already mentioned in Section 3.1.2, the description of the sea states should be done using the descriptors *wave height* and *wave period*. This is the most common way of describing seaways allowing it to display the in reality irregular sea state of a specific area by using scatter tables.

Within this work, the seaway tables of *Söding* as published in Söding (2001) have been used. The scatter diagrams given there indicate the 10^6 times relative frequency of occurrence of specific seaway combinations at 126 points (in the first place defined by Young and Holland (1996)) within the world's oceans. A map showing the allocation of these points is given in Figure 3.12. The different seaway conditions are indicated by their significant wave height $H_{1/3}$, indicating the average height (measured from crest to trough) of the largest one third of all occurring waves, and their corresponding center of gravity period T_1 . This period indicates the pass of the center of gravity of the waves' spectrum area and differs from the more widespread peak period T_p but can easily be converted via $T_p = T_1/0.77$ if necessary. The translation into the also commonly used zero upcrossing period T_z can be done via $T_z = T_1/1.086$ (Michel, 1999). An example for an extract from a Söding scatter table entry (Point 1 located at latitude -54° and longitude 2°) is given in Table 3.4. Thereby, the classification of the axis is done using the mean value of the summarized values within the respective bin. As an example, the combination of $H_{1/3} = 0.25\text{ m}$ and $T_1 = 1.5\text{ s}$ covers a range of waves with a significant height from 0 to 0.5 m and a period from 1 to 2 s .

When modeling the trade, the specific seaway points along the vessel's route can be assigned to the respective route segments in order to reflect the local weather conditions. As every route segment has to have constant properties, the route needs to be split up every time it crosses the borders between two different sea areas. Thereby, the decision about the extends of those sea areas or its derived route segments has to be done by special routing software or - if not available - simply by estimating (as done in all use cases presented in Section 6).

3. Scenario Development

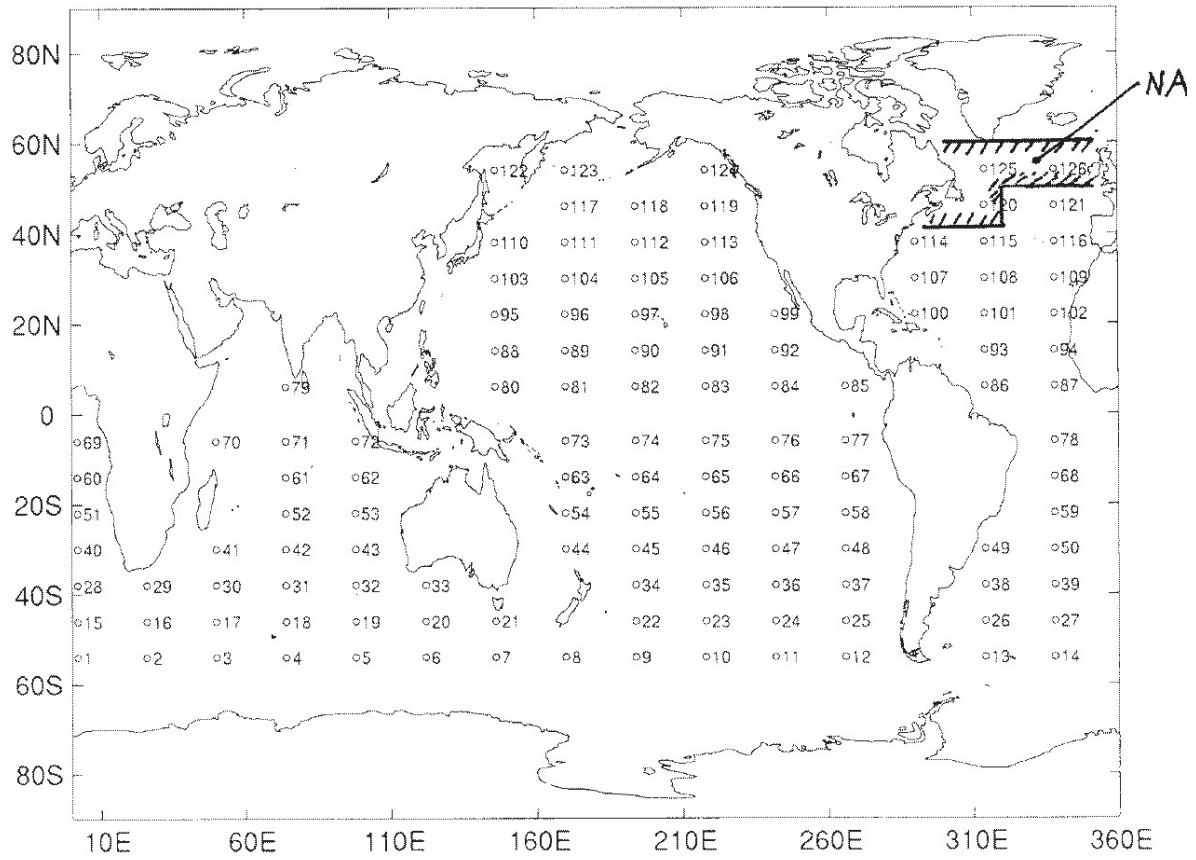


Figure 3.12.: Position of seaway points (Söding, 2001). The area marked with “NA” refers to the ISSC wave statistic covering the North Atlantic.

T_1 [s]	$H_{1/3}$ [m]						
	0.25	0.75	1.25	1.75	2.25	2.75	...
1.5	6	0	0	0	0	0	
2.5	88	20	0	0	0	0	
3.5	546	632	102	0	0	0	
4.5	2420	3826	3610	1768	0	0	
5.5	5411	8527	12343	14902	10117	2633	
⋮							

Table 3.4.: Exemplary extract of a seaway scatter table entry (Söding, 2001)

3. Scenario Development

This allocation of sea areas allows it to determine one particular wave height / wave period combination for each pass of the respective route segment, as it is described in Section 3.4.2. While in this way not reflecting reality at each particular route segment, the respective sea state profile of each segment converges the one given in its associated scatter table when combining this approach with the Monte-Carlo method presented in Section 3.5.

In compliance with the research project *PerSee* (Bronsart et al., 2016), it has been decided to consider the waves to always attack under an angle of 180° , meaning that the vessel always faces head seas. This decision is based on the idea of keeping the calculation effort as low as possible and can be considered to be reasonable when keeping in mind, that the most influential wave directions regarding added resistance are head and beam seas, of which the angle of 180° could be seen as the average. Furthermore, it would be very difficult to determine the distribution of wave directions for each sea area, which had to be coupled with the respective course of the vessel in order to find the relative angle of attack. Another suitable solution for this would be the assumption of uniformly distributed wave directions, which could also be applied easily.

In case the *Söding* tables do not cover all sea passages of a designated trade (which could be the case if the trade leads through the Mediterranean, Baltic or North Sea as well as through the Arctic Ocean), the tables can be amended if respective data is available. Otherwise, data of the closest or any other sea area considered to have matching characteristics can be used. A special case are ports. The scenario development algorithm necessitates the indication of a sea state within all route segments, including ports. As the sea state in ports is of no greater interest when optimizing a hull form respecting its added resistance in seaways, it has been decided to introduce a specific “port point” within the *Söding* tables having a 100 % probability of waves with a unique combination of $H_{1/3}$ and T_1 . As this combination does not come up throughout all other points, it can easily be identified as a “port sea state” and therefore filtered out afterwards when analyzing the scenario data.

3.4. Calculation of Scenario Descriptors

Within this section, the calculation of the manifestations of the four descriptors defining an operation condition will be described in detail. Thereby, the calculation within every route segment follows the schema given in Figure 3.13. It has to be noticed that the step sequence is of importance due to the fact that the manifestation of some descriptors rely on the manifestation of other descriptors. An example for this exists in the speed dependency from the current sea state. Based on the given sequence, detailed descriptions on how the respective scenario descriptors are determined are given within the next sections.

3.4.1. Dry Dock

The first descriptor to calculate is the detection of the vessel’s need to be dry docked. This need is driven by the descriptor *docking interval*. At the begin of each route segment, the algorithm checks, whether the vessel has reached its maintenance interval. If this is the case, the vessel will be sent into dry dock at the next opportunity. As it has already been mentioned in Section 3.3.1, there are no specific dry docks to be modeled. Instead, ports can be marked as *docking ports*, indicating a port close to a dry docking facility. If the vessels needs to be dry-docked when reaching such a docking port, it will remain there not only for the time needed for loading and unloading, but additionally for the docking time specified through the descriptor

3. Scenario Development

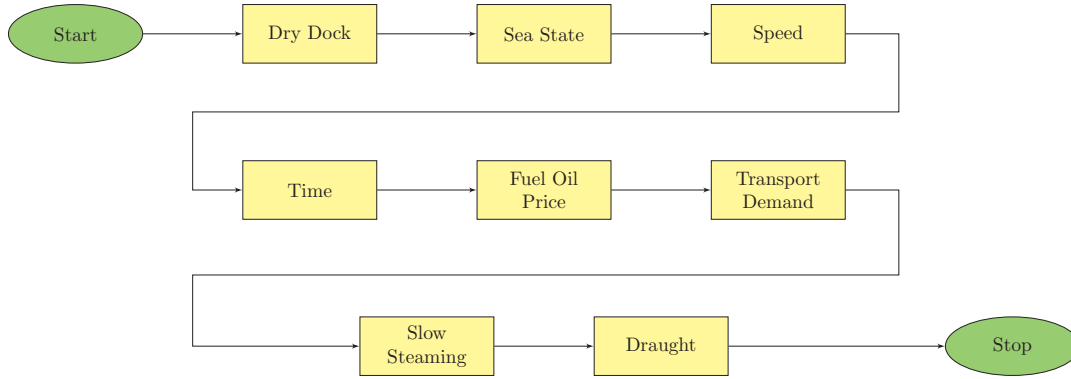


Figure 3.13.: Schema of manifestation calculation within each route segment

docking duration. Therefore, the docking time should include both, the net time to be spent for overhaul plus the time needed to travel from the port to the dry docking facility and back.

3.4.2. Sea State

As it has been mentioned in Section 3.3.4, one specific combination of wave height and period has to be determined each time the vessel crosses a route segment. This will be done on the basis of the scatter table assigned to the current route segment. As it has to be assured that when repeating the process multiple times the distribution of the resulting sea state combinations converges the original distribution gained from the *Söding* tables, the sampling of those combinations has to follow the probability distribution of the respective scatter table.

Therefore, the scatter table of the current sea area is read by the algorithm and converted into a one-dimensional cumulative distribution function (CDF) of sea state combinations. The combinations' frequencies are translated into probabilities summing up to 1 by dividing them by their overall occurrence frequency, which in case of the *Söding* tables mostly equals 10^6 . Written as a discrete probability mass function (PMF), the scatter diagram presented in Table 3.4 in Section 3.3.4 would have the form

$$f_X(x) = \begin{cases} 6.0 \cdot 10^{-6}, & x = x_1 \\ 0.0, & x \in \{x_1, \dots, x_{22}\} \\ 8.8 \cdot 10^{-5}, & x = x_{23} \\ 2.0 \cdot 10^{-5}, & x = x_{24} \\ \vdots & \end{cases} . \quad (3.7)$$

Thereby, the array indices mark the respective sea state combinations, while the corresponding values indicate their probability. Consequently, the first array entry x_1 indicates a wave period of $T_1 = 1.5 \text{ s}$ in conjunction with a wave height of $H_{1/3} = 0.25 \text{ m}$ and a corresponding probability of $6.0 \cdot 10^{-6}$.

On the basis of the resulting CDF, a random variate with the desired probability can be picked by uniformly sampling on the diagram's ordinate between 0 and 1, which is often referred to

3. Scenario Development

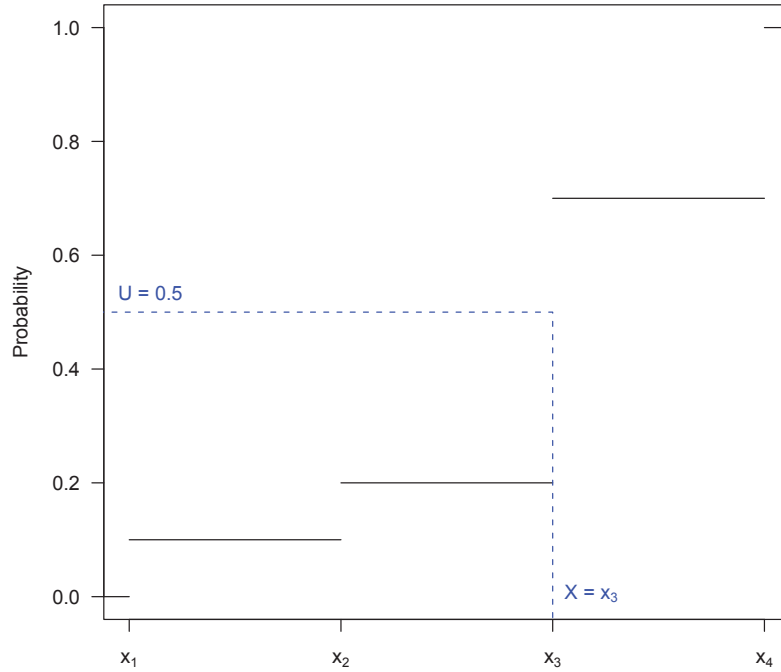


Figure 3.14.: Sampling from a discrete cumulative distribution function

as *inverse transform sampling*. In Figure 3.14, a discrete example CDF with

$$F_X(x) = \begin{cases} 0, & x < x_1 \\ 0.1, & x_1 \leq x < x_2 \\ 0.2, & x_2 \leq x < x_3 \\ 0.7, & x_3 \leq x < x_4 \\ 1, & x \geq x_4 \end{cases} \quad (3.8)$$

can be seen. When uniformly sampling a value U along the CDF's ordinate, the largest abscissa value $X \in x_{1,\dots,4}$, whose probability $P(-\infty \leq X)$ is smaller than the sampled probability value U can be determined via

$$X = x_i \iff F_X(x_{i-1}) \leq U < F_X(x_i). \quad (3.9)$$

In the given example, the sampled value $U = 0.5$ leads to

$$X = x_3, \text{ as } F_X(x_2) \leq 0.5 < F_X(x_3), \quad (3.10)$$

which could also be written as

$$F_X^{-1}(U = 0.5) = X = x_3, \quad (3.11)$$

3. Scenario Development

with F_X^{-1} being the inverse cumulative distribution function. When repeating this process multiple times, the generated abscissa values $U_{1,\dots,n}$ will converge their original cumulative distribution function. This behavior will be shown in Section 4.3 and makes this approach a suitable solution for simulating the sea state conditions along the vessel's route.

At the end of each route segment, the thus generated conditions will directly be handed over to the objective operating conditions detection algorithm (see Section 3.6).

3.4.3. Speed

The determination of the vessel's current speed is affected by the most restrictions and boundary conditions. The following influencing factors have to be considered during its calculation:

- local constraints,
- sea states,
- slow steaming,
- schedule.

Figure 3.15 presents the general approach of the speed calculation. In a first step, it is detected whether the vessel stays in port or operates in open waters. In the first case the speed will be set to 0 *kn*. Additionally and in case there was time to make up due to a delay in one of the previous route segments, this time will be preserved and passed over to the next segment.

If the vessel operates outside ports, more calculations have to be done, beginning with the determination of the initial speed value as stated within the trade description. Based on this value, corrections related to the influencing descriptors given above will be applied. The first step consists in checking, whether a decision for slow steaming has been done at the last main port (see Section 3.4.7). If so, the initial speed will be checked against the slow steaming speed that has been determined on the basis of the user defined decision table and in the following appropriately adjusted when being higher than this value.

Within the second step, the subject of a potential speed increase in order to make up for lost time is dealt with. Therefore, the current delay to cope with needs to be calculated on the basis of an intended passing time for the current and possible delays from previous route segments. While the latter ones are directly handed over from the last route segment, the intended passing time for the current route segment is determined by the quotient of the length of the current route segment and the speed value after a potential slow steaming correction. This reflects the idea that a ship operator does not decide for slow steaming without adapting his vessel's schedule. Consequently, the time intended to pass through a route segment calculates as

$$t_{intended,i} = \frac{s_i}{v_{ssc,i}} - t_{delay,i-1}, \quad (3.12)$$

with s_i being the length of the current route segment $i \in (0, \dots, n)$, $v_{ssc,i}$ the already slow steaming-corrected speed and $t_{delay,i-1}$ the delay time of the previous segments. In case the vessel serves a route segment with local speed restrictions, Equation 3.12 transforms into

$$t_{intended,i} = \frac{s_i}{\min(v_{ssc,i}, v_{max,local,i})} - t_{delay,i-1}. \quad (3.13)$$

As local speed restrictions are considered to be taken care of within the schedule planning of ship operators, Equation 3.13 is needed in order to prevent the simulation from further

3. Scenario Development

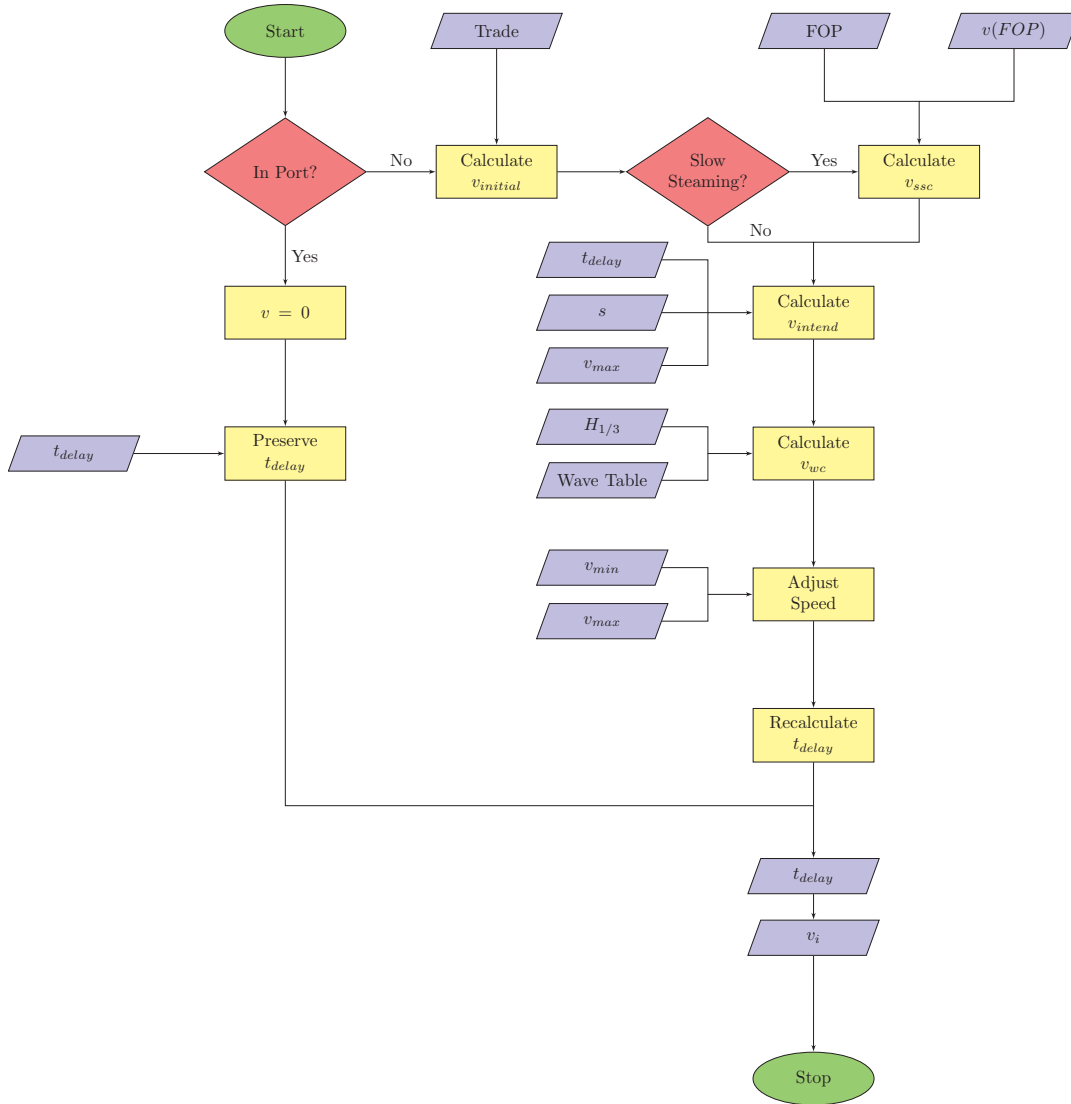


Figure 3.15.: Flow chart of speed calculation

increasing the delay when already being late and entering such a segment with a higher speed than allowed by the respective local restriction.

For the determination of the actually needed speed, it has been decided to make up for a delay as fast as possible, meaning at best within the next route segment. This approach has been favored over only slightly increasing the speed within all upcoming route segments until the next port, as with the second method a higher risk of still not arriving there on time due to further potentially upcoming interferences arises. It has furthermore been decided that keeping the schedule should be of higher importance than observing the slow steaming order. Therefore, the speed will be increased even during operating in slow steaming. Keeping this in mind, the delay-corrected speed value is calculated via

$$v_{intended,i} = \frac{s_i}{\frac{s_i}{v_{ssc,i}} - t_{delay,i-1}} = \frac{s_i}{t_{intended,i}}. \quad (3.14)$$

3. Scenario Development

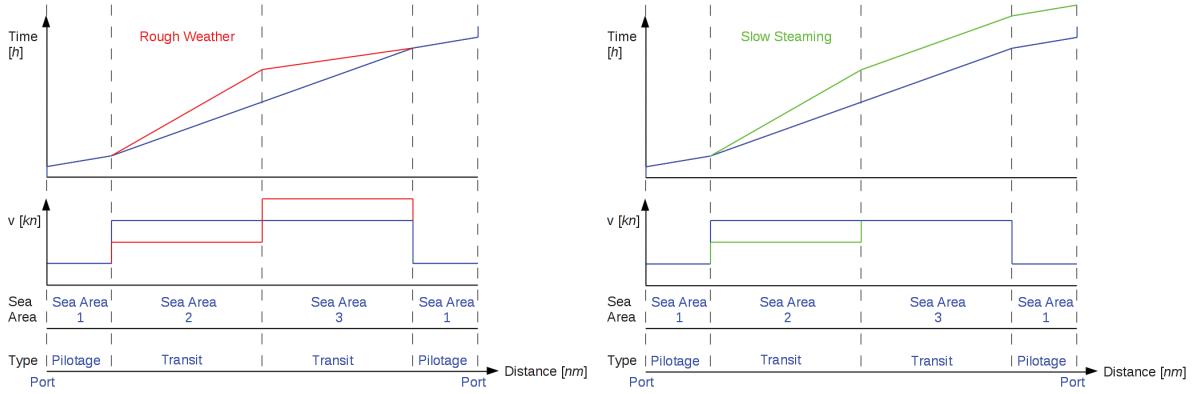


Figure 3.16.: Comparison of reactions to speed changes: rough weather (left) versus slow steaming (right)

$H_{1/3}$ [m]	v_{max} [kn]
≤ 3	20
> 3	18
> 5	17
> 8	15

Table 3.5.: Decision table for speed reductions due to wave height

Referring to the schematic trade description previously introduced in Figure 3.5, this leads to the behavior presented in Figure 3.16, where speed developments as a reaction to different delays from previous route segments are given. It can be seen that a speed deviation in the second route segment that has been caused by rough weather (marked red) results in an increased speed within the subsequent route segment, while a speed loss due to a slow steaming decision (green) does not.

In case the time to make up for becomes greater than the initially intended segment passing time and, resulting from that, $t_{intended,i}$ gets negative, the vessel's speed value will be set to the maximum speed allowed, while the remaining delay will be handed over to the next route segment.

Within step three of the speed calculation process, the weather detection takes place. According to the simplifications made when describing sea state conditions, the critical descriptor regarding speed reductions is the wave height $H_{1/3}$. In order to simulate the operator's decision to reduce speed, a decision table as already mentioned in Section 3.1.2 is applied, consisting of a list of wave height thresholds and its corresponding speed adjustments (see Table 3.5). In case the current speed exceeds the maximum value corresponding to the current wave height, it will be accordingly adjusted.

The last step consists in the examination of compliance to the maximum and minimum speed values. The global speed constraints are specified when setting up the scenario development process. While the maximum speed usually results from the vessel's characteristics, the minimum speed can be set due to technical limitations or it can be used to define an operator-predetermined velocity at which the vessel barely operates without becoming economically unviable. Additionally, the algorithm checks for local restrictions specified within

3. Scenario Development

the trade description and adapts the speed accordingly. It has to be noted that these local and global speed restrictions supersede all other decisions (slow steaming, schedule keeping and reductions due to bad weather). While being reasonable for the maximum, the minimum speed limits could theoretically collide with the targeted values resulting from slow steaming or bad weather. As in most cases the minimum speed reflects an economic decision, the operator would not decrease the slow steaming speed below this threshold value. Regarding the weather issues, it can be supposed that local speed restrictions do only appear in areas of generally calm sea states, such as inland waterways or coastal areas.

After the final speed manifestation for the current route segment has been found, the possibly remaining or newly developed time to make up for has to be determined in order to pass it over to the next segment. If the vessels stays in port, the delay time from the last segment remains unmodified as mentioned before. If not in port, the new delay time calculates as specified within Equation 3.15.

$$t_{delay,i} = \frac{s_i}{v_i} - t_{intended,i} \stackrel{!}{\geq} 0 \quad (3.15)$$

Thereby, $t_{delay,i}$ indicates the delay time of the current route segment and v_i the corresponding final speed manifestation. It has been decided that in the unlikely event of being faster than the initial schedule, for example due to a local minimum speed restriction being higher than the initially intended speed value provided within the trade description, the speed will not be reduced within the next segments although the delay time will be set to zero, based on the idea of having a buffer for upcoming delays. In case there are no further disturbances, this “negative delay” should be rather small, allowing the vessel to spend this time waiting in port.

3.4.4. Time

The time descriptor is an important element within the scenario development process as it is the main weighting factor for determining and evaluating the final operating conditions as it will be shown in Section 3.6. The calculation of the time spent within each route segment t_i differs according to the kind of segment the vessel stays in. As it can be seen in the flow chart of Figure 3.17, it is distinguished between open sea, docking port and other ports. In case the vessels operates outside ports, the passage time simply results from

$$t_i = \frac{s_i}{v_i}. \quad (3.16)$$

If the vessel is in a port not being marked as docking port, the time spent within this route segment is directly taken from the lay time specified for the current port within the trade description. The same applies in case of the vessel staying within a docking port while there is no need for dry docking. If this need has been detected, the time for traveling to the maintenance facility and the time needed for the maintenance procedure itself is added to the originally intended port lay time.

3.4.5. Fuel Oil Price

Due to the dependency of the FOP development from the step size used within the simulation method as it has been described in Section 3.3.2, the fuel oil prices can not be calculated “live” within each route segment. Thus, the whole development of the FOP over the vessel’s designated service time will be simulated in advance at the begin of each Monte-Carlo run

3. Scenario Development

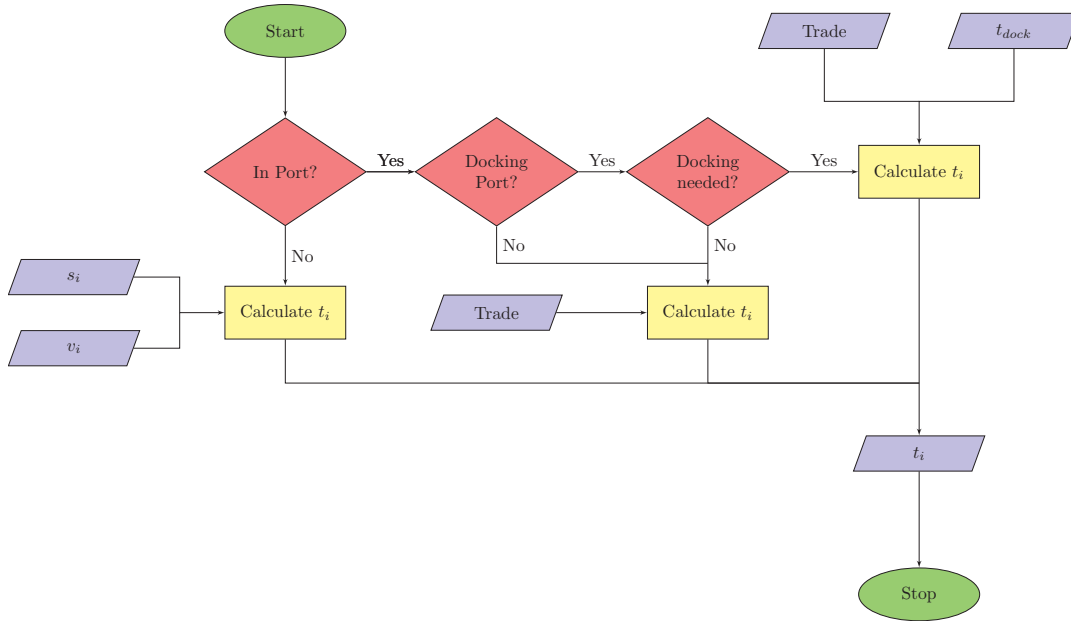


Figure 3.17.: Flow chart of time calculation

on the basis of a 24 hour step size. If at any time within the following scenario development process the algorithm needs to determine the current fuel oil price, it accesses this previously generated data and reads the value corresponding to the current operating time $t_{total,i}$.

When targeting at calculating the costs spent for fuel and in order to utilize those costs for the creation of a weighting, it has to be taken into consideration that not always the current fuel oil price but the one being current at the time of the last port visit has to be used. Therefore, the FOP manifestation is only updated within ports being referred to as *refueling ports*. The only exception to this exists, if the vessel passes an emission control area and is forced to switch to eco-friendly fuels or to take other environmental measures. In this case, the corresponding cost difference is added to the FOP of the respective route segment as it has been mentioned in Section 3.1.2. This reflects the assumption that the ship operator either knows how to anticipate the fuel consumption of his vessel on the following trip and fills his tanks with the exact amount of fuel needed for it or that he starts every trip with full tanks and re-fills them when arriving at a refueling port. Even though both cases might not reflect a realistic ship operator behavior as for example the possibility of bunkering more fuel in case of low prices can not be depicted by this method, this calculation approach can be considered to be sufficient within the context of this thesis.

Another matter to be taken care of when it later comes to financial assessment is the interest rate. In order to not distort the influence of costs appearing within the future, the net present value as introduced in Section 2.4.2 can be applied to the fuel oil price, wherefore a specific interest rate i_r has to be indicated when setting up the scenario development. The method calculates and preserves both, the original and the interest rate-adjusted FOP, allowing to create weightings considering both variants (see Section 3.6).

The flow chart of the calculation of the FOP manifestations is depicted in Figure 3.18.

3. Scenario Development

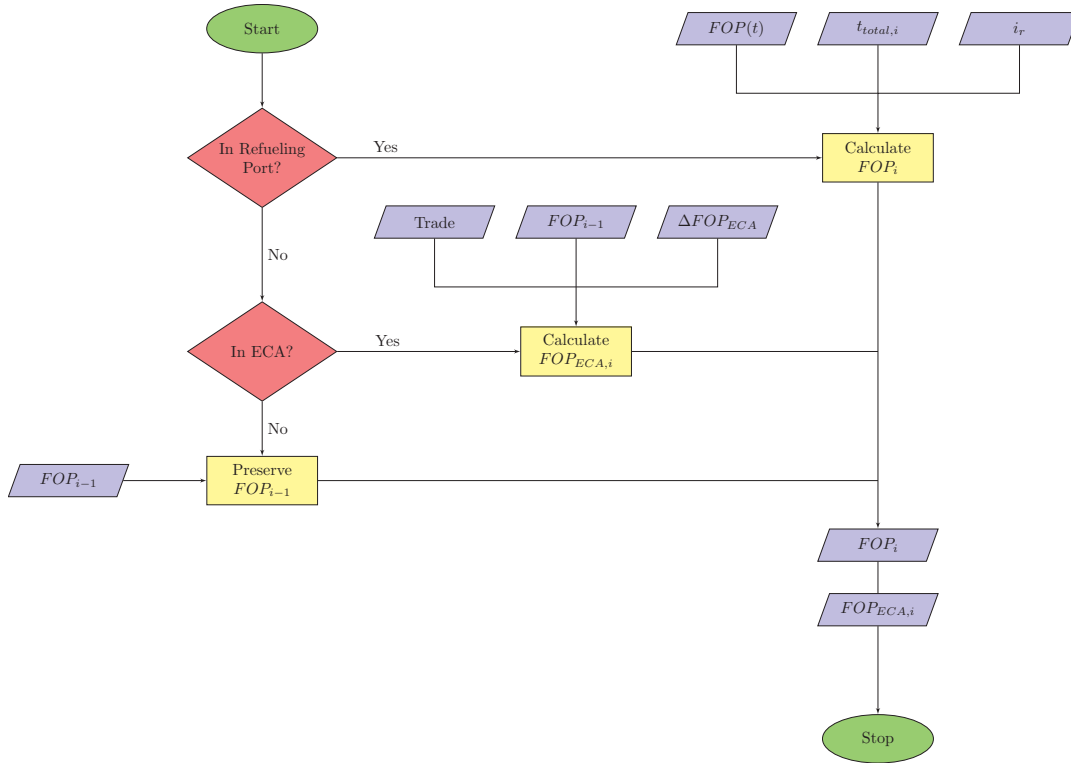


Figure 3.18.: Flow chart of fuel oil price calculation

3.4.6. Transport Demand

The transport demand calculation follows the same principles as previously introduced for the FOP development, including the approach of executing the complete TD development at the begin of each MC cycle in 24 hour steps, see Figure 3.19. As the manifestation of the transport demand only affects the loading of the vessel and resulting from that its draught, it is only calculated within ports and subsequently handed over to the draught calculation.

3.4.7. Slow Steaming

As it has already been mentioned within Section 3.4.3, the simulation of an operator's decision for slow steaming is vital when it comes to determining the vessel's speed. According to a ship owner's statement, the decision for slow steaming has a strategic character and would not be applied during an ongoing round trip due to the fact that this would lead to conflicts with the previously made time and port schedules. Therefore, specific ports along the vessel's designated trade can be marked, exclusively at which a possible slow steaming decision can be made. Within the setup of the scenario development, these ports are called *main ports*. Only in case the vessel reaches such a main port while the fuel oil price is higher than an operator-specified threshold, a slow steaming decision being valid at least until the next arrival at another main port will be made. By using this approach, it is secured that the scenario development does not simulate an unrealistic behavior of the vessel constantly hovering between slow steaming and normal operation mode in case the fuel oil price oscillates around the specified slow steaming threshold.

3. Scenario Development

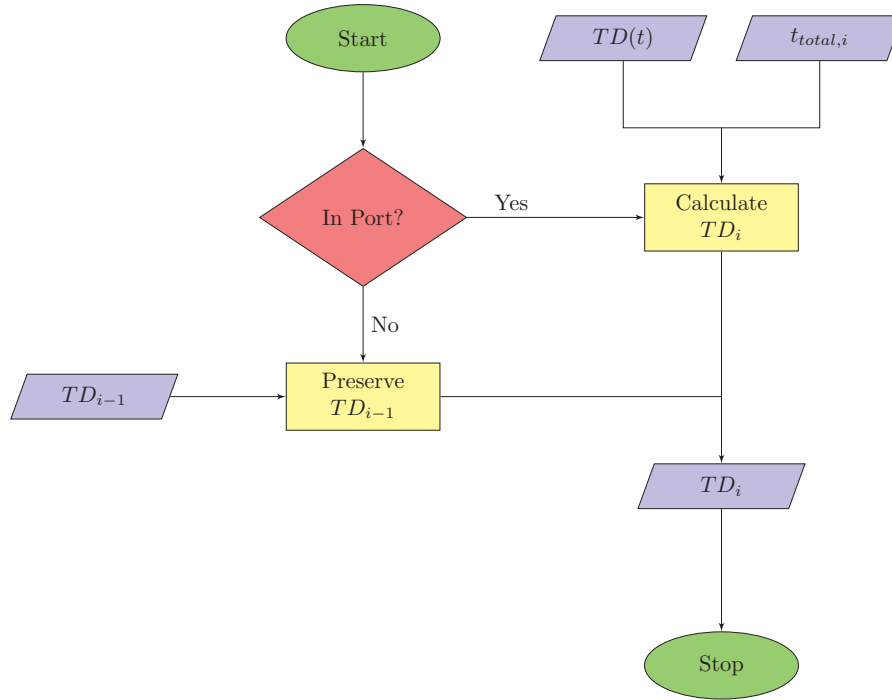


Figure 3.19.: Flow chart of transport demand calculation

If the vessel stays within a main port, the slow steaming detection itself is based on the current FOP and the slow steaming decision table as specified by the user. This table is checked against the current FOP manifestation and in case it matches one of the entries specified there, an indicator for a positive slow steaming decision and the respective maximum speed is handed over to the speed calculations of the next route segments.

Figure 3.20 shows the FOP and speed development of a vessel serving on an example trade. It can be seen that in case the fuel oil price reaches the slow steaming threshold (between segment 3 and 4), the vessel's speed is limited to the slow steaming velocity v_{SSC} . According to the explanations given above, the speed limitation applies from main port to main port, even if the FOP dropped below the threshold within any other non-main port (as between segment 6 and 7). Therefore, the vessel still operates at v_{SSC} even beyond route segment 7.

3.4.8. Draught

There are two different possibilities of calculating the vessel's draught. Based on the method specified within the scenario development setup, the draught of the current route segment can either be determined by

- utilizing an initial draught specified within the trade description or
- on the basis of a loading-draught-function.

The first method should be applied in case that not much is known about the hydrostatic characteristics of the vessel, for example if the scenario development needs to be done before the design spiral has successfully been run through. It could also be used in case the transportation task has not clearly been defined, remains vague or does not refer to standard containerized

3. Scenario Development

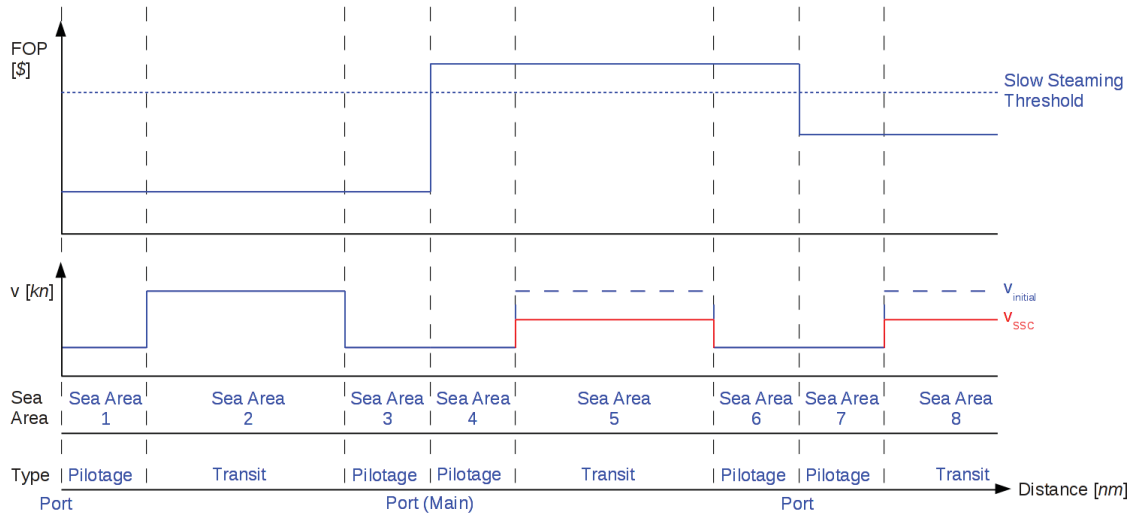


Figure 3.20.: Reaction to an exemplary slow steaming decision. The speed limitation (marked red) applies beyond the time span of the FOP staying above the slow steaming threshold.

or bulk goods. An example for the latter can be found in Section 6.3. The second method aims onto situations, at which the hull form and the transportation task can be specified with comparatively high accuracy, which includes the knowledge of a loading-draught-function. This function should be able to display the draught of the vessel depending on the number of loaded full and empty TEUs and has to be specified within the scenario development setup. It should be noted that potential changes to the loading-draught-function caused by a subsequent hull form optimization have been neglected due to its presumed low impact. An example for this could be the retrofitting of the bulbous bow or the fore body region of an existing vessel due to a changing trade as it will be presented in Section 6.2.

In both cases, the general calculation procedure follows a similar approach. Basically, the draught is only determined in ports and in the following kept constant over the rest of the trip up to the next port. Within each port, three calculation steps have to be done. The first consists in determining the originally intended draught detection, meaning the calculation of the current draught value on the basis of the draught given in the trade description or derived from the specified number of TEUs via the loading-draught-function. In order to reflect a developing transport demand, the current TD manifestation being calculated as described in Section 3.4.6 will be added to the initial draught value or the number of TEUs, respectively. For the latter case, only rounded integer numbers of full and empty containers are allowed. It has to be noted that when using the first method, a linear increase in the transport demand leads to a linear increase of the draught, which does not reflect a realistic behavior. While under the same conditions the second method should - depending on the accuracy of the loading-draught-function - lead to a more asymptotic development of the draught increase towards its maximum value, the application of the first method is only suitable at an early design stage.

Step two includes the determination of potentially upcoming local draught restrictions. As the scenario development process is not able to adjust the draught outside ports, the compliance to future local draught restrictions has already to be secured within the current port. In order to do this, the algorithm checks all upcoming route segments on the way to the next port for

3. Scenario Development

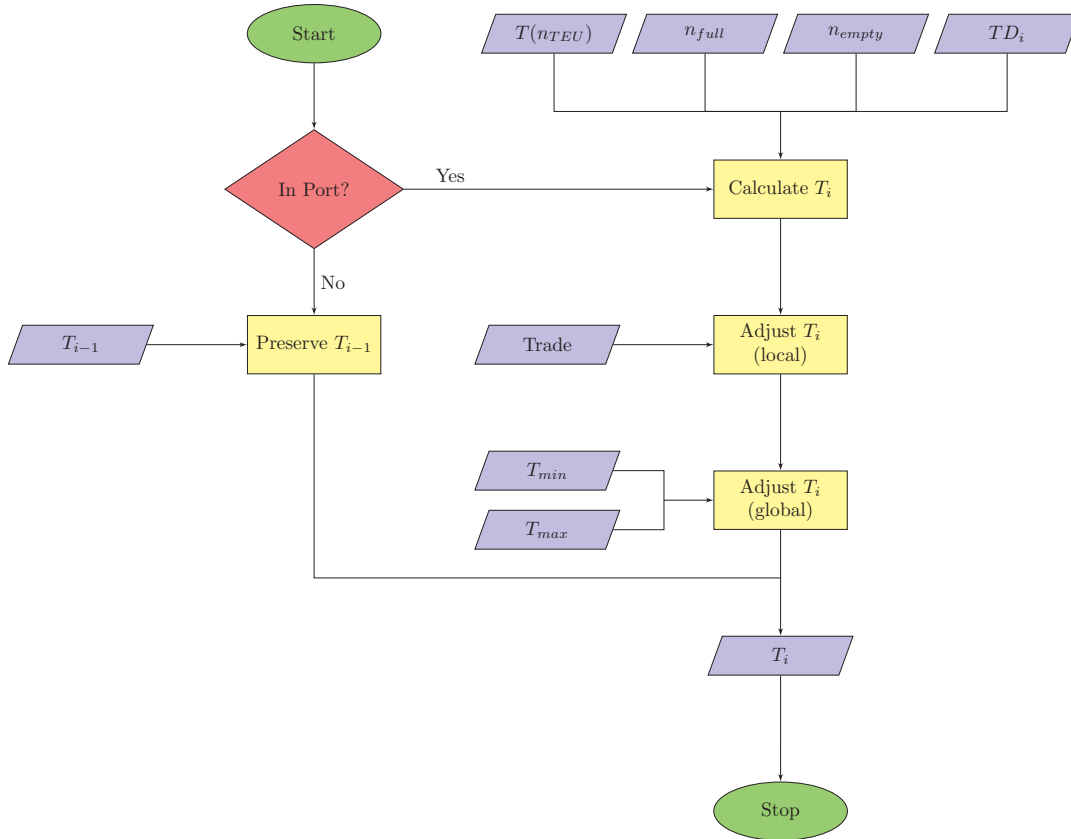


Figure 3.21.: Flow chart of draught calculation (using loading-draught-function)

local restrictions and accordingly adjusts the current draught if necessary.

Within the last step, the draught manifestation is tested against its global minimum and maximum values specified within the scenario setup. These boundaries can be set in order to fulfill safety regulations (freeboard) or to ensure a certain minimum draught via ballasting.

The resulting flow chart of the whole draught determination process using the loading-draught-function can be found in Figure 3.21.

3.5. Uncertainty Handling

With the help of the methods presented above it is possible to simulate a vessel's operational life. It has to be noted that due to the random events included within the simulation (seaway, fuel oil price and transport demand development) only one of many possible life cycles of the vessel is generated. Thus, it can not be ruled out that the simulated vessel life and the most frequent operating conditions derived therefrom represent an uncommon yet possible constellation. Referring to the picture of the scenario cone presented in Section 2.2, a scenario cycle run only once could lead to extreme scenarios at the edge of the cone. While being possible, the usage of such a scenario cycle would lead to wrong conclusions regarding the distribution of operating conditions. A scenario cycle with a more temperate outcome would also not be sufficient for determining the most common operating conditions as this on the other hand neglects less but still possible developments.

3. Scenario Development

In order to avoid this overvaluation (or undervaluation, respectively), the vessel's life needs to be simulated many times, each time with newly random-generated scenario developments. As this can be considered to be a random experiment, the distribution of the resulting operating conditions converge their theoretical but in this case unknown probability distribution with an increasing number of scenario cycles. This behavior is widely known as the law of huge numbers and sets the basis for the Monte-Carlo method (MCM) used within this thesis. In principle, Monte-Carlo methods are a stochastic tool applied for simulating and solving systems with many uncertainties and degrees of freedom, which otherwise could not or only at high computation costs be solved analytically. Comprehensive literature on these methods and their application can be found in Sobol (1991) and Binder and Heermann (2010). Using the Monte-Carlo approach, all random-based developments can be depicted in compliance with the specifications of the scenario setup, if the totality of all simulation cycles is considered. An example for this exists in the passing of a specific route segment and the simulation of the corresponding sea state conditions. For each single pass, a combination of T_1 and $H_{1/3}$ is simulated while assuming the sea state to remain constant within the whole route segment, which does not reflect a realistic behavior. But when passing through this segment many times, the sum of the respective simulated sea states will yield the originally intended distribution of wave heights and periods as given in the *Söding* tables. This behavior will exemplarily be shown in Section 4.3.

The advantage of MCMs against the direct and more accurate simulation of all possible developments consists in the fact that the computational effort regarding both memory and processor usage can be remarkably reduced. The main reason for this can be found in the necessity to create multi-dimensional weighted decision trees when doing a direct simulation. As an example, again the passing of a specific route segment and the calculation of the most probably upcoming sea states can be given. In order to directly simulate all possibilities and assuming a random generator, that would be able to perfectly reflect any given sea state distribution, the calculation of 10^6 cycles would be needed, resulting in a decision tree with the same number of branches. Even though branches with the same descriptor values (which sum up to $22 \cdot 20 = 440$) could be united and given a corresponding weighting, another 440 branches would diverge from each of the branches created within the previous segment, if the vessel proceeds to the next route segment. It can be seen that the number of branches equals the number of possible decisions per descriptor to the power of the number of route segments. Resulting, in case of already ten segments, the number of sea state branches would rise to $2.72 \cdot 10^{26}$ and in case of 100 segments to $2.21 \cdot 10^{264}$. If furthermore kept in mind that any further descriptor increases the number of possible decisions by multiplication, the decision tree grows too big to be computed at justifiable efforts or within a reasonable amount of time. The MCM reduces the needed resources as it does not simulate all possible developments but only a sufficient number of random samples. Even in case the MC simulation would need the same number of cycles as there are branches in the decision tree, their computation can be handled a lot easier due to the fact that each cycle can be treated independently from the others.

One important question when dealing with Monte-Carlo methods is, how many cycles are sufficient, in terms of at least being needed in order to achieve accurate results. Accuracy in this case means a certain level of similarity when comparing the resulting distribution with the theoretical distribution. While the topic of general asymptotic behavior of sampling methods has been addressed in Witting and Müller-Funk (1995), a comprehensive meta study focusing on the Monte-Carlo sampling of simple distribution functions has been presented in Mundform et al. (2011). Therein, the authors come to the conclusion that there is no universal and

3. Scenario Development

scientifically justified procedure for estimating the required minimum number of MC cycles. Despite this, there are ideas of calculating the required MC cycles on the basis of the theoretical distribution's properties and the targeted confidence interval, but as the theoretical distribution in case of the scenario development remains unknown³, those approaches are not applicable.

In this context, the definition of a maximum number of MC cycles has been replaced by a minimum number in conjunction with a convergence criterion, both of which to be specified during the scenario setup. The minimum MC cycle number $n_{MC,min}$ can exemplarily be set by using a multiple of the maximum number of possible descriptor combinations, which in this case and only considering the ones being of interest for the objective operational profile would lead to

$$n_{MC,min} = m \cdot n_T \cdot n_v \cdot n_{H_{1/3}} \cdot n_{T_1}, \quad (3.17)$$

with m being an arbitrary factor and n_x indicating the respective number of possible manifestations of T , v , $H_{1/3}$ and T_1 . It has to be noted that while $H_{1/3}$ and T_1 are discrete descriptors with a fixed number of possible manifestations (22 and 20, respectively), the number of manifestations of the continuous descriptors T and v depends on the bin widths that have been chosen in order to create the histogram of operating conditions.

All descriptor combinations (with each of them forming a single operating condition) resulting during the scenario simulations will be added up onto a four dimensional histogram at the end of each MC cycle. Due to the law of huge numbers, it can be assumed that with an increasing number of MC cycles the histogram converges a specific, yet unknown distribution. In order to determine the degree of convergence, a measurement for the similarity of the current and the histogram of the last MC cycle is needed. Since every histogram can be interpreted as a vector, simple distance measurement methods like the *Euclidean distance* or the L_2 distance can be applied. An introduction to and a comprehensive survey on various PDF distance measuring approaches can be found in Cha (2007). Within this thesis, it has been decided to use the *Hellinger distance*, which is commonly used within the field of asymptotic statistics (for example for image retrieval). For two discrete probability distributions $P = (p_1, \dots, p_k)$ and $Q = (q_1, \dots, q_k)$ with equal bin widths, the *Hellinger distance* can be written as

$$H(P, Q) = \frac{1}{\sqrt{2}} \cdot \sqrt{\sum_{i=1}^k (\sqrt{p_i} - \sqrt{q_i})^2}. \quad (3.18)$$

Possible values of $H(P, Q)$ can be all real numbers between 0 (no difference) and 1 (total difference, meaning that all bins of P are zero and one or more bins of Q are non-zero). In Green and Xu (2005), it has been shown that the *Hellinger distance* in contrast to other histogram distance measurements (for example the L_2 distance) gives higher value to differences in smaller bins than to differences in bigger ones. The example given there introduces three histograms (A , B and C) as shown in Figure 3.22, whose probability distributions' *Hellinger distances* calculate to

$$H(A, B) = 0.0396, \quad (3.19)$$

$$H(A, C) = 0.0826, \quad (3.20)$$

$$H(B, C) = 0.0916. \quad (3.21)$$

³As all involved functions and distributions are known, the resulting distribution is theoretically computable, but not at reasonable expenses.

3. Scenario Development

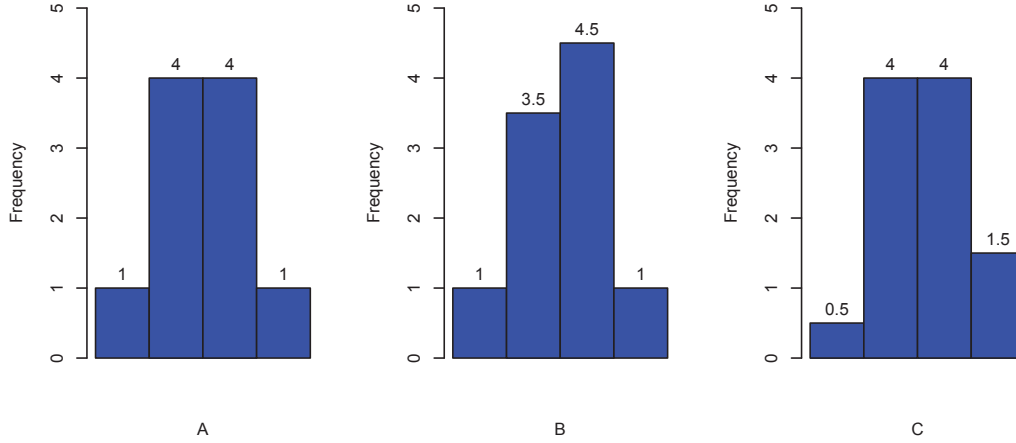


Figure 3.22.: Comparison of three histograms using *Hellinger distance*

It can be seen that the difference between A and B , whose lower bins are equal, is identified to be smaller than the difference between A and C , which equal in the higher and differ in the lower bins. Since the intention of the scenario method is to reveal and consider especially the more uncommon operating conditions, this behavior makes the *Hellinger distance* a suitable convergence criterion. Furthermore, the *Hellinger distance* only considers the relative distance between histograms. In case B and C are multiplied by an arbitrary factor, the distances between all three histograms would stay the same, which is a basic requirement for convergence detection. In case all bins of B and C are added an arbitrary constant (for example a value of 10), the *Hellinger distances* between these two and A increase and additionally assimilate, while the distance between B and C itself decreases,

$$H(A, B_{+10}) = 0.1847, \quad (3.22)$$

$$H(A, C_{+10}) = 0.1847, \quad (3.23)$$

$$H(B_{+10}, C_{+10}) = 0.0142. \quad (3.24)$$

When also applying the same addition to all bins of A , all *Hellinger distances* decrease in comparison to the ones of the original distributions, which is due to the fact that the distance between the respective bins become proportionally smaller,

$$H(A_{+10}, B_{+10}) = 0.0299, \quad (3.25)$$

$$H(A_{+10}, C_{+10}) = 0.0477, \quad (3.26)$$

$$H(B_{+10}, C_{+10}) = 0.0563. \quad (3.27)$$

Keeping this in mind, the *Hellinger distance* will decrease with increasing MC cycles. While possibly becoming zero in a few cases (if the outcome of one MC cycle exactly fits the overall distribution of the previous ones), it most certainly will converge a specific value. In Figure 3.23, the *Hellinger distances* over an exemplary Monte-Carlo simulation with 100 cycles is given. It can be seen that the development of the *Hellinger distance* converges to approximately $3 \cdot 10^{-3}$, which could be used as the convergence threshold for this specific example case.

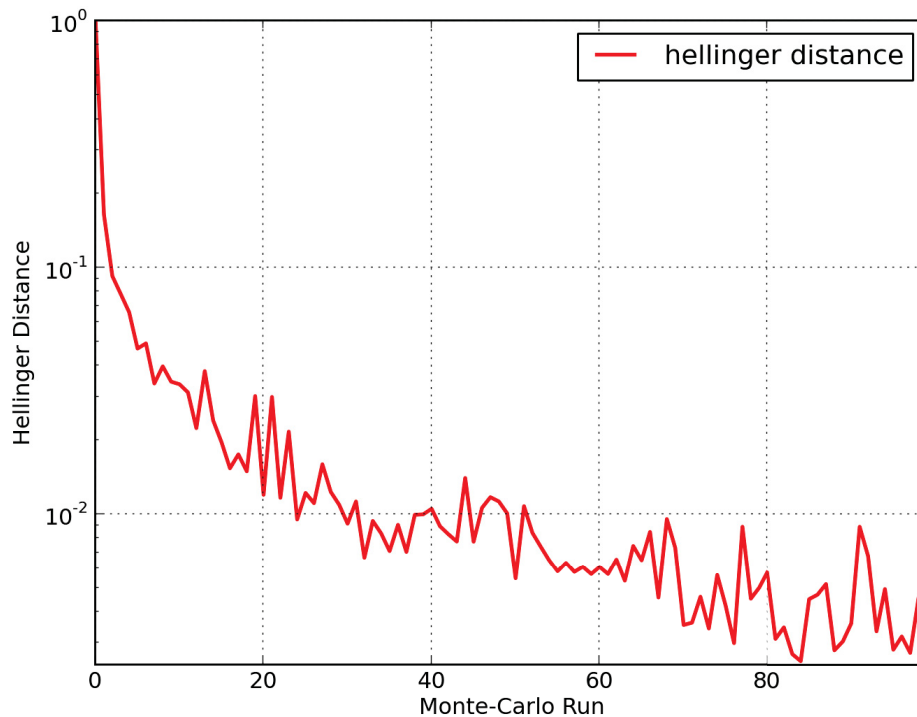


Figure 3.23.: Exemplary *Hellinger distance* development

Unfortunately, this value can not be considered to reflect a global indicator for convergence, since it is dependent on the problem setup and varies for example with the number of different sea areas, the development functions for fuel oil price and transport demand, the trade length, the binning, etc.. As the determination of a general formula for a problem-specific threshold value would need intensive analyses, in practice it is more applicable to set this value on the basis of experience. Examples of *Hellinger distance* values for different simulation setups can be found in Bronsart et al. (2016).

Within the approach presented in this thesis, the MC simulation will be stopped if the specified *Hellinger* threshold has been reached five times in a row (respecting the erratic behavior of its development) or the maximum number of MC cycles as specified within the scenario development setup has been reached.

3.6. Development of Objective Operating Conditions

The scenario development process results in a five-dimensional array containing the multivariate distribution of all operating conditions (OCs) the vessel has met during the simulations. Each operating condition is defined by specific information regarding

- speed,
- draught,

3. Scenario Development

- significant wave height,
- wave period and
- frequency of occurrence.

The first four values are binned according to specifications made during the scenario setup. The binning of the speed and draught values can be chosen freely by means of a specific bin width in combination with a maximum value. The bins will be determined by using the given maximum value as the center of the top bin and accordingly adjusting the following bins. Even though there won't come up for example speed values higher than the specified maximum, which lets the upper half of the last bin appear to be useless, this procedure has been chosen with respect to the following optimization as in general the mean value is considered to be representative for a bin and therefore chosen to be optimized onto. In case the maximum values would also reflect the upper boundaries of the last bins, the maximum speed or draught would not appear within the optimization, which would be inappropriate as those values should normally be the dominating ones within the top bins. In contrast to this, the binning of the sea state parameters depends on the shape of the sea state tables to be used within the development process (in this case the *Söding* tables, leading to 20 and 22 bins, respectively).

It has to be noted that the determination of the bin widths has a strong influence on the optimization's objective function, which has exemplarily been shown in Bronsart et al. (2016).

The last information contained within the array of operation conditions is the frequency of occurrence. As it has already been mentioned, there are two ways of determining this frequency. The first consists in summing up the time spent operating in the particular operating conditions, leading to a time-weighted distribution. In most cases where hull form optimizations are done with respect to multiple operating conditions, the focus is set on minimizing the vessel's resistance, power or fuel consumption. For these objectives, such time based distributions can be considered to be applicable and are usually used for determining the most relevant operating conditions. But considering the goal of finding a cost-optimized hull form, also the fuel oil price needs to be taken into account. Therefore, a second weighting is created based on the product of the time spent in the particular condition and the NPV of the fuel oil price at the time of the last refueling, which alters the frequencies' measurement unit from h to $h \cdot \$$. The scenario development outputs both variants, allowing to compare both results and to decide for one of them afterwards.

Regardless of which variant will be used, an important thing to be aware of when focusing on the probability of operating conditions is the consideration of joint instead of marginal probabilities. In Figure 3.24, an exemplary bivariate joint distribution of speed and draught values is given, indicated by I, II, III and a, b, c , respectively. The main peak is located at the combination (I, b) followed by (II, b) . The joint distribution is framed by the corresponding marginal frequency distributions, which can be derived by summing up the joint frequencies of the speed over the draught values and vice versa. It can be seen that a designer - when only using these marginal distributions - would most probably but wrongly consider the combination (II, b) to be the most relevant peak to optimize onto.

In order to determine a specific number of objective operating conditions, two different methods are offered. Using the first alternative, only a fixed number of operating conditions to be chosen needs to be specified. The algorithm will then evaluate the distribution from top down and stops after the given number has been reached. This approach is especially applicable if there are limitations regarding the duration or manageability of the following

3. Scenario Development

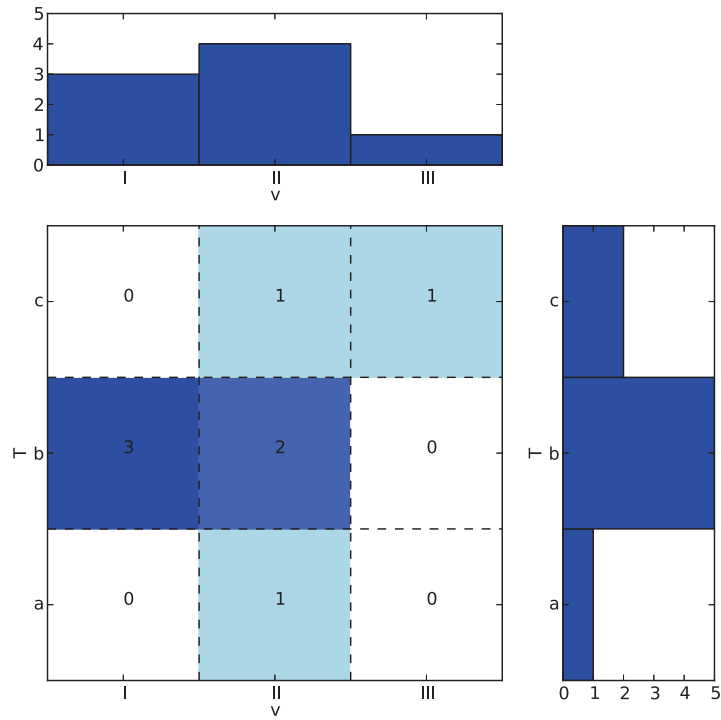


Figure 3.24.: Joint vs. marginal frequencies

hull form optimization. In that case, one would decide to consider only a limited amount of operating conditions at the expense of eventually not covering a sufficient percentage of the total operating time.

By using the second alternative, this percentage is the main concern as a minimum coverage of the total operating time can be specified. While not allowing to determine the resulting number of objective operating conditions, this approach assures a solid basis for the following optimization. On the other hand, it has to be noted that the number of objective operating conditions can quickly grow large, especially in case of a high coverage and small bin sizes.

Due to the fact that there is no use of including zero speed conditions (port and maintenance times), these will be filtered from the array before determining the objective operating conditions, regardless of the chosen method.

After determining the objective operating conditions, a weighting w with respect to the respective condition's relative occurrence frequency to the other chosen conditions is created, finally forming the optimization basis. An example of this basis that includes four operating conditions is given in Table 3.6. The objective function of the following hull form optimization with respect to the vessel's resistance would result to

$$\min \sum_{i=1}^4 R_{T,OC_i} \cdot w_{OC_i}, \quad (3.28)$$

3. Scenario Development

OC	v [kn]	T [m]	T_1 [s]	$H_{1/3}$ [m]	w [%]
1	20.50	14.00	4.00	1.75	28.00
2	18.50	14.00	6.50	1.75	25.62
3	20.50	14.00	4.00	1.25	23.91
4	23.00	15.00	4.50	1.25	22.46

Table 3.6.: Exemplary objective operating conditions

OC	v [kn]	T [m]	T_1 [s]	$H_{1/3}$ [m]	w [%]
1	20.50	14.00	4.00	1.75	31.09
2	23.00	15.00	4.50	1.75	27.57
3	18.50	14.00	6.50	1.75	24.04
4	20.50	13.50	5.00	1.75	17.30

Table 3.7.: Exemplary objective operating conditions including merged $H_{1/3}$ bins

with R_{T,OC_i} being the total resistance and w_{OC_i} the weighting of the respective operating condition.

In order to reduce the amount of operating conditions within the objective function, specific filters can be applied to the data. If for example a large container vessel mostly meets minor wave heights not significantly influencing its resistance, it is recommendable to merge all wave heights smaller than a specific threshold into one bin, which - in case of a coverage-based creation of the objective function - results in less operating conditions to be considered and therefore in a decreased optimization time. Vice versa in case of a fixed number of operating conditions, the corresponding coverage can be increased. Additionally, any particular or even a range of operating conditions (for example all conditions featuring an extremely low draught or high wave heights) can be excluded.

Based on the example presented in Table 3.6, merging all bins with significant wave heights smaller than 1.75 m into one bin results in the distribution given in Table 3.7. It can be seen that both $20.50\text{ kn} / 14.00\text{ m}$ conditions have merged into a single condition, while a new operating condition again with a speed of 20.50 kn but with a slightly lower draught has come up due to the fixed number of objective operating conditions. It can furthermore be noticed that the ranking order of the previous operating conditions number 2 and 4 has been swapped, which indicates that the vessel operates on higher speed in route segments with significant wave heights $\leq 1.25\text{ m}$ and on lower speed in segments with bigger waves.

This behavior proves the earlier mentioned strong influence of the bins' widths and positions onto the final objective function.

4. Proof of Concept

Within this chapter, the basic functionality of the methods developed in Chapter 3 will be demonstrated. Therefore, stripped down example cases will be used that allow to emphasize certain capabilities of the program but on some points might not reflect realistic assumptions or recommendable setups for a real life application.

Examples for the latter one can be found in Chapter 6, where the application and the results of both, the scenario development and the subsequent hull form optimization will be presented.

Additionally to the brief proof of concept, comprehensive studies on the functionality and sensitivity of the scenario development methodology have been done in the course of *PerSee* and been published in Bronsart et al. (2016). Therein, detailed analyses on the response of the objective operating conditions due to variations of the descriptors *fuel oil price*, *oil price crises probability* and corresponding characteristics, *transport demand*, *service time horizon* and *number of Monte-Carlo cycles* have been carried out.

4.1. Trade

In a first step, the correct reproduction of the original transport task is shown. Therefore, an exemplary trade description consisting of six segments with two of them being ports has been set up, whose details are given in Table 4.1. The trade has been designed in a way that makes it comprehensible and allows to easily keep track of all changes resulting from later to be added influences. Keeping that in mind, the trade features two distinctive speed / draught combinations, both being served for 200 hours as long as there aren't any disturbances. The trade furthermore leads through two distinctive sea areas, which will not become important until Section 4.3. The - referring to Section 3.3.1 - missing parameters have been omitted, kept on constant values or set to zero in order to keep the example as simple as possible. The time horizon spans 420 *h*, while any influence due to weather conditions, fuel oil prices or transport demand has been suppressed for the same reason and will later be dealt with in Section 4.4.

After running through 1000 Monte-Carlo cycles, the method indicates the top ten operating conditions presented in Table 4.2 (w_{Total} thereby indicates the share of each condition in relation

Segment	Type	Sea Area ID	Distance [nm]	Speed [kn]	Draught [m]
1	Port (10 <i>h</i>)	–	0	0	8
2	Transit	10	1000	10	8
3	Transit	79	1000	10	8
4	Port (10 <i>h</i>)	–	0	0	10
5	Transit	10	1200	12	10
6	Transit	79	1200	12	10

Table 4.1.: Example trade characteristics

4. Proof of Concept

v [kn]	T [m]	T_1 [s]	$H_{1/3}$ [m]	w_{Total} [%]
10.00	8.00	4.50	1.25	3.55
12.00	10.00	4.50	1.25	3.20
12.00	10.00	4.50	0.75	3.12
10.00	8.00	4.50	0.75	3.02
10.00	8.00	5.00	1.75	2.95
10.00	8.00	3.50	0.75	2.38
12.00	10.00	5.50	1.25	2.20
12.00	10.00	3.50	0.75	2.15
10.00	8.00	5.50	1.25	2.10
12.00	10.00	5.50	1.75	2.08

Table 4.2.: Exemplary objective operating conditions (initial case)

v [kn]	T [m]	w_{Total} [%]
12.00	10.00	48.65
9.00	8.00	27.03
10.00	8.00	24.32

Table 4.3.: Exemplary objective operating conditions (with local speed restriction)

to the total service time). These ten conditions have an overall share of 26.75%. It can be seen that - neglecting the varying sea state conditions - only the two expected speed draught combinations appear. Merging all sea states into one bin eventually leads to 10 kn / 8 m and 12 kn / 10 m, each with a share of exactly 50%. It has to be noted that the port laying conditions (whose lay times sum up to a share of 4.76%) have automatically been filtered out.

While appearing to work correctly, in a next step local speed restrictions are added to the route description. To be precise, route segment 2 is now considered to only allow a maximum speed of 9 kn. The three resulting OOCs are given in Table 4.3 (note that for reasons of comprehension, the objective operating conditions will in the following be presented without considering sea state conditions). It appears that not only the conditions itself but also the weightings changed due to the speed restriction. Regarding the share of the 8 m draught conditions, this can be explained with the increased time the vessel spends within route segment 2 (111.11 instead of 100 hours). As it has been mentioned in Section 3.2, the simulation does not immediately stop at the end of the time horizon but waits until the vessel finishes the current segment. This behavior leads to an increase of the overall simulation time, as a result of which the share of segments 5 and 6 decreases from 50 to 48.65%. It should be noted that there is no catching up of the time being lost due to the restricted speed as the ship operator is considered to know the trade particularities and to plan his schedule accordingly.

In the next step, an additional draught restriction is added. Assuming the port of route segment 4 being limited to a maximum draught of $T_{max} = 7$ m, the objective operating conditions of Table 4.4 arise. As mentioned in Section 3.4.8, draught restrictions within any port have an affect on both, the previous as well as the subsequent route segments. Consequently, the vessel's draught has been adapted within all modeled transit segments, so that Table 4.4 only differs in the draught values from the previous OOCs, while the speed as well as the weightings

4. Proof of Concept

v [kn]	T [m]	w_{Total} [%]
12.00	7.00	48.65
9.00	7.00	27.03
10.00	7.00	24.32

Table 4.4.: Exemplary objective operating conditions (with local speed and draught restrictions)

remain the same.

While these simple use cases demonstrate the basic functionality and the correct reproduction of the trade modeling, further examples on the simulation of transport demand, fuel oil prices and weather conditions as well as the vessel’s response to these influencing variables will be given in the following sections.

4.2. Fuel Oil Prices

As the simulation of the transport demand and the fuel oil price follows the same methodology, the proof of concept will only be done for the latter one. In a first step, the correct implementation of the basic development function and the fluctuations shall be reviewed. Therefore, a constant FOP development of 10 \$/y with a starting value of 300 \$ has been assumed. This development function has been added a normally distributed fluctuation of 1 \$ per day, while the probability for upcoming crises has been set to zero. Summing up all simulated FOP developments after 1000 Monte-Carlo cycles, the picture given in Figure 4.1 arises. It can be seen that the simulation works as intended and the expected cone of developments opens up around the targeted end price of 310 \$. Instead of a constant linear development, liberating, dithering and even partially contrary developments can be spotted. This is further emphasized within Figure 4.2, where four single developments of the FOP simulation are highlighted. Beginning at the top left and proceeding to the down right, each plot represents an example for different development types. The first one indicates a development closely following the specified base function, while in the second example the targeted FOP of approximately 310 \$ is reached after a strong price increase between two phases of stagnation. Within the third example, the fuel oil price shows a behavior contrary to the base function, while in the last case a long period of alternating development prevents the oil price from reaching its intended level.

Following Equation 3.1, the overall fluctuation’s standard deviation is expected to result in

$$\sigma_{FOP} = \sqrt{365} \cdot \sigma_{\mathcal{N}(0, \frac{1}{3})} = 6.37 \quad (4.1)$$

at the end of the time horizon. Figure 4.3 shows the resulting distribution of fuel oil prices, clustered into 1 \$ bins and showing the predetermined typical flat progression of random walk-based simulation models. An analysis of the data indicates a FOP distribution that features a mean value of $\mu_{FOP} = 309.97$ \$ and a standard deviation of $\sigma_{FOP} = 6.33$ \$, which is considered to approve the simulation procedure.

In order to demonstrate the impact of crises onto the FOP development, the whole simulation has been run through again under the same conditions as before but with the consideration of crises. The corresponding characteristics have been specified to feature an occurrence frequency of 50 % per year and a normally distributed duration of 2920 h (one third of a year) with a

4. Proof of Concept

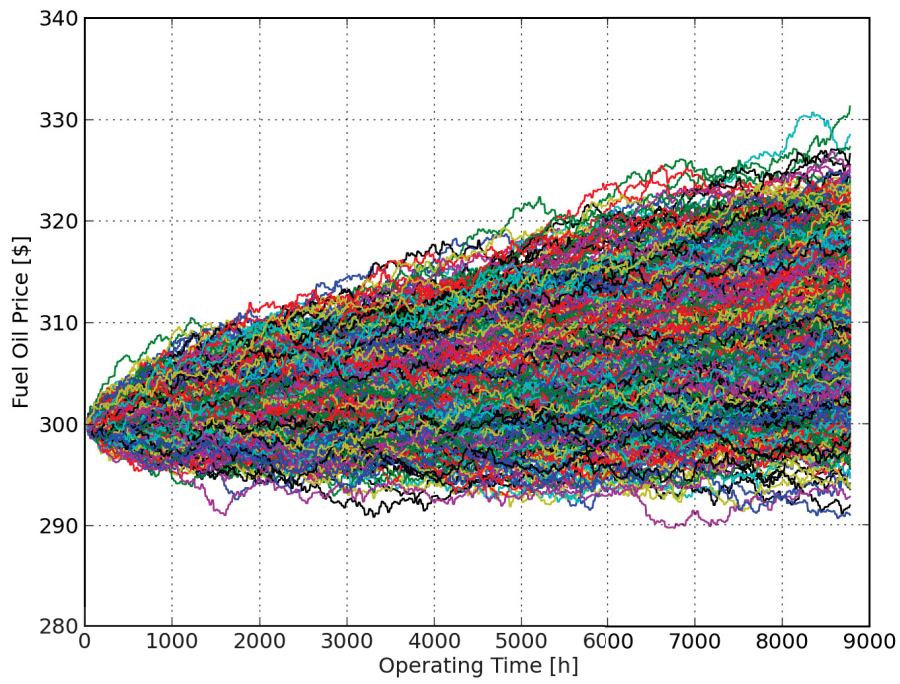


Figure 4.1.: Exemplary fuel oil price development after 1000 Monte-Carlo cycles

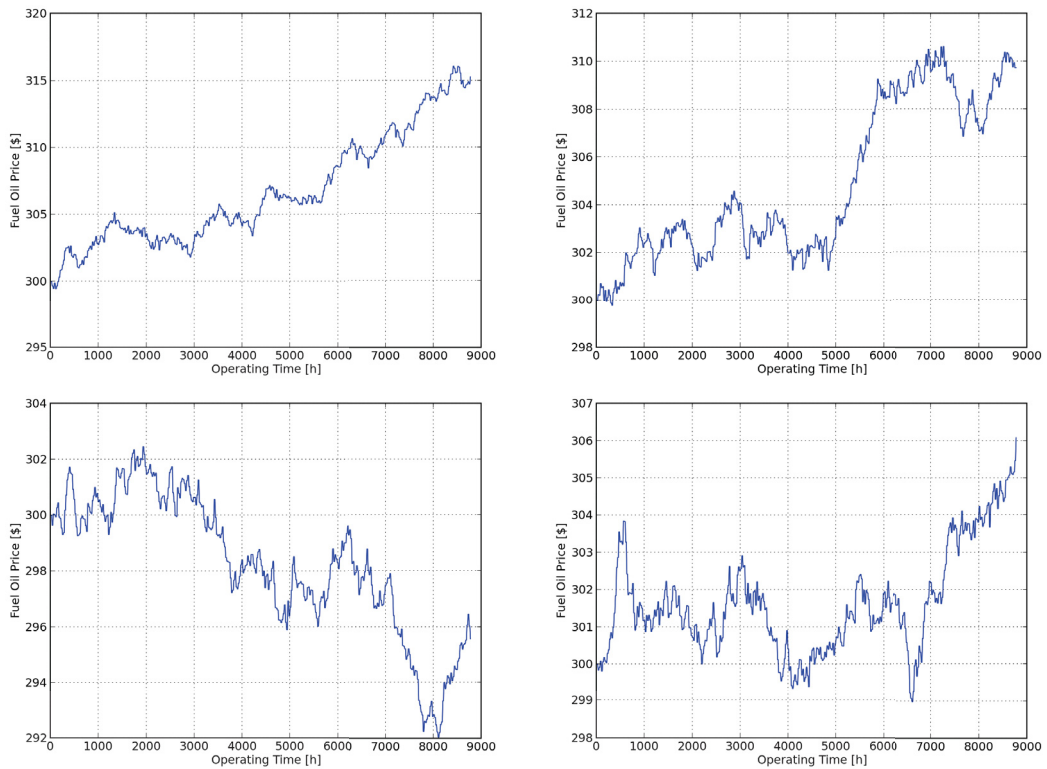


Figure 4.2.: Selected single fuel oil price developments

4. Proof of Concept

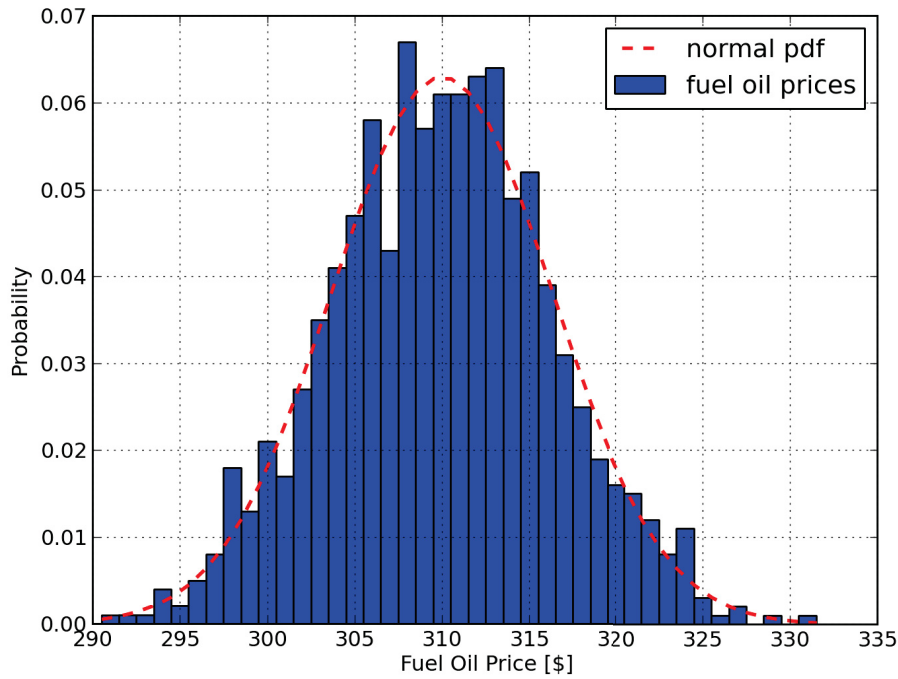


Figure 4.3.: Distribution of fuel oil prices after 1000 Monte-Carlo cycles. Red: normal distribution with $\mu = 309.97$ and $\sigma = 6.33$.

standard deviation of $1460h$. The probability for increasing prices has been set to 50%. The resulting FOP developments are depicted in Figure 4.4 and are - due to the high probability of crises appearances - dominated by segments of constantly in- or decreasing fuel oil prices. In order to further demonstrate the effect resulting from the crises simulation, Figure 4.5 exemplarily shows 4 out of the 1000 FOP developments. The upper two figures feature typical price drops with subsequent recoveries, while the lower left figure shows a contrary development and serves as a good example for a - except throughout the crisis period - development being closely related to the initial base function. The development of the bottom right example is interrupted by two shorter crises (although the duration of the second crisis appearance remains unknown) with rising prices and eventually reaches a FOP of 362 \$, which is one of the highest values of the whole simulation and makes this MC cycle easily identifiable within Figure 4.4.

Summing up all simulated price developments, it appears that the distribution of the prices at the end of the time horizon has grown wider, which is also reflected in the distribution's characteristics that veer away from being normally distributed (see Figure A.2 in the Appendix). While the mean value ($\mu_{FOP} = 309.74$ \$) almost remained the same, the minimum and maximum values changed to 234.86 and 393.91 \$, respectively. The same applies to the standard deviation that more than tripled to $\sigma_{FOP} = 21.16$ \$.

While the simulation of the fuel oil prices (and correspondingly the transport demand) has been proven to function as intended, its impact onto the vessel's operation will be presented in Section 4.4.

4. Proof of Concept

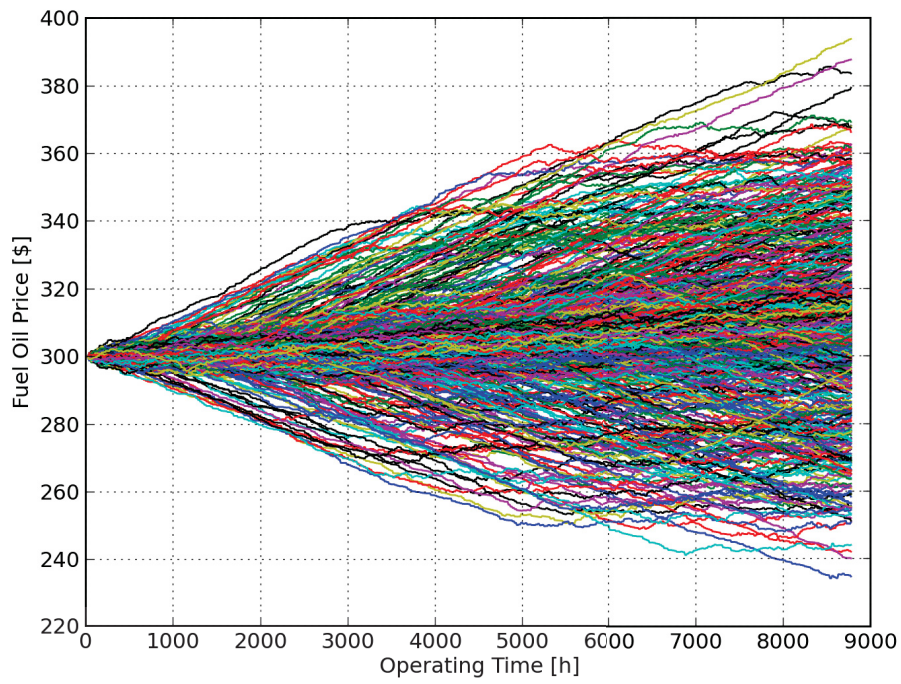


Figure 4.4.: Exemplary fuel oil price development including crises after 1000 Monte-Carlo cycles

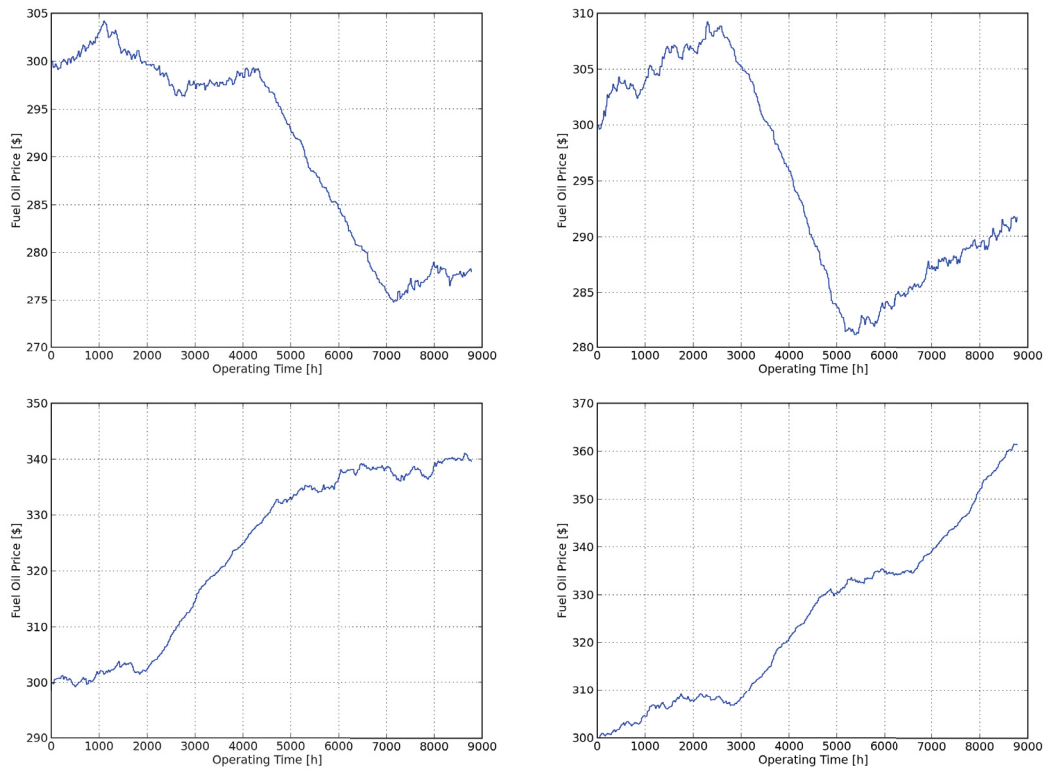


Figure 4.5.: Selected single fuel oil price developments including crises

4. Proof of Concept

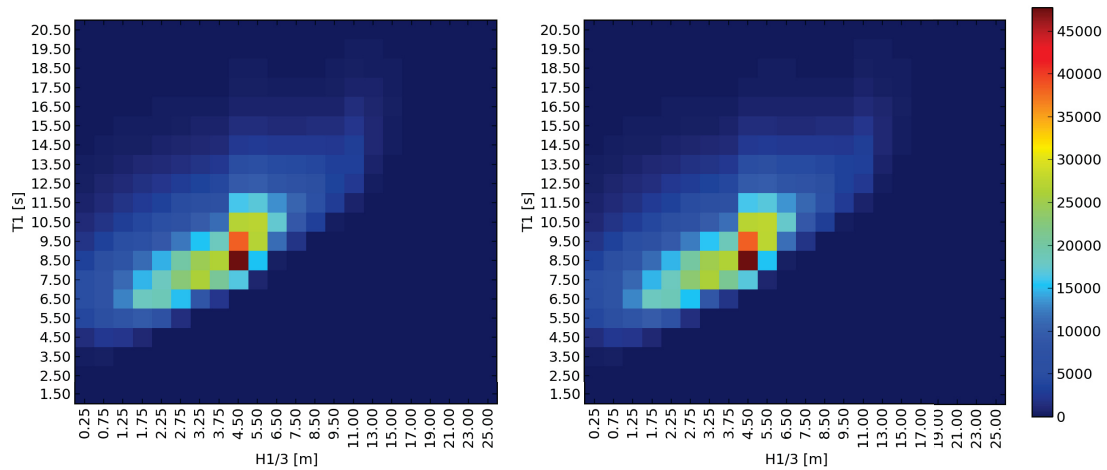


Figure 4.6.: Comparison between original (left) and simulated (right) sea state distribution. Both distributions match well in their overall tendency, small differences can only be noticed when focusing on comparatively rare combinations.

4.3. Weather

In order to proof the correct reproduction of weather conditions, a simple testing route consisting of a single route segment has been set up. This segment features seaway point 10 (located within the South Pacific Ocean) and will be run through 10^6 times. The resulting distribution of wave heights and periods is supposed to - of course not exactly but at least in its tendency - match the original distribution. Figure 4.6 shows both histograms, the original and the one resulting from the simulation. It can be seen that both bear good resemblance to each other, that would increase even further in case the number of simulations rises.

4.4. Vessel Response

The vessel's response with respect to the development of transport demand and fuel oil prices will be demonstrated by the help of the initial exemplary trade used within Section 4.1. Therefore, a linear yet unrealistically steep developing transport demand will be added that allows to identify resulting draught changes within the specified time horizon of 420 hours. Almost the same applies to the FOP development, albeit the development function features a discontinuity, which could be thought of as an additional environmental fee on HFO coming into effect during the vessel's service. In order to avoid a blurring of the demonstration, the fluctuation rate of both parameters has been kept at a low level, while the appearance of crises has been suppressed completely. The interest rate has also been omitted for the same reason. Summing up, the economic development parameters are given in Table 4.5. These specifications should lead to a draught increase of approximately 10% as of the visit of the second port, while the FOP will not have any influence onto the objective operating conditions as long as the scenario setup lacks any slow steaming instructions.

This assumption is approved by the resulting OOCs listed in the upper part of Table 4.6. Therein, only two operating conditions appear, each with a share 50%. The first one equals the

4. Proof of Concept

Parameter	Value	Unit
$FOP(t)$	300.00	\$
$fluc_{FOP}$	$t \cdot (1.00/24.00 h)$	\$
$TD(t)$	$t \cdot 10.00$	%
$fluc_{TD}$	$t \cdot (1.00/24.00 h)$	%
$P_{FOPCrisis}$	0.00	%
$P_{TDCrisis}$	0.00	%

Table 4.5.: Exemplary economic scenario development parameters

	$v [kn]$	$T [m]$	$w_{Total} [\%]$
no FOP	10.00	8.00	50.00
consideration	12.00	11.00	50.00
with FOP	12.00	11.00	57.69
consideration	10.00	8.00	42.31

Table 4.6.: Exemplary objective operating conditions (with and without considering fuel oil prices)

conditions resulting from the first two transit segments, which are not affected by the developing transport demand (as per definition the starting value of the TD development applies within the first port). When visiting the second port, the draught is modified on the basis of the current transport demand, whose mean value at that point is around 10%. Accordingly, the draught increases from the initial 10 to 11 meters.

Within the lower part of Table 4.6, the impact of the fuel oil price onto the objective operating conditions is reflected. Due to the higher fuel costs to be paid for the second part of the trade, the weighting shifts towards these more cost-intensive segments, ranking the operating condition with the increased draught approximately 15% higher than the unmodified one. As this condition does not appear within the initial trade description while having the largest share within the resulting objective operating conditions, this use case serves as a good example for the scenario method's capability for revealing future operating conditions that would otherwise not have been considered within the vessel's hull form optimization.

Regarding the FOP-based weightings, the influence of ECAs and the number of refueling ports is of further importance. In case trade segment 5 is assumed to completely pass through an emission control area while the price difference between HFO and MGO accounts for 250\$, the weightings of the OOCs that consider fuel oil prices diverge even further to 61.74 and 38.26%, respectively. The opposite can be observed if the type of the second port (segment 4) changes from the current status of a refueling port to a standard port. Resulting, the only fuel costs that will be taken into consideration for determining the OOCs' weightings are those of the fuel being bunkered at the first port. It has to be noted that the indicated emission control area still leads to a superior weighting of the latter transit segments (55.56 compared to 44.44%), as the vessel's operator is supposed to bunker prior to serving the next trade segment.

In order to depict the vessel's response to slow steaming decisions, a threshold of 350\$ has been added to the scenario development parameters of Table 4.5, at which the service

4. Proof of Concept

	v [kn]	T [m]	w_{Total} [%]
no FOP	11.00	11.00	52.17
consideration	10.00	8.00	47.83
with FOP	11.00	11.00	60.00
consideration	10.00	8.00	40.00

Table 4.7.: Exemplary objective operating conditions (considering slow steaming)

	v [kn]	T [m]	w_{Total} [%]
	11.00	11.00	48.92
	10.00	8.00	44.73
no FOP	8.00	11.00	2.23
consideration	8.00	8.00	1.94
	13.00	11.00	1.16
	18.00	8.00	1.01
	11.00	11.00	56.06
	10.00	8.00	37.60
with FOP	8.00	11.0	2.56
consideration	8.00	8.00	1.63
	18.00	11.00	1.16
	13.00	8.00	0.98

Table 4.8.: Exemplary objective operating conditions (considering slow steaming and weather conditions)

speed should be limited to 11 kn. Without considering the ECA influence, the OOCs given in Table 4.7 come up. According to this, the vessel sticks to the specified slow steaming speed while passing segments 5 and 6, due to the fuel oil price of 400 \$ in the second port. Resulting, the corresponding operating conditions increase in their weightings, both with and without including fuel oil prices. It should be noted that this result can only be achieved if the second port has been marked as a main port. In case it had been chosen to only represent a standard refueling port, there would be no reaction to the slow steaming instructions at all.

In a last step, the weather's influence onto the vessel's operating conditions will be demonstrated. As stated in Section 4.1, route segment 3 and 6 feature a sea area with comparatively calm conditions (seaway point 79). According to the scatter tables, there won't appear wave heights bigger than 8.50 m, which are a lot more common within the route segments 2 and 5, due to their assigned sea area 10. Therefore, a speed reduction on 8 kn has been applied in case the vessel meets seaways with $H_{1/3} > 8.50$ m. In order to ensure an accurate sea state sampling, the number of Monte-Carlo cycles has been increased to 10^6 . The resulting objective operating conditions are presented in Table 4.8. As given there, six new conditions (combining speeds of 8, 13 and 18 kn with draughts of 8 and 11 m) appear. Evidence for the two slower conditions being caused by reaching a wave height threshold can be found in Figure 4.7, where the vessel speeds are plotted against the simulated wave heights. While on the left side a range of speeds from 10 to 18 kn can be found, a distinct cut can be identified at the specified threshold value.

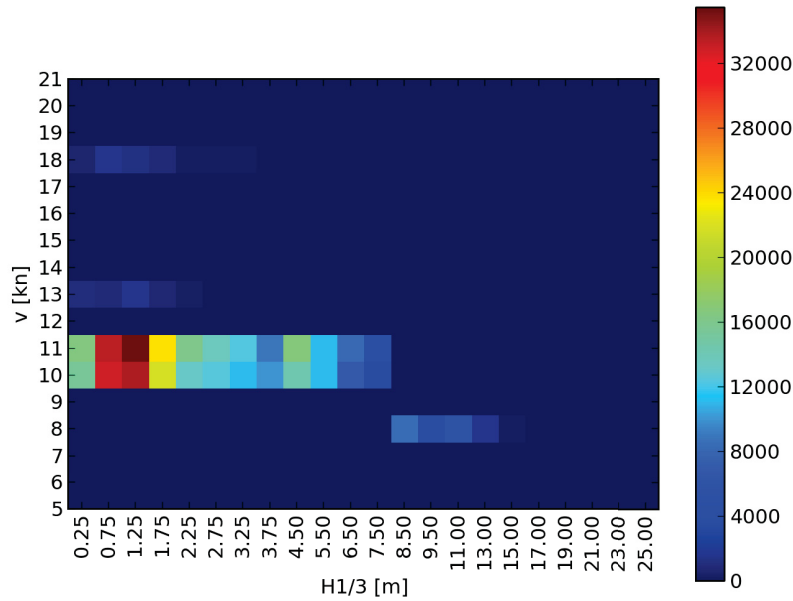


Figure 4.7.: Exemplary distribution of speed and wave heights

The remaining, faster conditions result from the need to keep the schedule.

In order to explain the resulting weightings, the simulation needs to be split up into its single route segments. When passing the first half of the transit passage (segment 2), the vessel potentially meets rough sea states, due to which its speed decreases to 8 kn . While causing a delay of 25 hours, this time needs to be made up for within the second half of the route segment. In order to arrive at port in time, the vessel speeds up to approximately 13 kn , allowing it to pass the 1000 nm within 75 hours. The chance of this situation to come up results from the *Söding* scatter tables (point 10) and calculates to 3.76%. When arriving in the second port, the fuel oil prices have met the slow steaming threshold, leading to a speed reduction onto 11 instead of 12 knots. In case the vessel again meets wave heights higher than 8.50 m during route segment 5, the transit time increases from 109.09 to 150 h^1 . In order to keep schedule, a speed of slightly more than 17.5 kn (due to the bin width of 1 kn classified into the 18 kn bin) is needed for arriving at port in 68.18 hours.

A detailed overview on the possible operating conditions along the trade and their corresponding probabilities is given in Table A.1 in the Appendix. Based thereon, the theoretical objective operating conditions (without considering fuel oil prices) calculate as given in Table 4.9. It can be seen that the ranking order as well as the theoretical weightings correspond to the simulated values. The minor deviations to Table 4.8 attribute to the stochastic nature of the simulation method. It should be noted that the condition featuring 18 kn - even though being operated on for a shorter period than the 13 kn condition - ranks higher when considering the fuel oil prices within the weightings.

¹As it has been mentioned in Section 3.4.3, potential slow steaming decisions do not trigger any speed-ups. Therefore, the targeted travel time for the 1200 nm segment amounts to 109.09 instead of 100 hours.

4. Proof of Concept

v [kn]	T [m]	w_{Total} [%]
11.00	11.00	50.00
10.00	8.00	45.83
8.00	11.00	1.34
8.00	8.00	1.13
13.00	8.00	0.69
18.00	11.00	0.61

Table 4.9.: Theoretical objective operating conditions (without fuel oil prices)

5. Implementation

Within this chapter, the implementation of the three example cases presented in the next chapter will briefly be illustrated. The overall scenario and optimization procedure follows the sequence previously given in Figure 3.2 on page 31. The algorithm dealing with the scenario development has been written in *Python 2.7* (Python Software Foundation, 2015), due to its characteristics of being open source and platform independent and its ability to offer comprehensive mathematic and stochastic libraries as well as support for multi-core execution.

The tools for evaluating and analyzing the results of the scenario development have furthermore been implemented in the statistical programming language *R*, which provides a wide variety of statistical and graphical modeling, testing, time-series analyzing and plotting techniques (The R Foundation, 2016). As well as *Python*, *R* is open source and runs on almost any platform.

The optimization part has been realized by the help of the *CAESES* modeling and optimization framework (FRIENDSHIP SYSTEMS AG, 2016). The framework allows a parametric modeling approach and offers an easy connection to external software tools. Furthermore, a wide range of Design of Experiment (DoE) and optimization algorithms are provided, making it possible to conduct and control the complete optimization task including the handling of in- and output files processed by the *CAESES* framework.

5.1. Scenario In- and Output

The input for the scenario development consists of three ASCII text files, each containing the trade description, the seaway scatter tables and the general settings including vessel-related information (such as service time, minimum and maximum draught or maintenance data), development functions and crises parameters as well as uncertainties and control commands. The scenario development output usually consists of

- the complete histogram data, with and without consideration of FOPs, each in form of a *Python* binary and a human readable ASCII file,
- a list of the objective operating conditions, in the same way as above with and without FOP consideration in form of an ASCII file.

In case of any filtering or merging of specific bins, additional output files concerning the histogram data as well as the objective function will appear. Furthermore, graphical output regarding FOP, TD and *Hellinger* criterion development accompanied by three-dimensional slices of the histogram data can be generated.

The - with respect to the optimization process - most relevant output consists in the list of objective operating conditions. Unfortunately, this list can not automatically be processed by the *CAESES* framework. Therefore, the optimization task (meaning the creation of the objective function that covers the number of computations to be done as well as their respective parameter configurations and weightings) needs to be set up manually.

5.2. Ship Model

Generally, all vessels used within this thesis have been modeled in *CAESES* on the basis of original line drawings or offset tables (in case of already existing vessels) or recreated from Initial Graphics Exchange Specification (IGES) files. Thereby, most parts of the hull form have been chosen to be modeled statically. The parametric modeling of the hull forms has been done with a focus on the bow region and especially the bulbous bow of the respective vessels only. It has been decided to exclusively apply hull form changes to this region due to its high influence onto the vessel's wave resistance and in order to keep the number of optimization parameters small. The specific details of the bow area modeling of each vessel will be given in the respective sections in Chapter 6.

5.3. Resistance Calculation

Within all examples presented in Chapter 6, the main focus of the optimization has been set on the respective vessel's total resistance (in- and excluding added resistance). Due to the fact that these examples have been done in the course of two different research projects and at three different facilities, varying methods and solvers have been applied.

The resistance calculations have been carried out by the help of two potential flow code solvers. In all exemplary cases it has been decided to not include Reynolds-Averaged Navier-Stokes Equation (RANSE)-based methods due to limited computational resources in conjunction with time constraints within the research project's schedules.

GL Rankine

Within the research project *PerSee*, the free surface potential solver *Rankine* developed by the DNV GL has come into operation. This program is capable of calculating calm water as well as added resistance of vessels on the basis of the *Rankine* panel method. For input, the program needs a hull form description in STL and some controlling data in XML format. The hull form is added an unstructured panel grid that covers the wetted surface up to the steady flow waterline, while the free surface is discretized by a block-structured grid that automatically adapts to the current wave length if necessary. After modeling the flow via *Rankine* point sources, *GL Rankine* calculates the vessel's calm water pressure distribution and wave resistance, its seakeeping behavior (up to first order) and resulting its added resistance as well as side drift forces in waves. As a faster alternative for determining the seakeeping behavior at low speeds, a linear seakeeping module based on zero-speed *Green functions* is offered (von Graefe et al., 2014).

The interaction between *GL Rankine* and the optimization framework has been modeled with the help of the *Software Connector* included within *CAESES*.

Shipflow

SHIPFLOW is a commercial free surface potential flow solver initially developed at the Swedish *SSPA* and currently being developed and sold by *FLOWTECH* (FLOWTECH International AB, 2015). It offers resistance calculations in both calm water and seaways via the modules *XPAN* and *MOTIONS*. Furthermore, thin turbulent boundary layer and RANSE calculations can be carried out but will not be used within this thesis.

5. Implementation

The hull form has to be handed over as a STL, IGES or offset file and is panelized by the internal meshing module *XMESH*, which is also responsible for the representation of the free surface. As above, *SHIPFLOW* then calculates the wave resistance by solving the *Laplace equation* along the singularities on the panels' surface, while the frictional resistance is computed by using the International Towing Tank Conference (ITTC) formula. The ship motions in seaways as well as the resulting added resistance are determined on the basis of non-linear boundary element methods, making the solver - in conjunction with its ability to threading - faster than conventional RANSE methods (FLOWTECH, 2015).

SHIPFLOW easily integrates into *CAESES*, as the framework offers a corresponding interface that allows the automatic exchange of all relevant in- and output data.

6. Optimization Examples

Within this chapter, the previously developed scenario-based optimization approach will be applied to three exemplary use cases, all of which differ in the type of vessel, its trade and the optimization objective and / or extent. While the first example especially focuses on the optimization's sensitivity to changes in the scenario development, the second optimization has its focus on the influence of considering more than one operating condition onto the vessel's hull form. The last example illustrates the method's usability for vessel types it has not specifically been developed for. Two of the example surveys have been carried out within the research project *PerSee* (and partially computed at participating facilities), while the remaining one has been done in the course of a collaboration with a German shipping company.

For all examples a short introduction on the optimization task itself and further details regarding the respective vessel and its main dimensions, the model, the scenario setup and outcomes, the following optimization and the corresponding results are given. Additionally, sensitivity studies will be carried out in the first two cases.

Further examples on the implementation and application of scenario-based optimizations have been published in Kleinsorge et al. (2016), Wagner et al. (2014) and Tun (2015), but will not be discussed within this thesis.

6.1. Case One: Duisburg Test Case

The first use case consists in the optimization of the Duisburg Test Case and has been done in the course of the research project *PerSee*. The main objective of this project has not only been the first application of a scenario based hull form optimization, but also a set of analyses covering the optimization results' sensitivity to varying input parameters. As many of the presented calculations have been carried out within *PerSee*, a few parts - especially of Sections 6.1.5 and 6.1.6 - are based on data of the project's final report given in Bronsart et al. (2016). A concluding summary of the optimizations done within this project has also been published in Kleinsorge et al. (2016).

The optimization is subjected to the Duisburg Test Case (DTC), a 14 000 *TEU* post-panmax, single-screw container vessel initially developed for benchmarking and validation reasons of numerical methods (el Moctar et al., 2012). Its hull form has been provided with a bulbous bow, a large bow flare and stern overhang and features the main dimensions given in Table 6.1.

6.1.1. Ship Model

As already mentioned in the previous chapter, main parts of the hull form have been modeled statically. The static description of the hull form has been provided by the project partners in form of a STL file and imported into the *CAESES* framework. The modification of the bulbous bow area has been realized by the help of so called *Image Trimeshes* in conjunction with *Surface Delta Shifts*, which allow the application of a variety of transformations to the

6. Optimization Examples

Dimension (Full Scale)		
L_{pp}	[m]	355.0
B_{wl}	[m]	51.0
T_D	[m]	14.5
∇	[m ³]	173 467.0
c_B	[-]	0.661
S	[m ²]	22 032.0
v_D	[kn]	25.0

Table 6.1.: Main dimensions of Duisburg Test Case (el Moctar et al., 2012)

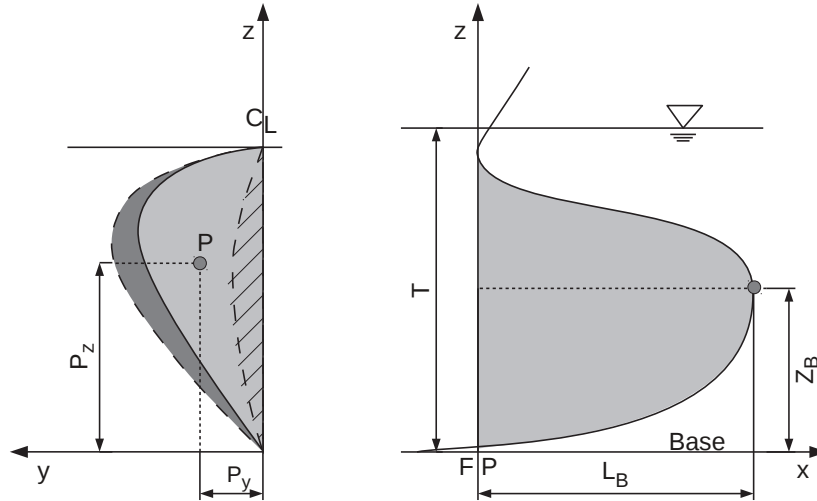


Figure 6.1.: Bulbous bow parameters. The dashed line represents the reference surface, whose curvature is controlled by the point P . A shift of P in transverse direction leads to a bow widening (marked in dark grey).

original STL geometry on the basis of user-defined surface coordinates. Further explanations on this modeling approach can be found in FRIENDSHIP SYSTEMS AG (2015). The bow area can be controlled via the parameters

- ΔL_B : transformation of the bulbous bow's tip in longitudinal direction,
- ΔZ_B : vertical transformation of the tip position,
- P_x : breadth shift in longitudinal direction,
- P_y : breadth shift in transverse direction,
- P_z : breadth shift in vertical direction.

These five parameters have been chosen according to the form-describing key factors of bulbous bows indicated by Kracht (1978). Their graphical representation and actual influence onto the hull form is presented in Figure 6.1. Figure 6.2 gives an impression on how the variation of the breadth parameter P influences the STL representation of the bulbous bow. In this context,

6. Optimization Examples

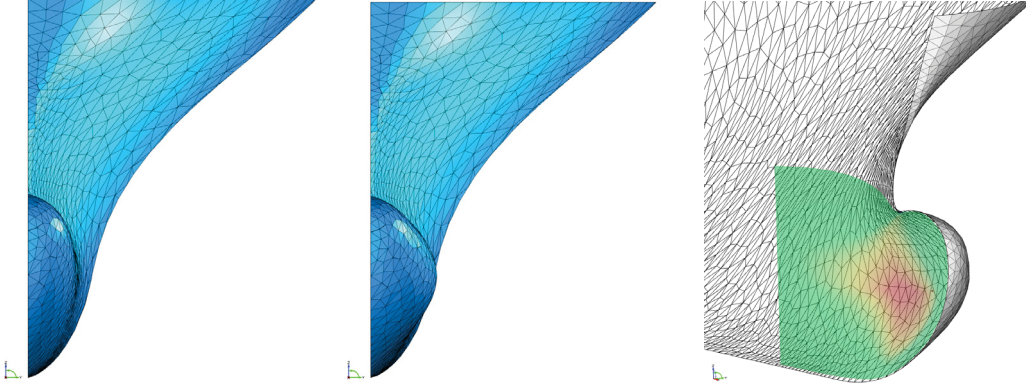


Figure 6.2.: Principle of bulbous bow breadth variation with $\Delta P_y = 3\text{ m}$. Left: original bow. Center: transformed bow. Right: provoking *Delta Surface* with heat map of transverse shift (Bronsart et al., 2016).

	ΔL_B	ΔZ_B	ΔP_x	ΔP_y	ΔP_z
Lower Bound	-4	-5	-10	-3	-5.75
Initial Value	0	0	0	0	0
Upper Bound	5	4	10	4	4.25

Table 6.2.: Boundaries of bulbous bow variation

it should be noted that in case of a breadth variation a ΔP_y of 3 m indicates the shift of the central control point of the reference surface (in this case a *B-Spline* surface) and therefore does not necessarily lead to a bow widening of the same length. In the above example, the 3 m shift of P_y results in a bow widening of 1.36 m , only. Further graphical examples on the working principle of the other parameters can be found in Section A.3.1 in the Appendix. In order to ensure a feasible design representation, parameter boundaries have been defined, which are given in Table 6.2.

The optimization focuses onto the DTC's effective power. The therefore required total resistance is determined using the potential solver *GL Rankine*. As it has - based on a series of RANSE calculations at varying draughts, speeds and sea states - been decided to not consider the added resistance due to its limited influence onto the vessel, the total resistance calculates via

$$R_T = (1 + k) \cdot R_F + R_W, \quad (6.1)$$

where R_F results from the ITTC 57 formula and R_W from the vessel's pressure distribution. The form factor has been determined to $k = 0.145$ on the basis of a range of RANSE calculations and is supposed to remain constant at all draughts¹. The hull form variations should also not notably affect the form factor, as they only apply to a small part of the vessel.

¹This assumption can be justified, as it will later be seen in Section 6.1.4 that the draught values contained within the objective operating conditions fall into a range of $\pm 1\text{ m}$ around T_D , at which changes in the hull form can be considered to stay at a moderate level.

6.1.2. Trade Description

Due to the fact that the DTC has initially been developed for benchmarking reasons only and has never been intended for serving a real trade, the transportation task to serve on had to be estimated on the basis of voyage data taken from similar vessels. Thanks to the contribution of a set of noon-to-noon reports from an Asian shipping company, an eastbound trading schedule serving the ports of

- Kaohsiung (China),
- Shanghai (China),
- Ningbo (China),
- Shekou (China),
- Tanjung Pelepas (Malaysia),
- Suez (Egypt),
- Piraeus (Greece),
- Felixstowe (United Kingdom),
- Rotterdam (Netherlands) and
- Hamburg (Germany)

could be developed. Thereby, all ports have been defined as possible refueling facilities, while Kaohsiung and Hamburg have been considered to be main ports. Additionally, the shipping company's maintenance facilities have been chosen to be located in Greece, nearby the port of Piraeus. A graphical representation of the trade is given in Figure A.5 in the Appendix.

The speed values of the respective transit segments as well as the port lay times have been derived on the basis of the given voyage data. According to these data, the vessel operates at almost 45 % of its time at speeds of 19.5 and 22.5 *kn*, both caused by the two-times passing of the comparatively long segment between Tanjung Pelepas and Suez on the way to and back from Europe. The remaining operating conditions are dominated by speed values ≥ 21 *kn*. In order to also determine the pilotage speeds, port schedules in conjunction with information on local port specifications have been utilized.

As the number of transported full and empty TEUs and FEUs as well as the corresponding draughts had been given within the reports, it has been decided to make use of the loading-draught-function as introduced in Section 3.4.8. Therefore, the loading conditions have directly been transferred into the trade description. The loading-draught-function has been approximated via a linear regression that resulted in

$$T = 7.8136 + (11.85 \cdot n_{full} + 2 \cdot n_{empty}) \cdot 6^{-5}, \quad (6.2)$$

with n_{full} and n_{empty} being the number of full and empty TEUs. This regression approach has been considered to be reasonably accurate as the hull form characteristics of the DTC differ from those of the provided ship in any case. Based on this input, the vessel is assumed to predominantly operate at draughts just below its designated design draught of 14.5 *m*.

6. Optimization Examples

$H_{1/3}$ [m]	4.5	5.5	6.5	7.5	8.5	9.5	10.5	11.5	12.5	13.5
v_{max} [kn]	22.8	20.6	18.4	16.2	14.0	11.8	9.6	7.4	5.2	3.0

Table 6.3.: Speed reduction due to wave height

The identification of the respective trade segments and their corresponding lengths has been done manually on the basis of graphical analyses. Therefore, an online routing and distance calculation tool (SeaRates LP, 2015) has been used for revealing the actual legs and corresponding travel distances. The results have then been matched to the seaway points defined by Young and Holland (1996) in order to detect the respective sea state areas, for which the *Söding* scatter tables have been processed in order to be usable for the scenario development program. Furthermore, the tables have been amended with a special sea area referring to port and inland waterways, where no considerable sea states are assumed. A picture of the allocation onto the seaway points can be found in Figure A.6 in the Appendix.

Regarding the local speed limitations a maximum speed of 10 *kn* has been assumed to apply for all pilotage segments. The maximum draughts have been determined via the respective port facilities' websites and vary between 13.5 (Shekou) and 19.0 *m* (Tanjung Pelepas). While passing the Suez Canal, a speed limit of 8.1 *kn* applies. Additionally, the vessel's draught is restricted to 18.56 *m*.

When traveling from Piraeus to Felixstowe, the vessel enters the North Sea (seaway point 116), which became an emission control area in 2005. As the vessel operates a few days within this area until it eventually leaves from Rotterdam back to Piraeus, the ECA indicator has been activated for all of these segments.

The complete route definition file as used for the scenario development process can be found in Section A.3.2 in the Appendix.

6.1.3. Scenario Setup

In order to allow the scenario development to have a noticeable impact onto the composition of the vessel's service, the service time has been decided to be set to ten years, even though this may not reflect a real life use case. For the sake of including leap years, the so-called *tropical year* equaling 8765.82 *h* has been used. The minimum and maximum draughts have been set to 10 and 16 *m*, while the maximum speed of 25 *kn* results from the vessel's main characteristics given in Table 6.1. A minimum speed has not been specified. The maintenance interval has - in accordance with a ship operator - been set to five years and the maintenance time to three weeks. The latter includes the time needed to move from the port of Piraeus to the maintenance shipyard.

Regarding the speed reductions caused by harsh weather conditions, it has been made use of the investigations done within *PerSee* (Riesner, 2013), whose results can be seen in Table 6.3. Due to lacking data on slow steaming decisions as a reaction to fuel costs, a simple assumption featuring speed reductions to 20, 18 and 16 *kn* due to fuel oil prices higher than 550, 600 and 700 $\$/mt$ has been made.

Coming to the economic aspects of the scenario setup, the development of the transport demand has been assumed on the basis of an analysis on the global container trade development presented by the United Nations Conference On Trade And Development in UNCTAD Secretariat (2015). From the corresponding graph of annual change as given in Figure 6.3 it

6. Optimization Examples

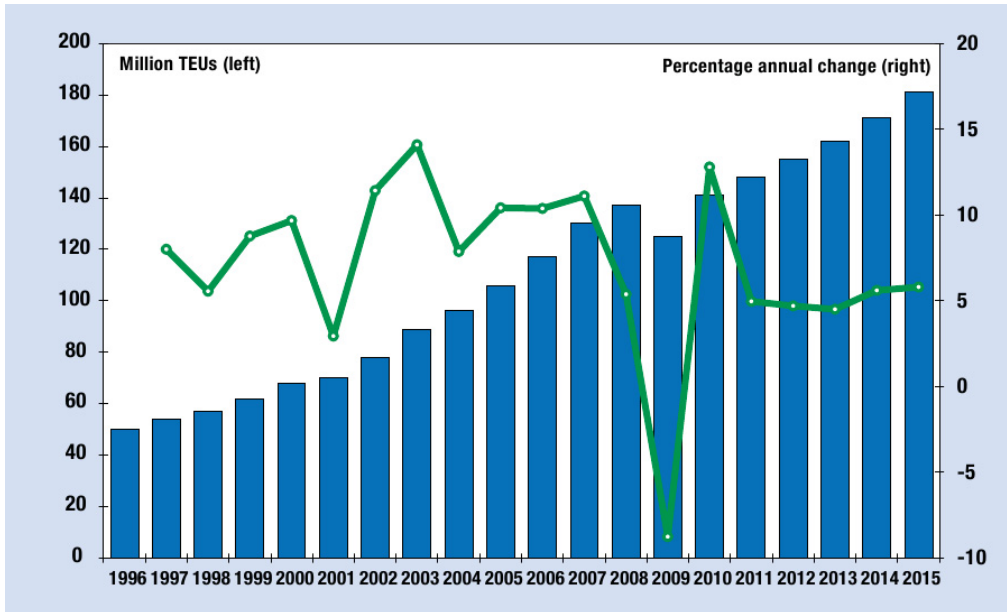


Figure 6.3.: Global container trade (UNCTAD Secretariat, 2015)

can be seen that the incremental growth rate of container trade for the post-crisis years can be averaged to approximately 5.0 % per year. It could be argued, whether this increase affects the loading conditions of single vessels or would rather be counteracted via the fleet management, but as there is no better data available, it has been decided to convert the growth rate at its face value onto the vessel's loading conditions. The properties of possible transport demand crises have also been determined on the basis of Figure 6.3. Resulting, a crisis is supposed to come up every seven and a half years at an average. Its duration follows a normal distribution with a mean value of one year and a standard deviation of two months. The probability of an increasing against a decreasing transport demand has been set to a ration of 1 : 3.

Regarding the fuel oil prices, it has been decided to model one year of constantly decreasing prices followed by a moderate increase until after ten years a FOP of approximately 675.00 \$/mt will be reached. The daily fluctuation rate has been set to 1.50 \$/mt as a result of external expertise from a German shipping company. As already mentioned within the Chapter 1, unexpected events regarding the development of fuel oil prices happen to appear within constantly shortening intervals. While the early FOP development before the year 2000 has only been interrupted by two oil crisis in 1973 and 1979 and the second Golf war in the 1990's, the occurrence frequency of fuel oil crises has notably risen since the Asian crisis in 1997 (see Figure 3.6 on page 38). This fact has been accommodated within the scenario setup by a crises occurrence probability of 40 %/y. As well as FOP crises are more likely to happen than those concerning the transport demand, they are considered to level out faster. Therefore, their averaged duration has been determined to be half a year. The corresponding standard deviation has been set to the same value, allowing for a wide range of crises durations.

In order to account for the higher fuel costs within the emission control areas, a constant HFO - MDO price gap of 250 \$/mt has been specified. Finally, the interest rate has been given a value of 3.0 %. A summary of all economic descriptors used for the scenario development of the DTC can be found in Table 6.4.

6. Optimization Examples

Parameter	Value
i_r	3.0 %
$FOP(t)$	$\begin{cases} 275.00 \$ - (50.00 \$/8765.82 h) \cdot t, & t \leq 8765.82 h \\ 225.00 \$ + (50.00 \$/8765.82 h) \cdot t, & t > 8765.82 h \end{cases}$
$fluc_{FOP}$	$(1.50 \$/24.00 h) \cdot t$
Δ_{FOP}	250.00 \$
$TD(t)$	$(7.50 \% / 8765.82 h) \cdot t$
$fluc_{TD}$	$(0.50 \% / 8765.82 h) \cdot t$
$P_{FOPCrisis}$	40.00 %
$P_{RiseFOP}$	50.00 %
$\mu_{FOPCrisisDur}$	4382.91 h
$\sigma_{FOPCrisisDur}$	4382.91 h
$P_{TDCrisis}$	13.33 %
P_{RiseTD}	25.00 %
$\mu_{TDCrisisDur}$	8765.82 h
$\sigma_{TDCrisisDur}$	1460.97 h

Table 6.4.: Economic scenario development descriptors

Regarding the scenario development methodology, the bin widths of the speed and draught values have been set to $0.5 kn$ and $0.5 m$, respectively. The draught will be calculated via the previously determined loading-draught-function. In order to keep the number of Monte-Carlo cycles n_{MC} as low as possible, a study on the impact of this number onto the ranking order of the resulting objective operating conditions has been carried out in Bronsart et al. (2016). This study revealed a ranking convergence of the top 33 operating conditions after a number of 25 000 MC cycles. Due to the fact that weather conditions will not be considered within the optimization, these 33 operating conditions covered more than 85 % of the vessel's total operational profile. Therefore, a n_{MC} of 25 000 cycles at the maximum has been considered to be sufficient. In case the scenario development reaches convergence faster than expected, the *Hellinger* threshold has been set to 10^{-10} . The minimum number of MC cycles has been set to 10 000.

The complete configuration file of the scenario development is given in Appendix A.3.3.

6.1.4. Objective Function and Optimization Setup

It has been decided to include a total of seven operating conditions within the objective function. Resulting from the scenario development, the seven objective operating conditions with an overall coverage of $w_{cum} = 46\%$ as presented in Table 6.5 arise. It has to be noted that the respective weightings have been calculated with considering the interest rate-adjusted fuel oil prices. The OOCs cover a wide range of speeds, from a Froude number of 0.14 to $Fn = 0.20$. It appears that the design speed does not show up within the top seven operating conditions, which can be seen as a confirmation of the statement made in Chapter 1. In general it can be seen that the operational profile is dominated by lower speeds than originally specified, which is a hint on the impact of rising fuel oil prices in conjunction with the long service horizon. This

6. Optimization Examples

	v [kn]	T [m]	w [%]	w_{cum} [%]
OC_1	16.00	15.50	10.78	10.78
OC_2	22.50	15.50	10.19	20.97
OC_3	18.00	15.50	7.61	28.58
OC_4	19.50	15.50	6.66	35.24
OC_5	19.00	14.00	4.66	39.90
OC_6	22.50	13.50	3.22	43.12
OC_7	19.50	15.00	2.88	46.00

Table 6.5.: Objective operating conditions (including fuel oil prices)

assumption is confirmed by the aggregation of all FOP developments as given in Figure 6.4 on page 88, which indicates a large number of FOPs crossing the slow steaming thresholds of 550, 600 and 700 Dollar. The distribution of the fuel oil prices at the end of the simulation horizon determines the share of FOP developments reaching at least one of the thresholds to 74 % (see Figure A.7). The question on how the objective operating conditions would look like without considering fuel oil prices will be addressed in Section 6.1.6.

The draught fluctuates around the design draught and covers values from 13.50 (appearing one time) to 15.50 m (four times), indicating a strong increase when keeping in mind that the draught has been limited to 15.50 m at maximum. This increase is owed to a constantly growing transport demand, which in average reaches a plus of $\approx 50\%$ at the end of the ten years time span (see Figure A.8 in the Appendix). After ten years, the vessel can be considered to operate fully loaded at all route segments. On the one hand, the lack of fleet management tools could be criticized at this point. On the other hand it could also be assumed that a ship operator will not acquire supplemental vessels until he reaches the capacity limit of his first ship.

The optimization goal consists in the minimization of the weighted effective power $P_{E,total}$ that calculates via

$$P_{E,total} = \sum_{i=1}^7 \frac{R_{T,OC_i} \cdot v_{OC_i} \cdot w_{OC_i}}{w_{cum}}, \quad (6.3)$$

with R_{T,OC_i} representing the total resistance of each operating condition, v_{OC_i} the corresponding speed and w_{OC_i} the operating condition's weighting.

Regarding the optimization algorithm it has been decided to use the Nelder Mead Simplex (NMS) method, which is closely related to the classic downhill simplex methods with the advantage of only evaluating the objective function itself instead of its derivative. A disadvantage of all simplex and related methods exists in their characteristic of often finding a local instead of the global minimum. In order to detect the global optimum of the objective function, the optimization process consists of two steps. Within the first step, a sobol algorithm, which produces quasi-random variations of the five design variables is run through 600 times. While the resulting quasi-random variants cover the whole design space, they shall be used to identify promising starting variants for a set of following NMS optimizations.

6.1.5. Results

Before discussing the newly developed hull form, it has to be noted that due to the high spread and the partly low Froude numbers of the OCs there have been difficulties to determine a fully

6. Optimization Examples

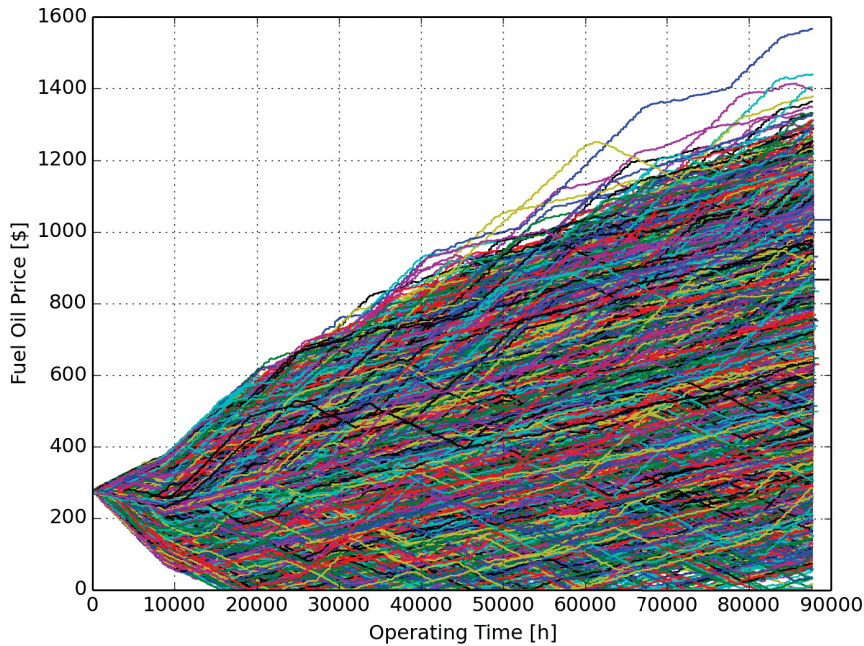


Figure 6.4.: Development of fuel oil prices of all 25 000 Monte-Carlo cycles

consistent configuration for the potential flow solver in order to produce accurate results at all OOCs. Even though the results have been verified against resistance model tests at design draught and a set of selected speeds (20 to 25 *kn*), all presented results should be perceived carefully.

Resulting from the optimization, a hull form with the bulbous bow parameters

- $\Delta L_B = -0.77$,
- $\Delta Z_B = -0.92$,
- $\Delta P_x = -1.60$,
- $\Delta P_y = -2.89$ and
- $\Delta P_z = 1.91$

has been developed. The new bulbous bow features a reduced length and a lowered bow tip, both of which are suspected to have happened in order to reduce the wetted surface and therefore the at lower speed values dominating frictional resistance. The same applies to the reduction of the bow's breadth via P_y and - with reservations - to the retraction of P_x . It should be noted that the impact of the design parameters P_x and especially P_z onto the vessel's resistance has been revealed to be almost insignificant.

While the initial hull form featured a weighted effective power of 20 737 *kW*, the $P_{E,total}$ of the optimized vessel has been decreased to 20 267 *kW*, equaling an improvement of 2.27%. In case this improvement might not be understood as a good result, it should be pointed out that these 2.27% relate to 46% of the vessel's total service time. In case one would seek to achieve

6. Optimization Examples

	v [kn]	T [m]	w [%]	w_{cum} [%]
OC_1	22.50	15.50	12.77	12.77
OC_2	19.50	15.50	7.09	19.86
OC_3	16.00	15.50	6.40	26.26
OC_4	19.00	14.00	5.61	31.87
OC_5	18.00	15.50	5.52	37.39
OC_6	22.50	13.50	4.13	41.52
OC_7	19.50	15.00	3.48	45.00

Table 6.6.: Objective operating conditions (excluding fuel oil prices)

the same performance improvement by optimizing onto a single operating condition only, he would have to reduce the effective power of - for example - OC_1 by 9.69%.

6.1.6. Sensitivity Analysis

In order to investigate the optimization's sensitivity with respect to changes in the scenario development, two surveys have been carried out within Bronsart et al. (2016), the first one focusing on the influence of the fuel oil prices and the second one targeting the number of operating conditions to be considered within the objective function. In the following, both results will briefly be summarized.

The objective operational profile without including fuel oil prices within the weightings has already been mentioned in Section 6.1.4. By removing the FOP influence from the weightings (while the influence on the slow steaming still remains), the objective operating conditions given in Table 6.6 arise. It appears that the distribution of these operating conditions is closer to the original route description. The two dominant speeds of 22.50 and 19.50 kn keep their leading position, while the combination of $v = 16.00$ kn and $T = 15.50$ m - in the previous case with a share of almost 11% representing the most common condition - diminished to 6.40%. This is due to the fact that omitting the FOP-based weighting mainly affects those operating conditions that are caused by high fuel oil prices. Therefore, the slow steaming as well as the ECA conditions have become less influential.

These modifications on the OOCs are reflected in modified optimum bulbous bow parameters. The best performing variant with respect to the seven only time-based operating conditions features the parameters

- $\Delta L_B = 1.36$,
- $\Delta Z_B = -0.76$,
- $\Delta P_x = 3.80$,
- $\Delta P_y = -1.59$ and
- $\Delta P_z = -0.11$.

The increased weightings of higher draughts result in a horizontally extended bow with its volume moved up front, representing a typical displacement bulbous bow. In the course of this, the weighted effective power could be reduced from $P_{E,total} = 22945$ kW to 22663 kW, equaling

6. Optimization Examples

No. of OOCs	ΔL_B [m]	ΔZ_B [m]	ΔP_x [m]	ΔP_y [m]	ΔP_z [m]	$P_{E,total}$
1	1.85	1.98	9.60	0.21	-2.68	32 168
2	1.90	0.91	-9.40	-0.59	-2.31	28 066
3	2.26	-0.71	-3.30	-0.76	3.39	24 288
5	1.68	-1.64	5.60	-1.89	3.84	22 243
7	1.36	-0.76	3.80	-1.59	-0.11	22 663

Table 6.7.: Best performing variants vs. number of objective operating conditions (excluding FOPs, Bronsart et al. (2016))

No. of OOCs	ΔL_B [m]	ΔZ_B [m]	ΔP_x [m]	ΔP_y [m]	ΔP_z [m]	$P_{E,total}$
1	1.30	-1.97	-7.60	-1.45	-1.87	17 079
2...7	-0.77	-0.92	-1.60	-2.89	1.91	n.a.

Table 6.8.: Best performing variants vs. number of objective operating conditions (including FOPs, Bronsart et al. (2016))

an improvement of 1.23%. In comparison to the hull form of the previous optimization, the bow characteristic changed notably, even though the changes in the objective operating conditions do not seem to be that severe. This issue can be solved by recapping that the optimization’s objective function targets the reduction of P_E instead of R_T . Hence, the vessel’s speed is included and serves as an additional multiplying factor for the faster operating conditions.

The second sensitivity study has been done with respect to the number of operating conditions considered within the objective function. Therefore, a set of optimizations onto one, two, three and five OOCs, each with and without consideration of the FOP-based weightings, has been carried out.

Starting with the optimization without FOP consideration, the best performing design variants of all five optimizations are presented in Table 6.7. When considering the top two operating conditions only, the vessel features an extended, comparatively wider bulbous bow with a risen tip, which is due to the domination of higher speeds. When increasing the number of objective operating conditions up to a value of five, the slower velocities’ influence grows, making the bow tip lower and the bow in general become more narrow. With the additional inclusion of two rather fast yet less influential conditions, this trend is slightly reversed, leading to the previously determined hull form. It should be noted that the behavior of the bow length could not finally be resolved. It appears logic to enlarge the bow at higher and to reduce it at lower speeds, which indeed applies to all cases except the optimization onto three operating conditions. It can only be assumed that the slightly increasing influence of the frictional resistance could be satisfied by the drastic lowering of the bow tip and the decreased width, both counteracting the bow’s extension in longitudinal direction.

In a second step, the optimization’s sensitivity with respect to varying numbers of objective operating conditions including the FOP-based weightings has been done. As it can be seen in Table 6.8, the best performing variant appears to be insensitive to the number of OOCs once the number gets bigger than one. The observed behavior can be explained with the structure of the objective operating conditions. While their speeds range from 16 to 22.50 *kn*, it could be seen in Table 6.5 that this bandwidth is already covered by the top two operating conditions.

6. Optimization Examples

Dimension (Full Scale)		
L_{oa}	[m]	231.0
L_{pp}	[m]	214.2
B_{wl}	[m]	32.2
T_D	[m]	12.0
∇	[m ³]	55 470.0
c_B	[-]	0.670
v_D	[kn]	25.0

Table 6.9.: Main dimensions of 3500 *TEU* container vessel

Representing the extreme objectives while additionally having the highest weightings, these conditions dictate the course of the optimization. This behavior could only be counteracted in case there was another single operating condition to optimize onto with a weighting being higher than one of the two extreme objectives.

Concluding, these sensitivity studies suggest that the decision on how many operating conditions to consider within the optimization’s objective function should not be made until the scenario development has been run through. Based on the structure and characteristic of the top ranked operating conditions, there are different optimization approaches that might save computational efforts without leading to worse results. Despite simply reducing the number of OOCs, similar or related conditions could be merged or temporarily omitted in order to subsequently verify the optimization results against these conditions.

6.2. Case Two: 3500 TEU Container Vessel

Within the context of this example, an optimization of the bow area of a 3500 *TEU* container vessel has been done. The whole process has been carried out on behalf of the vessel’s operator, a German shipping company. Originally being built as a panmax vessel, cascading effects arising due to the extension of the Panama Canal as it has already been described in Chapter 1 forced the displacement of the vessel from its initial trade to a service along the African and Asian coasts. Resulting from the shifting trade specifications, a whole new operational profile - mainly characterized by lower service speeds - developed, letting the original hull form and especially the bulbous bow area become ineffective. In order to cope with these changes, a scenario-based retrofitting has been targeted. The vessel’s main dimensions are given in Table 6.9, while the lines drawing is presented in Figure 6.5.

6.2.1. Ship Model

The ship model has been implemented within *CAESES* on the basis of a set of offsets, which have been supplied by the owning shipping company. The model features a ∇ -deviation of 0.14% in comparison to the original hull form and can be considered to be sufficiently accurate.

The modeling of the bulbous bow section has been done in the same way as described in the previous case with the exemption of using *Image Surfaces* instead of *Image Trimeshes*, due to the different surface representation approach. It has to be noted that - after an influence analysis and in order to decrease the computational calculation effort - only the design parameters L_B ,

6. Optimization Examples

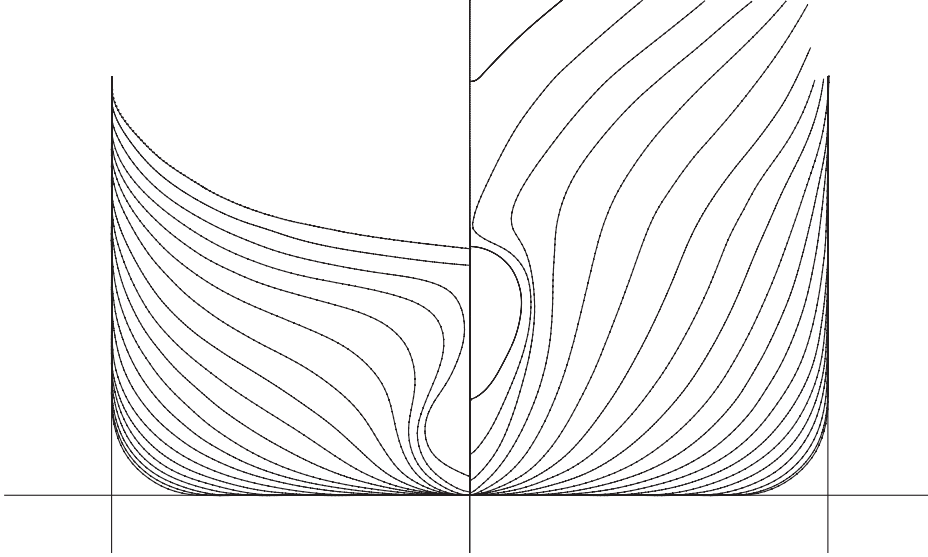


Figure 6.5.: Body plan of 3500 *TEU* container vessel

	ΔL_B	ΔZ_B	ΔP_y
Lower Bound	-2.0	-2.25	-1.5
Initial Value	0.0	0.00	0.0
Upper Bound	0.5	1.10	0.5

Table 6.10.: Boundaries of bulbous bow variation

Z_B and P_y have been varied during the optimization. The boundaries of these variations are given in Table 6.10. These boundaries ensure both, a feasible design as well as stable computations with reasonable results. The extension of the length and height parameters has furthermore been limited with respect to the requirement of the bulbous bow not piercing the water line (as this leads to problems with the potential solver) and not reaching beyond the peak of the vessel's fore end.

The computation of the vessel's resistance will be done using *SHIPFLOW*, with the total resistance being determined via

$$R_T = (1 + k) \cdot R_F + R_W. \quad (6.4)$$

When operating in seaways, the total resistance sums up to

$$R_T = (1 + k) \cdot R_F + R_W + R_{AW}, \quad (6.5)$$

with R_{AW} being the added resistance and k the vessel's form factor. As k has not been determined by RANSE calculations, it had to be approximated using a corresponding tool implemented within *CAESES*. Amongst others, this tool offered the form factor approximation according to Mewis (1989), which is based on the vessel's block coefficient and led to $k = 0.16$. As a control approximation on the basis of a block coefficient, depth, length and breadth-based method introduced by Holtrop resulted in $k = 0.157$, this assumption has been considered to

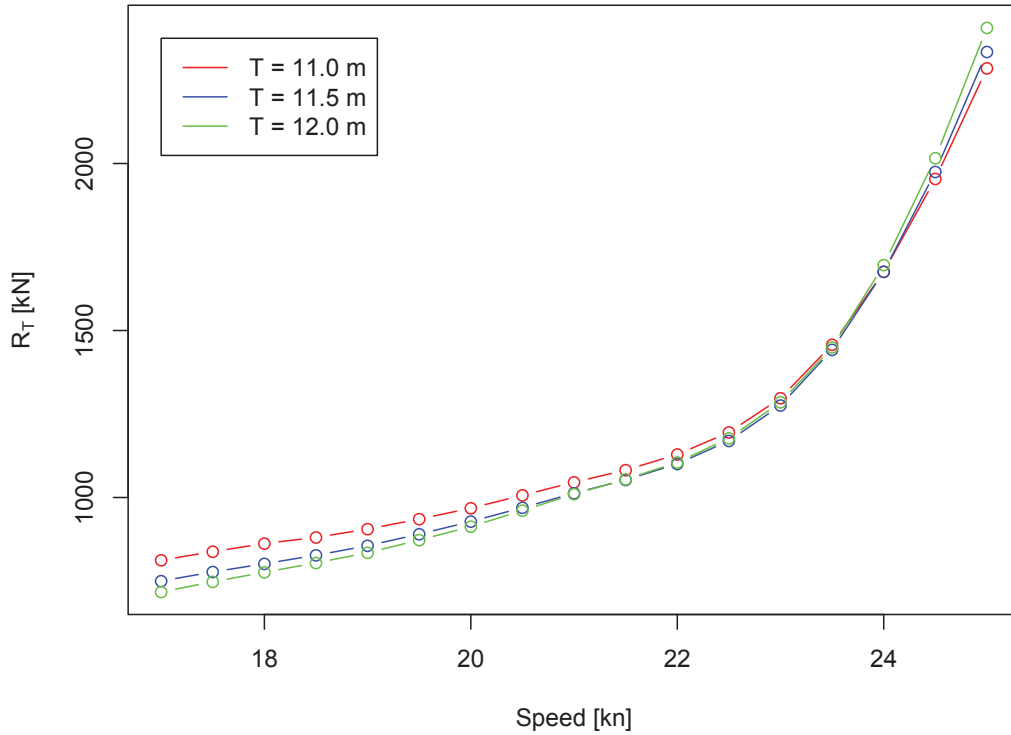


Figure 6.6.: Speed-resistance-curves of original hull form

be correct. As well as for the previous optimization example, the form factor has been assumed to remain constant at all variants.

The calm water speed-resistance-curves for draughts of 11.0, 11.5 and 12.0 *m* of the original hull form is given in Figure 6.6. The corresponding diagrams for R_W and R_F can be found in Section A.4.1 in the Appendix.

6.2.2. Trade Description

Contrary to the DTC and due to the real life nature of this example, there has been no need to preconceive the vessel's transport task. It has been intended by the owner to operate the vessel on the same route as some of its sister ships that have already been in service between varying ports around the Arabian Peninsula, Madagascar and Africa. Based on the 2014 noon-to-noon reports of one of these vessels, an eastbound service of approximately one year has been developed, during which the ports of

- Jebel Ali (United Arab Emirates),
- Sohar (Oman),
- Salalah (Oman),

6. Optimization Examples

- Le Port (Réunion),
- Port Louis (Mauritius),
- Toamasina (Madagascar),
- Durban (South Africa) and
- Port Elizabeth (South Africa)

will be called. Thereby, Jebel Ali has been set as main, maintenance and refueling port, while Salalah and Durban have been defined as refueling ports only. Overall, the three individual shorter round trips

- Jebel Ali - Salalah - Le Port - Port Louis - Toamasina - Durban - Port Elizabeth - Port Louis - Jebel Ali,
- Jebel Ali - Sohar - Salalah - Le Port - Port Louis - Toamasina - Durban - Port Elizabeth - Jebel Ali and
- Jebel Ali - Salalah - Le Port - Port Louis - Toamasina - Port Elizabeth - Durban - Port Louis - Jebel Ali

have been identified, which are served in changing order by the vessel. It has to be mentioned that due to the demands of the scenario development, the trade needs to be defined as a closed loop with one port being both the departure and the final arrival point. While the original trade featured the port of Mombasa (Kenya) as departure port before entering closed round trips, this port had to be excluded from the scenario development.

The speed values of the vessel have been taken over as listed in the noon-to-noon reports. As the vessel most of the time served at speeds between 11 and 17.5 *kn* (equaling Froude Numbers of 0.12 and 0.20, respectively), the speed values had to be adapted in order to perform the resistance calculations by the help of potential flow methods. Therefore, these values have been scaled up by a factor of 1.55².

As the port lay times have not specifically been given, they needed to be estimated using the averaged speed and the remaining distance to and from port as given in the last and following time step. In case this did not succeed, the lay times have been derived from previous or upcoming visits of this port under having comparable loading conditions.

Within the noon-to-noon reports the loading conditions in form of the number of full and empty TEUs and FEUs as well as the total payload amount in tonnes has been given for most of the route sections. Resulting and in conjunction with the consistently existing draught information, the loading-draught-function could be derived. Therefore, a regression of the draughts against the full and empty TEUs (FEUs have accordingly been converted) has been done in a first step. An earlier approach of determining the averaged container weights in order to calculate the total payload and gathering the draught on this basis led to insufficient results, even though additional loading information such as the carried ballast water and other goods were available. Hence, the resulting loading-draught-function

$$T = 5.5013054 + 0.0031827 \cdot n_{full} + 0.0007229 \cdot n_{empty}, \quad (6.6)$$

²This factor has been determined on the basis of serial tests, where the scaling factor has constantly been increased until the top six (see Section 6.2.4) operating conditions fulfilled the minimum draught and speed requirements for stable and dependable resistance calculations.

6. Optimization Examples

with n_{full} and n_{empty} being the number of full and empty TEUs led to a median draught deviation of 2.4% and a maximum draught deviation of 9.0%, which is equivalent to absolute values of approximately 25 cm and 90 cm. In order to meet the given draught values from the reports in spite of this error, the number of full and empty TEUs has been adapted within the trade description in compliance with their respective ratio. Due to this, the draught deviations - when being calculated via the loading-draught-function - have been limited to 0.5% at the maximum. It has to be noted that due to the scenario method's limitation of not being able to simulate draught changes resulting from the consumption of fuel or other goods, the draught has been kept constant along each trip. In case the noon-to-noon reports denoted reasonably varying draughts during a trip (unreasonable changes caused by measuring faults have been filtered out), the time-averaged draught value has been utilized.

The sea areas the vessel meets during its service have been determined in the same manner and with the same assumptions as done for the DTC by using the online distance and route calculator in conjunction with the *Söding* tables. According to these tools, the vessel stays most of the time in coastal waters, namely within the areas 29, 41, 70 and 79. As there are no emission control areas planned along the Arabian or African coasts, the ECA indicator has been set to zero for the whole trip.

As the vessel does not serve any inland ports and most of the ports along its route are directly located at the open sea, there have neither speed nor draught limitations been implemented within the trade description.

All details on the trade can be found in the trade description file included in Appendix A.4.2.

6.2.3. Scenario Setup

The whole scenario setup has been done in agreement with the shipping company. In cases where no information could be given, the assumptions already made for the DTC have been utilized.

Regarding the vessel-related data, the service time has been set to one year, which equals 8765.82 h. The maximum draught of 12 m has been taken from the vessel's drawings, while its minimum has been set to 5.5013054 m, indicating the light ship draught T_{LSW} according to Equation 6.6. The maximum speed has been set to 25 kn, a minimum has not been specified. Finally, maintenance interval and time have been stated to be five years and two weeks, respectively. As the interval is longer than the designated service time, the maintenance influence onto the scenario development will be neglected.

Concerning the operator's decisions at which fuel prices to go for slow steaming, the following assumptions have been made: as the speed values taken from the noon-to-noon reports have been considerably below 25 kn, the vessel has already been operating in a moderate slow steaming mode. In contrast to the previous example, the operator is thought to stick to this low speed values, even though the fuel oil price decreased since 2015 (which seems to be a valid assumption according to Ship & Bunker News Team (2015)). In case the prices would rise again to a level higher than 2014, the slow steaming will be intensified. Therefore, it has been decided to delimit the maximum speed to 20, 18 and 16 kn in case the FOP reaches above 550, 600 or 700 \$, respectively. As the speed adaption in response to demanding weather conditions falls to the ship operator only, the shipping company has not been able to provide any data regarding this issue. In a first approximation and based on the fact that this vessel is rather small compared to the DTC, it has been decided to use the DTC's speed reduction table and to scale the wave heights by a divisor of 1.5, which results in Table 6.11.

6. Optimization Examples

$H_{1/3}$ [m]	3.00	3.67	4.33	5.00	5.67	6.33	7.00	7.67	8.33	9.00
v_{max} [kn]	22.8	20.6	18.4	16.2	14.0	11.8	9.6	7.4	5.2	3.0

Table 6.11.: Speed reduction due to wave height

Parameter	Value
i_r	3.0 %
$FOP(t)$	$275.00 \$ + (325.00 \$/8765.82 h) \cdot t$
$fluc_{FOP}$	$(1.50 \$/24.00 h) \cdot t$
Δ_{FOP}	250.00 \$
$TD(t)$	$(3.00 \%/8765.82 h) \cdot t$
$fluc_{TD}$	$(1.00 \%/8765.82 h) \cdot t$
$P_{FOPCrisis}$	40.00 %
$P_{RiseFOP}$	50.00 %
$\mu_{FOPCrisisDur}$	4382.91 h
$\sigma_{FOPCrisisDur}$	4382.91 h
$P_{TDCrisis}$	13.33 %
P_{RiseTD}	25.00 %
$\mu_{TDCrisisDur}$	8765.82 h
$\sigma_{TDCrisisDur}$	1460.97 h

Table 6.12.: Economic scenario development descriptors

The economic part of the scenario setup is summarized in Table 6.12 and differs in the fuel oil price as well as in the transport demand development from the ones of the DTC example, while the crises parameters remain unaffected. Instead of decreasing prices, the shipping company targeted a more negative development in order to follow a more conservative approach and to be “on the safe side”. This is reflected in the constantly increasing FOP development base function starting at 275 \$/mt and reaching 600 \$/mt after one year. The transport demand development with its constant growth of 3.0%/y and its fluctuation rate of 1.0%/y is also characterized by a more cautious view. The interest rate and the crises parameters reflect the assumptions already presented in the previous section.

Regarding the control of the methodology itself, bin widths of 0.5 m for the speed and 0.5 kn for the draught have been specified. The calculation of the draught will be done using the loading-draught-function presented earlier. For the minimum and maximum number of Monte-Carlo cycles, values of 10 000 and respectively 1 000 000 have been chosen. Compared to the simulation of the DTC’s scenarios, the maximum cycle number strongly increased, which is owed to the fact that within the current scenario development weather conditions are to be considered within the objective operating conditions. This leads to a considerably higher number of possible operating conditions and, resulting, to a slower convergence of the OOCs’ histogram. In case the histogram of operating conditions converges faster than expected, a *Hellinger* threshold of 10^{-10} would lead to a premature termination.

6.2.4. Objective Function and Optimization Setup

Based on the input presented above, the scenario development ran through all 1 000 000 MC cycles without reaching the *Hellinger* criterion (whose corresponding development is given in Figure A.11 in the Appendix). The resulting top 50 operating conditions based on the weightings including the interest rate-adjusted FOPs is presented in Table 6.13.

v [kn]	T [m]	T_1 [s]	$H_{1/3}$ [m]	w_{Total} [%]
17.50	11.00	4.50	1.25	0.82
17.50	11.00	4.50	0.75	0.71
17.50	11.00	5.50	1.25	0.66
17.00	11.50	4.50	1.25	0.63
17.50	11.00	5.50	1.75	0.56
17.00	11.50	4.50	0.75	0.55
17.50	11.00	3.50	0.75	0.52
17.00	11.50	5.50	1.25	0.50
18.00	12.00	4.50	1.25	0.45
17.00	11.50	5.50	1.75	0.43
20.00	11.00	4.50	1.25	0.42
17.00	11.50	3.50	0.75	0.41
20.00	11.00	5.50	1.25	0.40
18.00	12.00	4.50	0.75	0.39
25.00	12.00	4.50	1.25	0.38
20.00	11.00	4.50	0.75	0.36
17.50	11.00	5.50	0.75	0.36
18.00	12.00	5.50	1.25	0.36
17.50	11.00	6.50	1.75	0.36
20.00	11.00	5.50	1.75	0.36
25.00	12.00	5.50	1.25	0.34
25.00	12.00	4.50	0.75	0.33
18.00	11.00	4.50	1.25	0.32
17.50	11.00	3.50	0.25	0.32
18.00	12.00	5.50	1.75	0.31
25.00	12.00	5.50	1.75	0.30
17.50	11.00	6.50	1.25	0.30
18.00	12.00	3.50	0.75	0.29
17.50	11.00	4.50	0.25	0.29
17.50	11.00	6.50	2.25	0.28
25.00	11.50	4.50	1.25	0.28
18.00	11.00	4.50	0.75	0.28
20.00	11.00	6.50	2.25	0.28
17.00	11.50	5.50	0.75	0.28
17.00	11.50	6.50	1.75	0.27
20.00	11.00	6.50	1.75	0.26
23.50	11.50	4.50	1.25	0.26
15.00	10.50	4.50	1.25	0.26

continued on next page

6. Optimization Examples

v [kn]	T [m]	T_1 [s]	$H_{1/3}$ [m]	w_{Total} [%]
18.00	11.00	5.50	1.25	0.26
20.00	11.00	3.50	0.75	0.25
17.00	11.50	3.50	0.25	0.25
25.00	11.50	5.50	1.25	0.24
25.00	11.50	4.50	0.75	0.24
25.00	12.00	3.50	0.75	0.23
18.50	11.00	8.50	4.50	0.23
15.00	10.50	4.50	0.75	0.23
23.50	11.50	5.50	1.25	0.23
17.00	11.50	6.50	1.25	0.22
23.50	11.50	4.50	0.75	0.22
20.00	11.00	5.50	0.75	0.22

Table 6.13.: List of top 50 operating conditions

These 50 operating conditions cover approximately 17.5 % of all conditions the vessel could possibly stay in during its service. A distribution of all upcoming speed / draught combinations can be found in Figure A.12 in the Appendix. It can be seen that four operating conditions amongst the top five feature the combination of a speed of 17.5 kn and a draught of 11 m, while the only difference exists in their respective sea state conditions. Due to the fact that these conditions do not heavily differ from each other, it has in a first step been decided to merge all bins into three major bins representing light, medium and heavy seaways. As wave height and wave period are usually connected, it has furthermore been decided to indicate these categories by wave heights only. In order to do this, a set of calculations similar to the ones done for the DTC has been carried out, whose results indicated R_{AW} -shares of approximately 5 to 15 % - depending on the particular operating condition - of the 3500 TEU container vessel's total resistance related to wave heights below 5 m. At the most common sea states around 1 m wave height and a corresponding wave period of roughly 5 s, the R_{AW} -share drops down to less than 5 %. Additionally, no notable changes in the added resistance could be identified when it comes to measuring changes due to smaller variations in the vessel's hull form as it will be done within the following bulbous bow optimization. Summing up, the influence of changes in the added resistance onto the vessel's total resistance due to bulbous bow variations can be considered to be limited. Keeping this in mind and looking at the total distribution of the wave heights and periods summed up over all draught and speed combinations given in Figure 6.7, it appears that bins containing wave heights of more than 4.5 m will be of almost no use, as they are very unlikely to appear within the objective function. Therefore, it has finally been decided to sum up all sea state conditions into one bin and to neglect the added resistance within the optimization process but to re-check the optimized variant against the original hull form on the basis of the chosen objective operating conditions, each with its particular most common sea state condition.

As it has been decided by the shipping company to optimize onto six operating conditions, the list given in Table 6.13 has been reduced to the one presented in Table 6.14. The six operating conditions indicated there cover slightly more than 30 % of the vessel's total service time, which can be considered to be a reasonable basis for the following hull form optimization.

6. Optimization Examples

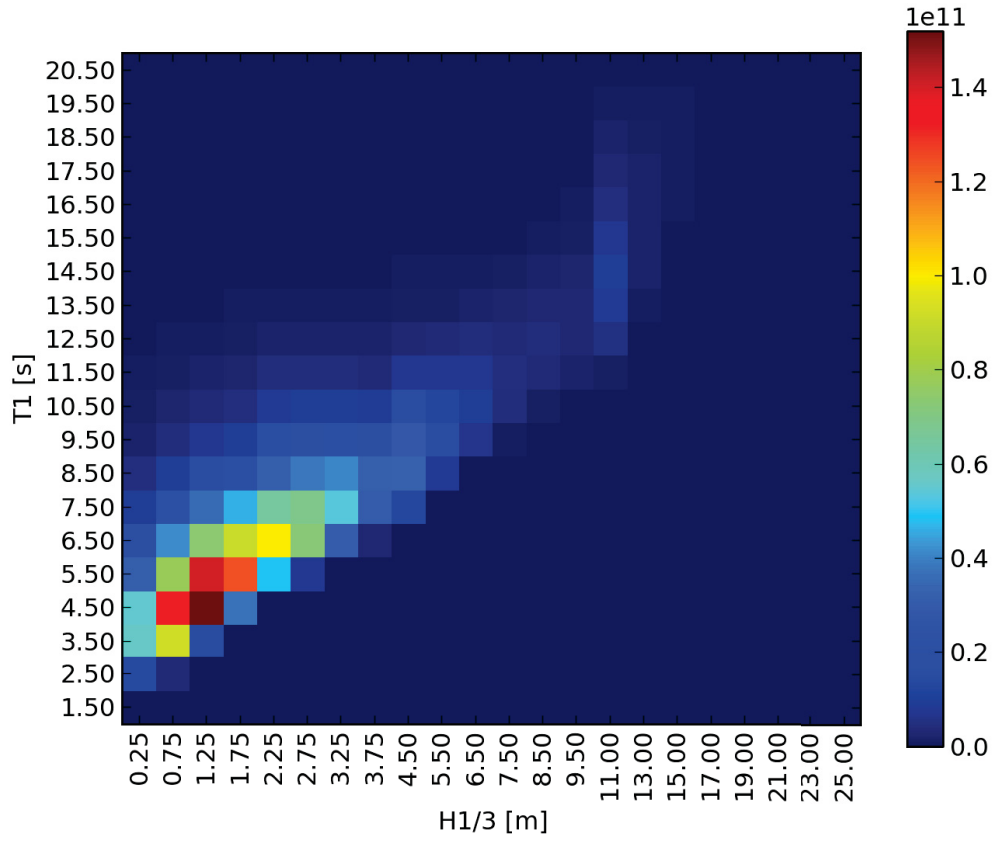


Figure 6.7.: Total wave height and period distribution of the 3500 *TEU* container vessel

	v [kn]	T [m]	w [%]	w_{Total} [%]
OC_1	17.50	11.00	24.54	7.58
OC_2	20.00	11.00	19.33	5.97
OC_3	17.00	11.50	18.53	5.72
OC_4	18.00	12.00	13.30	4.11
OC_5	25.00	12.00	12.75	3.94
OC_6	18.00	11.00	11.55	3.56

Table 6.14.: Objective operating conditions (including fuel oil prices)

6. Optimization Examples

	R_F [kN]	R_W [kN]	R_T [kN]
OC_1	515.31	240.06	837.82
OC_2	662.46	199.56	968.01
OC_3	505.57	163.31	749.77
OC_4	582.16	100.86	776.17
OC_5	1 080.34	1 153.08	2 406.27
OC_6	543.35	231.90	862.18
<i>Weighted</i>			1 041.26

Table 6.15.: Resistance values of initial variant

The objective function to be minimized during this optimization results to

$$\min R_{T,total} = \min \sum_{i=1}^6 R_{T,OC_i} \cdot w_{OC_i}, \quad (6.7)$$

with R_{T,OC_i} and w_{OC_i} representing the total resistance and the weighting of each of the six objective operating conditions. Due to the fact that four of the six operating conditions feature low speeds ($Fn = 0.191$ to 0.202), at which the share of the wave resistance is comparably small, it has been decided to optimize onto the total resistance R_T . Doing this, it should be avoided that the gainings in the wave resistance are consumed by an increased frictional resistance.

For the optimization algorithm it has been decided to make use of the Tangent Search (TS) method as originally presented in Hilleary (1966). In a first step, this method makes use of an initial exploration of the design space around the given starting point and along the variables' axes in order to detect a promising search direction. This search direction is then followed through until a certain minimum has been reached. This algorithm is known for being comparatively fast (especially when compared to the Nelder Mead Simplex) as well as being capable of dealing with variable boundaries and inequality constraints. On the downside, it lacks the ability for detecting an objective function's global maximum, which makes it necessary to primarily explore the design space in order to find suitable starting points. Here, an Ensemble Investigation (which can be understood as a systematic, stepwise variation of the three design variables covering the whole design space) has been used to achieve this task. Resulting from this, a set of promising starting variants have been identified for the following Tangent Search optimizations.

6.2.5. Results

As shown in Table 6.15, the weighted total resistance (excluding added resistance) of the initial variant calculates to $R_{T,total} = 1\,041$ kN, including the total resistance of each of the six objective operating conditions. As expected, the operating condition with the highest resistance is the one of OC_5 , while the lowest resistance value can be found in OC_3 . It has to be noted that the high frictional resistance values of OC_4 and OC_5 (in the latter case only partly) result from the increased draught at these conditions.

As mentioned above, an ensemble investigation has been set up in a first step that covers the whole design space spanned by the parameter boundaries previously being introduced in

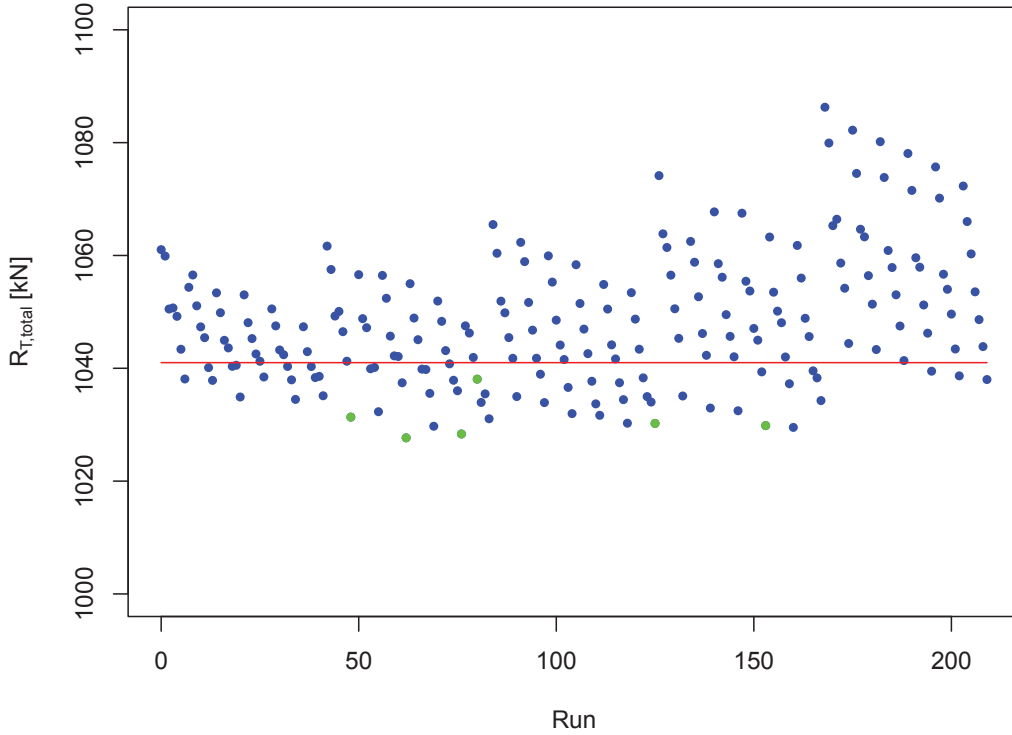


Figure 6.8.: Results of Ensemble Investigation. Tangent Search starting variants are marked green, the initial variant's performance is indicated in red.

Table 6.10. While it has been decided to split the design space into five segments for ΔP_y , six segments for ΔL_B and seven segments for ΔZ_B , 210 design variants have been created. Their resulting weighted total resistance values are displayed in Figure 6.8, with the reference resistance of the initial variant being indicated by a red line. At first sight it can be seen that most of the variants do not lead to an improvement of the hull form and that even the best performing variants do not feature large gainings in $R_{T,total}$, which is an issue that will be addressed later.

On second sight, a step-like behavior - caused by the systematic parameter variation - can be identified, which allows to deduce a first trend. Each of the five distinctive blocks represents an increase of ΔP_y , starting at its lower boundary of -1.5 . Furthermore, a clear structure can be identified within each of these blocks, which denotes that variants with a more slender bow in conjunction with a rising tip seem to rank first. This is supported by the fact that the - regarding their weighted total resistance - 15 best performing variants feature a bow tip that has risen up to the maximum possible value. The influence of the length of the bulbous bow can not be determined accurately, but it seems as if short variants perform worse than the ones having medium or long bulbous bows.

In order to not only consider variants of the denoted type as starting point for the Tangent Search, it has been decided to also include variants with a higher $R_{T,total}$ but a wider parameter

6. Optimization Examples

<i>Variant</i>	ΔP_y	ΔL_B	ΔZ_B
48	-1.0	-2.0	1.100
62	-1.0	-1.0	1.100
76	-1.0	0.0	1.100
80	-1.0	0.5	-0.575
125	-0.5	0.5	1.100
153	0.0	-0.5	1.100

Table 6.16.: Starting variants for Tangent Search optimization

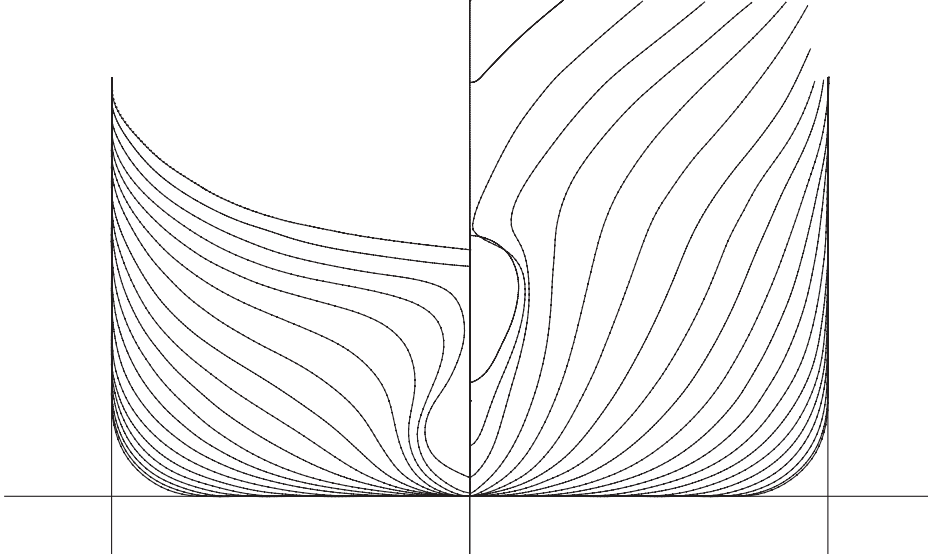


Figure 6.9.: Body plan of optimized hull form

distribution. The finally chosen starting variants for the TS optimization are given in Table 6.16 and are marked by green dots in Figure 6.8.

Resulting from the six Tangent Search optimizations, the best performing variant has finally been determined to feature a total weighted resistance of $R_{T,total} = 1025 \text{ kN}$. At this point it has to be noted that - due to the wide range of considered operating conditions - a lot of design variants with differing parameter constellations are comparatively close to each other with respect to their weighted total resistance. In fact, all hull forms resulting from the Tangent Search optimizations feature resistance values between 1015 and 1029 kN , while their design variables range from -1 to 0 for P_y , -2 to 0.5 for ΔL_B and -0.05 to 1.1 for ΔZ_B . Anyhow, the optimized hull form has been revealed to have a bulbous bow with the design parameters

- $P_y = -1.00$,
- $\Delta L_B = -0.15$ and
- $\Delta Z_B = 1.1$.

While the corresponding body plan is presented in Figure 6.9, the resulting form variation leads to a decrease in $R_{T,total}$ of 1.56 %. The trend previously derived from the ensemble investigation

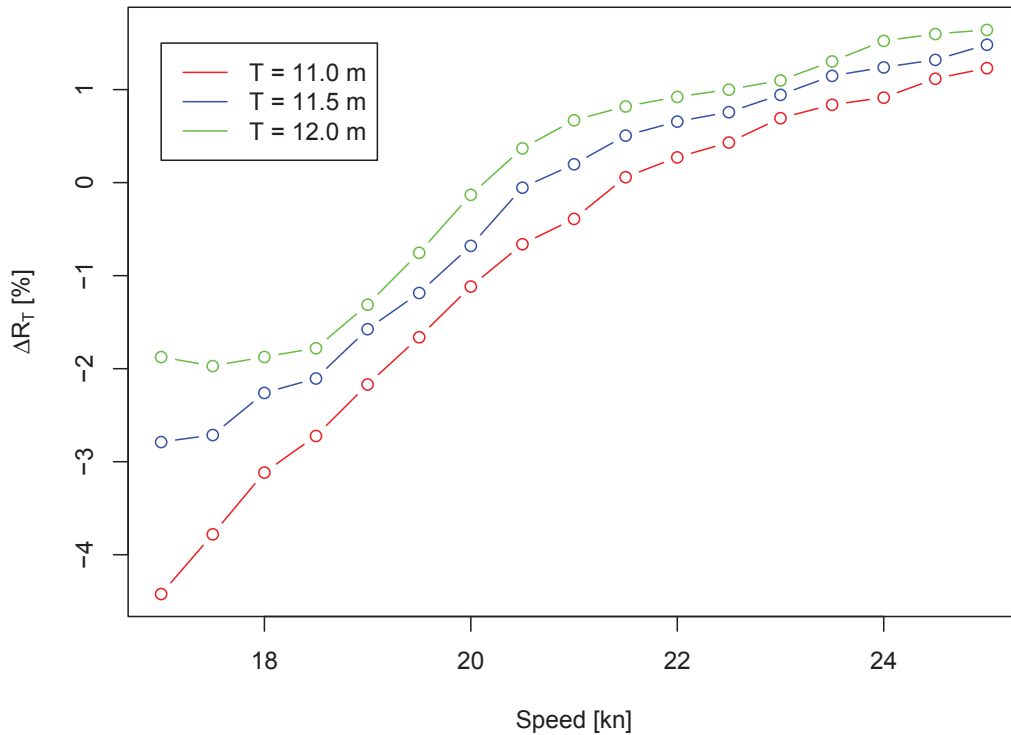


Figure 6.10.: Comparison of speed-resistance-curves

has been confirmed, as the resulting bulbous bow has an elevated tip, a slightly reduced length and is a bit more slender than its initial variant. The reason for the decreased length and width can be found in the comparatively high share of the frictional resistance. Due to the low Froude numbers of most of the OOCs in conjunction with the usage of a form factor, the reduction of the wetted surface becomes a major objective. Using operating condition 1 as an example, the share of the frictional resistance is - when considering the form factor - approximately four times bigger than the one of the wave resistance, which makes it profitable to apply changes that prefer reducing the surface to minimizing the wave resistance. Contrary, the elevation of the bow tip results from its high impact onto the wave resistance. Most probably, the bow tip would have risen even more if it wasn't for the limitations of the ship model and the potential solver as described in Section 6.2.1.

While the speed resistance curves of the optimum hull form can be found in Section A.4.5 in the Appendix, their changes in R_T compared to the initial variant's curves are given in Figure 6.10. In general, it can be seen that the optimized vessel achieves the highest gainings at lower speeds and draughts. When aiming towards higher speeds and draughts this advantage diminishes, until above 22 *kn* the optimized hull form at all draughts performs even worse than the original one.

Taking a closer look onto the optimized hull form's performance gainings at each of the objective operating conditions, it appears on first sight that especially OC₅ shows an opposing

6. Optimization Examples

	R_F [kN]	\pm [%]	R_W [kN]	\pm [%]	R_T [kN]	\pm [%]
OC_1	513.70	-0.31	208.95	-14.89	804.85	-4.02
OC_2	660.40	-0.31	188.71	-5.75	954.77	-1.39
OC_3	504.26	-0.26	142.64	-14.49	727.58	-3.05
OC_4	581.07	-0.19	85.00	-18.66	756.04	-2.26
OC_5	1078.31	-0.19	1192.12	+3.27	2442.96	+1.50
OC_6	541.65	-0.31	205.27	-12.97	833.59	-3.43
<i>Weighted</i>					1025.59	-1.56

Table 6.17.: Optimized vessel performance per objective operating condition

trend to the other conditions due to its high speed and draught values (see Table 6.17). One reason for this could be found in the fact that according to Table 6.9 on page 91, OC_5 represents the vessel's design condition. Therefore, its hull form inherently offers only a limited potential for further improvements. Furthermore, OC_5 outreaches the other five conditions both in its draught (OC_1 to OC_3 , OC_6) and its speed in such a way that the optimization had to take care of two opposing objectives, namely optimizing a slow vessel at moderate draughts and at the same time a fast vessel at full draught. Even though the latter condition has a weighting of only 12.75 %, its influence onto the weighted total resistance is rather strong, owed to its corresponding total resistance, which - with a value of 2443 kN - is more than twice as big as the one of the second ranked OC_2 . Considering the total share of each objective operating condition in $R_{T,total}$ (consisting of the respective weighting multiplied by its corresponding total resistance), the design condition accounts for 33 %, followed by the originally highest ranked OC_1 with a share of only 22 %. This further aggravates the situation, as therewith the minimization of the total resistance of OC_5 becomes the optimization's main objective, while the five remaining operating conditions individually fall behind.

The reason why there is still no improvement at OC_5 consists in the similarity of the other operating conditions. With their speed range of 1 kn (excluding OC_2) and their draught range of 1 m, they could be reckoned as one operating condition with an increased bin width. Thus having a cumulative share of 67 %, their resistance minimization again becomes the optimization's main objective. Operating condition 2 solely features a higher speed of 20 kn, which opposes this statement and is the reason for their comparatively low improvement of 1.39 %.

These effects can be observed on the example of the - with respect to the ship's speed - two extreme objective operating conditions 3 and 5. In order to give an impression on their altered resistance characteristics, Figures 6.11 and 6.12 show the comparisons of the hull form's wave elevation and pressure distribution before and after the optimization. It can be seen that - in accordance with the above mentioned effects - the wave profile of OC_3 has changed to the better. Due to the reduced stagnation point at the bow tip and the increased area of underpressure, the bow wave features a smaller elevation and has additionally been shifted forwards. Contrary, the pressure distribution of OC_5 deteriorated. Caused by the rising tip of the optimized variant, the bow wave elevation slightly increased. Thanks to the decreased breadth and the higher draught at OC_5 , these effects only show a limited impact onto the wave resistance, hence keeping the losses at a reasonable scale.

In order to check the vessel's performance in seaways, the original and the optimized hull form's weighted added resistance have been calculated. As mentioned earlier, each objective

6. Optimization Examples

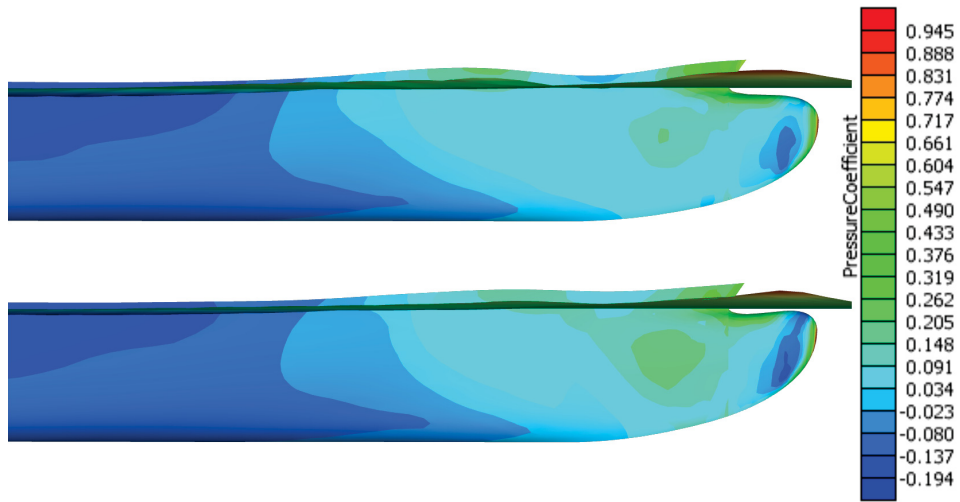


Figure 6.11.: Comparison of wave elevation and pressure distribution at OC_3 of original (top) and optimized hull form (bottom)

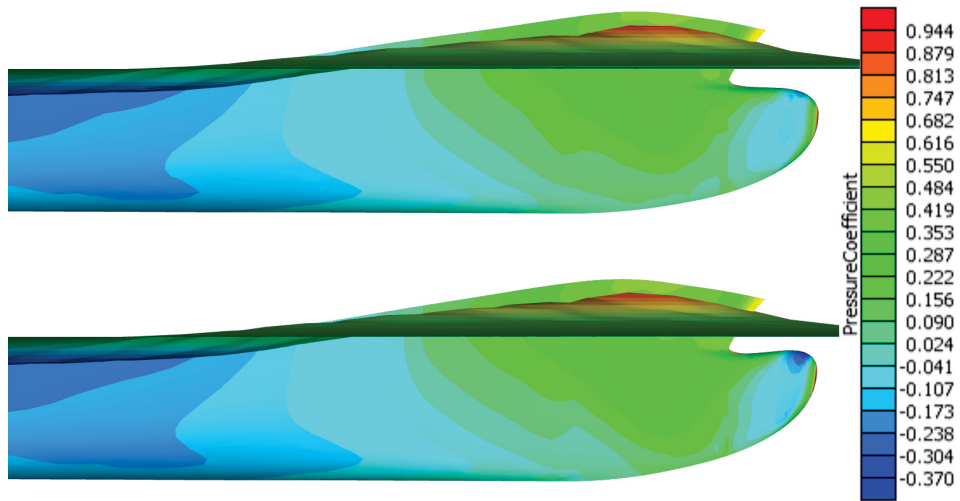


Figure 6.12.: Comparison of wave elevation and pressure distribution at OC_5 of original (top) and optimized hull form (bottom)

6. Optimization Examples

operating condition has for this reason been assigned its most common sea state, which in all cases turned out to be the combination of $H_{1/3} = 1.25\text{ m}$ and $T_1 = 4.2\text{ s}$. The weighted added resistance of the original hull form calculates to 183 kN , while $R_{AW,total}$ of the optimized variant results in 182 kN . Assuming the numerical error to remain constant for both variants, the change in $R_{AW,total}$ equals a small decrease of 0.3% . This corroborates the previously made assumption that the added resistance - at least when considering as moderate sea states as done within the course of this example - does not substantially contribute to the overall optimization gainings, even though its development confirms the tendency of the calm water resistance. In addition to that, the development of the added resistance values within the individual operating conditions obeys the same pattern as the calm water resistance. In fact, the ranking of the operating conditions with respect to their gainings is the same in both cases, including OC₅ being the only condition without a resistance improvement.

Even though an overall $R_{T,total}$ reduction of 1.56% might not be thought of as a good result, it has to be kept in mind that this decrease is related to 30% of the vessel's total operating time. In fact, the main reason for only getting these comparatively small $R_{T,total}$ gainings consists - as it has been described above - in the wide range of speeds and draughts covered by the six objective operating conditions. Concentrating onto the effective power P_E only (in order to avoid the problem of presumably drastic yet unknown changes in η_D due to the various draughts) and by using the time-averaged fuel oil price of $\overline{FOP} = 300\text{ \$/mt}$ and assuming a (constant) specific fuel consumption of $SFC = 200\text{ g/kWh}$, the averaged annual fuel costs of the six objective operating conditions of the optimized variant sum up to

$$8765.82\text{ h} \cdot SFC \cdot \overline{FOP} \cdot \sum_{i=1}^6 R_{T,OC_i} \cdot v_{OC_i} \cdot w_{Total,OC_i} = 1\,772\,888.58\text{ \$.} \quad (6.8)$$

It has to be noted that in this case w_{Total,OC_i} indicates the time-based instead of the time and fuel oil price-based weighting of each OC as introduced in Section 3.6. The respective weightings can be found in Table A.2 in the Appendix. Substituting the resistance values of the optimized with the ones of the initial variant, annual fuel costs of $1\,752\,954.51\text{ \$}$ arise, leading to overall gainings of $\approx 20\,000\text{ \$/year}$. This rough example demonstrates that even a small improvement can cause high economic gainings, when applied onto a vessel's operational profile³. It has furthermore to be noted that these estimated gainings should be considerably higher in real life, as Equation 6.8 only considers the vessel's top six operating conditions. Considering the full operational profile as given in Figure A.12, the high share of speed values below 20 kn should have a positive impact on the result⁴.

Regarding the environmental performance and considering a HFO mass to CO₂ mass conversion factor of 3.1144 as recommended by IMO (2009), an amount of 200 t of CO₂ can be saved per year only considering the top six OOCs. In accordance with the financial gainings, the CO₂ savings should increase even further in case all developed operating conditions would be taken into account.

³It should be mentioned that it is almost impossible to correctly determine the averaged annual fuel costs as well as the averaged fuel savings, as it is neither possible to determine the whole speed-draught-power-curve with potential flow code nor to exactly predict the vessel's future operational profile.

⁴Keeping in mind that the speed values have previously been multiplied by a factor of 1.5, even better results could have been achieved if it wasn't for the need to apply potential flow instead of RANSE methods.

6.2.6. Sensitivity Analysis

In order to check the scenario based optimization approach against its sensitivity to the number of operating conditions included within the objective operating conditions, two alternative optimizations of the vessel's hull form have been done. The first attempt considered the top four OCs of Table 6.14 (covering $\approx 23\%$ of the total operational profile), while the second optimization was reduced to the top three conditions with a coverage of $\approx 18\%$. Despite the objective function, no further changes have been applied in comparison to the ensemble investigation carried out earlier.

Interestingly, a best performing variant with the design parameters

- $P_y = -1.0$,
- $\Delta L_B = -2.0$ and
- $\Delta Z_B = 1.1$

came up from both optimizations. While sharing P_y and ΔZ_B with the initial optimization, the bulbous bow has been further reduced, most probably due to the relatively increased frictional resistance influence due to the elimination of the high-speed condition OC₅. Having a look onto the speed-resistance-curves given in Figure 6.13, this is reflected in the higher performance gainings at lower in conjunction with bigger losses at higher speeds. All in all, the optimization led to a reduction in $R_{T,total}$ of 2.75% for the four OOC-case and to 2.95% for the three OOC-case, which is a nominal better result than the one achieved in the previous optimization. It furthermore appears that with a decreasing number of objective operating conditions the percentaged gainings rise. In contrast, the application of Equation 6.8 on the basis of the top six objective operating conditions results in annual gainings of $\approx 5300\$$ and 55 tonnes CO₂ only.

It turns out that considering a smaller number of operating conditions - even though appearing to achieve better results - leads to reduced cost savings. In the above example, bisecting the optimization effort causes a saving reduction of approximately 75%. While the exact amount of this proportion might vary as the case arises, the optimization onto too few OOCs may become essential for the payoff of a new building or retrofitting measure. Again, and in accordance to the statements made in Section 6.1.6, this statement only applies for the current example as it is highly dependent on the structure and the characteristic of the OOCs.

6.3. Case Three: Passenger Vessel

The third example case deals with the optimization of the design of a passenger cruise vessel of a German shipyard. It has to be noted that this design only represents a - although typical - design study that has never been intended to be built in that way. The main dimensions of the vessel are given in Table 6.18.

The whole scenario simulation as well as the following optimization has been carried out within the research project *PerSee*. As the latter part has exclusively been done at the shipyard, some parts of the following sections (especially Sections 6.3.1 and 6.3.5) are based on Kreutzer (2015) and will be presented in condensed form.

Even though a passenger vessel can not be considered to be a common merchant vessel, this example has been included within this thesis in order to give an impression on the flexibility of the developed scenario-based design approach.

6. Optimization Examples

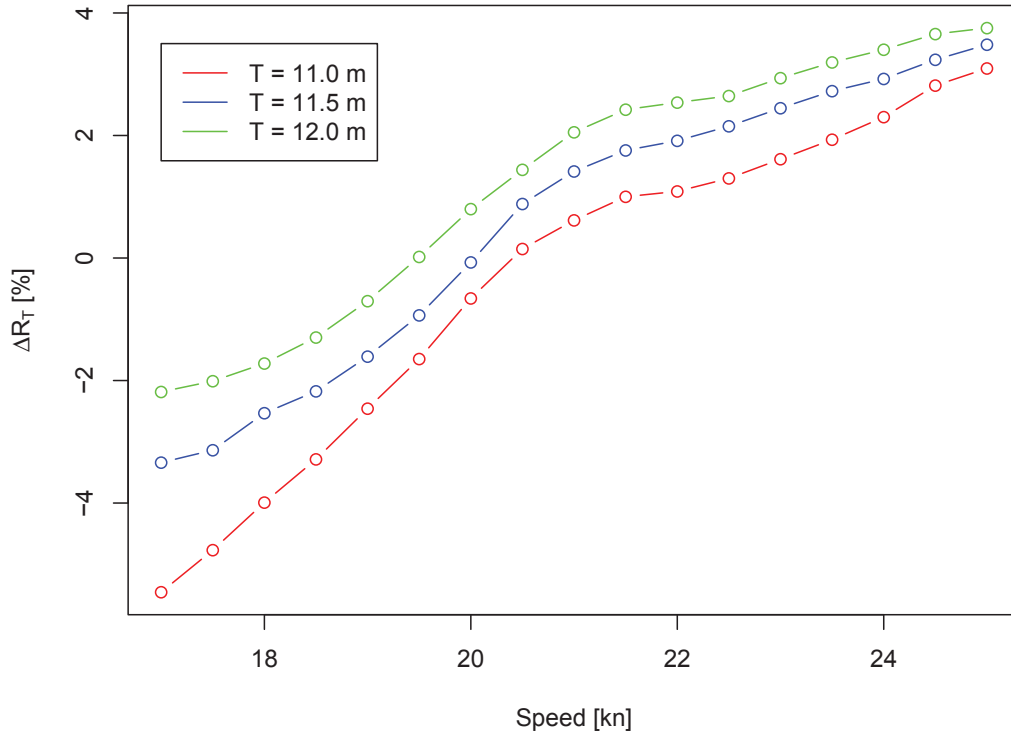


Figure 6.13.: Comparison of speed-resistance-curves (three / four objective operating conditions)

Dimension (Full Scale)		
L_{pp}	[m]	216.80
L_{OA}	[m]	238.00
B_{wl}	[m]	32.20
T_D	[m]	7.20
Δ	[t]	34 059.75
c_B	[-]	0.65
S	[m ²]	7822.80

Table 6.18.: Main dimensions of passenger vessel (Kreutzer, 2015)

6.3.1. Ship Model

As well as for the other examples, the ship hull form has been modeled and in the following been modified within the *CAESES* framework. The general manipulating process of the hull form has been divided into three parts, namely

- a global variation by means of an adjustment of the vessel's shoulder position, followed by a
- rough local variation that focuses onto the fairing of the shoulder, and at last a
- fine local variation, in this case meaning the modification of the bulbous bow by means of length, breadth and height.

In contrast to the other examples, not only the vessel's resistance but its delivered power P_D has been in focus of the optimization, including added resistance, wind resistance and losses due to maintaining the course. The total resistance of the passenger vessel has been determined via

$$R_T = R_W + (1 + k) \cdot R_F + R_{AW} + R_{Wind} + R_{Drift}, \quad (6.9)$$

with the values for R_W and R_{AW} being calculated by *GL Rankine*. It has been decided to assume the vessel meeting the waves under a constant angle of attack of 170° , as this has been determined to be the angle resulting in the highest resistance values. R_{Wind} and R_{Drift} result from various coefficients, either determined via RANSE planar motion mechanism (PMM) simulations or taken from literature. The form factor has - on the basis of RANSE computations - been determined to $k = 0.1$ and is assumed to remain constant throughout the form variations. Resulting, the delivered power calculates as

$$P_D = \frac{P_E}{\eta_D} = \frac{R_T \cdot v}{\eta_H \cdot \eta_R \cdot \eta_O}. \quad (6.10)$$

While η_H and η_R have been roughly approximated, η_O has been specified on the basis of the open water diagram of the vessel's assumed propeller.

It has to be noted that in addition to the power calculation algorithms rough stability calculations have been implemented in order to maintain a certain stability level.

6.3.2. Trade Description

Even though the vessel transports passengers instead of containerized cargo, the modeling of the transport task could be done as for the other examples. The voyage data has been provided by the shipyard in the course of the *PerSee* project. While representing an exemplary service profile of passenger vessels for one year, this voyage consists of the three main schedules

- summer schedule (operating in Europe and the Mediterranean Sea),
- winter schedule (serving the Carribean) and a
- cross of the Atlantic Ocean (twice a year).

These profiles subdivide into the five specific round trips

- Rome - Santorini - Istanbul - Ephesus - Mykonos - Athens - Naples - Rome (named MC01, service time ten days),

6. Optimization Examples

- Rome - Messina - Athens - Ephesus - Rhodes - Santorini - Mykonos - Naples - Rome (MC02, also ten days),
- Rome - Funchal - Basseterre - Philipsburg - Labadee - Miami (TAC01, 15 days),
- Miami - San Juan - Philipsburg - Basseterre - Miami (ECC01, seven days) and
- Miami - Tenerife - Malaga - Cartagena - Barcelona - Villefranche - Florence - Rome (TAC02, 15 days).

These trips should be served in the order of eleven times MC01, eleven times MC02, one time TAC01, 16 times ECC01 and one time TAC02.

Compared to the previously dealt with container ships, passenger vessels are supposed to serve on a constant draught. In this case, this is indicated by the vessel's design draught of $T_D = 7.2\text{ m}$ that has been assigned to all route segments. The speed values have been specified by the shipyard and therefore directly been adopted into the trade description. In contrast to the draught, a whole set of speeds could be found, ranging from 3.5 to 21 *kn*.

As the voyage data already included port lay times, only the port types needed to be defined. The port of Rome has been assumed to be the vessel's main and docking port, while all other ports have been defined as simple refueling facilities only.

As well as for the other examples, the sea areas have been detected by graphical analyses of the vessel's voyage description. It should be noted that the Mediterranean Sea is not covered by the *Söding* tables. Therefore, for each route segment the nearest of the adjacent seaway points has been identified (in most cases point 116) and inserted into the trade description. The remaining route segments' sea areas are mainly located within the Atlantic Ocean and feature seaway points such as 101, 102 and 107 to 109.

The complete trade description as handed over to the scenario development can be found in Section A.5.1 in the Appendix.

6.3.3. Scenario Setup

For the basic vessel setup, the minimum draught has been set to 5 and the maximum draught to 12 *m*. While the latter reflects the vessel's actual maximum draught, the former value is of theoretical nature only. Due to the fact that it is difficult to determine a loading-draught-function for a passenger vessel, its specification has been skipped for the benefit of using the draught values as specified within the transport task and modifying them directly via the TD development function. At this point it could already be mentioned that there will appear only small draught variations during the scenario simulation. None of the specified boundaries will be reached, which makes them almost obsolete. The speed limit has been set to 22 *kn* at the maximum, while a minimum value has not been defined. Regarding the service time, a value of ten (tropical) years has been proposed, the maintenance interval has again been set to five years and the corresponding maintenance time to three weeks.

According to the shipyard, it does not make sense to specify any slow steaming tables, which is mainly due to reasons of passenger satisfaction and higher efforts when it comes to schedule adaption. The same applies to speed reductions caused by rough seaways, as a cruise ship would always avoid any passage having weather conditions that would make its passengers feel uncomfortable.

6. Optimization Examples

Parameter	Value
i_r	5.0 %
$FOP(t)$	$500.00 \$ + (12.50 \$/8765.82 h) \cdot t$
$fluc_{FOP}(t)$	$(100 \$/8765.82 h) \cdot t$
$TD(t)$	0.00 %
$fluc_{TD}(t)$	1.00 %
$P_{FOPCrisis}$	15.00 %
$P_{RiseFOP}$	67.00 %
$\mu_{FOPCrisisDur}$	8765.82 h
$\sigma_{FOPCrisisDur}$	2920.00 h
$P_{TDCrisis}$	15.0 %
P_{RiseTD}	25.00 %
$\mu_{TDCrisisDur}$	8765.82 h
$\sigma_{TDCrisisDur}$	2920.00 h

Table 6.19.: Economic scenario development descriptors

At this point it can be seen that not all of the implemented features are useful when dealing with this kind of vessels, but even though many functions have been omitted, the simulation of the seaways for the vessel to meet is still of importance.

The economic setup features a FOP of 500 \$/mt as starting point (the scenario setup has been done in mid 2014) in conjunction with a constant linear increase of 2.5 % and a corresponding fluctuation rate of $fluc_{FOP} = 100 \$$ per year. The interest rate has been assumed to be at 5 %. As the vessel - even in case only half of the cabins would have been booked - won't face notable draught changes, it has been decided to keep the transport demand development at a constant level, while the fluctuation rate has been set to a fixed value of 1.0 % in order to reflect smaller stochastic loading variations. The probabilities for FOP and TD crises have in comparison to the other examples slightly been reduced to 15 %, each. The setup also differs in the respective crises durations and probabilities for in- or decreasing prices and transport demand, which can be seen in the summary of the economic scenario setup given in Table 6.19.

In accordance with the shipyard, the bin widths have been set to 1 kn and 1 m for speed and draught, respectively. As many scenario features (and therefore uncertainty sources) have been omitted within this simulation, the number of Monte-Carlo cycles could be reduced to 10 000. In order to achieve a high coverage, the resulting objective operating conditions should cover approximately 70 % of the vessel's total service time.

6.3.4. Objective Function and Optimization Setup

From the scenario simulation resulted a list of 140 operating conditions. As it could have been expected, these conditions did not show notable variations with respect to the draught and speed values but only in their sea state conditions. In fact, the only draught bin appearing within the objective conditions is the one of $T = 7.0 m$. As the vessel's design draught of 7.2 m is included within this bin, it appeared legit to use this value as objective draught. The most common speed could be found at 18 kn, followed by 20 and 14 kn. In order to reduce the amount

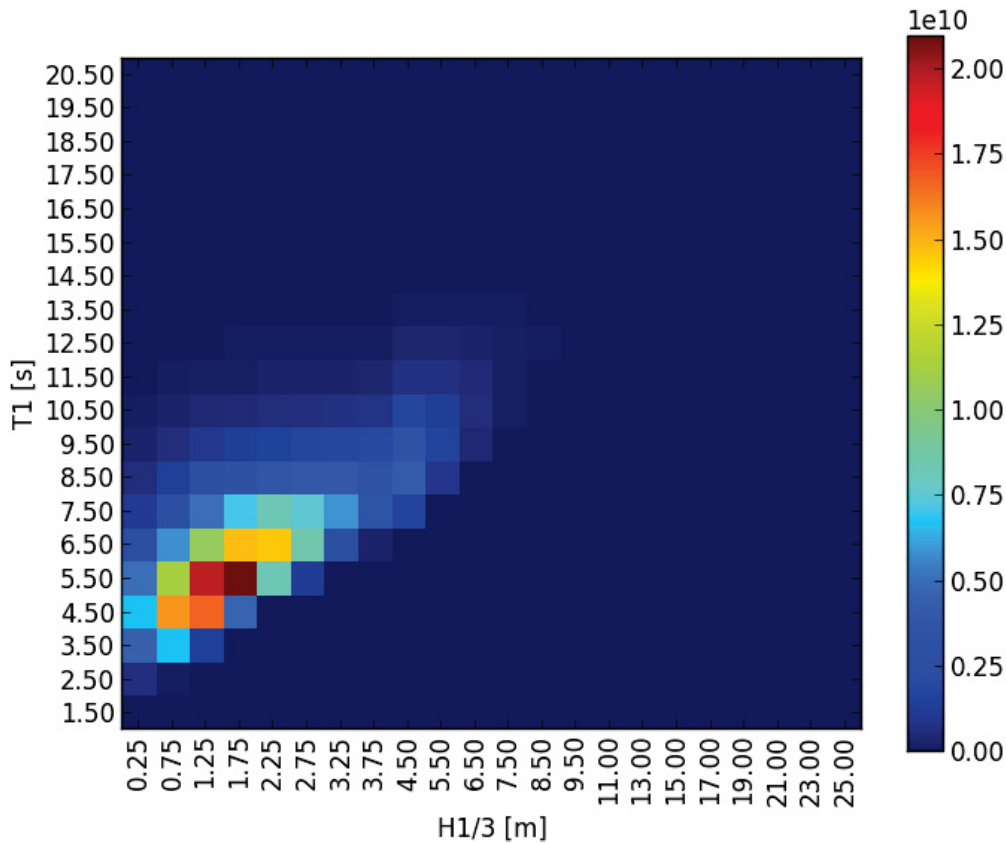


Figure 6.14.: Total wave height and period distribution of passenger vessel

of operating conditions, it has been decided to merge all sea state conditions (whose distribution is given in Figure 6.14) into three categories, the first indicating good weather conditions with wave heights up to 3.0 m , the second representing medium conditions of $3\text{ m} < H_{1/3} \leq 5\text{ m}$ and the last marking rough seas with wave heights $> 5\text{ m}$ (which do not appear within the objective conditions). The specific wave heights to represent each bin and to later optimize onto have then been determined by calculating their average value based on the weightings of each condition included within the respective bin. The same applied to the wave periods, finally leading to the six objective operating conditions listed in Table 6.20.

The form variation as well as the evaluation of the respective results have been done manually. Thereby, the former task has been carried out on the basis of the form variation steps introduced in Section 6.3.1. As the positioning of the vessel's shoulder has a notable impact onto its displacement as well as its stability, the development of both parameters has constantly been monitored and - if necessary - counteracted during the global and the rough local variation. A closer description of the optimization approach is given in Kreuzer (2015).

6.3.5. Results

Resulting from the optimization, an overall power decrease of 3.35% has been achieved. The optimized variant features an approximately 7 m backwards relocated shoulder in conjunction

6. Optimization Examples

	v [kn]	T [m]	w [%]	w_{Total} [%]
OC_1	18.00	7.20	46.00	32.00
OC_2	20.00	7.20	19.00	13.00
OC_3	14.00	7.20	13.00	9.00
OC_4	12.00	7.20	9.00	6.00
OC_5	18.00	7.20	7.00	5.00
OC_6	10.00	7.20	6.00	4.00

Table 6.20.: Objective operating conditions

with a 1.5 m extended bulbous bow. The bulbous bow has furthermore been thinned for 40 cm, while its peak moved about 1 m downwards.

It has to be noted that most of the gainings have been achieved due to improvements in the calm water resistance. Due to the fact that the added resistance has a small share of 2.1 % only, its relative reduction of approximately 10 % contributes to the overall powering improvement only in a limited way. The remaining resistance components (wind, rudder, oblique flow) could not notably be decreased, which in some cases might be caused by the calculation methods used within the optimization.

Referring to fuel costs, the form improvement leads to annual savings of approximately 250 000 \$. It should in this context be noted that this statement has been made based on the assumption of a FOP of 600 \$/mt. Regarding the ecological performance and under the assumptions of a specific fuel consumption of 200 g/kWh and carbon dioxide emissions of 0.28 kg/kWh, more than 580 tonnes of CO₂ could be saved per year. These results prove the scenario-based optimization approach to be applicable and to perform well even for - in this context - unconventional ship types.

7. Conclusion

Within this chapter, the results of the previous chapters will be summarized, reviewed and discussed. Additionally, an outlook on possible future improvements and enhancements will be given.

7.1. Summary

Within this thesis, a method for the scenario-based hull form optimization of merchant vessels has been introduced that fulfills the requirements mentioned in Section 1.1. To the author's knowledge, this marks the first attempt of including scenario methods within the ship design or re-design process.

In Chapter 2, an overview on scenario methods, their history, terminology and general structure as well as their current level of application within the maritime industry has been given. It could be shown that scenario methods - even though being widely used within other industries - have not been utilized within the maritime context until the economic crisis in 2008. Owing to that, they usually address "classic" issues, such as the forecasting of fuel oil price developments or business scenarios, while only a few approaches related to the design of ships could be found. Even though some of these approaches offer single capabilities similar to those of the methodology presented within this thesis, the coupling of mathematically modeled trade scenarios with fluctuating environmental conditions in order to develop the most likely upcoming operating conditions on the basis of joint probabilities has not been implemented yet. In addition to that, a short overview on assessment possibilities for ship design evaluations has been given.

The working principle and main characteristics of the scenario-based optimization approach has been presented in Chapter 3. It has been decided to target an explorative, quantitative chain scenario approach that is able to simulate a vessel's service life with respect to a set of stochastically fluctuating environmental influences. The most relevant of these influences have been identified to exist in the fuel oil price and the transport demand. Within the scenario development setup, both of them can be modeled by specifying an expected basic development function, to which - in order to depict the limited knowledge regarding the future - constantly growing uncertainties in form of a normally distributed fluctuation is added. Additionally, both developments can be subjected to disruptive events, such as crises or economic upturns. Despite these descriptors, the method considers potential slow steaming decisions, local draught and speed restrictions, the influence of passing through emission control areas, the need to keep schedule in case of delays, dry docking and port lay times and the operator's reaction to harsh weather conditions within the scenario development. The latter is thereby simulated on the basis of the scatter tables by Söding (2001). In order to deal with the appearing uncertainties, the scenario development makes use of Monte-Carlo methods, which have been introduced in Section 3.5.

Regarding the resulting operating conditions, it has been decided to include the vessel's speed, its draught and the sea state conditions indicated by $H_{1/3}$ and T_1 . Any combination of these four descriptors - clustered into customizable bins - represents a distinctive operating

condition. The most probably upcoming operating conditions are detected on the basis of exposure time and the at that time present fuel oil price. This has been done in order to also account for economic matters. A number of n top-ranked operating conditions are utilized to form the optimization's objective function, where n can either be directly specified or detected on the basis of a desired coverage. In this context, it should be noted that the ranking is based on joint instead of marginal probabilities as explained in Section 3.6.

The proof of concept concerning the scenario development has been done in Chapter 4. Therein, the approaches capabilities regarding the trade description, fuel oil prices, weather conditions and the vessel's response to these influences has been demonstrated.

While Chapter 5 gives a brief overview on the implementation of the scenario method as well as the optimization environment, Chapter 6 contains the application of the scenario-based optimization approach on three exemplary use cases. Within the first example, the 14 000 *TEU* container vessel DTC has been set on a realistic yet fictional eastbound trade. The optimization of the vessel's bulbous bow area has been carried out with respect to its weighted effective power based on the top six operating conditions with an overall coverage of 46 %. The optimization resulted in an $P_{E,total}$ -improvement of 2.27 %. Additionally, the optimization's sensitivity to changes in the scenario setup and the number of objective operating conditions has been demonstrated. It could be revealed that comparatively small changes in the objective operating condition's structure (weighting and ranking order) can result in strong modifications of the resulting hull form. Thereby, the sensitivity to the number of considered operating conditions depends on the structure of the objective operating conditions.

Within the second example, an existing 3500 *TEU* container vessel has been subjected to a trade change. In order to adapt its bulbous bow to the new, in general slower service profile, a hull form optimization with respect to six operating conditions with a coverage of 30 % of the vessel's service time has been done. The optimization led to a shorter, more slender bulbous bow with an elevated tip and a reduction of $R_{T,total}$ of 1.56 %. The added resistance has been proven to only play a secondary role in this case, even though it might become important when switching to a route featuring rougher sea states. The successive sensitivity study on the impact of the number of considered operating conditions onto the annual performance gainings illustrated the need to strive for a high coverage.

The last use case introduced the application of the scenario-based optimization approach onto a passenger vessel. Although not being developed for this vessel type, the approach generated six objective operating conditions with a coverage of 69 %. Focusing on the manipulation of the vessel's fore ship including the shoulder position and considering the added resistance, a decrease of the vessel's delivered power of 3.35 % could be achieved.

7.2. Limitations and Discussion

Within the presented optimization examples, different presumptions, calculation and optimization methods and objective functions have been applied. While the resulting savings vary in their extent, the application of the scenario-based optimization has in all three cases proven to generate notable benefits. The introduction of mathematically modeled scenario methods into the ship design process allows for the first time to catch a glimpse on a vessel's future operational profile. It has been demonstrated that the ability of scenarios to stretch peoples' thinking and to broaden their horizon can be applied to the ship design context in terms of revealing operating conditions that might not have come up when determining a vessel's service

7. Conclusion

conditions the traditional way. Resulting, the presented approach contributes to the goal of a holistic hull form optimization, whose application involves both, environmental and economic gainings. The latter issue is especially addressed by the possibility to include economic thoughts within in the selection of the objective operating conditions.

Besides these achievements, there are some limitations regarding the scenario development process as well as the optimization itself. The first issue addresses the scenario development and the basic decision to use a distance-based instead of a time-based modeling approach. Due to this decision, the vessel's route is fixed, making it impossible to simulate spontaneous route deviations, such as weather routing. The same applies to trade changes due to economic effects. Another important issue exists in the lack of fleet management possibilities. Especially when it comes to extreme economic developments (as for example in Section 6.1.4), a shipping company would rather seek for deploying new or shutting down old vessels than serving on extreme draughts and speeds. Additionally, some minor matters are not yet considered within the scenario simulation. As an example, there only exists a global transport demand and global fuel oil prices. Local developments being independent of the world economy can not be reflected. Regarding the simulation of the vessel's operating conditions, one could criticize that there is no function to reflect the vessel's fuel consumption within its draught. Also, there is no impact of the number of transported TEUs onto the port lay times.

While all of these issues can be fixed within future revisions of the scenario approach, there are a few topics to be discussed that address the determination of the objective operating conditions. First of all, it could be argued that even when using the presented approach, there are still operating conditions not being considered within the optimization. While this is generally true, it has to be taken into account that the optimization onto an operational profile covering 30 to almost 70% of a vessel's total service time nevertheless marks a significant improvement compared to the traditional way of designing ships. Additionally, it should be noted that comparatively unlikely operating conditions might still appear within the objective operating conditions in case their economic impact (high fuel oil price) is strong enough. Furthermore, it is possible to optimize onto all simulated operating conditions (even though this would not necessarily lead to better results, see Section 6.1.6), providing the existence of sufficient computational resources.

Related to that, it could be questioned whether it makes sense to allow the optimization onto a clearly unrealistic combination of operating conditions due to the (possible) multiple consideration of single route segments under varying conditions. An alternative procedure appears to exist in creating a separate distribution of operating conditions for each route segment and choosing the respective segment's most probable ones to form the objective operational profile. While this on the one hand would lead to an illustration of the most probable way of serving the trade, it would on the other hand antagonize the idea of considering uncertainties and the goal of a robust design approach.

Regarding the usability and the optimization procedure itself, there are a few issues that decide over the success of a scenario-based optimization. It should be mentioned that the binning of the operating conditions can have a significant impact on the optimization's computational efforts and results. While the position of the bins affects the justification of the objective function (a good example for this is the draught adaption of the passenger vessel in Section 6.3.4), the bin size is closely related to the objective function's accuracy and coverage. A reduced bin size allows to optimize onto more specific operating conditions but also leads - when keeping the number of objective operating conditions - to a reduced coverage. In order to achieve the same coverage, more operating conditions had to be included within the objective

function, which results in an increased computational effort. Therefore, it has previously been recommended to start the scenario development simulation with small bins in order to analyze and possibly later merge them into larger clusters before starting the optimization. The same applies to the amplitude of the stochastic fluctuations added to the FOP and TD developments. Larger values lead to an expansion and at the same time to a flattening of the operating conditions' probability density function, which implies the need to consider more conditions within the objective function. Smaller fluctuations result in a tighter distribution and less objective operating conditions but imply the risk of underestimating unexpected developments.

It should be noted that the presented approach in general is only applicable in case the main dimensions of the vessel already exist. When using this approach for an optimization of the complete hull form including the vessel's main dimensions instead of - for example - the bulbous bow area only, the draught determination becomes complex.

7.3. Outlook and further Work

Even though the scenario-based optimization approach as presented within this thesis contributes to the goal of improving the life-time efficiency of merchant vessels, this work can only be considered as a first step towards a truly holistic and robust hull form design.

In order to achieve this goal, the issues mentioned in the previous section have to be solved, which can easily be done due to the modular structure of the approaches implementation. In addition to that, it appears promising to include further parameters such as wind or the wave direction within the operating conditions.

The - referring to the numbers only - small performance gainings of 1.5 to 3.35 % partly result from the use of potential flow code for calculating the vessels' resistance. While the vessels in the presented examples mainly serve at low Froude numbers, it appears reasonable to apply RANSE methods for determining their total resistance, which would also allow for including the propulsion efficiency within the optimization. Especially when thinking of the appearing draught variations, there exists a huge potential for optimizing the propeller and its interaction with the hull form.

In order to speed up the - especially in case of many objective operating conditions in conjunction with the need to calculate the propulsion characteristics as well as the added resistance - long optimization process, other optimization methods could be applied, such as response surface methodologies or *Kriging*.

Another potential for improvement exists in enhancing the evaluation of the design variants. Due to lacking data, the optimizations presented within this thesis have been carried out with respect to their resistance or powering attributes only. In theory, it should be possible to link the scenario development to almost any performance indicator presented in Section 2.4 or given in Fet et al. (2001) or other related publications. As an example, the ship merit factor could be applied by simply logging the number of carried containers and defining a loading / unloading factor that determines the container exchange rate at all ports. This would make it possible to perform a hull form optimization with respect to the relative transport costs per mile and TEU.

Finally, there is a potential for further improving the optimization approach by introducing a parametric objective function. Currently, the objective operating conditions are fixed in their rank and weighting throughout the whole optimization, which is due to the weightings being exclusively based on the results of the scenario development process that has been carried

7. Conclusion

out prior to the optimization. As the best-ranked operating condition's performance indicator (for example R_T) must not have the highest share with respect to the total performance (see Section 6.2.5 for an example), the conditions' weightings should be accordingly adapted after each iteration of the optimization process.

A. Appendix

A.1. Introduction



Figure A.1.: Development of HARPEX Index since 2006 (Harper Peterson & Co. (GmbH & Cie. KG), 2016)

A.2. Proof of Concept

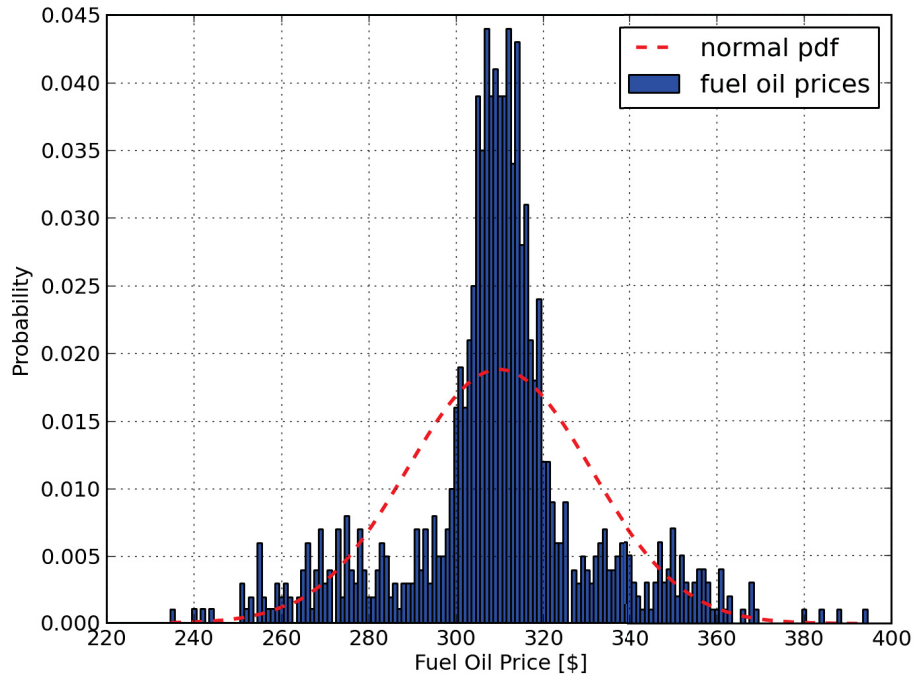


Figure A.2.: Distribution of fuel oil price development including crises after 1000 Monte-Carlo cycles

Route Segment	v [kn]	T [m]	Distance [nm]	Duration [h]	P [%]
2	10.00	8	1000	100.00	96.24
	8.00	8	1000	125.00	3.76
3	10.00	8	1000	100.00	96.24
	13.33	8	1000	75.00	3.76
5	11.00	11	1200	109.09	96.24
	8.00	11	1200	150.00	3.76
6	11.00	11	1200	109.09	96.24
	17.60	11	1200	68.18	3.76

Table A.1.: Calculation of route segment characteristics

A.3. Optimization of Duisburg Test Case

A.3.1. Ship Model

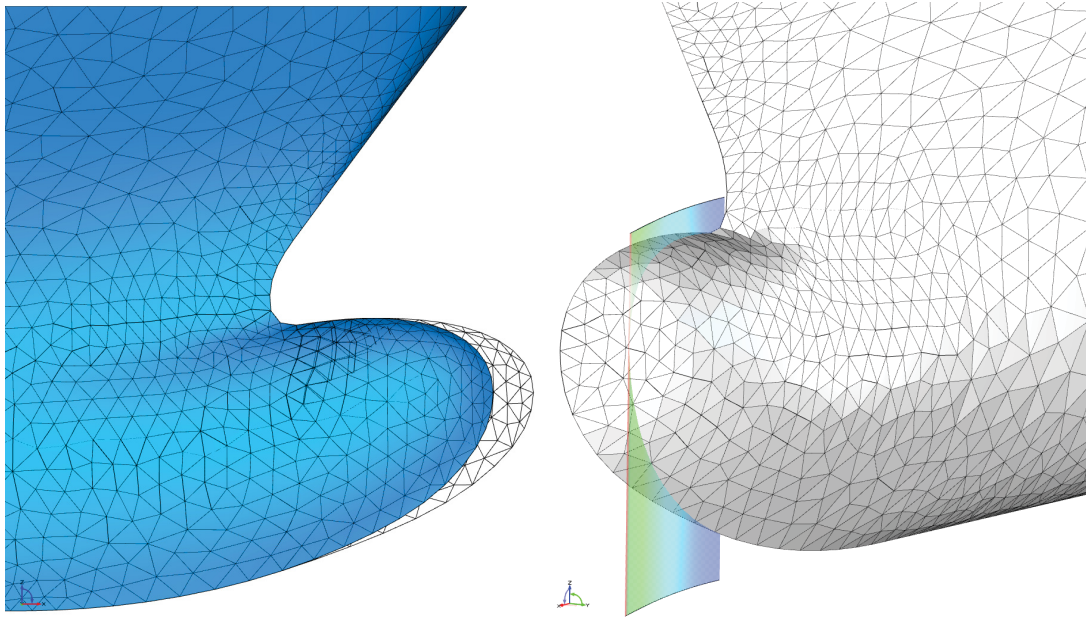


Figure A.3.: Principle of bulbous bow length variation (Bronsart et al., 2016)

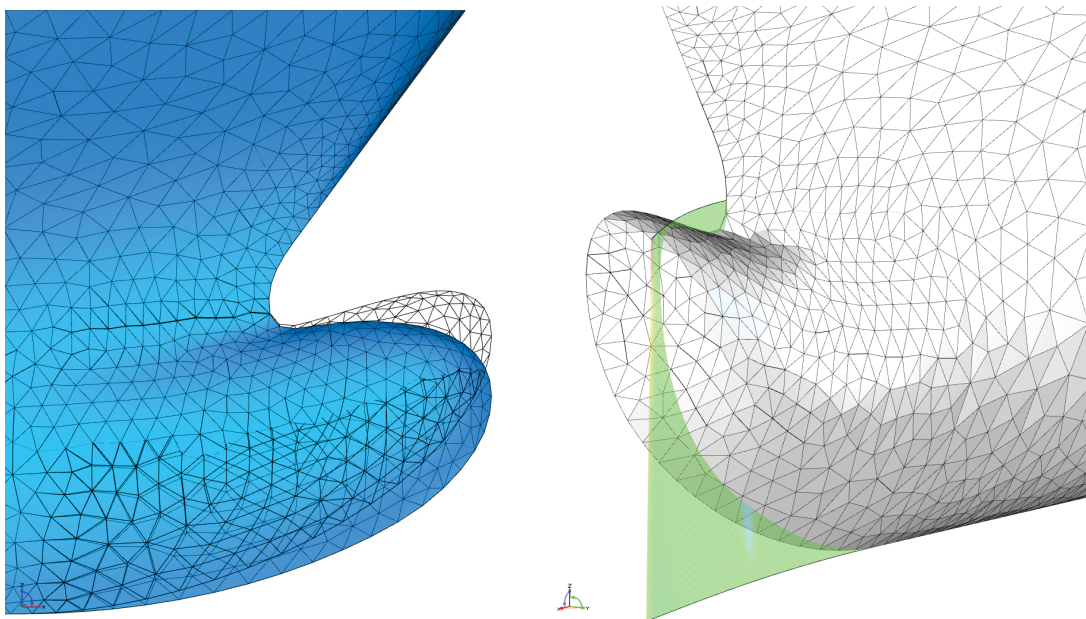


Figure A.4.: Principle of bulbous bow height variation (Bronsart et al., 2016)

A.3.2. Trade Description

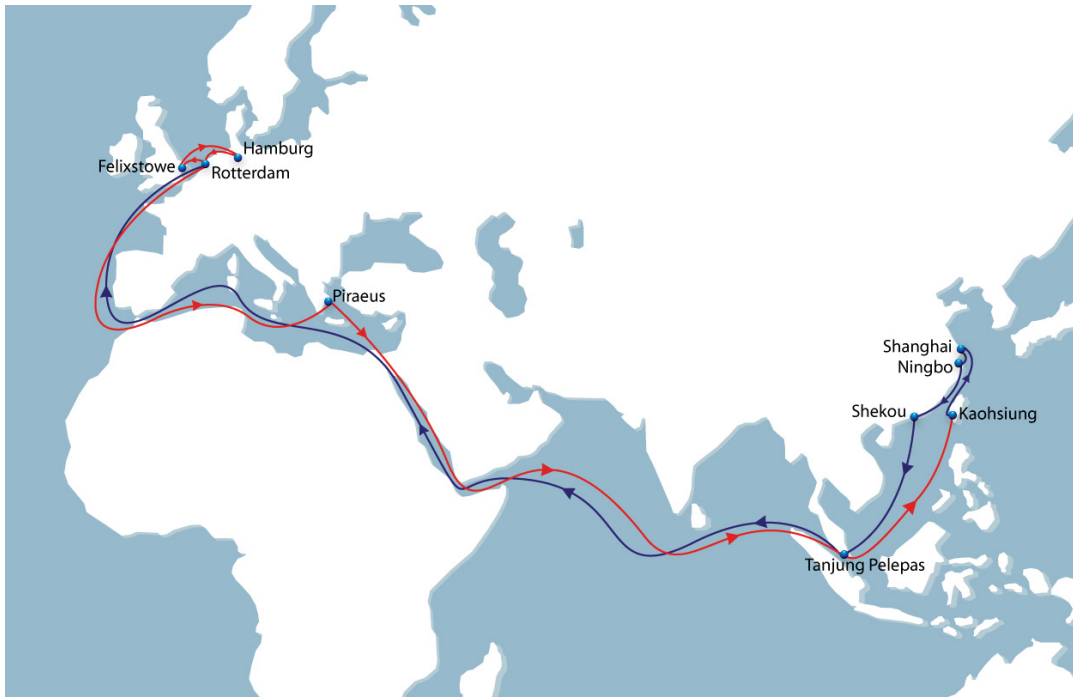


Figure A.5.: Transport task of Duisburg Test Case

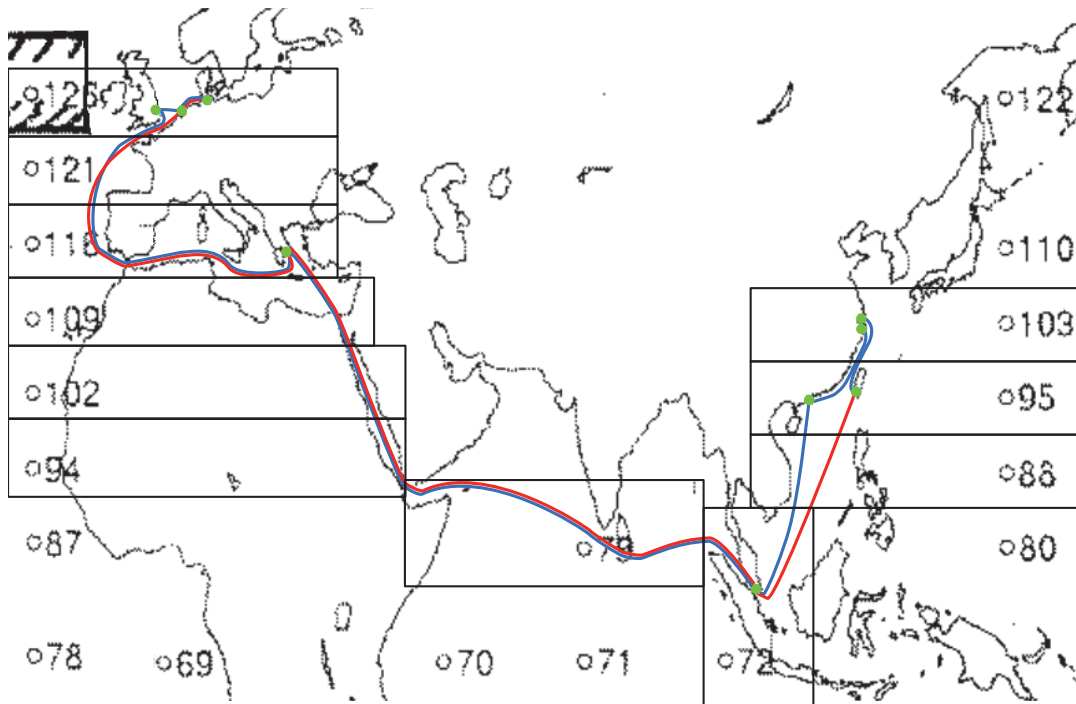


Figure A.6.: Allocation of transport task onto seaway points

A. Appendix

```

1 #Trade Description
2 #
3 #lines starting with '#' are treated as comments
4 #
5 #columns content:
6 #distance [nm], Soeding ID, speed [kn], draught [m], port lay time [h], port type, TEU (full),
7 #TEU (empty), min. local speed [kn], max local speed [kn], max. local draught [m], ECA share
8 #
9 0.0      95      0.0      0      49.33  5      6589    5230    0      0.0    14.00  0
10 2.4      95      6.3      0      0.00  0      6589    5230    0      10.0   0.00  0
11 233.8    95      14.9     0      0.00  0      6589    5230    0      0.0    0.00  0
12 300.6    103     14.9     0      0.00  0      6589    5230    0      0.0    0.00  0
13 1.1      103     6.3      0      0.00  0      6589    5230    0      10.0   0.00  0
14 0.0      103     0.0      0      56.50  4      6440    2368    0      0.0    0.00  0
15 1.1      103     6.3      0      0.00  0      6440    2368    0      10.0   0.00  0
16 37.9     103     11.0     0      0.00  0      6440    2368    0      0.0    0.00  0
17 17.3     103     8.8      0      0.00  0      6440    2368    0      10.0   0.00  0
18 0.0      103     0.0      0      29.00  4      8796    705     0      0.0    17.00  0
19 18.9     103     8.8      0      0.00  0      8796    705     0      10.0   0.00  0
20 233.2    103     21.0     0      0.00  0      8796    705     0      0.0    0.00  0
21 466.3    95      21.0     0      0.00  0      8796    705     0      0.0    0.00  0
22 1.1      95      6.3      0      0.00  0      8796    705     0      10.0   0.00  0
23 0.0      95      0.0      0      23.25  4      9088    227     0      0.0    13.50  0
24 1.1      95      6.3      0      0.00  0      9088    227     0      10.0   0.00  0
25 257.1    95      22.7     0      0.00  0      9088    227     0      0.0    0.00  0
26 514.3    88      22.7     0      0.00  0      9088    227     0      0.0    0.00  0
27 697.9    72      22.7     0      0.00  0      9088    227     0      0.0    0.00  0
28 1.1      72      6.3      0      0.00  0      9088    227     0      10.0   0.00  0
29 0.0      72      0.0      0      24.70  4      10009   23      0      0.0    19.00  0
30 1.1      72      6.3      0      0.00  0      10009   23      0      10.0   0.00  0
31 655.7    72      22.3     0      0.00  0      10009   23      0      0.0    0.00  0
32 2856.8   79      22.3     0      0.00  0      10009   23      0      0.0    0.00  0
33 655.7    94      22.3     0      0.00  0      10009   23      0      0.0    0.00  0
34 702.5    102     22.3     0      0.00  0      10009   23      0      0.0    0.00  0
35 46.8     109     22.3     0      0.00  0      10009   23      0      0.0    0.00  0
36 86.4     109     10.0     0      0.00  0      10009   23      0      8.1    18.56  0
37 393.8    109     20.6     0      0.00  0      10009   23      0      0.0    0.00  0
38 212.1    116     20.6     0      0.00  0      10009   23      0      0.0    0.00  0
39 1.1      116     6.3      0      0.00  0      10009   23      0      10.0   0.00  0
40 0.0      116     0.0      0      25.02  7      6948    191     0      0.0    18.00  0
41 1.1      116     6.3      0      0.00  0      6948    191     0      10.0   0.00  0
42 1847.1   116     22.9     0      0.00  0      6948    191     0      0.0    0.00  0
43 615.7    121     22.9     0      0.00  0      6948    191     0      0.0    0.00  0
44 326.0    126     22.9     0      0.00  0      6948    191     0      0.0    0.00  1
45 1.1      126     6.3      0      0.00  0      6948    191     0      10.0   0.00  1
46 0.0      126     0.0      0      37.72  4      6948    191     0      0.0    15.00  1
47 1.1      126     6.3      0      0.00  0      5683    1933    0      10.0   0.00  1
48 104.5    126     19.8     0      0.00  0      5683    1933    0      0.0    0.00  1
49 2.4      126     6.3      0      0.00  0      5683    1933    0      10.0   0.00  1
50 0.0      126     0.0      0      53.33  4      5683    1933    0      0.0    17.50  1
51 2.4      126     6.3      0      0.00  0      1804    1698    0      10.0   0.00  1
52 276.8    126     19.5     0      0.00  0      1804    1698    0      0.0    0.00  1
53 3.5      126     6.3      0      0.00  0      1804    1698    0      10.0   0.00  1
54 0.0      126     0.0      0      57.50  5      1804    1698    0      0.0    15.10  1
55 3.5      126     6.3      0      0.00  0      2569    2585    0      10.0   0.00  1
56 276.8    126     17.3     0      0.00  0      2569    2585    0      0.0    0.00  1
57 2.4      126     6.3      0      0.00  0      2569    2585    0      10.0   0.00  1
58 0.0      126     0.0      0      40.33  4      2569    2585    0      0.0    17.50  1
59 2.4      126     6.3      0      0.00  0      7629    5943    0      10.0   0.00  1
60 333.0    126     20.8     0      0.00  0      7629    5943    0      0.0    0.00  1
61 628.9    121     20.8     0      0.00  0      7629    5943    0      0.0    0.00  0
62 1886.8   116     20.8     0      0.00  0      7629    5943    0      0.0    0.00  0
63 1.1      116     6.3      0      0.00  0      7629    5943    0      10.0   0.00  0
64 0.0      116     0.0      0      30.33  7      7629    5943    0      0.0    18.00  0
65 1.1      116     6.3      0      0.00  0      7328    7103    0      10.0   0.00  0
66 212.1    116     24.9     0      0.00  0      7328    7103    0      0.0    0.00  0
67 393.8    109     24.9     0      0.00  0      7328    7103    0      0.0    0.00  0
68 86.4     109     10.0     0      0.00  0      7328    7103    0      8.1    18.56  0
69 46.8     109     19.5     0      0.00  0      7328    7103    0      0.0    0.00  0
70 702.5    102     19.5     0      0.00  0      7328    7103    0      0.0    0.00  0
71 655.7    94      19.5     0      0.00  0      7328    7103    0      0.0    0.00  0
72 2856.8   79      19.5     0      0.00  0      7328    7103    0      0.0    0.00  0
73 655.7    72      19.5     0      0.00  0      7328    7103    0      0.0    0.00  0
74 1.1      72      6.3      0      0.00  0      7328    7103    0      10.0   0.00  0
75 0.0      72      0.0      0      26.80  4      7328    7103    0      0.0    19.00  0
76 1.1      72      6.3      0      0.00  0      7096    5645    0      10.0   0.00  0
77 811.4    72      18.9     0      0.00  0      7096    5645    0      0.0    0.00  0
78 553.3    88      18.9     0      0.00  0      7096    5645    0      0.0    0.00  0
79 332.0    95      18.9     0      0.00  0      7096    5645    0      0.0    0.00  0
80 4.6      95      6.3      0      0.00  0      7096    5645    0      10.0   0.00  0

```

Listing A.1: Trade description

A.3.3. Scenario Setup

```

1 #Config-File for Scenario Development
2 #
3 #lines starting with '#' are treated as comments
4 #
5 #time horizon [h]
6 87658.2
7 #
8 #minimum draught [m]
9 10.0
10 #
11 #maximum draught [m]
12 15.5
13 #
14 #minimum speed [kn]
15 0.0
16 #
17 #maximum speed [kn]
18 25.0
19 #
20 #loading-draught-function (Lambda function), x / y = no. of full / empty TEUs
21 lambda x, y: 7.8136 + ((x * 11.85 + y * 2.0) * 6e-5)
22 #
23 #maintenance interval [h]
24 43829.1
25 #
26 #docking duration [h]
27 504.0
28 #
29 #slow steaming table
30 550, 600, 700
31 20, 18, 16
32 #
33 #speed reduction table
34 4.5, 5.5, 6.5, 7.5, 8.5, 9.5, 10.5, 11.5, 12.5, 13.5, 14.5
35 22.8, 20.6, 18.4, 16.2, 14.0, 11.8, 9.6, 7.4, 5.2, 3.0, 0.8
36 #
37 #bin width: speed [kn]
38 0.5
39 #
40 #bin width: draught [m]
41 0.5
42 #
43 #interest rate [%]
44 3.0
45 #
46 #FOP development (Lambda function) [$/h]
47 lambda x: 275.0 - 50.0 * (x / 8765.82) if x <= 8765.82 else 225.0 + 50.0 * (x / 8765.82 - 1.0)
48 #
49 #FOP fluctuation (Lambda function) [$/h]
50 lambda x: 1.5 * (x / 24.0)
51 #
52 #HFO-MDO difference (Lambda function) [$/h]
53 lambda x: 250.0
54 #
55 #TD development (Lambda function) [%/h]
56 lambda x: 0.05 * (x / 8765.82)
57 #
58 #TD fluctuation (Lambda function) [%/h]
59 lambda x: 0.005 * (x / 8765.82)
60 #
61 #FOP crisis: chance [%/y]
62 40.0
63 #
64 #FOP crisis: duration (averaged) [h]
65 4382.91
66 #
67 #FOP crisis: duration (standard deviation) [h]
68 4382.91
69 #
70 #FOP crisis: chance of rising FOP [%]
71 50.0
72 #
73 #TD crisis: chance [%/y]
74 13.33
75 #
76 #TD crisis: duration (averaged) [h]
77 8765.82
78 #
79 #TD crisis: duration (standard deviation) [h]
80 1460.97
81 #
82 #TD crisis: chance of rising TD [%]
83 25.0
84 #
85 #draught calculation: 0 = from draughts, 1 = from loading
86 1
87 #

```

A. Appendix

```
88 #minimum no. of MC cycles
89 10000
90 #
91 #Hellinger criterion (0 <= x <= 1)
92 1e-10
93 #
94 #maximum no. of MC cycles
95 25000
96 #
97 #OOC calculation: 0 = maximum no., 1 = coverage
98 1
99 #
100 #no. of OOCs
101 10
102 #
103 #OOC coverage [%]
104 100.0
```

Listing A.2: Scenario development setup

A.3.4. Objective Function

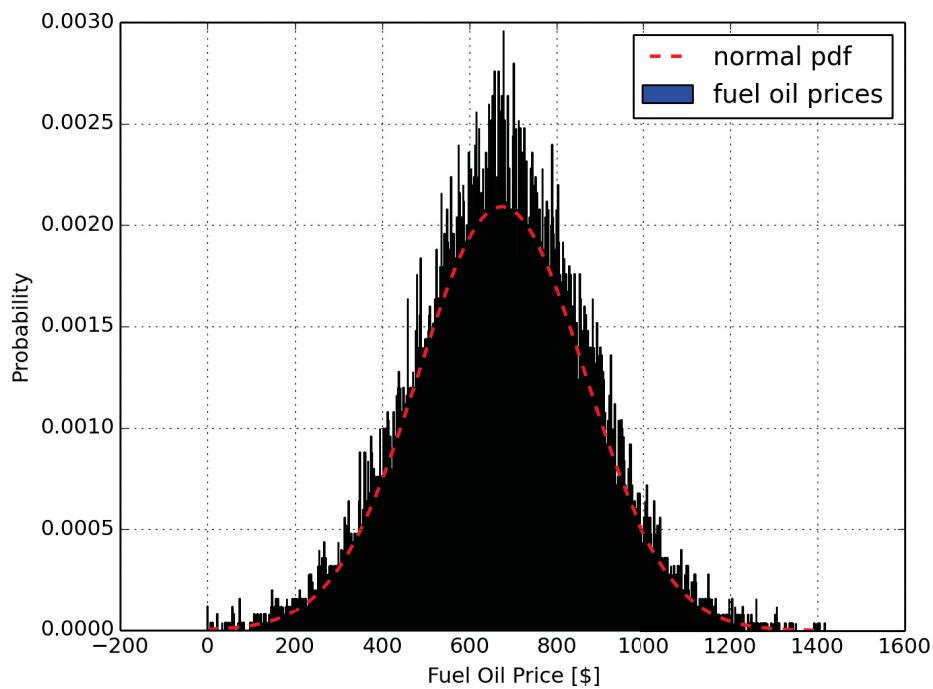


Figure A.7.: Distribution of fuel oil price values after ten years. Red: normal distribution with $\mu = 673.75$ and $\sigma = 190.82$.

A. Appendix

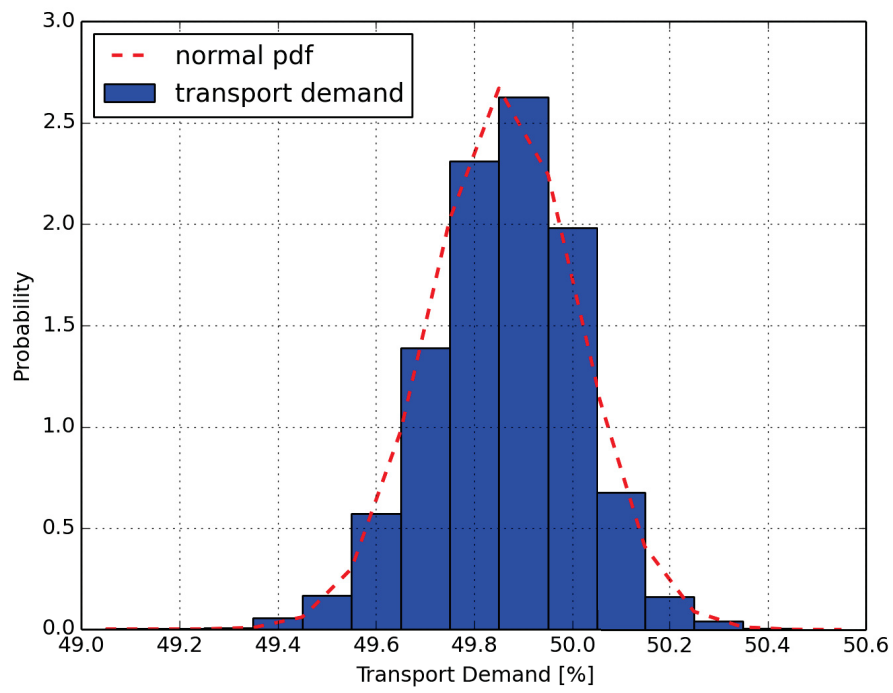


Figure A.8.: Distribution of transport demand values after ten years. Red: normal distribution with $\mu = 49.86$ and $\sigma = 0.15$.

A.4. Optimization of 3500 TEU Container Vessel

A.4.1. Ship Model

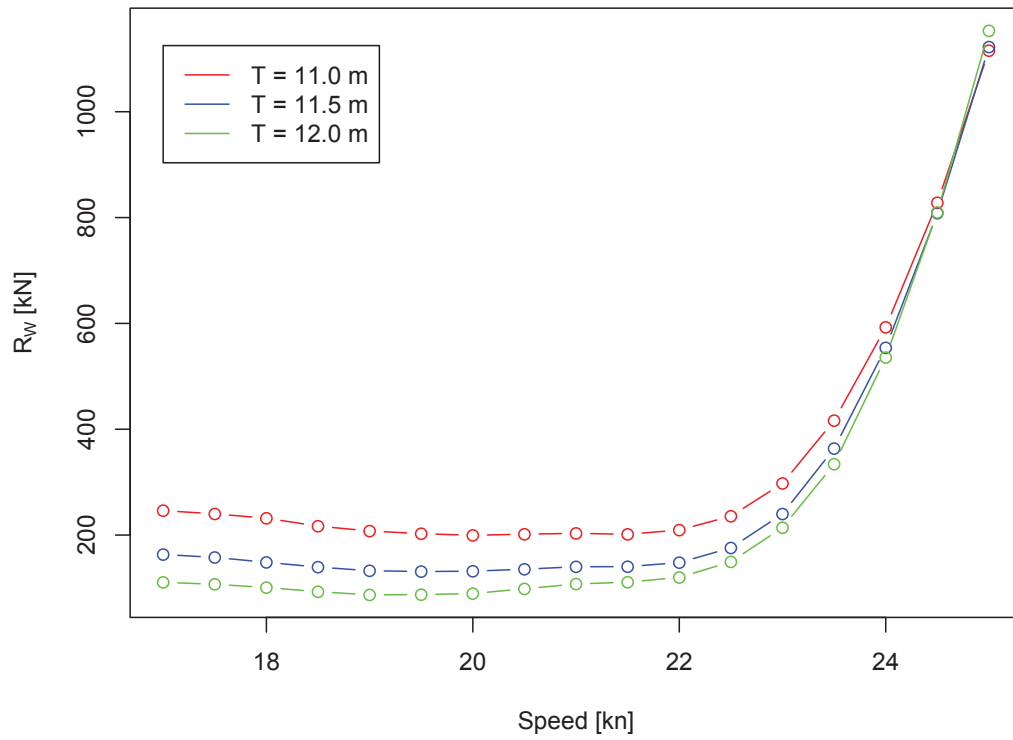


Figure A.9.: Wave resistance-curves of original hull form

A. Appendix

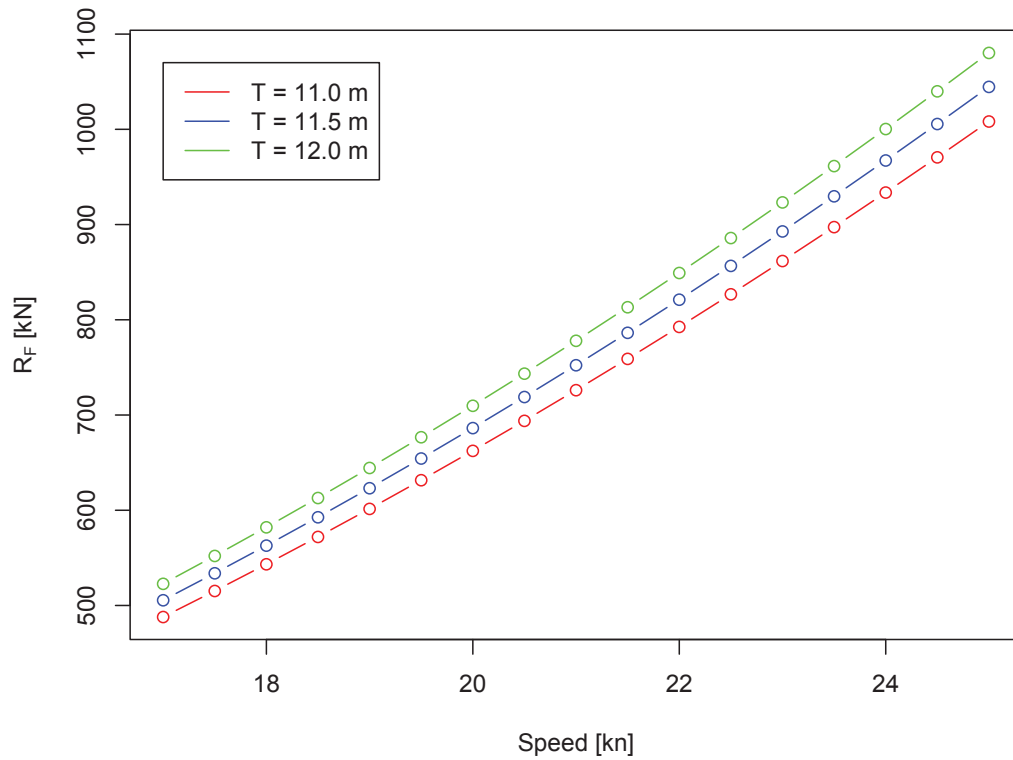


Figure A.10.: Frictional resistance-curves of original hull form

A.4.2. Trade Description

```

1 #Trade Description
2 #
3 #lines starting with '#' are treated as comments
4 #
5 #columns content:
6 #distance [nm], Soeding ID, speed [kn], draught [m], port lay time [h], port type, TEU (full),
7 #TEU (empty), min. local speed [kn], max local speed [kn], max. local draught [m], ECA share
8 #
9 # 1 - leg A
10 #
11 0 0 0.00 0.00 7 1489 1053 0.00 0.00 0.000 0
12 992 79 11.50 0.00 0.00 0 1489 1053 0.00 0.00 0.000 0
13 0 0 0.00 0.00 42.87 4 2034 0 0.00 0.00 0.000 0
14 580 79 17.43 0.00 0.00 0 2034 0 0.00 0.00 0.000 0
15 1574 70 17.43 0.00 0.00 0 2034 0 0.00 0.00 0.000 0
16 152 41 17.43 0.00 0.00 0 2034 0 0.00 0.00 0.000 0
17 0 0 0.00 0.00 24.00 8 1829 591 0.00 0.00 0.000 0
18 138 41 6.92 0.00 0.00 0 1829 591 0.00 0.00 0.000 0
19 0 0 0.00 0.00 24.00 8 1080 1605 0.00 0.00 0.000 0
20 474 41 6.92 0.00 0.00 0 1080 1605 0.00 0.00 0.000 0
21 0 0 0.00 0.00 31.66 8 787 648 0.00 0.00 0.000 0
22 1220 41 10.85 0.00 0.00 0 787 648 0.00 0.00 0.000 0
23 169 29 10.85 0.00 0.00 0 787 648 0.00 0.00 0.000 0
24 0 0 0.00 0.00 110.70 4 1436 1110 0.00 0.00 0.000 0
25 392 29 11.63 0.00 0.00 0 1436 1110 0.00 0.00 0.000 0
26 0 0 0.00 0.00 24.19 8 1797 1320 0.00 0.00 0.000 0
27 478 29 13.73 0.00 0.00 0 1797 1320 0.00 0.00 0.000 0
28 1411 41 13.73 0.00 0.00 0 1797 1320 0.00 0.00 0.000 0
29 0 0 0.00 0.00 34.77 8 1778 1300 0.00 0.00 0.000 0
30 110 41 11.49 0.00 0.00 0 1778 1300 0.00 0.00 0.000 0
31 1395 70 11.49 0.00 0.00 0 1778 1300 0.00 0.00 0.000 0
32 1519 79 11.49 0.00 0.00 0 1778 1300 0.00 0.00 0.000 0
33 0 0 0.00 0.00 24.12 7 1407 995 0.00 0.00 0.000 0
34 #

```

A. Appendix

35	# 2 - leg A											
36	#											
37	970	79	11.54	0.00	0.00	0	1407	995	0.00	0.00	0.000	0
38	0	0	0.00	0.00	36.63	4	1796	90	0.00	0.00	0.000	0
39	580	79	15.11	0.00	0.00	0	1796	90	0.00	0.00	0.000	0
40	1572	70	15.11	0.00	0.00	0	1796	90	0.00	0.00	0.000	0
41	152	41	15.11	0.00	0.00	0	1796	90	0.00	0.00	0.000	0
42	0	0	0.00	0.00	18.00	8	1166	1090	0.00	0.00	0.000	0
43	135	41	10.67	0.00	0.00	0	1166	1090	0.00	0.00	0.000	0
44	0	0	0.00	0.00	24.00	8	1188	978	0.00	0.00	0.000	0
45	483	41	10.67	0.00	0.00	0	1188	978	0.00	0.00	0.000	0
46	0	0	0.00	0.00	49.95	8	525	867	0.00	0.00	0.000	0
47	1235	41	11.03	0.00	0.00	0	525	867	0.00	0.00	0.000	0
48	171	29	11.03	0.00	0.00	0	525	867	0.00	0.00	0.000	0
49	0	0	0.00	0.00	115.37	4	838	1082	0.00	0.00	0.000	0
50	394	29	15.25	0.00	0.00	0	838	1082	0.00	0.00	0.000	0
51	0	0	0.00	0.00	21.57	8	1320	947	0.00	0.00	0.000	0
52	479	29	10.71	0.00	0.00	0	1320	947	0.00	0.00	0.000	0
53	1412	41	10.71	0.00	0.00	0	1320	947	0.00	0.00	0.000	0
54	0	0	0.00	0.00	23.18	8	1458	1051	0.00	0.00	0.000	0
55	110	41	11.48	0.00	0.00	0	1458	1051	0.00	0.00	0.000	0
56	1396	70	11.48	0.00	0.00	0	1458	1051	0.00	0.00	0.000	0
57	1520	79	11.48	0.00	0.00	0	1458	1051	0.00	0.00	0.000	0
58	0	0	0.00	0.00	20.45	7	1307	1300	0.00	0.00	0.000	0
59	#											
60	# 3 - leg A											
61	#											
62	971	79	9.62	0.00	0.00	0	1307	1300	0.00	0.00	0.000	0
63	0	0	0.00	0.00	34.72	4	1747	88	0.00	0.00	0.000	0
64	581	79	15.52	0.00	0.00	0	1747	88	0.00	0.00	0.000	0
65	1575	70	15.52	0.00	0.00	0	1747	88	0.00	0.00	0.000	0
66	152	41	15.52	0.00	0.00	0	1747	88	0.00	0.00	0.000	0
67	0	0	0.00	0.00	30.00	8	1205	1126	0.00	0.00	0.000	0
68	135	41	10.67	0.00	0.00	0	1205	1126	0.00	0.00	0.000	0
69	0	0	0.00	0.00	18.00	8	991	1308	0.00	0.00	0.000	0
70	474	41	10.67	0.00	0.00	0	991	1308	0.00	0.00	0.000	0
71	0	0	0.00	0.00	58.98	8	552	912	0.00	0.00	0.000	0
72	1215	41	9.35	0.00	0.00	0	552	912	0.00	0.00	0.000	0
73	168	29	9.35	0.00	0.00	0	552	912	0.00	0.00	0.000	0
74	0	0	0.00	0.00	73.49	4	1266	856	0.00	0.00	0.000	0
75	391	29	12.13	0.00	0.00	0	1266	856	0.00	0.00	0.000	0
76	0	0	0.00	0.00	37.26	8	1474	1082	0.00	0.00	0.000	0
77	480	29	12.91	0.00	0.00	0	1474	1082	0.00	0.00	0.000	0
78	1414	41	12.91	0.00	0.00	0	1474	1082	0.00	0.00	0.000	0
79	0	0	0.00	0.00	20.54	8	1647	1204	0.00	0.00	0.000	0
80	110	41	10.87	0.00	0.00	0	1647	1204	0.00	0.00	0.000	0
81	1394	70	10.87	0.00	0.00	0	1647	1204	0.00	0.00	0.000	0
82	1518	79	10.87	0.00	0.00	0	1647	1204	0.00	0.00	0.000	0
83	0	0	0.00	0.00	24.00	7	1771	744	0.00	0.00	0.000	0
84	#											
85	# 4 - leg B											
86	#											
87	268	79	11.73	0.00	0.00	0	1771	744	0.00	0.00	0	0
88	0	0	0.00	0.00	24.00	8	1582	664	0.00	0.00	0	0
89	756	79	11.73	0.00	0.00	0	1582	664	0.00	0.00	0	0
90	0	0	0.00	0.00	16.87	4	1724	87	0.00	0.00	0	0
91	580	79	15.77	0.00	0.00	0	1724	87	0.00	0.00	0	0
92	1573	70	15.77	0.00	0.00	0	1724	87	0.00	0.00	0	0
93	152	41	15.77	0.00	0.00	0	1724	87	0.00	0.00	0	0
94	0	0	0.00	0.00	18.00	8	1028	1560	0.00	0.00	0	0
95	133	41	10.67	0.00	0.00	0	1028	1560	0.00	0.00	0	0
96	0	0	0.00	0.00	18.00	8	973	1284	0.00	0.00	0	0
97	473	41	10.67	0.00	0.00	0	973	1284	0.00	0.00	0	0
98	0	0	0.00	0.00	63.28	8	474	1673	0.00	0.00	0	0
99	1219	41	10.16	0.00	0.00	0	474	1673	0.00	0.00	0	0
100	169	29	10.16	0.00	0.00	0	474	1673	0.00	0.00	0	0
101	0	0	0.00	0.00	157.56	4	1020	1317	0.00	0.00	0	0
102	393	29	9.08	0.00	0.00	0	1020	1317	0.00	0.00	0	0
103	0	0	0.00	0.00	24.40	8	1349	1554	0.00	0.00	0	0
104	646	29	12.86	0.00	0.00	0	1349	1554	0.00	0.00	0	0
105	775	41	12.86	0.00	0.00	0	1349	1554	0.00	0.00	0	0
106	1970	70	12.86	0.00	0.00	0	1349	1554	0.00	0.00	0	0
107	1518	79	12.86	0.00	0.00	0	1349	1554	0.00	0.00	0	0
108	0	0	0.00	0.00	30.47	7	1266	1259	0.00	0.00	0	0
109	#											
110	# 5 - leg A											
111	#											
112	972	79	10.33	0.00	0.00	0	1266	1259	0.00	0.00	0.000	0
113	0	0	0.00	0.00	20.43	4	1062	588	0.00	0.00	0.000	0
114	580	79	16.95	0.00	0.00	0	1062	588	0.00	0.00	0.000	0
115	1572	70	16.95	0.00	0.00	0	1062	588	0.00	0.00	0.000	0
116	152	41	16.95	0.00	0.00	0	1062	588	0.00	0.00	0.000	0
117	0	0	0.00	0.00	18.00	8	964	1462	0.00	0.00	0.000	0
118	136	41	10.79	0.00	0.00	0	964	1462	0.00	0.00	0.000	0
119	0	0	0.00	0.00	18.00	8	955	1261	0.00	0.00	0.000	0
120	477	41	10.79	0.00	0.00	0	955	1261	0.00	0.00	0.000	0
121	0	0	0.00	0.00	72.07	8	461	2054	0.00	0.00	0.000	0
122	1215	41	10.13	0.00	0.00	0	461	2054	0.00	0.00	0.000	0
123	168	29	10.13	0.00	0.00	0	461	2054	0.00	0.00	0.000	0
124	0	0	0.00	0.00	52.81	4	1266	856	0.00	0.00	0.000	0

A. Appendix

125	396	29	7.21	0.00	0.00	0	1266	856	0.00	0.00	0.000	0
126	0	0	0.00	0.00	53.71	8	1474	1082	0.00	0.00	0.000	0
127	480	29	13.43	0.00	0.00	0	1474	1082	0.00	0.00	0.000	0
128	1416	41	13.43	0.00	0.00	0	1474	1082	0.00	0.00	0.000	0
129	0	0	0.00	0.00	36.63	8	1560	1141	0.00	0.00	0.000	0
130	111	41	12.28	0.00	0.00	0	1560	1141	0.00	0.00	0.000	0
131	1397	70	12.28	0.00	0.00	0	1560	1141	0.00	0.00	0.000	0
132	1521	79	12.28	0.00	0.00	0	1560	1141	0.00	0.00	0.000	0
133	0	0	0.00	0.00	20.80	7	1807	705	0.00	0.00	0.000	0
134	#											
135	# 6 - leg A											
136	#											
137	970	79	9.32	0.00	0.00	0	1807	705	0.00	0.00	0.000	0
138	0	0	0.00	0.00	28.62	4	1817	91	0.00	0.00	0.000	0
139	580	79	17.17	0.00	0.00	0	1817	91	0.00	0.00	0.000	0
140	1574	70	17.17	0.00	0.00	0	1817	91	0.00	0.00	0.000	0
141	152	41	17.17	0.00	0.00	0	1817	91	0.00	0.00	0.000	0
142	0	0	0.00	0.00	18.00	8	1556	548	0.00	0.00	0.000	0
143	135	41	11.04	0.00	0.00	0	1556	548	0.00	0.00	0.000	0
144	0	0	0.00	0.00	18.00	8	1600	521	0.00	0.00	0.000	0
145	477	41	11.04	0.00	0.00	0	1600	521	0.00	0.00	0.000	0
146	0	0	0.00	0.00	66.98	8	570	941	0.00	0.00	0.000	0
147	1214	41	10.59	0.00	0.00	0	570	941	0.00	0.00	0.000	0
148	168	29	10.59	0.00	0.00	0	570	941	0.00	0.00	0.000	0
149	0	0	0.00	0.00	135.79	4	1249	1087	0.00	0.00	0.000	0
150	395	29	13.42	0.00	0.00	0	1249	1087	0.00	0.00	0.000	0
151	0	0	0.00	0.00	35.19	8	1324	949	0.00	0.00	0.000	0
152	478	29	17.92	0.00	0.00	0	1324	949	0.00	0.00	0.000	0
153	1410	41	17.92	0.00	0.00	0	1324	949	0.00	0.00	0.000	0
154	0	0	0.00	0.00	14.45	8	1386	985	0.00	0.00	0.000	0
155	111	41	11.13	0.00	0.00	0	1386	985	0.00	0.00	0.000	0
156	1398	70	11.13	0.00	0.00	0	1386	985	0.00	0.00	0.000	0
157	1523	79	11.13	0.00	0.00	0	1386	985	0.00	0.00	0.000	0
158	0	0	0.00	0.00	29.95	7	1767	794	0.00	0.00	0.000	0
159	#											
160	# 7 - leg C											
161	#											
162	974	79	10.91	0.00	0.00	0	1767	794	0.00	0.00	0.000	0
163	0	0	0.00	0.00	27.71	4	2097	0	0.00	0.00	0.000	0
164	579	79	15.35	0.00	0.00	0	2097	0	0.00	0.00	0.000	0
165	1572	70	15.35	0.00	0.00	0	2097	0	0.00	0.00	0.000	0
166	152	41	15.35	0.00	0.00	0	2097	0	0.00	0.00	0.000	0
167	0	0	0.00	0.00	24.00	8	1829	591	0.00	0.00	0.000	0
168	134	41	11.75	0.00	0.00	0	1829	591	0.00	0.00	0.000	0
169	0	0	0.00	0.00	18.00	8	1617	626	0.00	0.00	0.000	0
170	475	41	11.75	0.00	0.00	0	1617	626	0.00	0.00	0.000	0
171	0	0	0.00	0.00	67.80	8	732	859	0.00	0.00	0.000	0
172	1196	41	11.81	0.00	0.00	0	732	859	0.00	0.00	0.000	0
173	518	29	11.81	0.00	0.00	0	732	859	0.00	0.00	0.000	0
174	0	0	0.00	0.00	19.42	8	851	1022	0.00	0.00	0.000	0
175	405	29	10.21	0.00	0.00	0	851	1022	0.00	0.00	0.000	0
176	0	0	0.00	0.00	59.79	4	1145	1080	0.00	0.00	0.000	0
177	171	29	9.37	0.00	0.00	0	1145	1080	0.00	0.00	0.000	0
178	1408	41	9.37	0.00	0.00	0	1145	1080	0.00	0.00	0.000	0
179	0	0	0.00	0.00	42.91	8	1304	1595	0.00	0.00	0.000	0
180	110	41	11.36	0.00	0.00	0	1304	1595	0.00	0.00	0.000	0
181	1395	70	11.36	0.00	0.00	0	1304	1595	0.00	0.00	0.000	0
182	1519	79	11.36	0.00	0.00	0	1304	1595	0.00	0.00	0.000	0
183	0	0	0.00	0.00	24.54	7	1489	1053	0.00	0.00	0.000	0

Listing A.3: Trade description

A.4.3. Scenario Setup

```

1 #Config-File for Scenario Development
2 #
3 #lines starting with '#' are treated as comments
4 #
5 #time horizon [h]
6 8765.82
7 #
8 #minimum draught [m]
9 5.5013054
10 #
11 #maximum draught [m]
12 12.0
13 #
14 #minimum speed [kn]
15 0.0
16 #
17 #maximum speed [kn]
18 25.0
19 #
20 #loading-draught-function (Lambda function), x / y = no. of full / empty TEUs
21 lambda x, y: 5.5013054 + (x * 0.0031827 + y * 0.0007229)
22 #
23 #maintenance interval [h]
24 43829.1
25 #
26 #docking duration [h]
27 336.0
28 #
29 #slow steaming table
30 550, 600, 700
31 20, 18, 16
32 #
33 #speed reduction table
34 3.0, 3.67, 4.33, 5.0, 5.67, 6.33, 7.0, 7.67, 8.33, 9.0, 9.67
35 22.8, 20.6, 18.4, 16.2, 14., 11.8, 9.6, 7.4, 5.2, 3., 0.8
36 #
37 #bin width: speed [kn]
38 0.5
39 #
40 #bin width: draught [m]
41 0.5
42 #
43 #interest rate [%]
44 3.0
45 #
46 #FOP development (Lambda function) [$/h]
47 lambda x: 275.0 + 325.0 * x / 8765.82
48 #
49 #FOP fluctuation (Lambda function) [$/h]
50 lambda x: 1.5 * (x / 24.0)
51 #
52 #HFO-MDO difference (Lambda function) [$/h]
53 lambda x: 250.0
54 #
55 #TD development (Lambda function) [%/h]
56 lambda x: 0.03 * (x / 8765.82)
57 #
58 #TD fluctuation (Lambda function) [%/h]
59 lambda x: 0.01 * (x / 8765.82)
60 #
61 #FOP crisis: chance [%/y]
62 40.0
63 #
64 #FOP crisis: duration (averaged) [h]
65 4382.91
66 #
67 #FOP crisis: duration (standard deviation) [h]
68 4382.91
69 #
70 #FOP crisis: chance of rising FOP [%]
71 50.0
72 #
73 #TD crisis: chance [%/y]
74 13.33
75 #
76 #TD crisis: duration (averaged) [h]
77 8765.82
78 #
79 #TD crisis: duration (standard deviation) [h]
80 1460.97
81 #
82 #TD crisis: chance of rising TD [%]
83 25.0
84 #
85 #draught calculation: 0 = from draughts, 1 = from loading
86 1
87 #

```

A. Appendix

```
88 #minimum no. of MC cycles
89 10000
90 #
91 #Hellinger criterion (0 <= x <= 1)
92 1e-10
93 #
94 #maximum no. of MC cycles
95 1000000
96 #
97 #OOC calculation: 0 = maximum no., 1 = coverage
98 1
99 #
100 #no. of OOCs
101 6
102 #
103 #OOC coverage [%]
104 100.0
```

Listing A.4: Scenario development setup

A.4.4. Objective Function

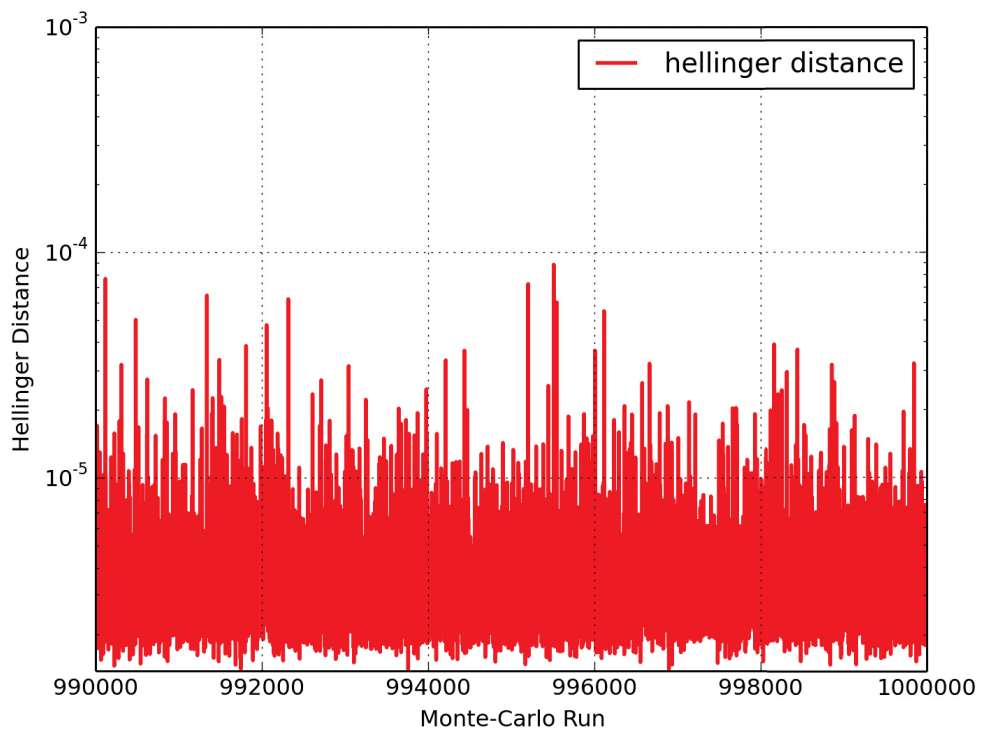


Figure A.11.: *Hellinger* criterion development of last 10 000 Monte-Carlo cycles

A. Appendix

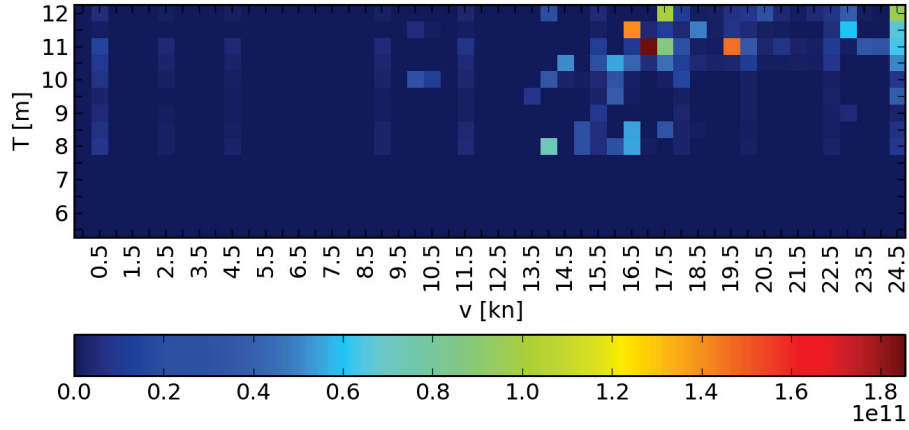


Figure A.12.: Total speed and draught distribution of 3500 *TEU* container vessel

v [kn]	T [m]	w [%]	w_{Total} [%]
17.50	11.00	23.61	7.22
20.00	11.00	18.70	5.72
17.00	11.50	17.51	5.35
18.00	12.00	14.38	4.40
25.00	12.00	13.68	4.18
18.00	11.00	12.12	3.71

Table A.2.: Objective operating conditions (without fuel oil prices)

A.4.5. Results

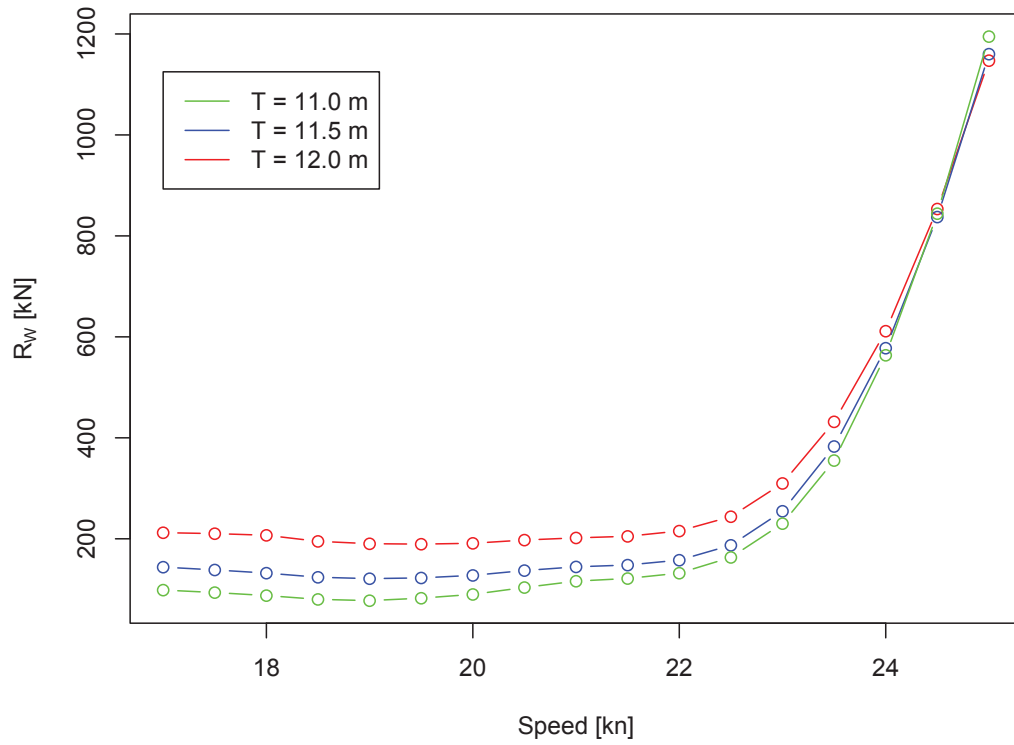


Figure A.13.: Wave resistance-curves of optimized hull form

A. Appendix

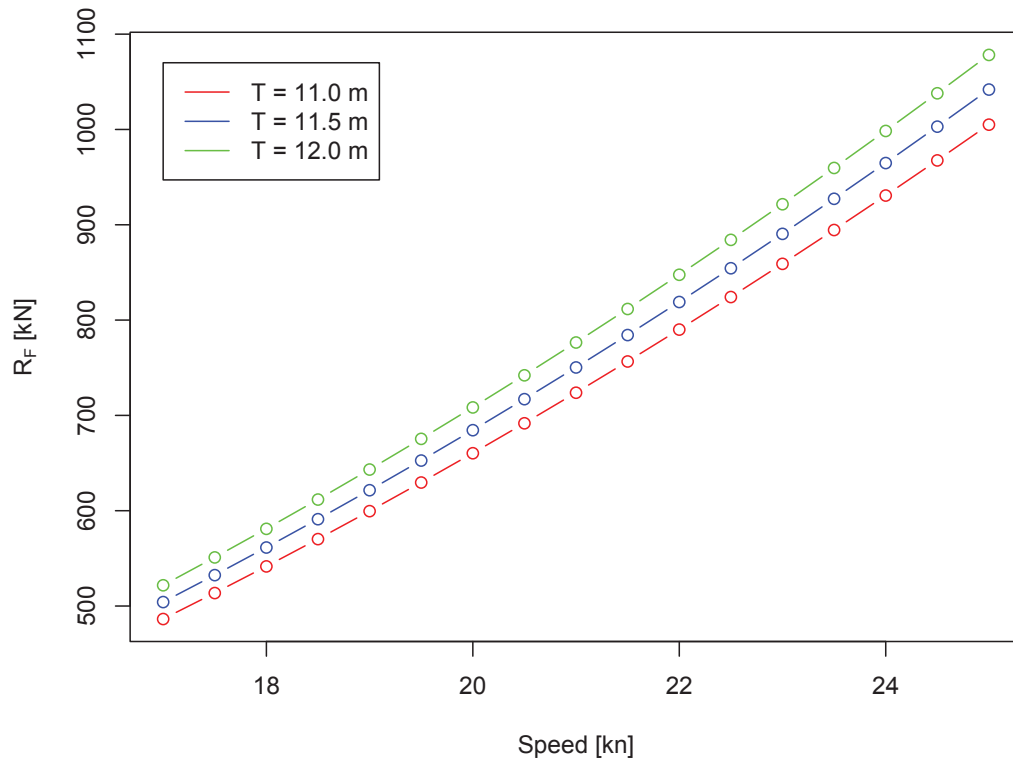


Figure A.14.: Frictional resistance-curves of optimized hull form

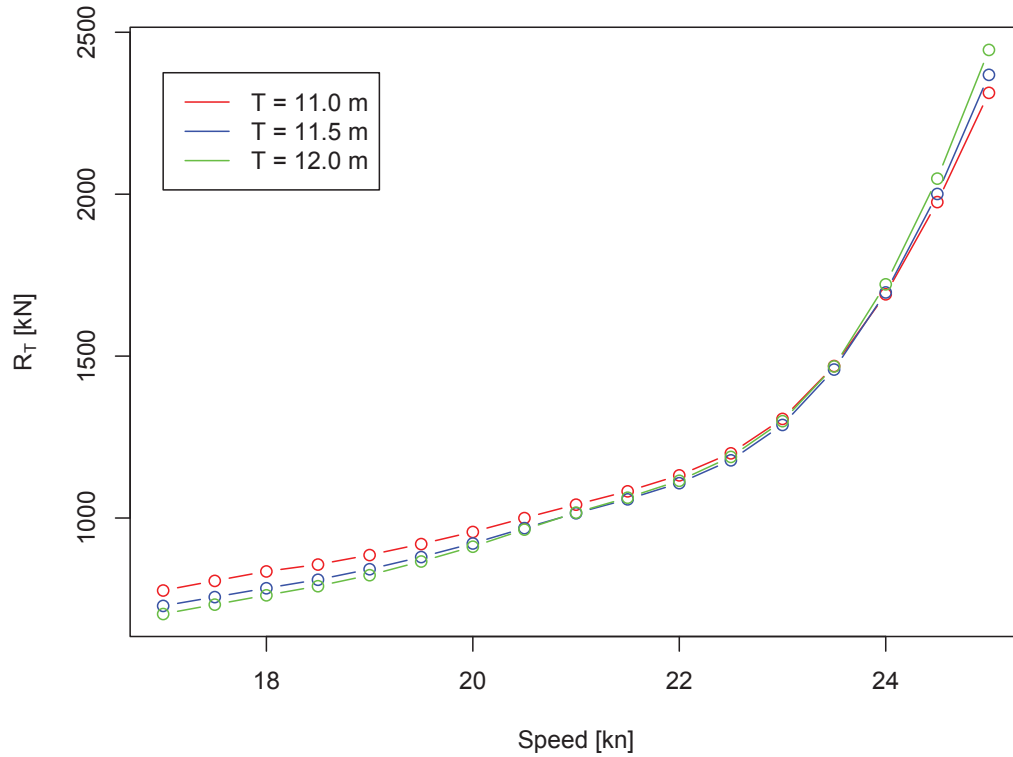


Figure A.15.: Total resistance-curves of optimized hull form

A.5. Optimization of Passenger Vessel

A.5.1. Trade Description

```

1 #Trade Description
2 #
3 #lines starting with '#' are treated as comments
4 #
5 #columns content:
6 #distance [nm], Soeding ID, speed [kn], draught [m], port lay time [h], port type, TEU (full),
7 #TEU (empty), min. local speed [kn], max local speed [kn], max. local draught [m]
8 #
9 0 0 0 7.2 12 2 0 0 0 0 0
10 810 116 18 7.2 0 0 0 0 0 0 0
11 0 0 0 7.2 8 4 0 0 0 0 0
12 328 116 10 7.2 0 0 0 0 0 0 0
13 0 0 0 7.2 10 4 0 0 0 0 0
14 273 116 12.5 7.2 0 0 0 0 0 0 0
15 0 0 0 7.2 6 4 0 0 0 0 0
16 153 116 14 7.2 0 0 0 0 0 0 0
17 0 0 0 7.2 10 4 0 0 0 0 0
18 97 116 8 7.2 0 0 0 0 0 0 0
19 0 0 0 7.2 12 4 0 0 0 0 0
20 661 116 18 7.2 0 0 0 0 0 0 0
21 0 0 0 7.2 11.5 4 0 0 0 0 0
22 147 116 14 7.2 0 0 0 0 0 0 0
23 0 0 0 7.2 12 2 0 0 0 0 0
24 810 116 18 7.2 0 0 0 0 0 0 0
25 0 0 0 7.2 8 4 0 0 0 0 0
26 328 116 10 7.2 0 0 0 0 0 0 0
27 0 0 0 7.2 10 4 0 0 0 0 0
28 273 116 12.5 7.2 0 0 0 0 0 0 0
29 0 0 0 7.2 6 4 0 0 0 0 0
30 153 116 14 7.2 0 0 0 0 0 0 0

```

A. Appendix

31	0	0	0	7.2	10	4	0	0	0	0	0
32	97	116	8	7.2	0	0	0	0	0	0	0
33	0	0	0	7.2	12	4	0	0	0	0	0
34	661	116	18	7.2	0	0	0	0	0	0	0
35	0	0	0	7.2	11.5	4	0	0	0	0	0
36	147	116	14	7.2	0	0	0	0	0	0	0
37	0	0	0	7.2	12	2	0	0	0	0	0
38	810	116	18	7.2	0	0	0	0	0	0	0
39	0	0	0	7.2	8	4	0	0	0	0	0
40	328	116	10	7.2	0	0	0	0	0	0	0
41	0	0	0	7.2	10	4	0	0	0	0	0
42	273	116	12.5	7.2	0	0	0	0	0	0	0
43	0	0	0	7.2	6	4	0	0	0	0	0
44	153	116	14	7.2	0	0	0	0	0	0	0
45	0	0	0	7.2	10	4	0	0	0	0	0
46	97	116	8	7.2	0	0	0	0	0	0	0
47	0	0	0	7.2	12	4	0	0	0	0	0
48	661	116	18	7.2	0	0	0	0	0	0	0
49	0	0	0	7.2	11.5	4	0	0	0	0	0
50	147	116	14	7.2	0	0	0	0	0	0	0
51	0	0	0	7.2	12	2	0	0	0	0	0
52	810	116	18	7.2	0	0	0	0	0	0	0
53	0	0	0	7.2	8	4	0	0	0	0	0
54	328	116	10	7.2	0	0	0	0	0	0	0
55	0	0	0	7.2	10	4	0	0	0	0	0
56	273	116	12.5	7.2	0	0	0	0	0	0	0
57	0	0	0	7.2	6	4	0	0	0	0	0
58	153	116	14	7.2	0	0	0	0	0	0	0
59	0	0	0	7.2	10	4	0	0	0	0	0
60	97	116	8	7.2	0	0	0	0	0	0	0
61	0	0	0	7.2	12	4	0	0	0	0	0
62	661	116	18	7.2	0	0	0	0	0	0	0
63	0	0	0	7.2	11.5	4	0	0	0	0	0
64	147	116	14	7.2	0	0	0	0	0	0	0
65	0	0	0	7.2	12	2	0	0	0	0	0
66	810	116	18	7.2	0	0	0	0	0	0	0
67	0	0	0	7.2	8	4	0	0	0	0	0
68	328	116	10	7.2	0	0	0	0	0	0	0
69	0	0	0	7.2	10	4	0	0	0	0	0
70	273	116	12.5	7.2	0	0	0	0	0	0	0
71	0	0	0	7.2	6	4	0	0	0	0	0
72	153	116	14	7.2	0	0	0	0	0	0	0
73	0	0	0	7.2	10	4	0	0	0	0	0
74	97	116	8	7.2	0	0	0	0	0	0	0
75	0	0	0	7.2	12	4	0	0	0	0	0
76	661	116	18	7.2	0	0	0	0	0	0	0
77	0	0	0	7.2	11.5	4	0	0	0	0	0
78	147	116	14	7.2	0	0	0	0	0	0	0
79	0	0	0	7.2	12	2	0	0	0	0	0
80	810	116	18	7.2	0	0	0	0	0	0	0
81	0	0	0	7.2	8	4	0	0	0	0	0
82	328	116	10	7.2	0	0	0	0	0	0	0
83	0	0	0	7.2	10	4	0	0	0	0	0
84	273	116	12.5	7.2	0	0	0	0	0	0	0
85	0	0	0	7.2	6	4	0	0	0	0	0
86	153	116	14	7.2	0	0	0	0	0	0	0
87	0	0	0	7.2	10	4	0	0	0	0	0
88	97	116	8	7.2	0	0	0	0	0	0	0
89	0	0	0	7.2	12	4	0	0	0	0	0
90	661	116	18	7.2	0	0	0	0	0	0	0
91	0	0	0	7.2	11.5	4	0	0	0	0	0
92	147	116	14	7.2	0	0	0	0	0	0	0
93	0	0	0	7.2	12	2	0	0	0	0	0
94	810	116	18	7.2	0	0	0	0	0	0	0
95	0	0	0	7.2	8	4	0	0	0	0	0
96	328	116	10	7.2	0	0	0	0	0	0	0
97	0	0	0	7.2	10	4	0	0	0	0	0
98	273	116	12.5	7.2	0	0	0	0	0	0	0
99	0	0	0	7.2	6	4	0	0	0	0	0
100	153	116	14	7.2	0	0	0	0	0	0	0
101	0	0	0	7.2	10	4	0	0	0	0	0
102	97	116	8	7.2	0	0	0	0	0	0	0
103	0	0	0	7.2	12	4	0	0	0	0	0
104	661	116	18	7.2	0	0	0	0	0	0	0
105	0	0	0	7.2	11.5	4	0	0	0	0	0
106	147	116	14	7.2	0	0	0	0	0	0	0
107	0	0	0	7.2	12	2	0	0	0	0	0
108	810	116	18	7.2	0	0	0	0	0	0	0
109	0	0	0	7.2	8	4	0	0	0	0	0
110	328	116	10	7.2	0	0	0	0	0	0	0
111	0	0	0	7.2	10	4	0	0	0	0	0
112	273	116	12.5	7.2	0	0	0	0	0	0	0
113	0	0	0	7.2	6	4	0	0	0	0	0
114	153	116	14	7.2	0	0	0	0	0	0	0
115	0	0	0	7.2	10	4	0	0	0	0	0
116	97	116	8	7.2	0	0	0	0	0	0	0
117	0	0	0	7.2	12	4	0	0	0	0	0
118	661	116	18	7.2	0	0	0	0	0	0	0
119	0	0	0	7.2	11.5	4	0	0	0	0	0
120	147	116	14	7.2	0	0	0	0	0	0	0

A. Appendix

121	0	0	0	7.2	12	2	0	0	0	0	0
122	810	116	18	7.2	0	0	0	0	0	0	0
123	0	0	0	7.2	8	4	0	0	0	0	0
124	328	116	10	7.2	0	0	0	0	0	0	0
125	0	0	0	7.2	10	4	0	0	0	0	0
126	273	116	12.5	7.2	0	0	0	0	0	0	0
127	0	0	0	7.2	6	4	0	0	0	0	0
128	153	116	14	7.2	0	0	0	0	0	0	0
129	0	0	0	7.2	10	4	0	0	0	0	0
130	97	116	8	7.2	0	0	0	0	0	0	0
131	0	0	0	7.2	12	4	0	0	0	0	0
132	661	116	18	7.2	0	0	0	0	0	0	0
133	0	0	0	7.2	11.5	4	0	0	0	0	0
134	147	116	14	7.2	0	0	0	0	0	0	0
135	0	0	0	7.2	12	2	0	0	0	0	0
136	810	116	18	7.2	0	0	0	0	0	0	0
137	0	0	0	7.2	8	4	0	0	0	0	0
138	328	116	10	7.2	0	0	0	0	0	0	0
139	0	0	0	7.2	10	4	0	0	0	0	0
140	273	116	12.5	7.2	0	0	0	0	0	0	0
141	0	0	0	7.2	6	4	0	0	0	0	0
142	153	116	14	7.2	0	0	0	0	0	0	0
143	0	0	0	7.2	10	4	0	0	0	0	0
144	97	116	8	7.2	0	0	0	0	0	0	0
145	0	0	0	7.2	12	4	0	0	0	0	0
146	661	116	18	7.2	0	0	0	0	0	0	0
147	0	0	0	7.2	11.5	4	0	0	0	0	0
148	147	116	14	7.2	0	0	0	0	0	0	0
149	0	0	0	7.2	12	2	0	0	0	0	0
150	810	116	18	7.2	0	0	0	0	0	0	0
151	0	0	0	7.2	8	4	0	0	0	0	0
152	328	116	10	7.2	0	0	0	0	0	0	0
153	0	0	0	7.2	10	4	0	0	0	0	0
154	273	116	12.5	7.2	0	0	0	0	0	0	0
155	0	0	0	7.2	6	4	0	0	0	0	0
156	153	116	14	7.2	0	0	0	0	0	0	0
157	0	0	0	7.2	10	4	0	0	0	0	0
158	97	116	8	7.2	0	0	0	0	0	0	0
159	0	0	0	7.2	12	4	0	0	0	0	0
160	661	116	18	7.2	0	0	0	0	0	0	0
161	0	0	0	7.2	11.5	4	0	0	0	0	0
162	147	116	14	7.2	0	0	0	0	0	0	0
163	0	0	0	7.2	12	2	0	0	0	0	0
164	300	116	17.5	7.2	0	0	0	0	0	0	0
165	0	0	0	7.2	9	4	0	0	0	0	0
166	486	116	14	7.2	0	0	0	0	0	0	0
167	0	0	0	7.2	12	4	0	0	0	0	0
168	204	116	15.5	7.2	0	0	0	0	0	0	0
169	0	0	0	7.2	11	4	0	0	0	0	0
170	235	116	18	7.2	0	0	0	0	0	0	0
171	0	0	0	7.2	11	4	0	0	0	0	0
172	162	116	12.5	7.2	0	0	0	0	0	0	0
173	0	0	0	7.2	11	4	0	0	0	0	0
174	162	116	12.5	7.2	0	0	0	0	0	0	0
175	0	0	0	7.2	11	4	0	0	0	0	0
176	676	116	18	7.2	0	0	0	0	0	0	0
177	0	0	0	7.2	11.5	4	0	0	0	0	0
178	147	116	14	7.2	0	0	0	0	0	0	0
179	0	0	0	7.2	12	2	0	0	0	0	0
180	300	116	17.5	7.2	0	0	0	0	0	0	0
181	0	0	0	7.2	9	4	0	0	0	0	0
182	486	116	14	7.2	0	0	0	0	0	0	0
183	0	0	0	7.2	12	4	0	0	0	0	0
184	204	116	15.5	7.2	0	0	0	0	0	0	0
185	0	0	0	7.2	11	4	0	0	0	0	0
186	235	116	18	7.2	0	0	0	0	0	0	0
187	0	0	0	7.2	11	4	0	0	0	0	0
188	162	116	12.5	7.2	0	0	0	0	0	0	0
189	0	0	0	7.2	11	4	0	0	0	0	0
190	162	116	12.5	7.2	0	0	0	0	0	0	0
191	0	0	0	7.2	11	4	0	0	0	0	0
192	676	116	18	7.2	0	0	0	0	0	0	0
193	0	0	0	7.2	11.5	4	0	0	0	0	0
194	147	116	14	7.2	0	0	0	0	0	0	0
195	0	0	0	7.2	12	2	0	0	0	0	0
196	300	116	17.5	7.2	0	0	0	0	0	0	0
197	0	0	0	7.2	9	4	0	0	0	0	0
198	486	116	14	7.2	0	0	0	0	0	0	0
199	0	0	0	7.2	12	4	0	0	0	0	0
200	204	116	15.5	7.2	0	0	0	0	0	0	0
201	0	0	0	7.2	11	4	0	0	0	0	0
202	235	116	18	7.2	0	0	0	0	0	0	0
203	0	0	0	7.2	11	4	0	0	0	0	0
204	162	116	12.5	7.2	0	0	0	0	0	0	0
205	0	0	0	7.2	11	4	0	0	0	0	0
206	162	116	12.5	7.2	0	0	0	0	0	0	0
207	0	0	0	7.2	11	4	0	0	0	0	0
208	676	116	18	7.2	0	0	0	0	0	0	0
209	0	0	0	7.2	11.5	4	0	0	0	0	0
210	147	116	14	7.2	0	0	0	0	0	0	0

A. Appendix

211	0	0	0	7.2	12	2	0	0	0	0	0
212	300	116	17.5	7.2	0	0	0	0	0	0	0
213	0	0	0	7.2	9	4	0	0	0	0	0
214	486	116	14	7.2	0	0	0	0	0	0	0
215	0	0	0	7.2	12	4	0	0	0	0	0
216	204	116	15.5	7.2	0	0	0	0	0	0	0
217	0	0	0	7.2	11	4	0	0	0	0	0
218	235	116	18	7.2	0	0	0	0	0	0	0
219	0	0	0	7.2	11	4	0	0	0	0	0
220	162	116	12.5	7.2	0	0	0	0	0	0	0
221	0	0	0	7.2	11	4	0	0	0	0	0
222	162	116	12.5	7.2	0	0	0	0	0	0	0
223	0	0	0	7.2	11	4	0	0	0	0	0
224	676	116	18	7.2	0	0	0	0	0	0	0
225	0	0	0	7.2	11.5	4	0	0	0	0	0
226	147	116	14	7.2	0	0	0	0	0	0	0
227	0	0	0	7.2	12	2	0	0	0	0	0
228	300	116	17.5	7.2	0	0	0	0	0	0	0
229	0	0	0	7.2	9	4	0	0	0	0	0
230	486	116	14	7.2	0	0	0	0	0	0	0
231	0	0	0	7.2	12	4	0	0	0	0	0
232	204	116	15.5	7.2	0	0	0	0	0	0	0
233	0	0	0	7.2	11	4	0	0	0	0	0
234	235	116	18	7.2	0	0	0	0	0	0	0
235	0	0	0	7.2	11	4	0	0	0	0	0
236	162	116	12.5	7.2	0	0	0	0	0	0	0
237	0	0	0	7.2	11	4	0	0	0	0	0
238	162	116	12.5	7.2	0	0	0	0	0	0	0
239	0	0	0	7.2	11	4	0	0	0	0	0
240	676	116	18	7.2	0	0	0	0	0	0	0
241	0	0	0	7.2	11.5	4	0	0	0	0	0
242	147	116	14	7.2	0	0	0	0	0	0	0
243	0	0	0	7.2	12	2	0	0	0	0	0
244	300	116	17.5	7.2	0	0	0	0	0	0	0
245	0	0	0	7.2	9	4	0	0	0	0	0
246	486	116	14	7.2	0	0	0	0	0	0	0
247	0	0	0	7.2	12	4	0	0	0	0	0
248	204	116	15.5	7.2	0	0	0	0	0	0	0
249	0	0	0	7.2	11	4	0	0	0	0	0
250	235	116	18	7.2	0	0	0	0	0	0	0
251	0	0	0	7.2	11	4	0	0	0	0	0
252	162	116	12.5	7.2	0	0	0	0	0	0	0
253	0	0	0	7.2	11	4	0	0	0	0	0
254	162	116	12.5	7.2	0	0	0	0	0	0	0
255	0	0	0	7.2	11	4	0	0	0	0	0
256	676	116	18	7.2	0	0	0	0	0	0	0
257	0	0	0	7.2	11.5	4	0	0	0	0	0
258	147	116	14	7.2	0	0	0	0	0	0	0
259	0	0	0	7.2	12	2	0	0	0	0	0
260	300	116	17.5	7.2	0	0	0	0	0	0	0
261	0	0	0	7.2	9	4	0	0	0	0	0
262	486	116	14	7.2	0	0	0	0	0	0	0
263	0	0	0	7.2	12	4	0	0	0	0	0
264	204	116	15.5	7.2	0	0	0	0	0	0	0
265	0	0	0	7.2	11	4	0	0	0	0	0
266	235	116	18	7.2	0	0	0	0	0	0	0
267	0	0	0	7.2	11	4	0	0	0	0	0
268	162	116	12.5	7.2	0	0	0	0	0	0	0
269	0	0	0	7.2	11	4	0	0	0	0	0
270	162	116	12.5	7.2	0	0	0	0	0	0	0
271	0	0	0	7.2	11	4	0	0	0	0	0
272	676	116	18	7.2	0	0	0	0	0	0	0
273	0	0	0	7.2	11.5	4	0	0	0	0	0
274	147	116	14	7.2	0	0	0	0	0	0	0
275	0	0	0	7.2	12	2	0	0	0	0	0
276	300	116	17.5	7.2	0	0	0	0	0	0	0
277	0	0	0	7.2	9	4	0	0	0	0	0
278	486	116	14	7.2	0	0	0	0	0	0	0
279	0	0	0	7.2	12	4	0	0	0	0	0
280	204	116	15.5	7.2	0	0	0	0	0	0	0
281	0	0	0	7.2	11	4	0	0	0	0	0
282	235	116	18	7.2	0	0	0	0	0	0	0
283	0	0	0	7.2	11	4	0	0	0	0	0
284	162	116	12.5	7.2	0	0	0	0	0	0	0
285	0	0	0	7.2	11	4	0	0	0	0	0
286	162	116	12.5	7.2	0	0	0	0	0	0	0
287	0	0	0	7.2	11	4	0	0	0	0	0
288	676	116	18	7.2	0	0	0	0	0	0	0
289	0	0	0	7.2	11.5	4	0	0	0	0	0
290	147	116	14	7.2	0	0	0	0	0	0	0
291	0	0	0	7.2	12	2	0	0	0	0	0
292	300	116	17.5	7.2	0	0	0	0	0	0	0
293	0	0	0	7.2	9	4	0	0	0	0	0
294	486	116	14	7.2	0	0	0	0	0	0	0
295	0	0	0	7.2	12	4	0	0	0	0	0
296	204	116	15.5	7.2	0	0	0	0	0	0	0
297	0	0	0	7.2	11	4	0	0	0	0	0
298	235	116	18	7.2	0	0	0	0	0	0	0
299	0	0	0	7.2	11	4	0	0	0	0	0
300	162	116	12.5	7.2	0	0	0	0	0	0	0

A. Appendix

301	0	0	0	7.2	11	4	0	0	0	0	0
302	162	116	12.5	7.2	0	0	0	0	0	0	0
303	0	0	0	7.2	11	4	0	0	0	0	0
304	676	116	18	7.2	0	0	0	0	0	0	0
305	0	0	0	7.2	11.5	4	0	0	0	0	0
306	147	116	14	7.2	0	0	0	0	0	0	0
307	0	0	0	7.2	12	2	0	0	0	0	0
308	300	116	17.5	7.2	0	0	0	0	0	0	0
309	0	0	0	7.2	9	4	0	0	0	0	0
310	486	116	14	7.2	0	0	0	0	0	0	0
311	0	0	0	7.2	12	4	0	0	0	0	0
312	204	116	15.5	7.2	0	0	0	0	0	0	0
313	0	0	0	7.2	11	4	0	0	0	0	0
314	235	116	18	7.2	0	0	0	0	0	0	0
315	0	0	0	7.2	11	4	0	0	0	0	0
316	162	116	12.5	7.2	0	0	0	0	0	0	0
317	0	0	0	7.2	11	4	0	0	0	0	0
318	162	116	12.5	7.2	0	0	0	0	0	0	0
319	0	0	0	7.2	11	4	0	0	0	0	0
320	676	116	18	7.2	0	0	0	0	0	0	0
321	0	0	0	7.2	11.5	4	0	0	0	0	0
322	147	116	14	7.2	0	0	0	0	0	0	0
323	0	0	0	7.2	12	2	0	0	0	0	0
324	300	116	17.5	7.2	0	0	0	0	0	0	0
325	0	0	0	7.2	9	4	0	0	0	0	0
326	486	116	14	7.2	0	0	0	0	0	0	0
327	0	0	0	7.2	12	4	0	0	0	0	0
328	204	116	15.5	7.2	0	0	0	0	0	0	0
329	0	0	0	7.2	11	4	0	0	0	0	0
330	235	116	18	7.2	0	0	0	0	0	0	0
331	0	0	0	7.2	11	4	0	0	0	0	0
332	162	116	12.5	7.2	0	0	0	0	0	0	0
333	0	0	0	7.2	11	4	0	0	0	0	0
334	162	116	12.5	7.2	0	0	0	0	0	0	0
335	0	0	0	7.2	11	4	0	0	0	0	0
336	676	116	18	7.2	0	0	0	0	0	0	0
337	0	0	0	7.2	11.5	4	0	0	0	0	0
338	147	116	14	7.2	0	0	0	0	0	0	0
339	0	0	0	7.2	12	2	0	0	0	0	0
340	995.71	116	17.5	7.2	0	0	0	0	0	0	0
341	337.1	116	17.5	7.2	0	0	0	0	0	0	0
342	157.19	109	17.5	7.2	0	0	0	0	0	0	0
343	0	0	0	7.2	9	4	0	0	0	0	0
344	908.37	109	19.5	7.2	0	0	0	0	0	0	0
345	556.36	108	19.5	7.2	0	0	0	0	0	0	0
346	857.29	101	19.5	7.2	0	0	0	0	0	0	0
347	320.98	100	19.5	7.2	0	0	0	0	0	0	0
348	0	0	0	7.2	9	4	0	0	0	0	0
349	50	100	3.5	7.2	0	0	0	0	0	0	0
350	0	0	0	7.2	10	4	0	0	0	0	0
351	580	100	15	7.2	0	0	0	0	0	0	0
352	0	0	0	7.2	9	4	0	0	0	0	0
353	516	100	15	7.2	0	0	0	0	0	0	0
354	0	0	0	7.2	12.5	4	0	0	0	0	0
355	930	100	20	7.2	0	0	0	0	0	0	0
356	0	0	0	7.2	7	4	0	0	0	0	0
357	200	100	20	7.2	0	0	0	0	0	0	0
358	0	0	0	7.2	9	4	0	0	0	0	0
359	50	100	3.5	7.2	0	0	0	0	0	0	0
360	0	0	0	7.2	9	4	0	0	0	0	0
361	1122	100	18	7.2	0	0	0	0	0	0	0
362	0	0	0	7.2	9.5	4	0	0	0	0	0
363	930	100	20	7.2	0	0	0	0	0	0	0
364	0	0	0	7.2	7	4	0	0	0	0	0
365	200	100	20	7.2	0	0	0	0	0	0	0
366	0	0	0	7.2	9	4	0	0	0	0	0
367	50	100	3.5	7.2	0	0	0	0	0	0	0
368	0	0	0	7.2	9	4	0	0	0	0	0
369	1122	100	18	7.2	0	0	0	0	0	0	0
370	0	0	0	7.2	9.5	4	0	0	0	0	0
371	930	100	20	7.2	0	0	0	0	0	0	0
372	0	0	0	7.2	7	4	0	0	0	0	0
373	200	100	20	7.2	0	0	0	0	0	0	0
374	0	0	0	7.2	9	4	0	0	0	0	0
375	50	100	3.5	7.2	0	0	0	0	0	0	0
376	0	0	0	7.2	9	4	0	0	0	0	0
377	1122	100	18	7.2	0	0	0	0	0	0	0
378	0	0	0	7.2	9.5	4	0	0	0	0	0
379	930	100	20	7.2	0	0	0	0	0	0	0
380	0	0	0	7.2	7	4	0	0	0	0	0
381	200	100	20	7.2	0	0	0	0	0	0	0
382	0	0	0	7.2	9	4	0	0	0	0	0
383	50	100	3.5	7.2	0	0	0	0	0	0	0
384	0	0	0	7.2	9	4	0	0	0	0	0
385	1122	100	18	7.2	0	0	0	0	0	0	0
386	0	0	0	7.2	9.5	4	0	0	0	0	0
387	930	100	20	7.2	0	0	0	0	0	0	0
388	0	0	0	7.2	7	4	0	0	0	0	0
389	200	100	20	7.2	0	0	0	0	0	0	0
390	0	0	0	7.2	9	4	0	0	0	0	0

A. Appendix

391	50	100	3.5	7.2	0	0	0	0	0	0	0
392	0	0	0	7.2	9	4	0	0	0	0	0
393	1122	100	18	7.2	0	0	0	0	0	0	0
394	0	0	0	7.2	9.5	4	0	0	0	0	0
395	930	100	20	7.2	0	0	0	0	0	0	0
396	0	0	0	7.2	7	4	0	0	0	0	0
397	200	100	20	7.2	0	0	0	0	0	0	0
398	0	0	0	7.2	9	4	0	0	0	0	0
399	50	100	3.5	7.2	0	0	0	0	0	0	0
400	0	0	0	7.2	9	4	0	0	0	0	0
401	1122	100	18	7.2	0	0	0	0	0	0	0
402	0	0	0	7.2	9.5	4	0	0	0	0	0
403	930	100	20	7.2	0	0	0	0	0	0	0
404	0	0	0	7.2	7	4	0	0	0	0	0
405	200	100	20	7.2	0	0	0	0	0	0	0
406	0	0	0	7.2	9	4	0	0	0	0	0
407	50	100	3.5	7.2	0	0	0	0	0	0	0
408	0	0	0	7.2	9	4	0	0	0	0	0
409	1122	100	18	7.2	0	0	0	0	0	0	0
410	0	0	0	7.2	9.5	4	0	0	0	0	0
411	930	100	20	7.2	0	0	0	0	0	0	0
412	0	0	0	7.2	7	4	0	0	0	0	0
413	200	100	20	7.2	0	0	0	0	0	0	0
414	0	0	0	7.2	9	4	0	0	0	0	0
415	50	100	3.5	7.2	0	0	0	0	0	0	0
416	0	0	0	7.2	9	4	0	0	0	0	0
417	1122	100	18	7.2	0	0	0	0	0	0	0
418	0	0	0	7.2	9.5	4	0	0	0	0	0
419	930	100	20	7.2	0	0	0	0	0	0	0
420	0	0	0	7.2	7	4	0	0	0	0	0
421	200	100	20	7.2	0	0	0	0	0	0	0
422	0	0	0	7.2	9	4	0	0	0	0	0
423	50	100	3.5	7.2	0	0	0	0	0	0	0
424	0	0	0	7.2	9	4	0	0	0	0	0
425	1122	100	18	7.2	0	0	0	0	0	0	0
426	0	0	0	7.2	9.5	4	0	0	0	0	0
427	930	100	20	7.2	0	0	0	0	0	0	0
428	0	0	0	7.2	7	4	0	0	0	0	0
429	200	100	20	7.2	0	0	0	0	0	0	0
430	0	0	0	7.2	9	4	0	0	0	0	0
431	50	100	3.5	7.2	0	0	0	0	0	0	0
432	0	0	0	7.2	9	4	0	0	0	0	0
433	1122	100	18	7.2	0	0	0	0	0	0	0
434	0	0	0	7.2	9.5	4	0	0	0	0	0
435	930	100	20	7.2	0	0	0	0	0	0	0
436	0	0	0	7.2	7	4	0	0	0	0	0
437	200	100	20	7.2	0	0	0	0	0	0	0
438	0	0	0	7.2	9	4	0	0	0	0	0
439	50	100	3.5	7.2	0	0	0	0	0	0	0
440	0	0	0	7.2	9	4	0	0	0	0	0
441	1122	100	18	7.2	0	0	0	0	0	0	0
442	0	0	0	7.2	9.5	4	0	0	0	0	0
443	930	100	20	7.2	0	0	0	0	0	0	0
444	0	0	0	7.2	7	4	0	0	0	0	0
445	200	100	20	7.2	0	0	0	0	0	0	0
446	0	0	0	7.2	9	4	0	0	0	0	0
447	50	100	3.5	7.2	0	0	0	0	0	0	0
448	0	0	0	7.2	9	4	0	0	0	0	0
449	1122	100	18	7.2	0	0	0	0	0	0	0
450	0	0	0	7.2	9.5	4	0	0	0	0	0
451	930	100	20	7.2	0	0	0	0	0	0	0
452	0	0	0	7.2	7	4	0	0	0	0	0
453	200	100	20	7.2	0	0	0	0	0	0	0
454	0	0	0	7.2	9	4	0	0	0	0	0
455	50	100	3.5	7.2	0	0	0	0	0	0	0
456	0	0	0	7.2	9	4	0	0	0	0	0
457	1122	100	18	7.2	0	0	0	0	0	0	0
458	0	0	0	7.2	9.5	4	0	0	0	0	0
459	930	100	20	7.2	0	0	0	0	0	0	0
460	0	0	0	7.2	7	4	0	0	0	0	0
461	200	100	20	7.2	0	0	0	0	0	0	0
462	0	0	0	7.2	9	4	0	0	0	0	0
463	50	100	3.5	7.2	0	0	0	0	0	0	0
464	0	0	0	7.2	9	4	0	0	0	0	0
465	1122	100	18	7.2	0	0	0	0	0	0	0
466	0	0	0	7.2	9.5	4	0	0	0	0	0
467	930	100	20	7.2	0	0	0	0	0	0	0
468	0	0	0	7.2	7	4	0	0	0	0	0
469	200	100	20	7.2	0	0	0	0	0	0	0
470	0	0	0	7.2	9	4	0	0	0	0	0
471	50	100	3.5	7.2	0	0	0	0	0	0	0
472	0	0	0	7.2	9	4	0	0	0	0	0
473	1122	100	18	7.2	0	0	0	0	0	0	0
474	0	0	0	7.2	9.5	4	0	0	0	0	0
475	930	100	20	7.2	0	0	0	0	0	0	0
476	0	0	0	7.2	7	4	0	0	0	0	0
477	200	100	20	7.2	0	0	0	0	0	0	0
478	0	0	0	7.2	9	4	0	0	0	0	0
479	50	100	3.5	7.2	0	0	0	0	0	0	0
480	0	0	0	7.2	9	4	0	0	0	0	0

A. Appendix

481	1122	100	18	7.2	0	0	0	0	0	0	0
482	0	0	0	7.2	8	4	0	0	0	0	0
483	1249.94	107	21	7.2	0	0	0	0	0	0	0
484	1190.48	108	21	7.2	0	0	0	0	0	0	0
485	3417	109	21	7.2	0	0	0	0	0	0	0
486	0	0	0	7.2	7	4	0	0	0	0	0
487	783	109	19	7.2	0	0	0	0	0	0	0
488	0	0	0	7.2	9	4	0	0	0	0	0
489	188	116	15	7.2	0	0	0	0	0	0	0
490	0	0	0	7.2	8	4	0	0	0	0	0
491	283	116	17	7.2	0	0	0	0	0	0	0
492	0	0	0	7.2	29	4	0	0	0	0	0
493	270	116	15	7.2	0	0	0	0	0	0	0
494	0	0	0	7.2	9	4	0	0	0	0	0
495	180	116	15	7.2	0	0	0	0	0	0	0
496	0	0	0	7.2	11	4	0	0	0	0	0
497	176	116	15	7.2	0	0	0	0	0	0	0

Listing A.5: Trade description

A.5.2. Scenario Setup

```

1 #Config-File for Scenario Development
2 #
3 #lines starting with '#' are treated as comments
4 #
5 #time horizon [h]
6 87658.2
7 #
8 #minimum draught [m]
9 5.0
10 #
11 #maximum draught [m]
12 12.0
13 #
14 #minimum speed [kn]
15 0.0
16 #
17 #maximum speed [kn]
18 25.0
19 #
20 #loading-draught-function (Lambda function), x / y = no. of full / empty TEUs
21 lambda x, y: 5 + (x * 14. + y * 2.33) / 5000.
22 #
23 #maintenance interval [h]
24 43829.1
25 #
26 #docking duration [h]
27 504.0
28 #
29 #slow steaming table
30 25
31 20
32 #
33 #speed reduction table
34 25
35 20
36 #
37 #bin width: speed [kn]
38 1.0
39 #
40 #bin width: draught [m]
41 1.0
42 #
43 #interest rate [%]
44 5.0
45 #
46 #FOP development (Lambda function) [$/h]
47 lambda x: 500.0 + 500.0 * 0.025 * (x / 8765.82)
48 #
49 #FOP fluctuation (Lambda function) [$/h]
50 lambda x: 100.0 * (x / 8765.82)
51 #
52 #TD development (Lambda function) [%/h]
53 lambda x: 0.015 * (x / 8765.82)
54 #
55 #TD fluctuation (Lambda function) [%/h]
56 lambda x: 0.1 * (x / 8765.82)
57 #
58 #FOP crisis: chance [%/y]
59 15.0
60 #
61 #FOP crisis: duration (averaged) [h]
62 8765.82
63 #

```

A. Appendix

```
64 #FOP crisis: duration (standard deviation) [h]
65 2920.0
66 #
67 #FOP crisis: chance of rising FOP [%]
68 67.0
69 #
70 #TD crisis: chance [%/y]
71 15.0
72 #
73 #TD crisis: duration (averaged) [h]
74 8765.82
75 #
76 #TD crisis: duration (standard deviation) [h]
77 2920.0
78 #
79 #TD crisis: chance of rising TD [%]
80 25.0
81 #
82 #draught calculation: 0 = from draughts, 1 = from loading
83 0
84 #
85 #minimum no. of MC cycles
86 0
87 #
88 #Hellinger criterion (0 <= x <= 1)
89 1e-10
90 #
91 #maximum no. of MC cycles
92 10000
93 #
94 #OOC calculation: 0 = maximum no., 1 = coverage
95 1
96 #
97 #no. of OOCs
98 100
99 #
100 #OOC coverage [%]
101 70.
```

Listing A.6: Scenario development setup

Bibliography

- Andrews, D., Papanikolaou, A., and Singer, D. J. (2012). Design for X. In IMDC2012 Secretariat, editor, *Proceedings of the 11th International Marine Design Conference (IMDC)*, volume 1, pages 109–146. State of the Art Report.
- Arcade, J. (1999). *Structural Analysis with the MICMAC Method & Actors' Strategy with MACTOR Method*. Laboratory for Investigation in Prospective and Strategy (LIPS), Paris, France.
- Argyros, D., Raucci, C., Sabio, N., and Smith, T. (2014). Global Marine Fuel Trends 2030.
- Aspen, D. M., Magerholm Fet, A., and Johansen, B. A. (2012). Life cycle system analysis methods in ship design - a review of current status, opportunities and challenges. In IMDC2012 Secretariat, editor, *Proceedings of the 11th International Marine Design Conference (IMDC)*, volume 2, pages 39–48.
- Ayob, A. F. M., Ray, T., and Smith, W. F. (2011). Scenario-based hydrodynamic design optimization of high speed planing craft for coastal surveillance.
- Bardi, U. (2011). *The Limits to Growth Revisited*. Springer.
- Barney, G. O. (1980). *The Global 2000 Report to the President*. US Government Printing Office, Washington DC, United States.
- Benford, H. (1980). A second look at measures of merit for ship design. The University of Michigan, College of Engineering, The Department of Naval Architecture and Marine Engineering.
- Bergh, I. (2010). Optimum speed - from a shipper's perspective. In *Container Ship Update*, number 2, pages 10–13.
- Beyer, H.-G. and Sendhoff, B. (2007). Robust optimization - a comprehensive survey. *Computational Methods in Applied Mechanics and Engineering*.
- Binder, K. and Heermann, D. W. (2010). *Monte Carlo Simulation in Statistical Physics: An Introduction*. Graduate Texts in Physics. Springer, Berlin, Germany, fifth edition.
- Bronsart, R., Binkowski, E., Garke, S., Lindner, H., Schenk, S., and Wagner, J. (2016). Performance von Schiffen im Seegang (PerSee) - Abschlussbericht. Technical report, Universität Rostock, Fakultät für Maschinenbau und Schiffstechnik.
- Carlton, J. S. (2012). *Marine Propellers and Propulsion*. Butterworth-Heinemann, Oxford, UK, third edition.

Bibliography

- Cha, S.-H. (2007). Comprehensive survey on distance/similarity measures between probability density functions. *International Journal of Mathematical Models and Methods in Applied Sciences*, 1(4):300–307.
- Cheng, H. M. (1968). Performance comparisons of marine vehicles. Naval Ship Research and Development Center, Washington, D.C.
- Chuang, Z. and Steen, S. (2012). Experimental and numerical study of stem shape influence on speed loss in waves. *Ship Technology Research*, 59(2):4–17.
- Cole, H. S. D. (1973). *Models of Doom: A Critique of the Limits to Growth*. Universe Books, New York, New York, United States.
- Diez, M., Chen, X., Campana, E. F., and Stern, F. (2013). Reliability-based robust design optimization for ships in real ocean environment. In *Proceedings of the 12th International Conference on Fast Sea Transportation (FAST)*.
- Diez, M. and Peri, D. (2009). Global optimization algorithms for robust optimization in naval design. In Bertram, V., editor, *Proceedings of the 8th International Conference on Computer Applications and Information Technology in the Maritime Industries (COMPIT)*.
- Diez, M. and Peri, D. (2010). Two-stage stochastic programming formulation for ship design optimisation under uncertainty. *Ship Technology Research*, 57(3):172–181.
- DNV (2010). Quantum - a container ship concept for the future. *DNV Container Ship Update*, (1).
- DNV (2012). Shipping 2020.
- DNV and MAN Diesel & Turbo (2011). *Quantum 9000 Two Stroke LNG*.
- el Moctar, O., Shigunov, V., and Zorn, T. (2012). Duisburg Test Case: Post-panmax container ship for benchmarking. *Ship Technology Research*, 59(3):50–64.
- Eljardt, G. (2010). *Entwicklung einer statistikbasierten Simulationsmethodik für Schiffsentwürfe unter realistischen Betriebsbedingungen*. PhD thesis, Technische Universität Hamburg Hamburg.
- Erikstad, S. O., Fagerholt, K., and Solem, S. (2011). A ship design and deployment model for non-cargo vessels using contract scenarios. *Ship Technology Research*, 58(3):132–141.
- Fang, I., Cheng, F., Incecik, A., and Carnie, P. (2013). Global Marine Trends 2030.
- Federal Reserve Bank of St. Louis (2015). Crude Oil Prices: Brent - Europe.
- Fet, A. M., Michelsen, O., and Karlsen, H. (2001). Environmental performance of transportation - a comparative study. Norwegian University of Science and Technology, Trondheim, Norway.
- Fet, A. M. and Sjørgård, E. (1999). Life cycle evaluation of ship transportation - development of methodology and testing. Technical Report HIA10/B101/R-98/008/00, Ålesund College.
- Fischer, N., Wurst, S., Nagel, R., and Witolla, T. (2012). Life cycle performance assessment as decision support for ship design - multipurpose rooms on cruise ships as example.

Bibliography

- FLOWTECH (2015). *SHIPFLOW 6.0 Users Manual*. Flowtech International AB, Gothenburg, Sweden.
- FLOWTECH International AB (2015). Shipflow basic. <http://www.flowtech.se/>.
- FRIENDSHIP SYSTEMS AG (2015). *CAESES Documentation*.
- FRIENDSHIP SYSTEMS AG (2016). Friendship systems. <https://www.caeses.com/>.
- GAUSS (2011). Ship life cycle assessment and management. Technical report, Gesellschaft für angewandten Umweltschutz und Sicherheit im Seeverkehr mbH (GAUSS), Bremen, Germany.
- Gershanik, V. (2011). Verringerung des Brennstoffverbrauchs und der Umweltbelastung von Seeschiffen.
- Godet, M. (1987). *Scenarios and Strategic Management*. Butterwoths, London, Boston, USA.
- Green, L. A. and Xu, K.-M. (2005). Comparison of Histograms for Use in Cloud Modeling. Technical report, National Aeronautics and Space Administration (NASA).
- Greeuw, S. C. H., van Asselt, M. B. A., Grosskurth, J., Storms, C. A. M. H., Rijkens-Klomp, N., Rothman, D. S., and Rothmans, J. (2000). *An Assessment of recent European and global scenario studies and models*. International Centre for Integrative Studies (ICIS).
- Harper Peterson & Co. (GmbH & Cie. KG) (2016). Harper peterson & co. <http://www.harperpetersen.com/>. as of Mai 2016.
- Hauke, W. (1992). *Darstellung struktureller Zusammenhänge und Entwicklungen in Input-Output-Tabellen*. Eul-Verlag, Bergisch-Gladbach, Germany.
- Henze, N. (2013). *Irrfahrten und verwandte Zufälle (Ein elementarer Einstieg in die stochastischen Prozesse)*. Springer Spektrum, Wiesbaden, Germany.
- Hilleary, R. R. (1966). The tangent search method of constrained minimization. Technical Report 59, United States Naval Postgraduate School.
- Hochkirch, K. and Bertram, V. (2012). Hull optimization for fuel efficiency - past, present and future. In Bertram, V., editor, *Proceedings of 11th International Conference on Computer and IT Applications in the Maritime Industries (COMPIT)*, pages 39–49.
- Hollenbach, U. and Reinholz, O. (2011). Hydrodynamic trends in optimizing propulsion. In *Proceedings of Second International Symposium on Marine Propulsors (SMP)*.
- Holtrop, J. (1984). A statistical re-analysis of resistance and propulsion data. *International Shipbuilding Progress*, (363):272–276.
- ICCT (2011). The Energy Efficiency Design Index (EEDI) for New Ships. In *Policy Update*, volume 15. The International Council on Clean Transportation.
- IMO (2009). *Guidelines for voluntary Use of the Ship Energy Efficiency Operational Indicator (EEOI)*.
- IMO (2012a). EEDI - rational, safe and effective. <http://www.imo.org/>.

Bibliography

- IMO (2012b). Marine Environment Protection Committee (MEPC), 63rd session, 27 February to 2 March. <http://www.imo.org>.
- IPCC (2014). *Climate Change 2014: Synthesis Report. Contribution of Working Groups I, II and III to the Fifth Assessment Report of the Intergovernmental Panel on Climate Change*. The Intergovernmental Panel on Climate Change (IPCC), Geneva, Switzerland.
- IPCC (2015). IPCC Assessment Reports. <http://www.ipcc.ch/>.
- Jah, M. and Christie, N. (2015). Baltic dry shipping index drops to all-time low. <http://www.bloomberg.com/>.
- Jammazi, R. and Aloui, C. (2012). Crude oil forecasting: Experimental evidence from wavelet decomposition and neural network modeling. *Energy Economics*, 34(3):828–841.
- Kaboudan, M. A. (2001). Compumetric forecasting of crude oil prices. In *Proceedings of the 2001 Congress on Evolutionary Computation*, volume 1, pages 283–287. IEEE.
- Kilian, L. (2014). Oil price shocks: Causes and consequences. Number DP9823 in CEPR Discussion Paper. Centre for Economic Policy Research.
- Kleinsorge, E., Lindner, H., Wagner, J., and Bronsart, R. (2016). Ship hull form optimization using scenario methods. In *Proceedings of the 13th International Symposium on Practical Design of Ships and Other Floating Structures (PRADS 2016)*, Copenhagen, Denmark.
- Kossow, H. and Gaßner, R. (2007). Methods of future and scenario analysis: Overview, assessment, and selection criteria. In *DIE Research Project "Development Policy: Questions for the Future"*, volume 39. Deutsches Institut für Entwicklungspolitik (DIE), Bonn.
- Kossow, H. and Gaßner, R. (2008). *Methoden der Zukunfts- und Szenarioanalyse - Überblick, Bewertung und Auswahlkriterien*. Institut für Zukunftsstudien und Technologiebewertung, Berlin, Germany.
- Koutroukis, G., Papanikolaou, A., Nikolopoulos, L., Sames, P., and Köpke, M. (2013). Multi-objective optimization of container ship design. *Mediterranean Marine Science*.
- Kracht, A. M. (1978). Design of Bulbous Bows. *SNAME Transactions*, 86:197–217.
- Krajnc, D. and Glavič, P. (2005). A model for integrated assessment of sustainable development. *Resources, Conservation and Recycling*, (43):189–208.
- Kramer, M., Motley, M., and Young, Y. L. (2010). Probabilistic-based design of waterjet propulsors for surface effect ships. In *The 29th American Towing Tank Conference*, pages 269–278.
- Kreutzer, K. (2015). Optimierung der Vorschiffsgeometrie einer Kreuzfahrtschiffsform in Hinblick auf die Minimierung der Propulsionsleistung für den Schiffsbetrieb im moderaten See-gang. Master's thesis, Technische Universität Hamburg-Harburg.
- Lawler, G. F. and Limic, V. (2010). *Random Walk: A Modern Introduction*. Cambridge University Press.

Bibliography

- Lohr, S. (1998). Long boom or bust; a leading futurist risks his reputation with ideas on growth and high technology. *The New York Times*.
- Meadows, D. H. (1982). *Groping in the Dark: The First Decade of Global Modelling*. John Wiley & Sons.
- Meadows, D. H., Meadows, D. L., Randers, J., and Behrens III, W. W. (1972). *The Limits to Growth*. Universe Books, New York, New York, United States.
- Meadows, D. H., Randers, J., and Meadows, D. (2004). *Limits to Growth: The 30-Year Update*. Chelsea Green Publishing.
- Meadows, D. L. (1973). *The dynamics of growth in a finite world: A technical report on the global simulation model World 3*. Thayer School of Engineering, Dartmouth College, Hanover, New Hampshire, United States.
- Meng, Q. and Wang, T. (2011). A scenario-based dynamic programming model for multi-period liner ship fleet planning. *Transportation Research Part E: Logistics and Transportation Review*, 47(4):401–413.
- Mewis, F. (1989). Zum Einfluß des Formfaktors k auf die berechnete Leistung. *Schiffbau-forschung*, 28(3).
- Michel, W. H. (1999). Sea spectra revisited. *Marine Technology*, 36(4):211–227.
- Mietzner, D. (2009). *Strategische Vorausschau und Szenarioanalysen - Methodenevaluation und neue Ansätze*. Innovation und Technologie im modernen Management. Gabler Research, Wiesbaden, Germany.
- Mietzner, D. and Reger, G. (2004). Scenario-approaches: History, differences, advantages and disadvantages. In *Proceedings of the EU-US Scientific Seminar: New Technology Foresight, Forecasting & Assessment Methods*, Sevilla, Spain.
- Minsaas, K. J., Thon, H. J., and Kauczynski, W. (1986). Influence of ocean environment on thruster performance. In *Proceedings of International Symposium on Propeller and Cavitation*.
- Mißler-Behr, M. (1993). *Methoden der Szenarioanalyse*. Deutscher Universitätsverlag, Wiesbaden, Germany.
- Mundform, D. J., Schaffer, J., Myoung-Jin, K., Dale, S., Ampai, T., and Supawan, P. (2011). Number of Replications Required in Monte Carlo Simulation Studies: A Synthesis of Four Studies. *Journal of Modern Applied Statistical Methods*, 10(1):19–28.
- Mutschler, J. (2013). Drehen an vielen Stellschrauben. <http://www.vdma.org>.
- Narayan, P. K. and Narayan, S. (2007). Modelling oil price volatility. *Energy Policy*, 35(12):6549–6553.
- Papanikolaou, A. (2010). Holistic ship design optimization. *Computer-Aided Design*, (42):1028–1044.

Bibliography

- Park, G.-J., Lee, T.-H., Kwon, H. L., and Hwang, K.-H. (2006). Robust design: An overview. *AIAA Journal*, 44(1).
- Python Software Foundation (2015). Welcome to Python.org. <https://www.python.org/>.
- Rehrl, T. and Friedrich, R. (2006). Modelling long-term oil price and extraction with a hubbert approach: The LOPEX model. *Energy Policy*, 34(15):2413–2428.
- Reibnitz, U. (1991). *Szenario-Technik: Instrumente für die unternehmerische und persönliche Erfolgsplanung*. Gabler, Wiesbaden, Germany.
- Riesner, M. (2013). Performance von Schiffen im Seegang - Arbeitspaket 1.1: Ermittlung betriebsnaher Bedingungen für Schiffe im Seegang. Technical report, Universität Duisburg-Essen, Institut für Schiffstechnik und Transportsysteme.
- Ringland, G. (1998). *Scenario planning: managing for the future*. John Wiley & Sons, Chichester, United Kingdom.
- Scarce, D. and Fulton, K. (2004). *What if? The Art of Scenario Thinking for Nonprofits*. Global Business Network.
- Schirwitz, B. and Vogt, G. (2005). Die gesamtwirtschaftlichen Auswirkungen einer Ölpreiserhöhung. Technical report, Ifo Institute - Leibniz Institute for Economic Research.
- Schlegel, H. (2011). Erfolg durch flexibles Handeln und Konzentration auf wachsende Märkte. *Schiff & Hafen*, (1):44–46.
- SeaRates LP (2015). Routes explorer. <http://www.searates.com/>.
- Shell International BV (2008). Scenarios: An explorer's guide. Edition 2.
- Shell International BV (2011). Energy needs, choices and possibilities - scenarios to 2050.
- Ship & Bunker News Team (2015). Maersk line says slow steaming will continue as "we want to be as energy-efficient as possible". <http://shipandbunker.com/>.
- Shoemaker, P. J. H. (1993). Multiple scenario development: Its conceptual and behavioral foundation. *Strategic Management Journal*, 14:193–213.
- Simmons, M. R. (2000). Revisiting the limits to growth: Could the club of rome have been correct, after all?
- Singh, R. K., Murty, H. R., Gupta, S. K., and Dikshit, A. k. (2009). An overview of sustainability assessment methodologies. *Ecological Indicators*, (9):189–212.
- Sobol, I. M. (1991). *Die Monte-Carlo Methode*. Deutscher Verlag der Wissenschaften, Berlin.
- Söding, H. (2001). Global seaway statistics. *Ship Technology Research*, 48:147–153.
- Spitzer, F. (2001). *Principles of Random Walk*. Springer-Verlag, second edition.
- Stefanakos, C. N. and Schinas, O. (2014). Forecasting bunker prices; a nonstationary, multivariate methodology. *Transportation Research Part C: Emerging Technologies*, 38:177–194.

Bibliography

- Temple, D. W. and Collette, M. (2012). Multi-objective hull form optimization to compare build cost and lifetime fuel consumption. In IMDC2012 Secretariat, editor, *Proceedings of the 11th International Marine Design Conference (IMDC)*, volume 2, pages 391–403.
- The R Foundation (2016). The R project for statistical computing. <https://www.r-project.org/>.
- Tun, T. Y. (2015). Ship hull optimization in calm water and moderate sea states. Master’s thesis, University of Rostock.
- UNCTAD Secretariat (2010). Oil prices and maritime freight rates: An empirical investigation. Technical report, United Nations Conference On Trade And Development.
- UNCTAD Secretariat (2013). Review of maritime transport 2013. Technical report, United Nations Conference On Trade And Development.
- UNCTAD Secretariat (2015). Review of maritime transport 2015. Technical report, United Nations Conference On Trade And Development.
- van Notten, P. W., Rotmans, J., van Asselt, M. B. A., and Rothman, D. S. (2003). An updated scenario typology. *Futures*, 35:423–443.
- Vassallos, D. (2012). Design for safety: Risk-based design life-cycle risk management. In Secretariat, I., editor, *Proceedings of the 11th International Marine Design Conference (IMDC)*, volume 1, pages 83–106. State of the Art Report.
- von Graefe, A., El Moctar, B., and Shigunov, V. (2014). *GL Rankine: User Manual*. DNV GL.
- Wagner, J., Binkowski, E., and Bronsart, R. (2014). Scenario based optimization of a container vessel with respect to its projected operating conditions. *International Journal of Naval Architecture and Ocean Engineering (IJNAOE)*, 6:496–506.
- Wagner, J. and Bronsart, R. (2011). A contribution to scenario based ship design. In *Proceedings of the 15th International Conference on Computer Applications in Shipbuilding (ICCAS)*, volume 1, pages 47–52, Trieste, Italy.
- Wagner, J. and Bronsart, R. (2012). Build-up of scenarios for ship life-cycle - methods for descriptor analysis. In IMDC2012 Secretariat, editor, *Proceedings of the 11th International Marine Design Conference (IMDC)*, volume 1, pages 251–262, Glasgow, UK.
- Wärtsilä (2010a). Shipping Scenarios 2030. <http://www.shipping-scenarios.wartsila.com/>.
- Wärtsilä (2010b). Shipping Scenarios 2030 (Global Scenarios of Shipping in 2030).
- Wessels, H. (1981). Triangulation und Blocktriangulation von Input-Output-Tabellen und ihre Bedeutung. In *Beiträge zur Strukturforchung*, volume 63. Deutsches Institut für Wirtschaftsforschung (DIW), Duncker & Humblot, Berlin.
- Witting, H. and Müller-Funk, U. (1995). *Mathematische Statistik II - Asymptotische Statistik: Parametrische Modelle und nichtparametrische Funktionale*. B. G. Teubner, Stuttgart.
- World Shipping Council (2008). Record fuel prices place stress on ocean shipping.

Bibliography

- Young, I. R. and Holland, G. J. (1996). *Atlas of the Oceans: Wind and wave climate*. Pergamon Press, Oxford, United Kingdom.
- Zhang, X., Lai, K. K., and Wang, S.-Y. (2008). A new approach for crude oil price analysis based on empirical mode decomposition. *Energy Economics*, 30(3):905–918.

Related Publications

Publications

- 2016 Kleinsorge, E., Lindner, H., Wagner, J., Bronsart, R.: Ship Hull Form Optimization using Scenario Methods. *Proceedings of the 13th International Symposium on Practical Design of Ships and Other Floating Structures (PRADS)*, Copenhagen, Denmark
- 2014 Wagner, J., Binkowski, E., Bronsart, R.: Scenario based Optimization of a Container Vessel with Respect to its projected Operating Conditions. *International Journal of Naval Architecture and Ocean Engineering (IJNAOE)*, Korea
Selected and enhanced paper from the proceedings of PRADS 2013
- 2013 Wagner, J., Binkowski, E., Bronsart, R.: Scenario based Optimization of a Container Vessel with Respect to its Projected Operating Conditions. *Proceedings of the 12th International Symposium on Practical Design of Ships and Other Floating Structures (PRADS)*, Changwon City, Korea
- 2012 Wagner, J. and Bronsart, R.: Build-up of Scenarios for Ship Life-Cycle - Methods for Descriptor Analysis. *Proceedings of the 11th International Marine Design Conference (IMDC)*, Glasgow, UK
- 2011 Wagner, J. and Bronsart, R.: Considering the Life Cycle Performance in Ship Design. *Proceedings of the 1st International Symposium on Naval Architecture and Maritime (INT-NAM)*, Istanbul, Turkey
- 2011 Wagner, J. and Bronsart, R.: A Contribution to Scenario based Ship Design. *Proceedings of the 15th International Conference on Computer Applications in Shipbuilding (ICCAS)*, Trieste, Italy

Lectures

- 2013 Practical Application of Scenario based Ship Hull Form Optimizations. *Technical Talk organised by the Society of Naval Architects & Marine Engineers Singapore (SNAMES), the Joint Branch of the RINA and the IMarEST (Singapore) and the Centre for Offshore Research and Engineering (CORE), National University of Singapore (NUS), Singapore, Republic of Singapore*
- 2013 An Introduction to the Scenario based Hull Form Optimization of Merchant Vessels. Shanghai Jiao Tong University (SJTU), School of Naval Architecture, Ocean and Civil Engineering, Shanghai, China
- 2013 Scenario based Optimization of a Container Vessel with Respect to its projected Operating Conditions. *12th International Symposium on Practical Design of Ships and Other Floating Structures (PRADS), Changwon City, Korea*
- 2012 Scenario Methods to predict the Ships' Life-Cycle in the Design Process. *5th European Conference on Production Technologies in Shipbuilding (ECPTS), Bremerhaven, Germany*
- 2012 Build-up of Scenarios for Ship Life-Cycle - Methods for Descriptor Analysis. *11th International Marine Design Conference (IMDC), Glasgow, UK*
- 2011 Considering the Life Cycle Performance in Ship Design. *1st International Symposium on Naval Architecture and Maritime (INT-NAM), Istanbul, Turkey*
- 2011 A Contribution to Scenario based Ship Design. *15th International Conference on Computer Applications in Shipbuilding (ICCAS), Trieste, Italy*

Curriculum Vita

Personal Data

Name Jonas Wagner
Date of Birth April 28, 1982
Place of Birth Stuttgart
Nationality German
Personal Status Unmarried

Dissertation

07.2011 - 08.2018 University of Rostock, Faculty of Mechanical Engineering and Marine Technology, Chair of Ship Design
Subject: Scenario-based Optimization of Merchant Vessels

Professional Experience

since 05.2016 German Shipbuilding and Ocean Industries Association
Technical Advisor
07.2009 - 07.2015 University of Rostock, Faculty of Mechanical Engineering and Marine Technology, Chair of Ship Design
Research Assistant

Education

07.2009 Diploma
10.2001 - 07.2009 Academic Studies, University of Rostock, Faculty of Mechanical Engineering and Marine Technology
Specialization: Fundamentals of Ship Design and Ocean Technology and Ship Design / Ship Theory
06.2001 Abitur
08.1992 - 06.2001 Secondary School, Rhein-Maas-Gymnasium, Aachen

Acknowledgements

The author would like to thank the following people:

First of all, a big thank you to Prof. Bronsart for providing the initial idea and for his constant support and guidance even beyond my employment at the chair of ship design. Another big thank you goes to Prof. Kaeding for reviewing this thesis.

Special thanks go to Steffen Garke for his short but fruitful contribution and his ability to instantly and at any time follow my crazes and to reduce them to practice. Also special thanks to Eva Kleinsorge for her efforts in the course of *PerSee* and her constant supply of sweets.

I would furthermore like to thank all my colleagues at the chair of ship design (in alphabetical order): Desta Milkessa Edessa for making our trip to Asia such an incredible experience, Mr. Greshake for his enthusiasm regarding all kind of nerdy things, Lutz Kleinsorge for backing me up, Thomas Lindemann for our frequent meetings at special places, Hannes Lindner for his ~~destructive~~ input, Sebastian Schenk for the constant badgering and Kersten Ziesemer for the virus-safe mouse pad. Thanks to all of you for making my employment at the chair of ship design such a wonderful time.

Again special thanks go to Frank Krüger for the fuzzy yet excessive discussions on methods and algorithms without knowing their purpose. Still looking forward to the *R* lecture.

Also a big thank you to János Zierath for proof-reading and all the paddling.

Additional thanks go out to Leif Broberg and Björn Walther for supporting this thesis by supplying me with software and lots of data.

Your contribution to this work is highly appreciated!

Finally, I would like to express my deepest gratitude to Romanița for all her love and patience.

Noroc!

Declaration of Authorship

I hereby declare that this dissertation has been composed by myself and describes my own work unless otherwise acknowledged in the text.

All references and verbatim extracts have been quoted and all sources of information have been specifically acknowledged. This thesis has not been submitted in any previous application for a degree.

Rostock, September 25, 2018

Jonas Wagner